HORIZONTAL & MULTILATERAL WELLS' PERFORMANCE PREDICTION IN UNDERSATURATED RESERVOIRS

BY

ALI SALMAN AL-MASHHAD

A Thesis Presented to the

DEANSHIP OF GRADUATE STUDIES

KING FAHD UNIVERSITY OF PETROLEUM & MINERALS

DHAHRAN, SAUDI ARABIA

In Partial Fulfillment of the

Requirements for the Degree of

MASTER OF SCIENCE

In

PETROLEUM ENGINEERING

DECEMBER 2018

KING FAHD UNIVERSITY OF PETROLEUM & MINERALS

DHAHRAN 31261, SAUDI ARABIA

DEANSHIP OF GRADUATE STUDIES

This thesis, written by **Ali Salman Al-Mashhad** under the direction of his thesis advisor and approval by his thesis committee, has been presented to and accepted by the Dean of Graduate Studies, in partial fulfilment of the requirements for the degree of **MASTER OF SCIENCE IN PETROLEUM ENGINEERING.**

Dr. Dhafer Al-Shehri
(Advisor)

Dr. Abdulazeez Abdulraheem
(Member)

Dr. Bashirul Haq
(Member)

Dr. Dhafer Al-Shehri
(Department Chairman)

Dr. Salam A. Zummo
(Dean of Graduate Studies)

19/12/18

Date

DEDICATION

My Parents, My Wife and My Daughters

ACKNOWLEDGMENTS

First and foremost, I praise and thank God Almighty for all the countless blessings and vast grace upon me. I would like to express my sincere gratitude to my thesis advisor Dr. Dhafer Al-Shehri for his guidance, supervision and friendship. I would have not been able to complete this work if it was not for the support and expertise of him and the rest of the committee members Dr. Abdulazeez Abdulraheem and Dr. Bashirul Haq.

Special thanks are due to my lovely family, my amazing parents Salman and Masoomah, my brothers and sisters, my daughters Zahra & Anwar and last but not least, to my soul mate and my wonderful wife, Zainab. I thank them all for their love, encouragement and support during my studies.

It is also a complete privilege to be a member of the great family of King Fahd University of Petroleum & Minerals which did not only award me with my Bachelor and Master degrees but also endowed me with the valuable gift of knowledge. Finally, I would like to thank my employer and sponsor, Saudi Aramco for its support, patience, and for providing me with such a great opportunity to continue my education.

TABLE OF CONTENTS

LIST OF FIGURES

LIST OF TABLES

LIST OF ABBREVIATIONS

H	Horizontal
ML	Multilateral
AI	Artificial Intelligence
ANN	Artificial Neural Network
FL	Fuzzy Logic
DT	Decision Tree
SVM	Support Victor Machine
Q_o	Oil flow rate
ΔP	Differential Pressure
B_o	Formation Volume Factor
h	Reservoir Thickness
J_o	Productivity Index
K	Permeability
μ_o	Oil Viscosity
S	Skin Factor
L	Horizontal Length
L_e	Effective Horizontal Length
r_e	Boundary Radius
r_w	Wellbore Radius
R^2	Coefficient of Determination
AAPE	Average Absolute Percentage Error
CC	Correlation Coefficient

ABSTRACT

NAME OF STUDENT	:	Ali Salman Al-Mashhad
TITLE	:	Horizontal & Multilateral wells' Performance Prediction in Undersaturated Reservoirs
MAJOR FIELD	:	Petroleum Engineering
DATE OF DEGREE	:	December 2018

Horizontal & multilateral (H & ML) wells are advance revolution transformation of vertical wells. The capitalization on these complex wells has many advantages, such as ensuring higher drainage and productivity of reservoirs, minimizing gas and water coning, achieving high productivity in a confined space and improving areal and vertical sweep efficiency. The performance of oil and gas production in highly deviated wells are predicted by many methods that range from simple to sophisticated techniques.

In the literature, several correlations have been developed to estimate the performance of H & ML wells. Reservoir data are incorporated in these correlations to come up with a rigid estimation mechanism. These correlations, however, are giving errors when used to calculate the productivity of complex wells. Another powerful forecasting tool in petroleum engineering technology is the numerical simulation software. However, the modelling process with numerical simulator is time-consuming and necessitates expertise in dealing with the simulation program. One of the novel predicting approaches is the Artificial Intelligence (AI) tool that is capable of characterizing, quantifying and forecasting many parameters in different application within the petroleum engineering industry.

The development of AI models that are competent in predicting the H & ML wells' performance in many under-saturated reservoirs is presented in this study. Results were compared to previously published correlations that are widely used in estimating the performance of the complex wells. The comparison between both methods in reference to the actual field data was obtained in this research.

The final results showed that all AI models are capable to predict oil rate with errors less than the existing correlations. Artificial Neural Network (ANN) models offered the highest accuracy among the other AI techniques. The lowest Average Absolute Percentage Error (AAPE) value of 6.9% was obtained with ANN while the minimum value of AAPE in the corrections was 38% in reference to the actual oil rate. New empirical correlations from ANN were derived to predict oil flow rates in complex wells.

The new AI models will shorten the lengthy computational process encountered with reservoirs simulator. Moreover, they will efficiently evaluate the performance of the wells in a simple way with higher accuracy through utilizing surface and subsurface data for many wells drilled in distinct under-saturated reservoirs.

ملخص الرسالة

أسم الطالب : علي سلمان المشهد

عنوان الرسالة : تقدير أداء الابار الأفقية ومتعددة الأطراف في المكامن الغير مشبعة

التخصص : هندسة البترول

تاريخ التخرج : ربيع ثاني 1440 هـ

الآبار الأفقية والمتعددة الأطراف هي تحول ثوري متقدم في الآبار الرأسية. تتمتع هذه الآبار المتقدمة بميزات عدة مثل ضمان ارتفاع معدلات الصرف وإنتاجية الخزانات النفطية، التقليل إلى الحد الأدنى من إنتاج الغاز والماء المصاحبين، تحقيق إنتاجية عالية في مكامن ذات مسامية محدودة جداً، وتحسين كفاءة الازاحتين الرأسية والسطحية. يتم التنبؤ بأداء إنتاج النفط والغاز في مثل هذه الآبار المتقدمة من خلال العديد من الطرق التي تتراوح بين التقنيات البسيطة والمتطورة.

في الدراسات السابقة تم تطوير العديد من النماذج الرياضية والقياسية لتقدير أداء الآبار الأفقية والمتعددة الأطراف. يتم إدراج بيانات الخزان في هذه النماذج الرياضية بهدف التوصل إلى آلية تقدير دقيقة. ومع ذلك، فإن هذه النماذج تعطي أخطاء عند أستخدامها في حساب إنتاجية الآبار الافقية وذات الاطراف. يمكن كذلك التنبؤ وتقدير الانتاجية عن طريق برمجيات المحاكاة العددية. ومع ذلك، فإن عملية تصميم برامج المحاكاة تستغرق وقت طويل وتستلزم معرفة وقدرة عالية للتعامل مع برنامج المحاكاة. توفر تقنيات الذكاء الأصطناعي واحداً من أهم أساليب التبؤ الجيدة والواعدة التي لديها القدرة على قياس وتوقع العديد من المجالات المختلفة في صناعة هندسة البترول.

تم تطوير نماذج الذكاء الاصطناعى للتنبؤ بأداء الآبار الأفقية ومتعددة الأطراف في العديد من المكامن غير المشبعة في هذه الدراسة. تمت مقارنة النتائج التي تم الحصول عليها من نماذج الذكاء الصناعي مع النتائج التقديرية التي تم حسابها النماذج الرياضية التي تستخدم على نطاق واسع في تقدير أداء الآبار المتقدمة. تم الحصول على المقارنة بين الطريقتين بالرجوع إلى قياسات حقيقية في هذا البحث.

أظهرت النتائج النهائية أن جميع نماذج الذكاء الاصطناعي قادرة على التنبؤ بمعدل الزيت مع وجود أخطاء أقل من جميع النماذج الرياضية الموجودة. كما قدمت نماذج الشبكات العصبية الاصطناعية أعلى دقة بين تقنيات الذكاء الاصطناعي الأخرى. حيث أشارة النتائج إلى أن نماذج الشبكات العصبية الاصطناعية تعطي أدنى خطأ للنسبة المئوية المطلقة بنسبة 6.9٪ مقارنة بالمعادلات الرياضية التي تعطي أقل خطأ للنسبة المئوية المطلقة بنسبة 38٪ مقارنة إلى قياسات أنتاج حقيقية. تم عمل نماذج رياضية جديدة من خلال الشبكة العصبية الاصطناعية والتي سوف تساعد على تقدير معدل تدفق النفط في الآبار شديدة التعقيد.

ستعمل النماذج الرياضية الجديدة على تقصير العملية الحسابية المطولة التي تُواجه خلال أعداد برمجيات المحاكاة العددية. علاوة على ذلك، سوف تقوم النماذج بتقييم أداء الآبار بكفاءة وبساطة عالية من خلال استخدام البيانات السطحية والجوفية للعديد من الآبار التي تم حفرها في خزانات معقدة غير مشبعة.

Chapter 1

INTRODUCTION

1.1 Background

Horizontal & multilateral (H & ML) wells are a revolutionary transformation of vertical wells. They are considered to be a magnificent contribution to the oil industry, since 1990s. The implementation of these techniques allows higher drainage of reservoirs utilizing diverse configurations. Also, they help in increasing the production of producible reserves by combining multiple targets which are separate uneconomic, achieving high productivity in a confined space limited with vertical wells, improving areal and vertical sweep efficiency, and reduce gas and water handling costs through minimizing gas and water coning. These wells are also superior to vertical wells in reservoirs with geological obstacles that are influencing vertical drilling. Reservoirs with large conductive faults in which the water cut is relatively high would have higher productivity indices if they drilled as H or ML wells. This will reduce the water flooding effects as well. However, these wells cost more than typical vertical wells, due to higher capital and operational expenditures. The general schematic of a typical H and vertical wells are illustrated in **Figure 1.1**. With the increasing demand of oil and gas, enhancing the productivity of oil reservoirs is very critical to make field development a worthwhile investment. Meanwhile, emphasis is currently being placed on the use of multilateral fishbone wells in tight (low permeable) and thin layered formations, fractured reservoirs, heavy oil reservoirs, and mature fields.

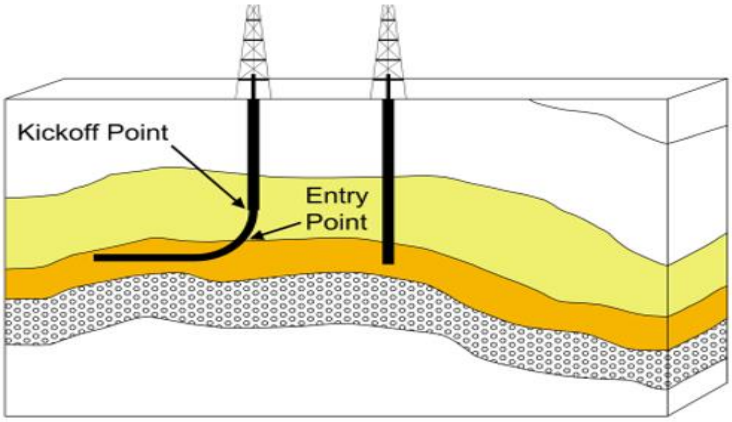

Figure 1.1: Schematic of Vertical & Horizontal Wells (Lynn 2011)

Based on The Technical Advancement of Multilaterals Group (TAML), a ML well is defined as: “Wells having one or more branches (laterals) tied back to a mother wellbore, which conveys fluids to or from the surface. ML fishbone wells technology provide significant leverage where conventional vertical wells cannot efficiently maintain a profitable development. The branch or lateral may be vertical or any inclination up to or greater than H” (2002). Hence, saving in the capital expenditure will be achieved with ML wells through minimizing the drilling & operating number of wells and facilities constructions. **Figure 1.2 & 1.3** shows the different types of ML wells and their complex deviations in reservoirs.

The success of the H & ML wells depends on well geometry, completion type, downhole equipment used, and junction selection. Geology, geometry, and production are the three main factors to design these wells. The well geometry and completion type depend essentially on the lithology and reservoir parameters, such as the number of pay zones, reservoir size, drive mechanism, vertical permeability, and fluid properties. Targeted production and estimated reserves dictate the size of the well to ensure that recovery can pay for such an expensive well.

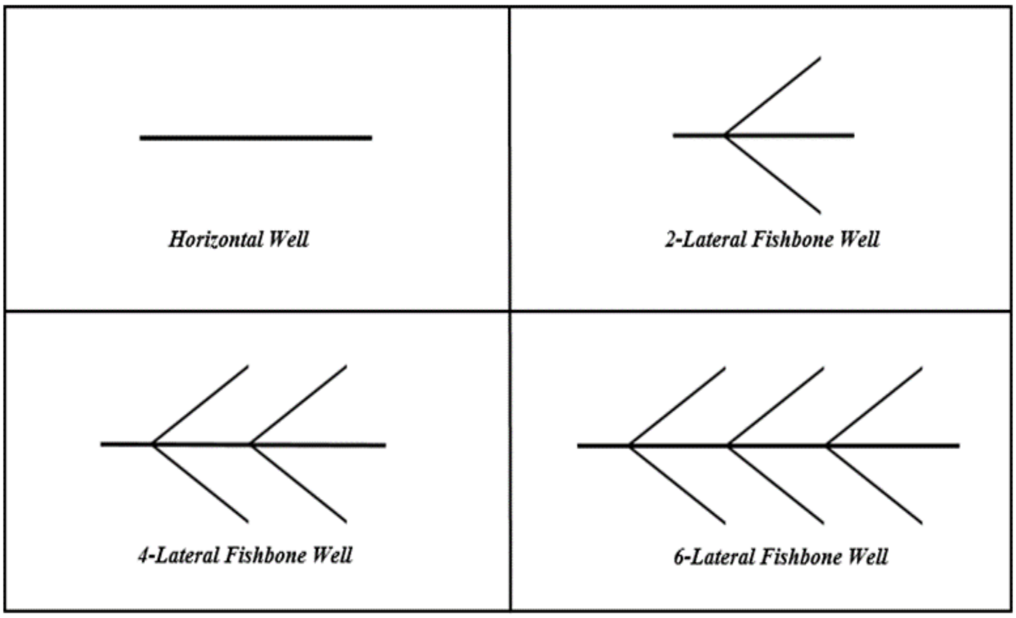

Figure 1.2: Complex Wells Configurations (TAML, 2002)

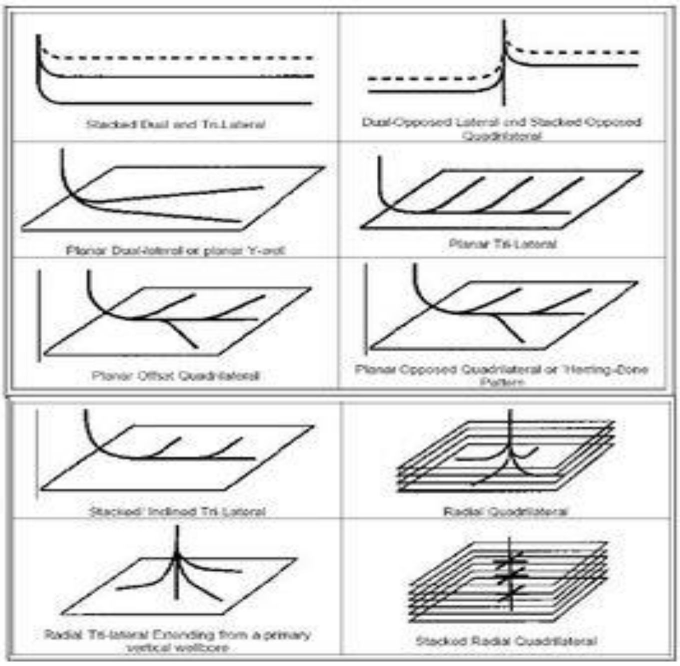

Figure 1.3: Multilateral well Configuration Types (TAML, 2002)

Inflow performance relationship for H & ML wells is influenced mainly by wellbore's rock and fluid characteristics. There are various methods to evaluate H & ML well performance such as: cross-sectional area, formation anisotropic properties (heterogeneity) and formation thickness.

Exploration, development, and production of oil and gas fields are all based on data acquisition processes. Geologist, geophysicist, and petroleum altogether rely on the data gathered from the sampling of rocks, seismic surveys, logging, and well testing operations in basic leadership handle. In any case, considering the physical necessities, time, and expenses of such field operations, procuring more information for reservoir simulation, drilling operation, well stimulation, and different purposes should be monetarily legitimate. Thus, engineers are regularly challenged to make the most out of the information officially gathered. One of these important factors that should be quantified regularly is the production performance of the wells in term of oil productivity especially on complex configurations which cost more than traditional vertical wells.

1.2 Statement of the Problem

Many correlations were derived based on inflow and outflow performance. The fundamental of these correlations are Dary law which simply estimates the productivity of vertical wells. However, applying these correlations to calculate the productivity of highly deviated wells like H & ML wells are associated with high uncertainties due to their well geometry and complex flow pattern.

Reservoir simulation is a very powerful tool used to ensure a sound decision-making process. It is used to forecast the reservoir performance and evaluate the productivity of the wells. It can model primary, secondary, and enhanced hydrocarbon recovery processes in complex heterogeneous, dual porosity and dual permeability reservoirs. Simulation results are used in economic studies to evaluate the validity of developing a specific field or use of complex well completions. However, the challenge with the reservoir simulation is related to its tedious process that requires highly skilled expedite and powerful computational capabilities.

Artificial Intelligence (AI) techniques have proven its capability to predict various parameters associated with high uncertainties in the oil industry. It employs simple math functions into a pattern recognition process to solve complex problems. The use of AI eliminates the need for excessive computations and time consumptions.

1.3 Thesis Objective

The objective of this research is to forecast production performance in term of oil flow rates in H & ML wells with high accuracy through utilizing different AI models. Actual data including reservoir parameters, well configurations, fluid properties and rate tests measurements will be collected from different under-saturated reservoirs. The obtained data will be applied to many well-known correlations available in the literature to estimate the oil flow rates of complex wells. The forecasted results from the AI models and the estimated results from the published correlations will be compared to the actual oil rate measurements. Rigorous statistical error analyses will be obtained. New empirical correlations from AI will be derived for future industry utilization to predict oil rates in highly deviated wells.

1.4 Approach

In this research, four efficient AI techniques have been implemented using Matlab software to develop many AI models for predicting oil flow rates for H wells, ML wells and combination of H & ML wells. The actual data were gathered from many fields including surface and subsurface measurements. Many scenarios with different input data combinations were faded to AI to come up with optimum models for estimating surface oil flow rates as a target. Statistical and graphical analyses were conducted to compare the results obtained from AI models and published correlation against the actual oil rates. The model with the lowest absolute relative error percentage was recommended for industry use. New correlations from ANN modelling were obtained.

1.5 Thesis Organization

The Thesis is divided into six chapters arranged as follows:

- **Chapter 1:** Introduction, Problem statement, Objective and Approach of the research
- **Chapter 2:** Literature review on existing productivity correlations for H & ML well and highlight relevant studies done with AI techniques.
- **Chapter 3:** Overview of the AI techniques implemented in this research.
- **Chapter 4:** Methodology followed in this study.
- **Chapter 5:** Data preparation & developed models, results comparison statistically and graphically and derives new empirical correlations.
- **Chapter 6:** Conclusions and recommendations.

CHAPTER 2

LITERATURE REVIEW

In this chapter, there are two sections, which are: Productivity correlations of H & ML wells, and the application of AI in oil and gas industry.

2.1 Productivity Correlations

After a broad literature review, estimation of the productivity index (PI) or inflow performance relationships (IPR) are obtained based on wells' configurations, fluid phase and time dependence. Many of the studies conducted for evaluating the performance of H & ML wells and came up with analytical correlations.

There are many correlations derived based on infinite drain hole conductivity of single phase in complex well configurations. They are widely adopted in the petroleum industry since they are easy to use through applying simple math with certain field and well data. The main source of errors with these correlations is that they are giving an over-estimation of well productivity since they ignore friction losses. However, petroleum engineers applied them to obtain a quick estimation of well productivity. Some well-known correlations in the literature were done by: Borisov (1984), Joshi (1988), Renard (1990), Economides (1994), Butler (1994), Furui (2003) and Escobar (2004). All the correlations were rearranged to be in the form of oil flow rates in this research and will be applied to a single oil phase reservoir, H & ML wells configurations at steady state conditions. A thorough analysis of these correlations with real field data to estimate the flow rates is presented in this thesis.

Darcy law has been used for a century to estimate flow rates in steady state condition for vertical well configuration. Direct application of Darcy low to calculate oil flow rates in H and/or ML wells is giving ambiguous results.

Darcy equation is given in the following form:

$$Q_o = J_o \Delta P = \frac{Kh\ \Delta P}{141.2 B_o \mu_o \left[\ln(\frac{r_e}{r_w})\right] + S} \tag{2.1}$$

Where:

Q_o: Oil flow rate, BPD

J_o: Productivity index, BPD/psia

ΔP: Differential Pressure, psia

K: Permeability, ft

B_o: Formation volume Factor

h: Reservoir thickness, ft

μ_o: Oil Viscosity, cp

S: Skin factor

r_e: Boundary Radius, ft

r_w: Wellbore Radius, ft

2.1.1 Analytical Correlations

Eight analytical productivity correlations have been used in this research for estimating oil flow rates in H & ML wells. Actual field data have been utilized to validate in practical the estimation accuracy of these correlations.

In superior of the analytical flow & productivity models, **Borisov (1984)** introduced one of the earliest models for oil production using H & ML wells with assuming a constant drainage pressure and single phase oil reservoir.

Borisov correlation for H wells (Equation-2.2):

$$Q_o = \frac{K_h h\ \Delta P}{141.2 B_o \mu_o * \left(\ln\left(4\frac{r_e}{L}\right) + \frac{h}{L}\ln\left(\frac{h}{2\pi r_w}\right)\right)} \tag{2.2}$$

Where:

L: Horizontal Length, ft

K_h: Average horizontal Permeability, md

Borisov's correlation for ML wells (Equation-2.3):

$$Q_o = \frac{K_h h \, \Delta P}{141.2 B_o \mu_o * \left(\ln\left(F \frac{r_e}{L}\right) + \frac{h}{n\,L} \ln\left(\frac{h}{2\pi r_w}\right) \right)} \tag{2.3}$$

Where:

F is 4, 2, 1.86, 1.78 for n=1, 2, 3, 4, respectively.

Joshi (1988) proposed a new correlation on H wells performance estimation at steady state condition on a single phase well. **Joshi correlation is (Equation-2.4):**

$$Q_o = \frac{K_h h \, \Delta P}{141.2 B_o \mu_o * \left(\ln\left[\frac{a + \sqrt{a^2 - \left(L/2\right)^2}}{\left(\frac{L}{2}\right)}\right] + \left(\frac{I_{ani}\, h}{L}\right) \ln\left(\frac{I_{ani}\, h}{2 r_w}\right) \right)} \tag{2.4}$$

Where:

$$a = \frac{L}{2} \left\{ 0.5 + \left[0.25 + \left(\frac{r_e}{L/2} \right)^4 \right]^{0.5} \right\}^{0.5}$$

$$I_{ani} = \sqrt{\frac{k_h}{k_v}}$$

Renard et al. (1990) presented a correlation for calculating the productivity on a steady state of anisotropic reservoir on H well configurations. **The Renard correlation is (Equation-2.5):**

$$Q_o = \frac{K_h h \, \Delta P}{141.2 B_o \mu_o} \left[\frac{1}{\cosh^{-1}(x) + \left(I_{ani}\, h / L \right) \ln\left[h / 2\pi r'_w \right]} \right] \tag{2.5}$$

Where:

$$r'_w = \frac{1+I_{ani}}{2\,I_{ani}} r_w$$

$$I_{ani} = \sqrt{\frac{k_h}{k_v}}$$

$$x = \frac{2a}{L}$$

$$a = \frac{L}{2}\left\{0.5 + \left[0.25 + \left(\frac{r_e}{L/2}\right)^4\right]^{0.5}\right\}^{0.5}$$

Economides at al. (1994) derived an analytical formula to assess the well performance of H wells on arbitrary direction which is applicable for transient, mixed and no flow boundary conditions. **Economides correlation is (Equation-2.6):**

$$Q_o = \frac{K_h h\,\Delta P}{141.2 B_o \mu_o \left(\ln\left\{ \frac{a + \sqrt{a^2 - \left(\frac{L}{2}\right)^2}}{\left(\frac{L}{2}\right)} \right\} + \left(\frac{I_{ani} h}{L}\right)\left\{ \ln\left(\frac{I_{ani}\,h}{r_w(I_{ani}+1)}\right) + S \right\} \right)} \qquad (2.6)$$

Where:

$$I_{ani} = \sqrt{\frac{k_h}{k_v}}$$

$$a = \frac{L}{2}\left\{0.5 + \left[0.25 + \left(\frac{r_e}{L/2}\right)^4\right]^{0.5}\right\}^{0.5}$$

$$L/2 < 0.9\, r_e$$

Butler et al. (1994) used a box-shaped reservoir to develop an IPR model to predict the PI for H wells. **Butler correlation is (Equation-2.7):**

$$Q_o = \frac{k\,L\,\Delta P}{141.2 B_o \mu_o * \left(I_{ani} \ln\left[\frac{h\,I_{ani}}{r_w\,(I_{ani}+1)}\right] + \left(\frac{Y_b\,\pi}{h}\right) - 1.14\, I_{ani} \right)} \qquad (2.7)$$

Where;

$$K = \sqrt{K_h K_v}$$

$$Y_b = 400$$

Furui et al. (2003) presented an IPR model for H wells that assumed the flow regime is linear away from wellbore while it radial near the wellbore. **Furui Correlation is (Equation-2.8):**

$$Q_o = \frac{k\, L\, \Delta P}{141.2 B_o \mu_o * \left(I_{ani} \ln\left[\frac{h\, I_{ani}}{r_w\,(I_{ani}+1)}\right] + \left(\frac{Y_b\, \pi}{I_{ani}\, h}\right) - 1.224 + S \right)} \quad (2.8)$$

Where;

$K = \sqrt{K_h K_v}$

$Y_b = 400$

Escobar et al. (2004) presented a modified model of Joshi correlations for H wells productivity calculation. Based on using the regression, two constant numbers were incorporated to the correlation. **Escobar correlation is (Equation-2.9):**

$$Q_o = \frac{K_h\, h\, \Delta P}{141.2 B_o \mu_o * \left(\operatorname{Cosh}^{-1}\left[1.075 \left(0.5 + \sqrt{0.25 + \left(\frac{2\, r_e}{L}\right)^4} \right) \right]^{0.5} + 0.874 \left(\frac{h}{L}\right) \ln\left(\frac{h}{2 r_w}\right) \right)} \quad (2.9)$$

In the literature, there are also numerical models done based on simulation software for estimating the productivity of the wells. These models are rigorous in field applications, but need skilful personnel to use them. Another challenge with the numerical software is that they costly and time consuming. Some studies conducted on well and reservoir performance evaluation with numerical models are: Folefac et al. (1991), Seines et al. (1993), Su & Lee (1998), Siu & Subramanian (1995), Yuan et al. (1998), Ouyang et al. (1998), Ouyang & Huang (2005) and Guo et al. (2006).

2.2 Application of Artificial Intelligence in the Oil and Gas Industry

Artificial Intelligence (AI) applications are widely used in engineering, science, business, and many other fields. Implementation of AI has provided the ability of learning, pattern recognition, real-time data processing, data clustering, correlation, and optimization. Joined with advanced computation tools, AI is able to solve many complex problems in a much shorter time than they formerly required. Consequently, the use of AI tools in the oil and gas industry has increased tremendously since the late eighties. In particular, its application showed a huge success in areas of drilling, reservoir simulation, well testing, and enhanced oil recovery.

2.2.1 Relevant Case Studies with Artificial Intelligence models

Boomer (1995) built a neural network model to forecast production profile for vertical wells drilled in Vacuum Field that was discovered in New Mexico City. Real Production data including oil & water rates, percent oil, injection rate, and injection withdrawal ratio for both current and cumulative rate bases were collected from 250 wells. All the data were used as an input for the model while the cumulative production volume was used as an output to be predicted for the newly proposed drilling wells. Data from 164 wells were used for network training process. The remaining data from 86 wells were utilized to test and verify the accuracy of the model. The final results showed that the model was underestimating the actual production with a deviation of 39%. He presumed that lack of geological/geophysical data as an input is the main reason for this uncertainty in the prediction of the cumulative production with AI modelling.

Okazan, et al. (1998) analysed the effect of design parameters of dual-lateral wells on pressure transient behaviour in oil reservoirs with employing AI. Parameters including lateral lengths, phase angle between the laterals & motherboard, and H and vertical separation between laterals were used. They observed that the pressure drop decreases as the phase angle increases. Also, they noticed that drilling a wider H separation between laterals will increase the drainage area of the well and hence, dimensionless pressure decreases. On the other hand, the study heightened that the influence of the vertical separation between the laterals is negligible, especially for long production intervals.

Weiss at al. (2002) applied fuzzy ranking and neural networks modelling for predicting oil production. The fuzzy rank tool was employed in his study to filter out the noisy data and select the related input variables from 34 wells from a field located in the New Mexico. The neural networks were built initially to predict secondary to primary ratio of water flooding in that field. Moreover, the model was used to generate pseudo-bulk volume oil logs from conventional logs run in the 34 wells. The oil rates of the first year for the wells were then predicted from the pseudo-bulk volume. With applying the models, they were able to reduce the errors with large data sets obtained from the actual well logging.

Yeten et al., (2003) applied a genetic algorithm combined with an Artificial Neural Network (ANN), a hill climber, and an up scaling method to optimize the non-conventional well type, configuration, and location. The objective of the study was to find maximum cumulative production or net present values (NPV) for wells completed in different reservoir conditions with varying fluid properties. The genetic algorithm was the main optimization tool used in the developed approach, while the ANN was used to mimic the numerical simulator in order to analyse a wide range of scenarios. The hill climber and up scaling procedure were used to improve the solution and accelerate the convergence of the finite-difference iterations.

Alkhalifah et al. (2009) developed ANN models to predict flow rate and choke size with using 4031 data sets points. The final results showed that developed models were providing errors less than existing correlations. The average absolute error were 3.7% and 6.7% for predicted choke size and flow rates respectively.

Alarfaj et al. (2012) utilized 4 different AI methods to estimate production rate for each layer in multi-layered gas reservoirs from four fields. The data were collected from 100 wells from well logging and pressure data. The overall results showed that the normalized Support Vector Machine (SVM) Model had performed the best with a mean absolute error of 2.25% comparing with other AI models. The accuracy of the model can be improved by adding additional samples that cover a wider range of the data.

Olivares et al. (2012) developed a workflow that combines AI techniques with nodal analysis to process and understand the production behaviour and validate well testing for oil wells. The models were generated from actual measured data obtained from operating conditions, well testing data history and other data set such as estimated flow rate from correlations. Three case studies were done with AI for (1) estimate flow rates using operating condition and well testing, (2) estimate flow rate using nodal analysis, operational conditions and wells testing, and (3) estimate volume in transfer pipeline using high-frequency data. The overall accuracy of the models was reaching around 90% compared with the actual data.

Almousa et al. (2013) presented an approach that successfully delivers a total of five distinct artificial expert systems in areas of production forecasting, ML well design, and reservoir evaluation in shale gas reservoirs. The developed toolbox consists of three expert systems that serve as proxies to simulators by predicting cumulative oil and gas productions, estimating the end of plateau and abandonment times, and forecasting cumulative fluid production. Furthermore, the fourth and fifth expert systems covered single phase gas reservoirs with dual-lateral wells and stacked ML (up to five laterals) wells completed within different reservoirs properties.

Alajmi et al. (2015) conducted a study to predict choke performance and well testing validation using ANN. From 595 actual data sets for 31 wells, they calculated critical and subcritical multiphase choke performance using five existing correlations and model the choke performance with ANN to predict the rate. Comparing the estimated and predicted results against actual values, ANN has the least absolute error percentage which proves its reliability and accuracy in predicting the choke performance in order to estimate the oil flow rate as a function of choke size and operational condition.

Alarifi et al. (2015) presented a study to predict the productivity index for a hundred oil H wells using different AI techniques including ANN, fuzzy logic (FL) and functional network (FN). The results showed that AI models have less errors than the existing correlations in estimating the productivity index, which proves its reliability as a powerful prediction tool.

Chukwuka et al. (2017) created a set of artificial expert models to predict the performance of advanced well structure in tight oil reservoirs. Synthetic data from commercial numerical simulator were utilized to build the neural network system. The input data fed into the models includes reservoir data, rock and fluid properties, relative permeability, capillary pressure data and well design and operating condition data for wide range data sets. The output targets from the systems were cumulative oil, water, gas production as well as bottom hole pressure profile. The final expert systems were giving an average mean absolute error of 8% compared with the results obtained from the numerical simulator for the same data sets.

Zeechan (2018) presented an new empirical model with ANN to forecast the flowing bottom hole pressure in verticals wells with using surface production data. In the study, 206 data points have been used with applying nine input parameters including oil, water and gas rate. The results showed that ANN model was offered an AAPE of 2% while existing correlations gave an AAPE of 15%.

CHAPTER 3

ARTIFICIAL INTELLIGENCE

This chapter will illustrate the definition of the Artificial Intelligence techniques used in the petroleum industry and have been applied in this research.

3.1 Background of Artificial Intelligence

Artificial Intelligent (AI) is the state-of-art system which has many definitions by scientists and engineers started back in 1945. Two definitions of which AI are clearly defined at the desired interest. Haugeland (1985) defined AI as “The exciting new effort to make computers think, machine with minds, in the full and literal sense.” Partridge (1991) has defined AI as “a collection of algorithms that are computationally tractable, adequate approximations of intractably specified problems.” AI can sometimes simulate human intelligence through solving problems by observing other parameters utilizing new methods or approaches. One of the approaches to perform and design AI is to define certain agents for a specific problem. In which specific inputs that are related to one single aspect can be integrated to solve the problem. In order to design the AI model, four components to define a specific agent shall be quantified which are: precepts, actions, goals and the environment.

3.2 Artificial Intelligence Techniques

In this research, four AI techniques will be implemented which are Artificial Neural Network (ANN), Fuzzy Logic (FL), Decision Tree (DS) and Support Vector Machine (SVM).

3.2.1 Artificial Neural Network

Following section will discuss the Artificial Neural Network (ANN) in detail.

A) History

The modern concept of ANN started by the work of Warren MaCulloch and Walter Pitts in 1940s, when they proved ANN could in principle compute arithmetic or logical functions. It was in the late 1950s when the first application of ANN came to life. This happened with the invention of perceptron network along with learning rule by Frank Rosenblatt. He and his contemporaries illustrated the ability of perceptron networks to perform pattern recognition, but unluckily this network had its limitations. These limitations discouraged others who started to believe that research on ANN had reached a dead end. Besides, computers at that time were not powerful and hence ANN research was mostly suspended. Fortunately, in 1980s a dramatic increase has occurred to the computational capabilities of computers which in turn overcame the main obstacle facing ANN. Two new concepts which brought these networks back to life. First was the use of statistical mechanics, which explained the operation of certain class of current networks. Second and the key improvement of the 1980s was the back propagation algorithms discovered by David Rumelhart and James MaClelland. Nowadays, ANN has invaded all fields, because of their ability to solve problems in many areas in life, including the petroleum engineering industry. This expansion of the use in ANN is a result of current fast computers which made it possible to solve complex problems that formerly required too much time and computations.

B) Artificial Neuron

ANN is a model which works similarly to a human biological neural network. The biological neural network basic building block is neurons. Similarly, the ANN has an artificial neuron as its basic building component as shown in **Figure 3.1**.

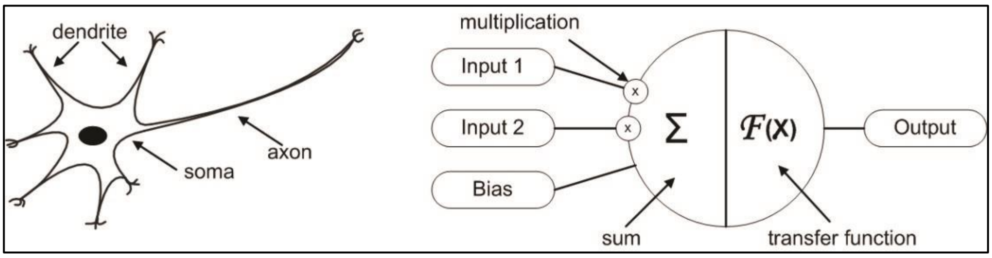

Figure 0.1: Biological Neuron vs Artificial Neuron (Robert 2011)

At the beginning of an ANN, the inputs are given to the artificial neuron after being multiplied by initial weights. The neuron then sums the weights of all inputs and bias. The sum is passed through an activation function or what is also called a transfer function. These working principles and simple mathematical calculations become powerful and more useful when the neurons start to interconnect forming an ANN (**Figure 3.2)**. Although, it uses simple math, but it can solve complex problems with the fact that complexity can grow from just a few basic rules through hidden layers between inputs and outputs as shown in **Figure 3.3**.

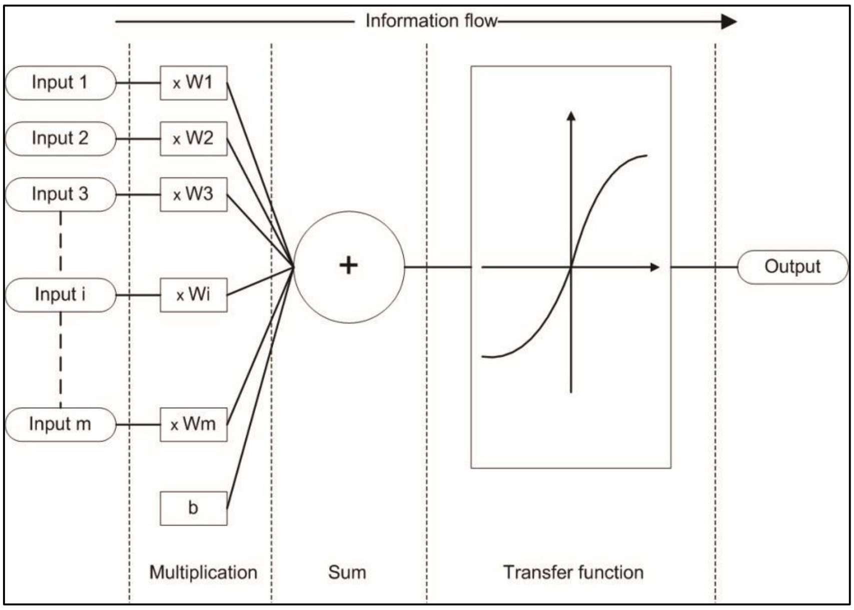

Figure 0.2: Working principle of an ANN (Robert 2011)

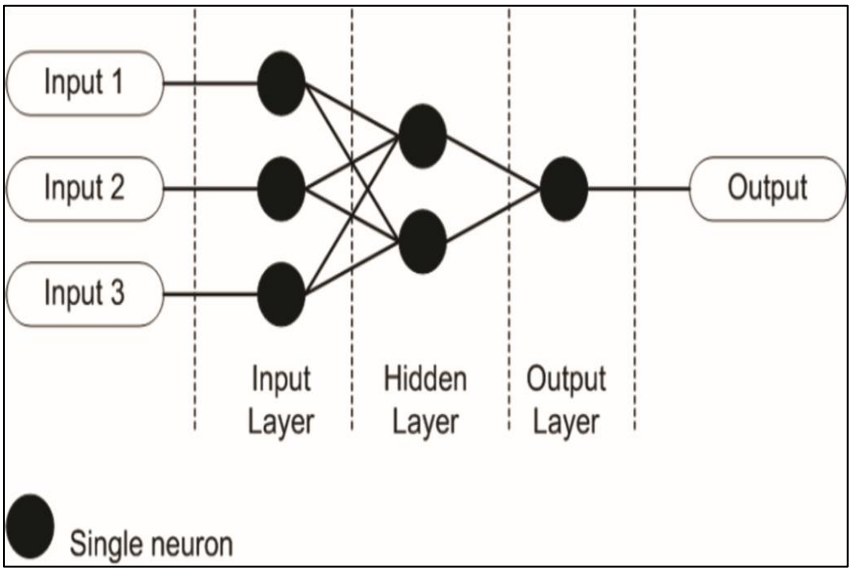

Figure 0.3: Hidden Layers in Simple ANN (Demuth 1995)

Now, to understand the benefit of the mathematical complexity achieved by interconnecting the individual artificial neurons, it is important to understand how these neurons are connected especially they are not interconnected randomly. The first step is to choose the appropriate topography for the problem being solved then manipulate it in order to get better results. After that, it is followed by teaching the network on a set of data representing a given problem. After completing the training of the network along with the manipulation of the chosen topography, the network is ready to be used. Similar to a biological neuron, ANN receives the information from inputs that have weights and bias. The neuron sums the weights and bias then process them via the transfer function and presents them as an output.

C) Transfer Function

Transfer functions are used to explain the mathematical properties of ANN function (**Table 3.1**). The functions are selected upon the problem being evaluated. For this research, all the transfer functions have been applied to the data sets and found that the Hyperbolic Tangent Sigmoidal was giving lower error than other activation functions.

Table 0.1: Transfer Functions (Chidambaram, 2009)

Name	Input/Output Relation	Icon	MATLAB Function
Hard Limit	$a = 0 \quad n < 0$ $a = 1 \quad n \geq 0$		hardlim
Symmetrical Hard Limit	$a = -1 \quad n < 0$ $a = +1 \quad n \geq 0$		hardlims
Linear	$a = n$		purelin
Saturating Linear	$a = 0 \quad n < 0$ $a = n \quad 0 \leq n \leq 1$ $a = 1 \quad n > 1$		satlin
Symmetric Saturating Linear	$a = -1 \quad n < -1$ $a = n \quad -1 \leq n \leq 1$ $a = 1 \quad n > 1$		satlins
Log-Sigmoid	$a = \frac{1}{1 + e^{-n}}$		logsig
Hyperbolic Tangent Sigmoid	$a = \frac{e^{n} - e^{-n}}{e^{n} + e^{-n}}$		tansig
Positive Linear	$a = 0 \quad n < 0$ $a = n \quad 0 \leq n$		poslin
Competitive	$a = 1$ neuron with max n $a = 0$ all other neurons	C	compet

D) Neurons Layers

ANN can have a single layer of neurons or multiple layers based on the problem being solved (**Figures 3.4 & 3.5**). The number of layers and neurons in each layer are chosen by the user. Each layer will have its own set of parameters including: weight matrix, summation and transfer function.

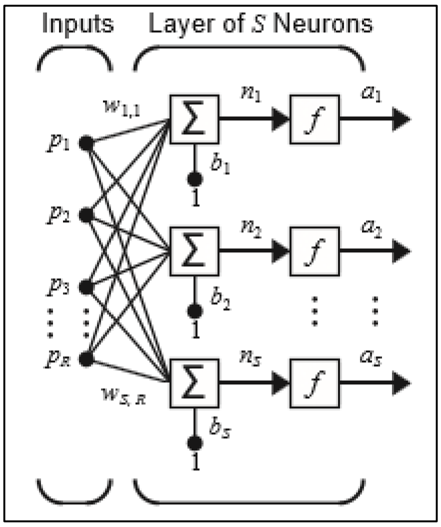

Figure 0.4: One Layer Network (Hagan, 2002)

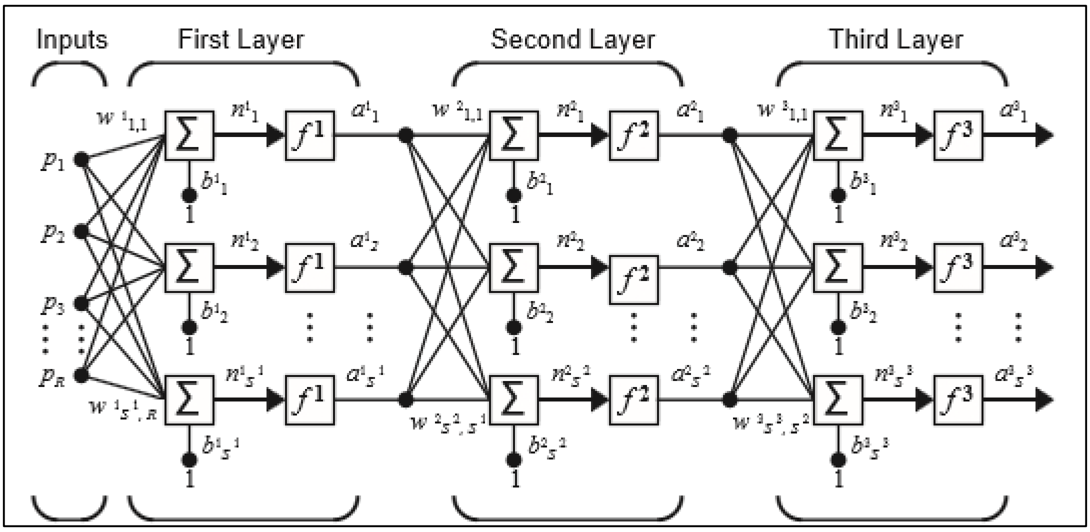

Figure 0.5: Multi-layer network (Hagan, 2002)

ANN can be classified into many models. Two of the most common networks used in engineering practices are feed forward back-propagation and cascade back-propagations networks. The feed forward back-propagation network consists of a back-propagation learning algorithm, input, hidden, and output layers. In this forward network, the flow of learning is from input to the neurons in the hidden layer and then to the output (**Figure 3.6**). Another method is the Cascade forward back-propagation model which is working based a weight connection from the input to each out layer and from each layer to the proceeding layers

(**Figure 3.7**). Back-propagation means that the error is calculated at the output and then the initial weights are updated accordingly.

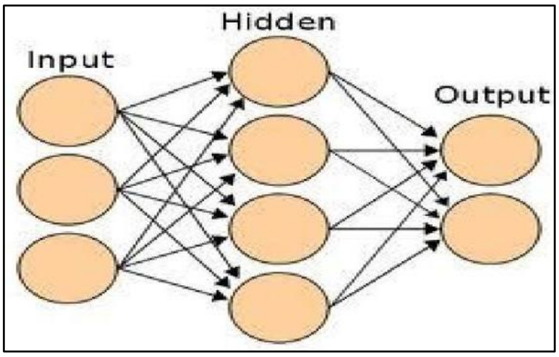

Figure 0.6: Feed Forward Network (Badde 2011)

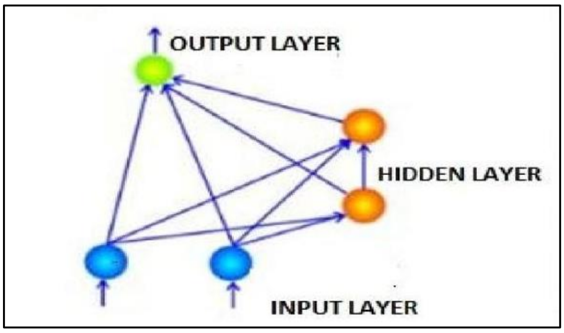

Figure 0.7: Cascade Network (Badde 2011)

E) Training Functions

On modelling ANN, there are many training functions to choose from (**Table 3.2**). Based on previous studies, “trainscg” and “trainrp” are fast, efficient and do not easily memorize the given data set. There are other learning algorithms in MATLAB that are compatible with the back-propagation. In this study, “trainlm” and “trainscg” were giving the best forested results. All the ANN algorithm applied in this thesis are presented in **Table 3.3**.

Table 0.2: Training functions (Demuth 2009)

Function	Algorithm
trainlm	Levenberg-Marquardt
trainbr	Bayesian Regularization
trainbfg	BFGS Quasi-Newton
trainrp	Resilient Backpropagation
trainscg	Scaled Conjugate Gradient
traincgb	Conjugate Gradient with Powell/Beale Restarts
traincgf	Fletcher-Powell Conjugate Gradient
traincgp	Polak-Ribiére Conjugate Gradient
trainoss	One Step Secant
traingdx	Variable Learning Rate Gradient Descent
traingdm	Gradient Descent with Momentum
traingd	Gradient Descent

Table 0.3: Training Functions Applied in the Research

Function	Definition
Trainlm	Mathematical optimization technique to solve non-linear least square curve fitting problems. It is used to update weights and biases during the learning process.
Traingd	It is applied on derivative functions through applying the gradient descent algorithm
traingdx	It is a combination of adaptive learning rate with momentum training.
trainbfg	It is using BFGS Quasi Newton method to update the weight and bias values. The previous trained epoch are used for the next epoch at the beginning.
trainscg	Updating Wight and bias on the learning process with application of Bayesian Regularization.
trainoss	Its working principle is based on the using of one step secant method to update weights and bias. It is using the roots of the lines to find the roof of a function.
Trainrp	Resilient Back propagation are used to update weight and bias values this technique
Trainbr	Updating Wight and bias on the learning process with application of Bayesian Regularization

3.2.2 Fuzzy Logic

Fuzzy Logic (FL) is another technique of AI models used in prediction and solving of complex problems with building models from inputs and outputs data sets. It is a logical system that extension of multivalued logic. FL is almost identical with the theory of fuzzy set in which it relates to classes of objects with unsharp boundaries. It is also widely used in the petroleum industry and other aspects of life. The operation principle of FL technique is based on decision making. As the name suggests, it is a model that is based on logic operations to make decisions for two options with outputs either TRUE with (0) value or FALSE with a value of (1). It is operating on the partial degree of truth which is located in between the two values 0-1. The main programing steps of it are: (1) Fuzzify the input values to fuzzy membership functions, (2) Execute the user-selected rules to compute fuzzy output functions and (3) De-Fuzzify the output to obtain real values. The two types of FL are Subtractive Gradient (Cluster radius) & Grid partitioning. Cluster radius is used for grouping the data by giving a membership degree for each data points. Centers of the clusters are updated with every iteration until a minimum distance is achieved between the centers and their data points. The cluster radius method has used in this research. The second technique in FL is Grid partitioning which is working by partitioning the input variable range to create a single output fuzzy system.

3.2.3 Decision Tree

The process of Decision Tree (DT) is using a branch series of Boolean tests to model the input data. The parameters of each decision point compose of Nodes, Actions, Choices and Paths. The nodes on the decision points are moving from one stage to another until achieving the target which is specified as a specific fact to predict the output.

3.2.4 Support Vector Machine

Support Vector Machine (SVM) is a learning algorithm used for solving mathematical and engineering problem with using regression analysis and classification. Its application showed success in many areas, such as bioinformatics and texting recognition. SVM is building of hyper-plane in an infinite dimensional space. It is using Kernel Neuron Functions which helps in solve complex problems. The data points lay close to hyper-plane are known as support vectors. These points are difficult to classify. Therefore, SVMs rule is to improve the margin around the separating hyper-plane. In the SVMs, a decision function is built with specified small training samples. The main issues with SVM include that the input data must be labelled and algorithms have to be applied to minimize the multi class task in several binary problems. Gaussian Kernel function which uses nonlinear separators is one of common methods used in SVM and has been applied in this study. It is transferring the input data to a point in an n-dimensional space. Other Kernel functions are Polynomial, Polyhomogenous and JCB kernel.

Figure 4.10 is showing all the AI techniques used in this thesis.

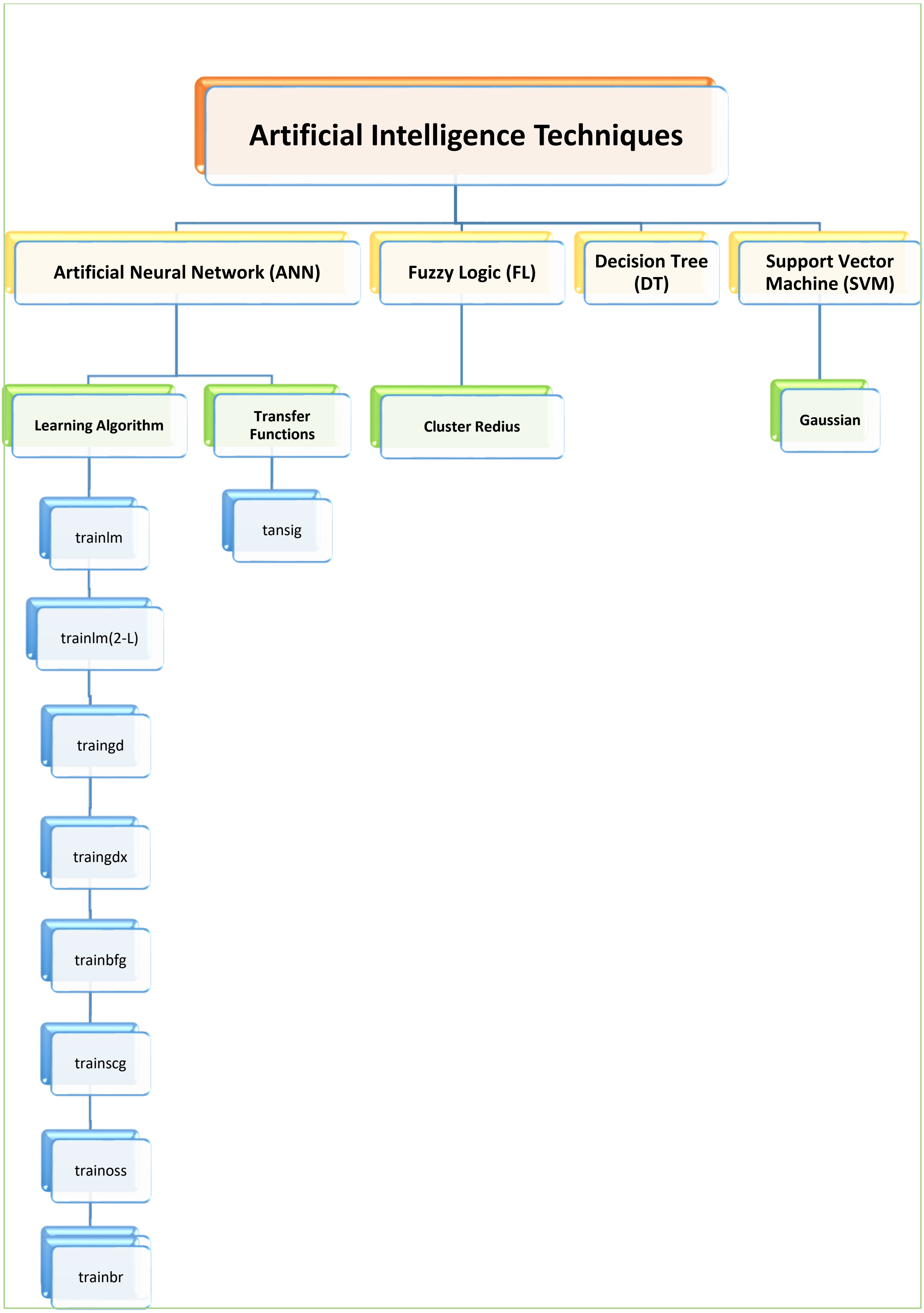

Figure 0.8: AI techniques implemented in the Research

CHAPTER 4

METHODOLOGY

This chapter will discuss the framework of the procedure followed in the thesis, for meeting the objective of this study. Data description and statistical analysis are also presented in this section.

4.1 Solution Procedures

To explore the potential of this research, which will lead to a cost optimization and acquiring full benefits of the available data for predicting performance of wells in a faster and easier way with higher accuracy, the below methodology will be followed:

- Gather relevant data from actual well testing measurements from many fields including: oil rate, water cut, gas oil ratio, upstream flowing wellhead pressure, downstream flowing wellhead pressure, ESP frequency and choke size.
- Collect reservoir fluid data that consist of oil viscosity and oil formation volume factor.
- Gather reservoir parameters including reservoir pressure, reservoir thickness, skin factor and average permeability.
- Obtain downhole parameters and well configurations that involve: flowing bottom hole pressure, number of laterals, effective horizontal lengths and hole diameters.
- Data preparation & processing for creating a data base.
- Estimate oil flow rate from several productivity correlations and compare the results with the actual measurement.
- Create AI models for H wells, ML wells and the combination of all data H & ML wells with the applying the following AI techniques:

  - Artificial Neural Network (ANN)
  - Fuzzy Logic (FL)
  - Decision Tree (DT)
  - Support Vector Machine (SVM)
- Analyse the output results to evaluate the best AI techniques.
- Populate a statistical and graphical error analysis of the results obtained from AI models & correlations and compare the results against the actual data.
- Come up with recommendation and conclusion with the most potential method for future application and utilization.

4.2 Selection of Independent Variables

To meet the objective of this research on accurately estimating oil flow rates of H and ML wells, thorough evaluations of many parameters from fields and wells were performed. Many independent variables were selected based on inflow performance equations with adding surface & subsurface parameters that proved in practical operations they have direct effect on wells performance.

4.3 Data Collections & Descriptions

The data used in this thesis were collected from 230 H and ML wells drilled in different under-saturated reservoirs from nine fields. The data were gathered from 180 H wells and 50 ML wells. The collected data are including surface & subsurface parameters, reservoir data and fluid properties.

Surface parameters were either collected from mechanical or electrical instrumentations like wellhead pressure, ESP frequency and choke size or obtained from measuring equipment namely 3-phase separators or multiphase flow meters (MPFM) for oil flow rates, water cut and gas oil ratio. The measured oil rates were calibrated from the field to surface conditions with PVT (Pressure, Volume and Temperature) data that were analysed at the laboratory. Downhole data like flowing bottom hole pressures were measured either through using temporary gauges carried downhole with wireline and lift at the well for certain time and then retrieved or with the application of permanent downhole gauges know are PDHM (Permanent downhole monitoring System) to measure downhole pressures and temperatures while the wells at the flowing conditions. Using similar measurement methods with keeping the well at shut in condition, reservoir pressures were estimated. Additional reservoir data such as reservoir thicknesses which were obtained from the well logging and horizontal average reservoir permeability were collected from all the wells. Well configurations parameters like number of laterals, horizontal lengths and hole diameters were acquired from drilling information. Deliverability tests were used to gathered skin factors. The fluid properties for all the different reservoirs in the nine fields were used to obtain oil formation volume factors and oil viscosities.

4.4 Data Analysis

In this part, a comprehensive statistical description of the data to understand each parameter was created. Statistical description of the data involves the following:

- **Correlation Coefficient (CC):** A statistical relationship between input and target parameters. Its' value is ranging between -1 to 1. As the value of CC reached 0, it indicates there is no or weak interrelationship between input and target parameters. On the other hand, a strong relationship between the two parameters as the CC approached -1 or 1. The equation of CC is given by:

$$cc = \frac{N\sum xy-(\sum x)(\sum y)}{\sqrt{N(\sum x^2)-(\sum y)^2}\ \sqrt{N(\sum b^2)-(\sum b)^2} \qquad (4.1)$$

Where:

N: Size of the data

x: Target Parameter

y: Input Parameter

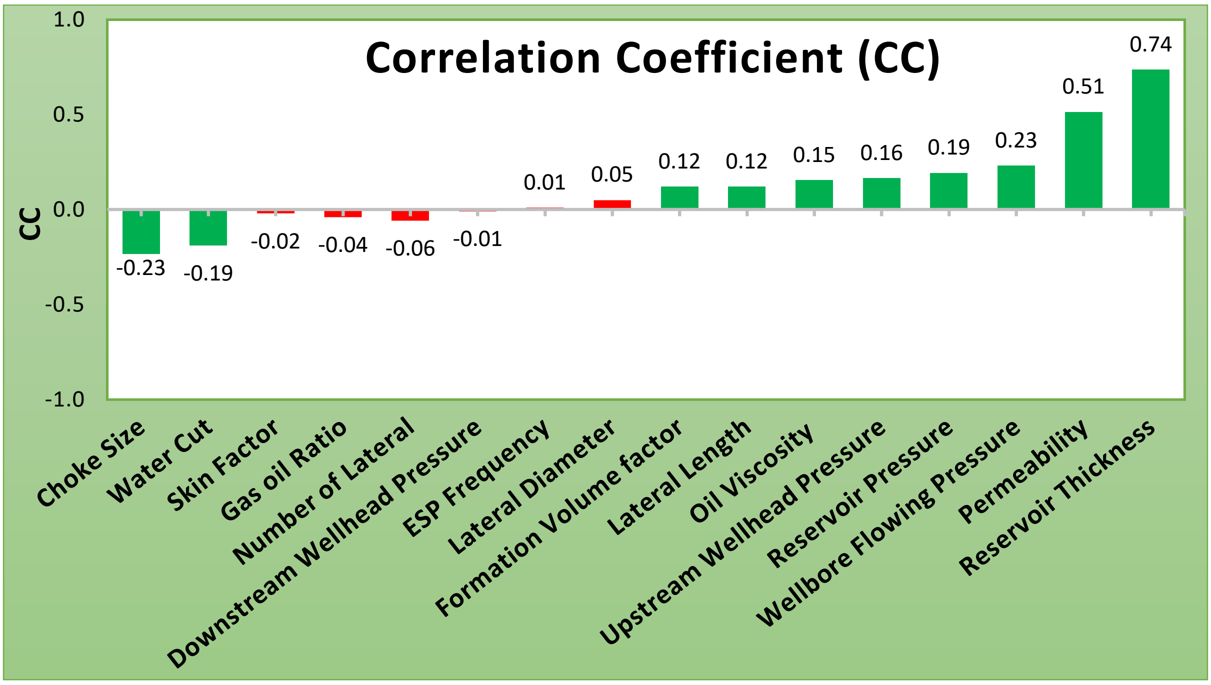

Figure 0.1: Relative Importance of Input Data

- **Minimum Value:** is the smallest values in each input and target parameters.
- **Maximum Value:** is the largest values in each input and target parameters.
- **Mean:** an arithmetic mean that is obtained by summation all the valves in each parameter and divided them by their total number. The form of arithmetic mean equation is:

$$\bar{x} = \frac{1}{n}\sum_{i=1}^{n} x_i \qquad (4.2)$$

- **Mode:** is the most frequently repeated number in each input and target parameter.

4.5 Data Preparations

One of the most significant step before feeding the input data to the AI models and helps in achieving well trained models with efficient target results is the data preparation and handling. Data handling steps involve transforming the input data into a suitable form like normalizing and rearranging them to fall within the same order of magnitude. The most prevalent normalization techniques in the mathematics is through applying the common logs which minimized the digest numbers. Likewise, normalizing the mean furthermore, standard deviation of the preparation set is viewed as one of the ground-breaking system inputs and targets scaling methods. On the current study, some input parameters were transformed into a suitable form by:

- ❑ Apply Logarithmic on Parameters for:
  - Effective horizontal length (L_e)
  - Upstream wellhead pressure parameters (P_w)
- ❑ Combine Parameters by:
  - Combination of Flowing Bottom Hole Pressure (P_{wf}) with Reservoir Pressure (P_r) with a form of: ($\Delta P = P_r - P_{wf}$)
  - Combination of Average Permeability (K), Formation Volume Factor (B_o) and Oil Viscosity (μ_o) with a form of ($\frac{k}{B_o \mu_o}$)

For building the AI models, 1840 points from all wells were utilized from seven input data and one target data. The target and input parameters are:

- ❑ **Target Parameter**
  - Oil Flow rate (Q_o)
- ❑ **Input Parameters**
  - Choke Size (CS)

- Water Cut (WC)
- Reservoir Thickness (H)
- Log of Wellhead Pressure (P_w)
- Log of Effective Horizontal Length (L)
- Combination of Reservoir Pressure (P_r) & Wellbore Pressure (P_f)
- Combination of Average Permeability (K), Formation Volume Factor (B_o) and Oil Viscosity (μ_o)

This research work involves the development of models for three data sets which are:

1) H Wells Data Sets (**Table-4.1**)
2) ML Wells Data Sets (**Table-4.2**)
3) Combination H & ML Wells Data Sets (**Table-4.3**)

Table 0.1: Descriptive Statistics of H Wells Data

Parameter	Minimum	Maximum	Mean
Oil Flow Rate (MBPD)	1.1	10	5.1
Water Cut (%)	0	81	7.8
Choke Size (%)	5	100	54
Upstream Wellhead Pressure (psia)	218	1162	601
Formation Volume Factor	1.001	1.7	1.2
Oil Viscosity (cp)	0.3	4.3	1.7
Wellbore Flowing Pressure (psia)	1103	3682	2476
Reservoir Pressure (psia)	1477	4220	2721
Average Permeability (md)	2	856	263
Reservoir Thickness (ft)	18	320	113
Effective Horizontal Length (ft)	469	2079	1269

Table 0.2: Descriptive statistics of ML Wells Data

Parameter	Minimum	Maximum	Mean
Oil Flow Rate (MBPD)	1.3	8.7	4.6
Water Cut (%)	0	49	6.6
Choke Size (%)	12	97	48
Upstream Wellhead Pressure (psia)	240	1168	721
Formation Volume Factor	1.1	1.7	1.4
Oil Viscosity (cp)	0.3	2.7	0.7
Wellbore Flowing Pressure (psia)	1195	3630	2263
Reservoir Pressure (psia)	1488	4057	2533
Average Permeability (md)	5	500	121
Reservoir Thickness (ft)	25	243	92
Effective Horizontal Length (ft)	1879	6002	3120

Table 0.3: Descriptive statistics of Combination of H & ML Wells Data

Parameter	Minimum	Maximum	Mean
Oil Flow Rate (MBPD)	1.1	10	5
Water Cut (%)	0	81	7.5
Choke Size (%)	5	100	53
Upstream Wellhead Pressure (psia)	218	1186	627
Formation Volume Factor	1.001	1.7	1.2
Oil Viscosity (cp)	0.3	4.3	1.5
Wellbore Flowing Pressure (psia)	1103	3682	2436
Reservoir Pressure (psia)	1477	4220	2680
Average Permeability (md)	2	856	232
Reservoir Thickness (ft)	18	320	108
Effective Horizontal Length (ft)	469	6002	1617

4.6 Model Optimizations

During building AI models, the data sets were grouped into two parts to be used for training and testing. On training stage, 70% of the data were used to build and modify the network through feeding it with input and output parameter and let the model predict the targets. On the testing stage, the remaining 30% of the data were used to examine the model through hiding the output and feeding the model with only input and let it predict the output. It’s worth mentioning that data selection for each stage were set randomly distributed to ensure having typical solid models.

AI modelling in this research started with ANN technique which is not only simple and fast predicting method, but it has been proven in the literature it's advancement amongst other AI techniques in predicting many aspects in the life. Searching for the optimization of architecture network and combination data is length process and complicated since it is achieved through trial and error. In this thesis, different number of neurons, layers, and transfer functions were applied to explore the best modelling architecture that will give a strong prediction results. Additionally, many random combinations of the input data was were fed to the ANN network and predict the targets. The final best data combination achieved in the ANN was applied to the other AI techniques for predicting oil flow rates as targets. For evaluation the performance of models at each case, many statistically errors such as Mean Absolute Error, Mean Squared Error, Root Mean Squared Error, Mean Absolute Relative Error, Mean Squared Relative Error, Root Mean Squared Relative Error, Mean Absolute Percentage Error, Mean Squared Percentage Error, Root Mean Squared Percentage Error and Coefficient of Determinations were calculated for all trained and tested models and arranged them in a tabular form for selecting the optimum model in this thesis. All these statistical results are presented in the **Appendix B**.

The optimum form of ANN models were selected based on the lowest Average Absolute Percentage Errors (AAPE) during the testing phase for the data sets of H Wells (**Table 4.4**), ML wells (**Table 4.5**) and combination of data from H & ML wells (**Table 4.6**).

Table 0.4: Optimum ANN Models for H Wells

Case	Training Function	# of Layers	# of Neurons	Transfer Function
1	Trainlm	One Layer	6	tansig
2	Trainlm -2L	Two Layer	5 - 4	tansig
3	Traingd	Two Layer	9 - 6	tansig
4	Traingdx	Two Layer	10 - 5	tansig
5	Trainbfg	Two Layer	20 - 15	tansig
6	trainscg	Two Layer	7 - 4	tansig
7	trainoss	Two Layer	13 - 4	tansig
8	Trainrp	Two Layer	10 - 5	tansig
9	Trainb	Two Layer	20 - 10	tansig

Table 0.5: Optimum ANN Models for ML Wells

Case	Training Function	# of Layers	# of Neurons	Transfer Function
1	Trainlm	One Layer	18	tansig
2	Trainlm -2L	Two Layer	10 - 18	tansig
3	Traingd	Two Layer	10 - 9	tansig
4	Traingdx	Two Layer	10 - 11	tansig
5	Trainbfg	Two Layer	10 - 18	tansig
6	trainscg	Two Layer	20 - 9	tansig
7	trainoss	Two Layer	10 - 17	tansig
8	Trainrp	Two Layer	20 - 17	tansig
9	Trainb	Two Layer	14 - 20	tansig

Table 0.6: Optimum ANN Models for H & ML Wells

Case	Function	# of Layers	# of Neurons	Transfer Function
1	Trainlm	One Layer	10	tansig
2	Trainlm -2L	Two Layer	7 - 3	tansig
3	Traingd	Two Layer	7 - 4	tansig
4	Traingdx	Two Layer	7 - 4	tansig
5	Trainbfg	Two Layer	20 - 15	tansig
6	trainscg	Two Layer	8 - 3	tansig
7	trainoss	Two Layer	7 - 4	tansig
8	Trainrp	Two Layer	7 – 3	tansig
9	Trainb	Two Layer	10 – 11	tansig

The results of prediction functions for ANN models for H, ML and combination data of both well types are presented in **Table 4.7, 4.8 & 4.9**. The parameters of ANN linear functions are:

- Slope of linear regression (S)
- Intercept of linear regression (P)
- Regression Value (R)

Table 0.7: ANN Models Function Results for H Wells

Case	Training Function	S	P	R
1	Trainlm	0.99	0.027	0.99
2	Trainlm -2L	0.98	0.13	0.98
3	Traingd	0.85	0.62	0.92
4	Traingdx	0.70	1.30	0.84
5	Trainbfg	0.94	0.3	0.97
6	trainscg	0.85	0.84	0.93
7	trainoss	0.89	0.45	0.93
8	Trainrp	0.91	0.31	0.94
9	Trainb	0.88	0.43	0.92

Table 0.8: ANN Models Function Results for ML Wells

Case	Training Function	S	P	R
1	Trainlm	0.71	1.7	0.64
2	Trainlm -2L	0.71	1.4	0.91
3	Traingd	0.87	0.6	0.64
4	Traingdx	0.44	2.5	068
5	Trainbfg	0.83	1.0	0.89
6	trainscg	0.48	2.3	0.77
7	trainoss	0.47	2.3	0.54
8	Trainrp	0.69	1.3	0.71
9	Trainb	0.41	2.5	0.50

Table 0.9: ANN Models Function Results for H & ML Wells

Case	Training Function	S	P	R
1	Trainlm	0.99	0.006	0.96
2	Trainlm	0.98	0.065	0.94
3	Traingd	0.79	0.67	0.88
4	Traingdx	0.89	0.31	0.93
5	Trainbfg	0.84	0.66	0.9
6	trainscg	0.94	0.42	0.97
7	trainoss	0.95	0.15	0.95
8	Trainrp	0.94	0.34	0.91
9	Trainb	0.76	0.95	0.89

More detail about modelling of ANN are illustrated at **Appendix A**.

On FL model development, the Subtractive clustering technique was applied for creating the models. The final optimum FL models that are giving less errors for H wells, ML wells and combination of data from both types of wells are shown in **Table 4.10**.

Table 0.10: Optimum FL Models

Parameters	H Wells	ML Wells	H & ML Wells
Radii	0.9	1.4	0.8
Epoch	900	100	200
Number of nodes	58	42	74
Number of linear parameters	24	16	32
Number of nonlinear parameters	42	28	56
Total number of parameters	66	44	88
Number of training data pairs	120	34	154
Number of fuzzy rules	3	2	4

On DT model development, manipulating branch node splits for creating deep or shallow tree is the main parameters to be tuned for achieving best predicting DT model. The optimum DT model for the three data sets of H wells, ML wells and combination of data from H & ML wells has node splits shown in **Table 4.11**.

Table 0.11: Constructed DT Models

Parameters	H Wells	ML Wells	H & ML Wells
Node Split	5	10	5

On the development of the SVM technique, “Gaussian” technique was applied to create the model. The Main parameters of the final form of SVM models for the data sets collected from H wells, ML wells and combination of data from H & ML wells are shown in **Table 4.12.**

Table 0.12: Optimum SVM Models

Parameters	H Wells	ML Wells	H & ML Wells
Kernel option	155	300	115
Regularization Parameter (C)	450	450	450
lambda	0.0085	0.012	0.0085
Penalty of Over Fitting (epsilon)	0.2	0.91	0.2

The summary of the optimized values applied in developing the models for all AI techniques for H wells, ML wells and combination H & ML wells data sets are shown in **Table 4.13, 4.14 & 4.15** respectively.

Table 0.13 : Optimized values for all AI Techniques in H Wells

AI Technique	Parameter	Optimized Value
ANN	ANN Type	Feed Forward Neural Network
	Number of Hidden layers	1
	Number of Neurons	6
	Training Function	Levenberg-Marquadt
	Transfer function	TanSigmoidal
FL	Cluster Radius	0.9
DT	Node Split	5
SVM	Type of Kernel	Gaussian
	Kernel Option	155
	Regularization Parameter (c)	450
	Penalty of Over fitting, (epsilon)	0.2

Table 0.14 : Optimized values for all AI Techniques in ML Wells

AI Technique	Parameter	Optimized Value
ANN	ANN Type	Feed Forward Neural Network
	Number of Hidden layers	2
	Number of Neurons	(18, 10)
	Training Function	Scale Conjugate Gradient
	Transfer function	TanSigmoidal
FL	Cluster Radius	1.4
DT	Node Split	10
SVM	Type of Kernel	Gaussian
	Kernel Option	300
	Regularization Parameter (c)	450
	Penalty of Over fitting, (epsilon)	0.91

Table 0.15 : Optimized values for all AI Techniques in H & ML Wells

AI Technique	Parameter	Optimized Value
ANN	ANN Type	Feed Forward Neural Network
	Number of Hidden layers	1
	Number of Neurons	10
	Training Function	Levenberg-Marquadt
	Transfer function	TanSigmoidal
FL	Cluster Radius	0.8
DT	Node Split	5
SVM	Type of Kernel	Gaussian
	Kernel Option	115
	Regularization Parameter (c)	450
	Penalty of Over fitting, (epsilon)	0.2

CHAPTER 5

RESULTS & DISCUSSIONS

This chapter is discussing the results of the developed AI models and estimated values from correlations and compare the results with actual measurement through statistical and graphical errors analysis. New empirical correlations from ANN models will be introduced in this section that will illustrate the superiority of the developed models over any other estimation methods.

5.1 Statistical Error Analysis

The statistical error analysis is a process performed in the results to evaluate the accuracy of the methods and techniques applied. In this study, two main common error analysis were calculated which are: Coefficient of Determination (R^2), Average Absolute Percentage Error (AAPE).

5.1.1 Coefficient of Determination

Coefficient of Determination (R^2) which is also known as R-square is used to measure how well fitted the data on the regression curve. The range of R^2 is from zero to one. While the goodness fit of data acquired when R^2 reached one, the dispersion of the data of the mean when R^2 is close to zero.

5.1.2 Average Absolute Percentage Error

Average Absolute Percentage Error (AAPE) is measuring the accuracy of the forecasted values with respect to the actual values. The formula of AAPE is given by:

$$\mathrm{AAPE} = \frac{100\%}{n}\sum_{i=1}^{n}\left|\frac{A_t - F_t}{A_t}\right| \tag{5.1}$$

Where,

A_t: Actual measurement

F_t: Forecasted Measurement

n: Number of Data Points

As the value of AAPE reached zero, matching between predicted and actual values is achieved. However, a high deviation between the two values when AAPE approached 100%.

5.1.3 Statistical Error Analysis of Analytical Correlations

Oil flow rates in this research were estimated with using eight analytical correlations. The maximum R^2 was around 0.67 obtained by Borisov (H) correlation while Furui method gave the minimum R^2 with a value of 0.1. The lowest AAPE was 38% from Renard correlation. On the other hand, 61.4% was the highest AAPE given by Butler correlation. **Table-5.1** is showing statistical errors for the existing correlations used in this study.

Table 0.1: Statistical Errors from Correlations

Correlation	**R^2**	**AAPE (%)**
Borisov (ML)	0.65	40.5
Borisov (H)	0.67	49.4
Joshi	0.57	40.1
Renard	0.47	38.0
Economides	0.58	40.4
Butler	0.15	61.4
Furui	0.1	56.0
Escobar	0.63	38.8

5.1.4 Statistical Error Analysis of Artificial Intelligence Models

All developed AI models in the research have provided superior results compared to the correlations for predicting oil flow rates for H and ML wells. The maximum AAPE value obtained from all AI models were less than the lowest value of the AAPE from the calculated correlations. Gathered data were divided into three groups from building AI models for H wells data sets, ML wells data sets and combination of data sets from H & ML wells. The statistical error analysis for all data sets are shown in **Table 5.2, 5.3 & 5.4.**

The predicted oil flow rates for H wells data set from **Table 5.2** showed the best estimation results were achieved with DT on training models and ANN on testing models with reference to the actual rates. The highest R^2 from AI models for H data sets was achieved from SVM which gave the value of 0.99 for training models and 0.98 for testing models. For AAPE, the minimum values were 6.9% for testing models from ANN and 4% for training models that were given from DT.

Table 0.2: Statistical Errors for H AI Models

Training Models			
#	**Model**	**R^2**	**AAPE (%)**
1	ANN	0.98	5.0
2	FL	0.97	7.5
3	DT	0.98	4.0
4	SVM	0.99	5.4
Testing Models			
#	**Model**	**R^2**	**AAPE (%)**
1	ANN	0.98	6.9
2	FL	0.92	16.6
3	DT	0.83	19.2
4	SVM	0.98	7.2

On ML data sets at **Table 5.3**, the best estimation result was obtained from SVM which gave the highest R^2 of 0.83 on testing model. Moreover, it provided the lowest AAPE of values equal to 11.7% while the minimum AAPE on training model was achieved DT technique with 17% from.

Table 0.3: Statistical Errors for ML AI Models

Training Models			
#	**Model**	$\mathbf{R^2}$	**AAPE (%)**
1	ANN	0.80	17.5
2	FL	0.89	10.3
3	DT	0.85	17.5
4	SVM	0.81	18.9
Testing Models			
#	**Model**	$\mathbf{R^2}$	**AAPE (%)**
1	ANN	0.59	19.2
2	FL	0.2	36.8
3	DT	0.45	32.6
4	SVM	0.83	11.7

On the statistical errors analysis in **Table 5.4** for the combined data of H & ML wells from all AI models, the best prediction models of oil flow rates were achieved by ANN on the testing model with AAPE of 9.5% and DT on with AAPE of 4.3% on the training model. The maximum R^2 on training models was 0.98 offered by ANN, DT and SVM. On the testing model, the highest R^2 was of 0.94 achieved SVM.

Table 0.4: Statistical Errors for H & ML AI Models

Training Models			
#	**Model**	$\mathbf{R^2}$	**AAPE (%)**
1	ANN	0.98	5.1
2	FL	0.94	8.7
3	DT	0.98	4.3
4	SVM	0.98	7.5
Testing Models			
#	**Model**	$\mathbf{R^2}$	**AAPE (%)**
1	ANN	0.92	9.5
2	FL	0.89	18.0
3	DT	0.87	15.8
4	SVM	0.94	9.6

The Overall statistical errors for all correlations and AI models from all data sets are shown in **Table 5.5**. On AI methods, the results are presenting of the results obtained from the testing models for all AI techniques. The lowest AAPE of 6.9% was achieved by ANN model on H wells data sets while the Butler correlation gave the highest AAPE of 61.4%. The highest R^2 was equal to 0.98 from SVM at H wells data sets while R^2 of 0.1 done from Furui correlation was the minimum R^2 in all techniques.

Table 0.5: Statistical Errors for all Methods

Type	Method	R^2	AAPE (%)
Correlations	Borisov (ML)	0.65	40.5
	Borisov (H)	0.67	49.4
	Joshi	0.57	40.1
	Renard	0.47	38.0
	Economides	0.58	40.4
	Butler	0.15	61.4
	Furui	0.1	56.0
	Escobar	0.63	38.8
AI Models (H Wells)	ANN	0.98	6.9
	FL	0.92	16.6
	DT	0.83	19.2
	SVM	0.98	7.2
AI Models (ML Wells)	ANN	0.59	19.2
	FL	0.2	36.8
	DT	0.45	32.6
	SVM	0.83	11.7
AI Models (H & ML Wells)	ANN	0.92	9.5
	FL	0.89	18.0
	DT	0.87	15.8
	SVM	0.94	9.6

5.2 Graphical Error Analysis

In graphical error analysis, the comparison plot bar charts and cross plots were used for evaluating the results of oil flow rates obtained from the correlations and AI models. Bar chart is one of the common technique for graphical error analysis that is used to categorize the data with a vertical line to represent the proportional values with respect to the other parameters. Cross plot is another graphical error analysis that is widely used through plotting the predicted results versus the target values over a 45° straight line in between them. As the values scattered near the straight line, the accuracy of the estimation techniques becomes higher, while less accuracy is obtained when the points are scattered away from the 45° straight line.

5.2.1 Graphical Error of Analytical Correlations

The estimated results of R^2 for the oil flow rates from H & ML wells for all the applied correlations are illustrated in **Figure 5.1**. The values are arranged in ascending order and is showing that Furui and Bulter's methods gave the least R^2. Borisov (H) & (ML) corrections gave the best R^2 among the other correlation.

In **Figure 5.2**, the distribution of AAPE values in ascending order are shown bar chart for the estimated oil flow rates in the complex wells from the correlations. The results showed that average AAPE for all correlations is around 50%. Bulter was giving the highest AAPE comparing with the other correlations. The figure also indicated that Joshi, Borisov (ML), and Ecomindes gave almost similar AAPE with around 40% for the calculated oil flow rates. The lowest values of AAPE were achieved from Renard and Escobar with 38 and 39% respectively.

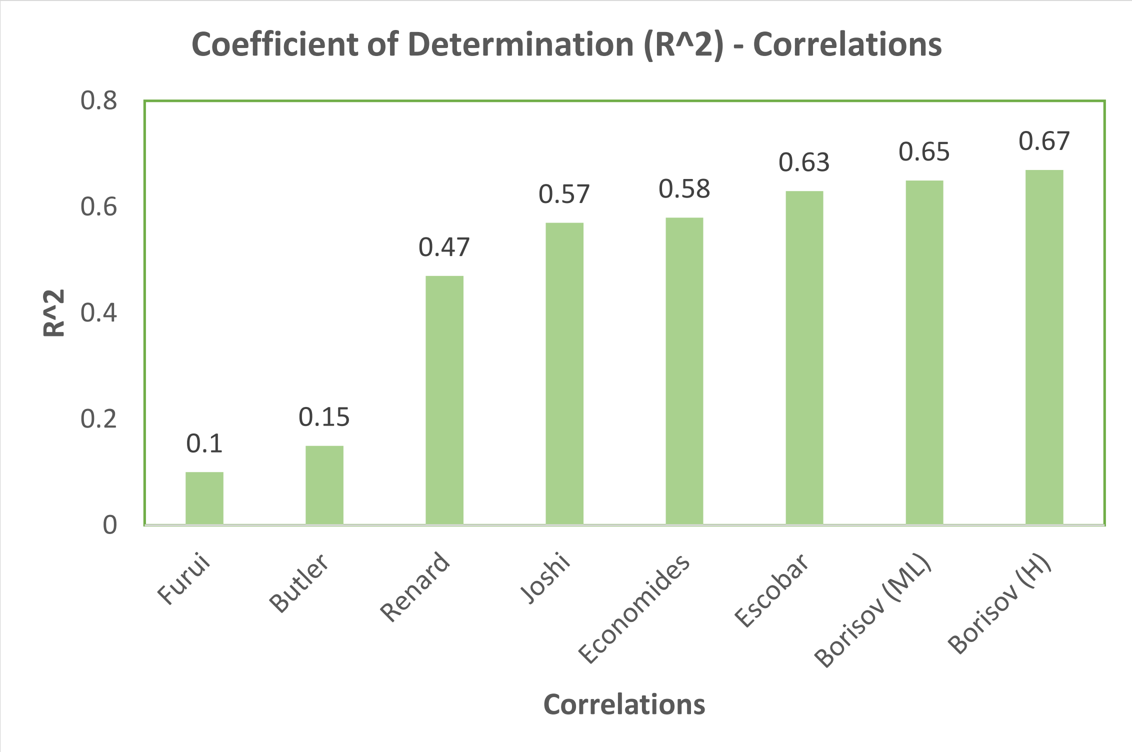

Figure 0.1: R-Square for Estimated Oil Rates from Correlations

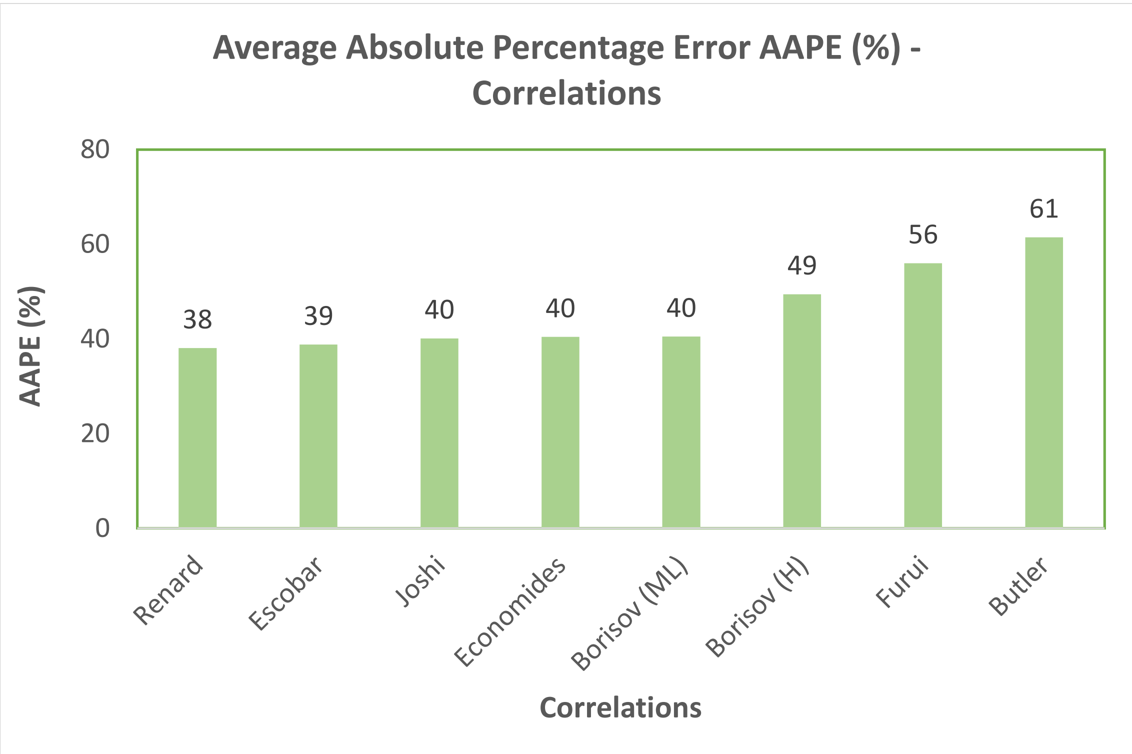

Figure 0.2: AAPE for Estimated Oil Rates from Correlations

The crossplots for the estimated oil flow rates from the eight correlations versus the actual flow rates in H and ML wells are shown in **Figures 5.3, 5.4, 5.5, 5.6, 5.7, 5.8, 5.9 & 5.10.**

Figure 5.3 is showing the plotted results of the calculated oil rates from the Borisov (ML) versus the actual oil rate from 50 ML wells. The value of AAPE is 40.5% and R^2 is 0.65.

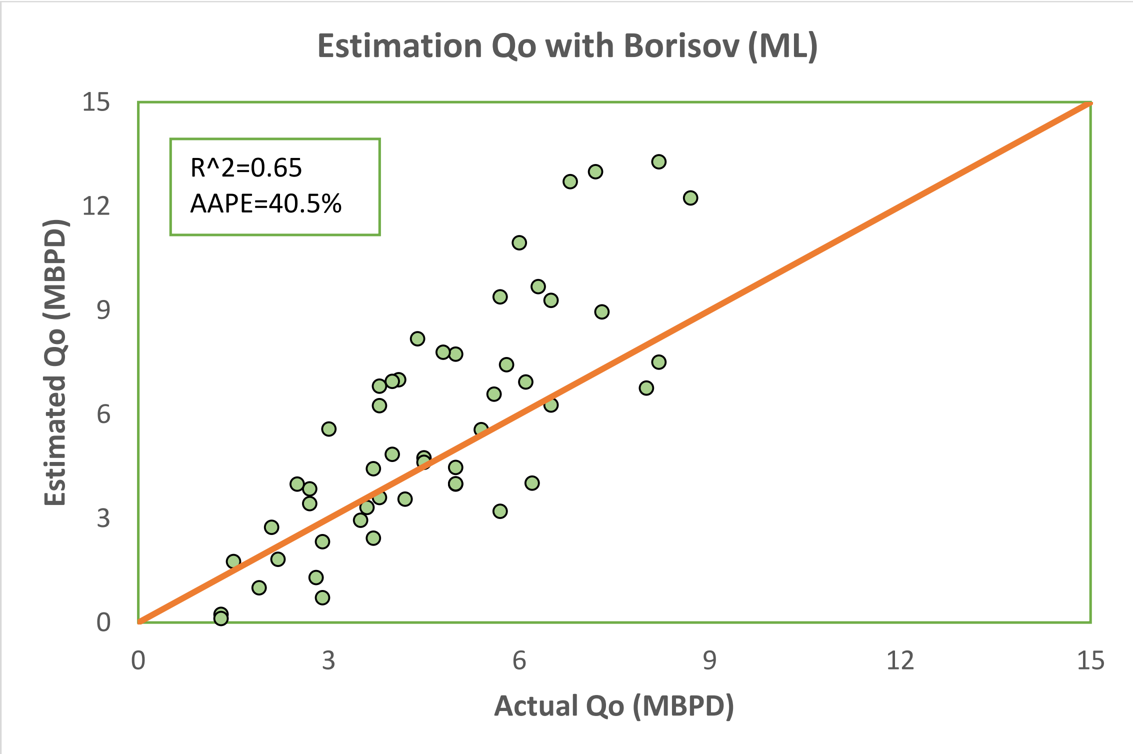

Figure 0.3: Crossplot of Estimated Oil Rates with Borisov (ML) Correlation

Figure 5.4 is illustrating the cross-plot results of the calculated oil rates from Borisov (H) correlation versus actual oil rates. The results showed the value of R^2 is 0.67 which is the highest R^2 obtained from all correlations. Moreover, it gave AAPE of 49.4%

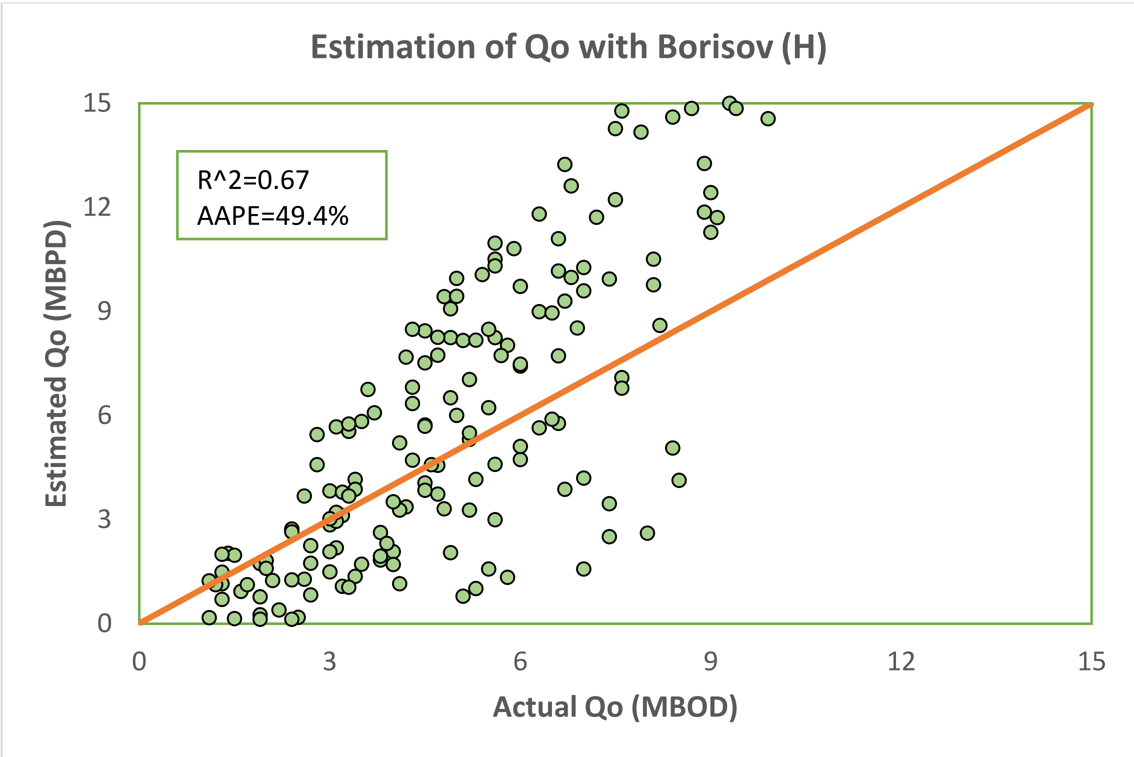

Figure 0.4: Crossplot of Estimated Oil Rates with Borisov (H) Correlation

Figure 5.5 is demonstrating the cross-plot results of the calculated oil rates from Joshi correlation versus the actual oil rates for oil H wells. The results showed the value of R^2 is 0.57 and 40.1% for AAPE.

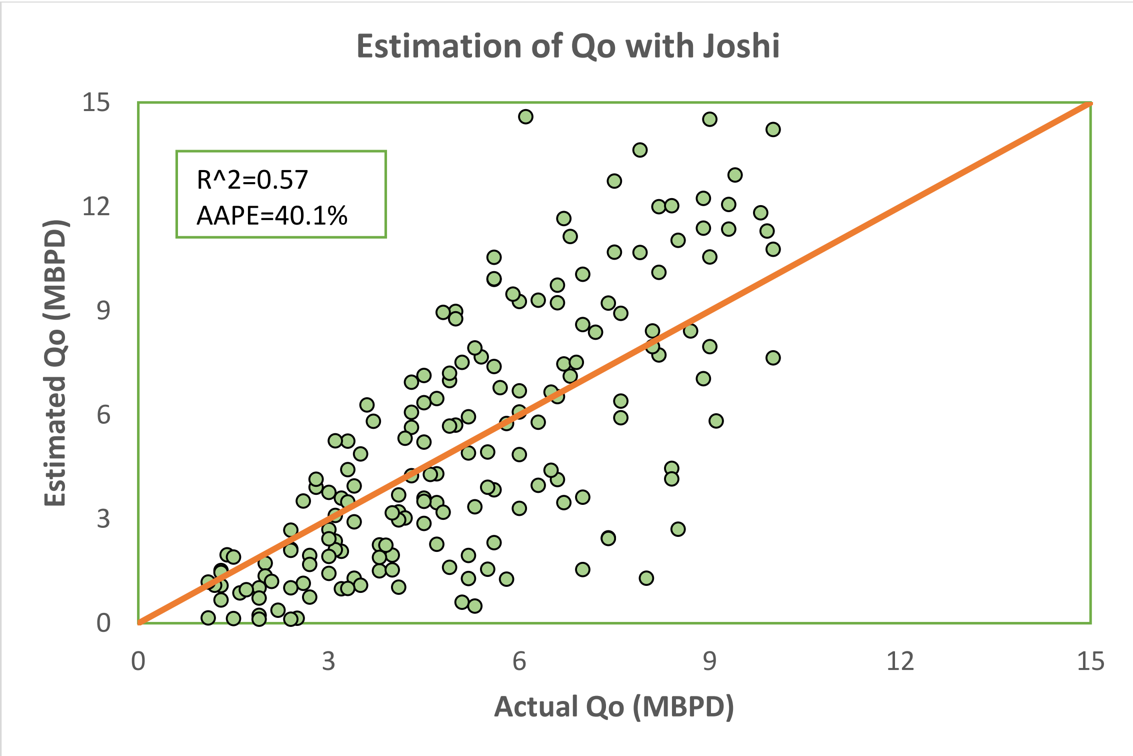

Figure 0.5: Crossplot of Estimated Oil Rates with Joshi Correlation

Figure 5.6 is illustrating the cross-plot results of the calculated oil rates from Renard correlation versus the actual oil rates of H wells. The results showed that Renard method was giving the best estimation over the other correlations with an AAPE of 38% and R^2 of 0.47.

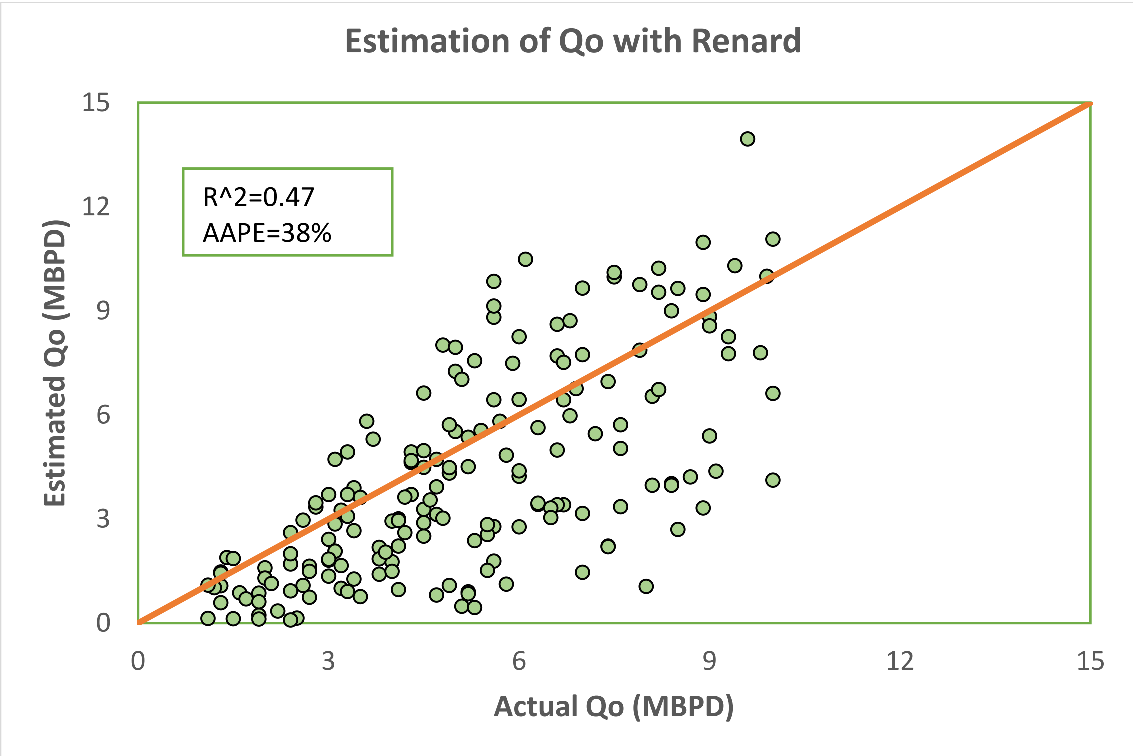

Figure 0.6: Crossplot of Estimated Oil Rates with Renard Correlation

Figure 5.7 is showing the results of the estimated oil rates from Economides correlation versus the actual oil rates of H wells. The values of Economides method were providing an AAPE of 40.4% and 0.58 of R^2.

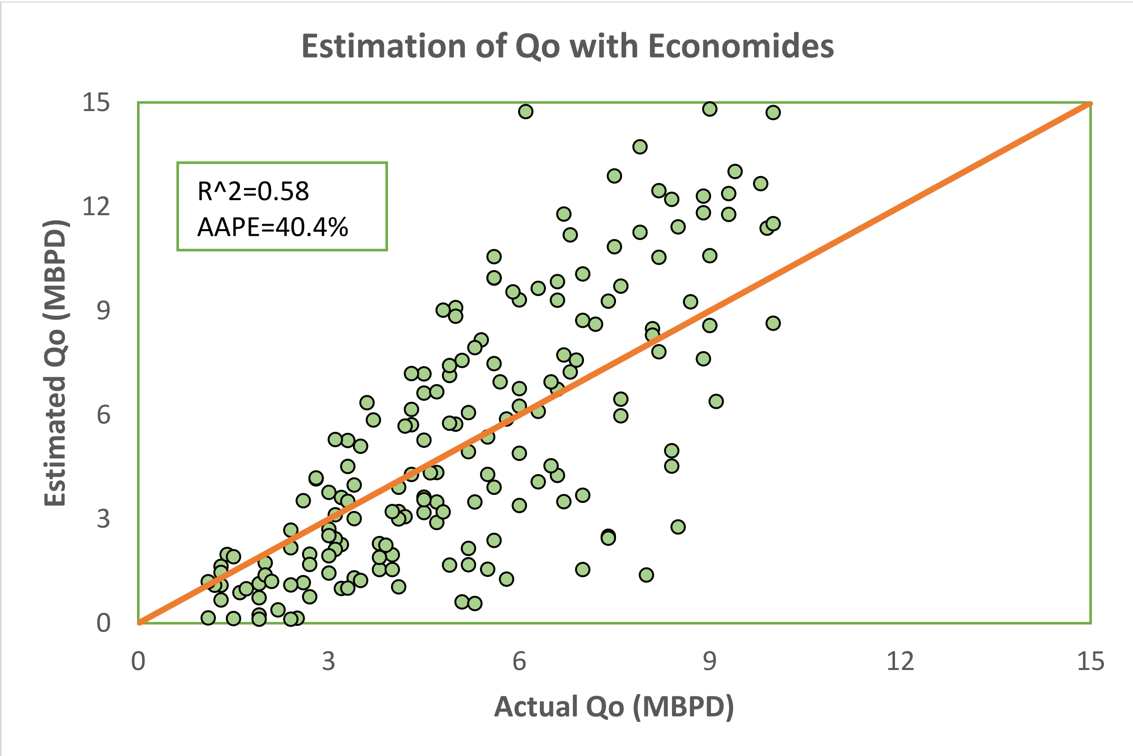

Figure 0.7: Crossplot of Estimated Oil Rates with Economides Correlation

Figure 5.8 is plotting the results of the estimated oil rates from Butler correlation versus the actual oil rates of H wells. The results showed Butler method was giving 0.15 of R^2 and 61.4% of AAPE. As shown in the plot, the most of the estimated oil rates values are below the 45° straight line which is showing a deficiency of this method in predicting of oil rates with the current data sets.

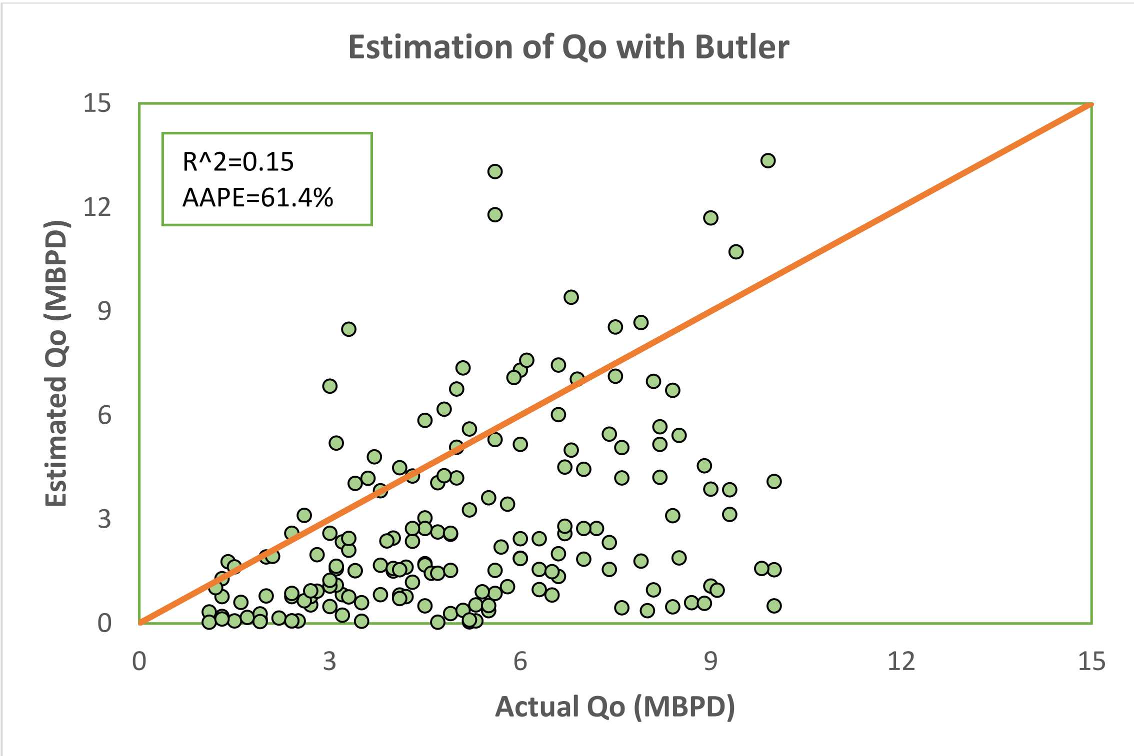

Figure 0.8: Crossplot of Estimated Oil Rates with Butler Correlation

Figure 5.9 is illustrating the cross-plot results of the calculated oil rates from Furui correlation versus the actual oil rates of H wells. The results showed Furui method was giving the least R^2 value of 0.1 comparing to the remaining the other correlations. The obtained values of AAPE was 56%.

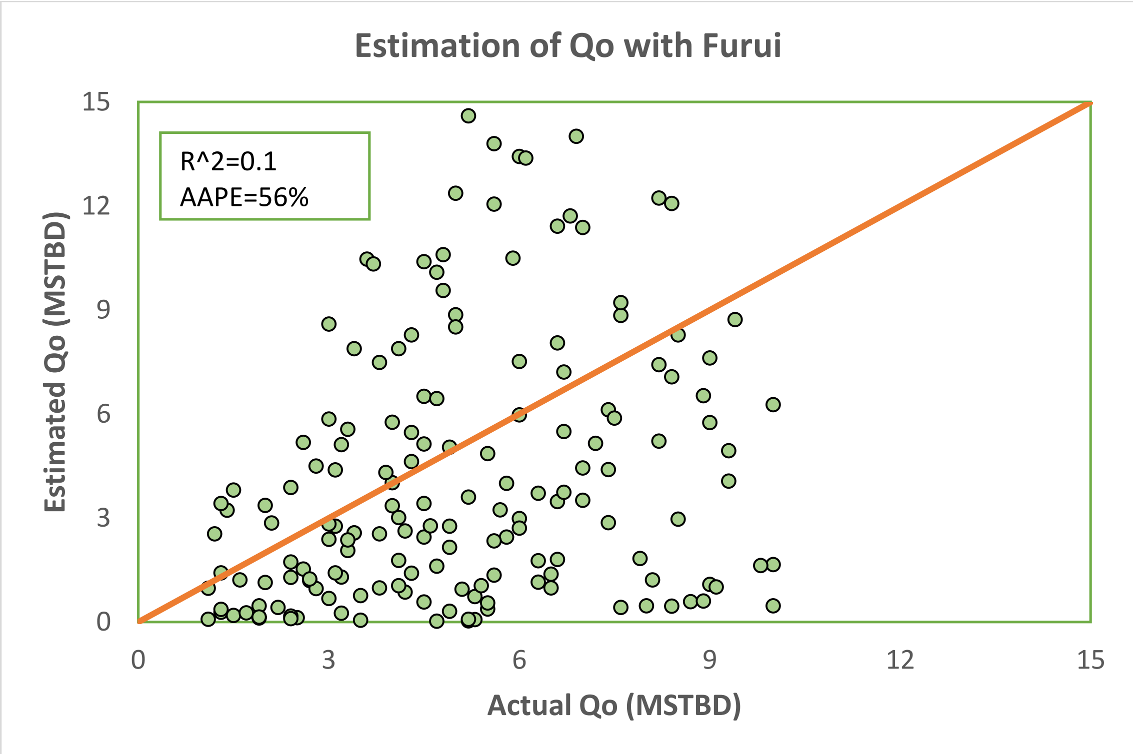

Figure 0.9: Crossplot of Estimated Oil Rates with Furui Correlation

Figure 5.10 is demonstrating the cross-plot results of the calculated oil rates from Escobar correlation versus the actual oil rates for H wells. The results showed the value of R^2 is 0.63 and AAPE is 38.8%

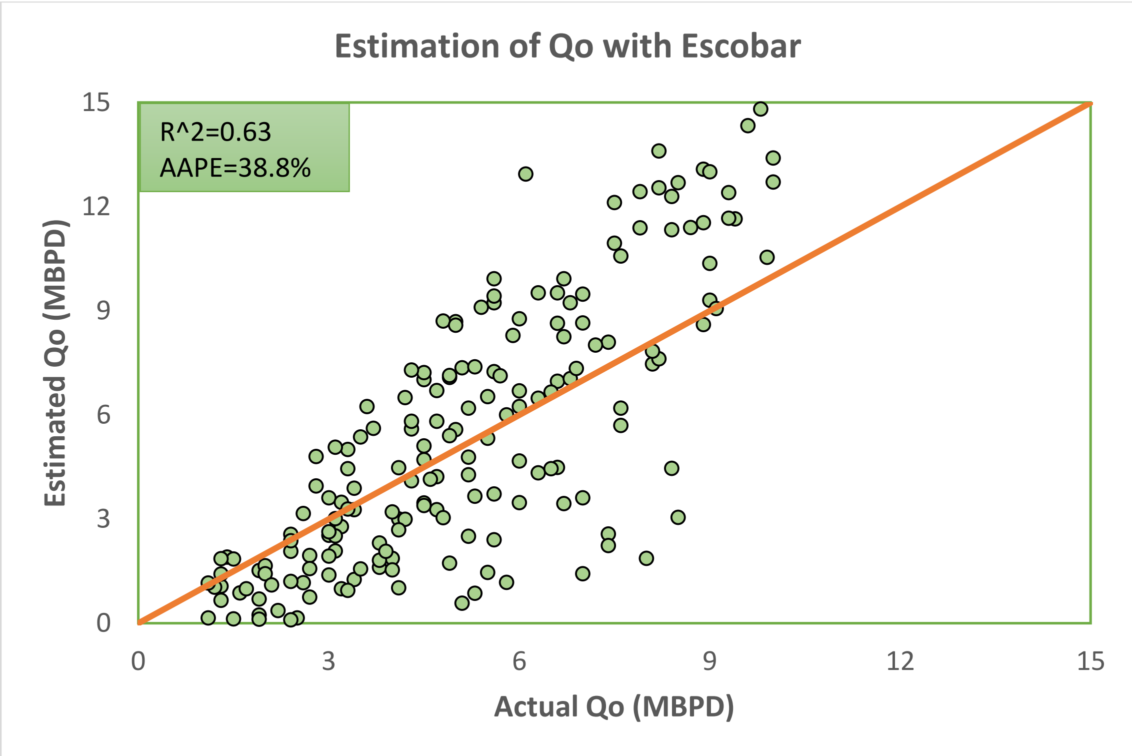

Figure 0.10: Crossplot of Estimated Oil Rate with Escobar Correlation

5.2.2 Graphical Error of Artificial Intelligence models

The graphical errors analysis for all AI models are shown in bar charts and crossplots for three different data sets which are: H Wells Data Sets, ML Wells Data Set and combination of H & ML Wells Data Sets. The results are plotted for training and testing models for ANN, FL, DT and SVM for R^2 and AAPE.

Figure 5.11 & 5.12 are showing the predicted results of R^2 for the oil rates for H wells from all AI techniques for training and testing models. In training models, the highest values of R^2 was 0.99 and obtained from SVM while the lowest value was 0.97 done by FL. For the testing model, the minimum R^2 results were done by DT while SVM & ANN gave the highest R^2 of 0.98.

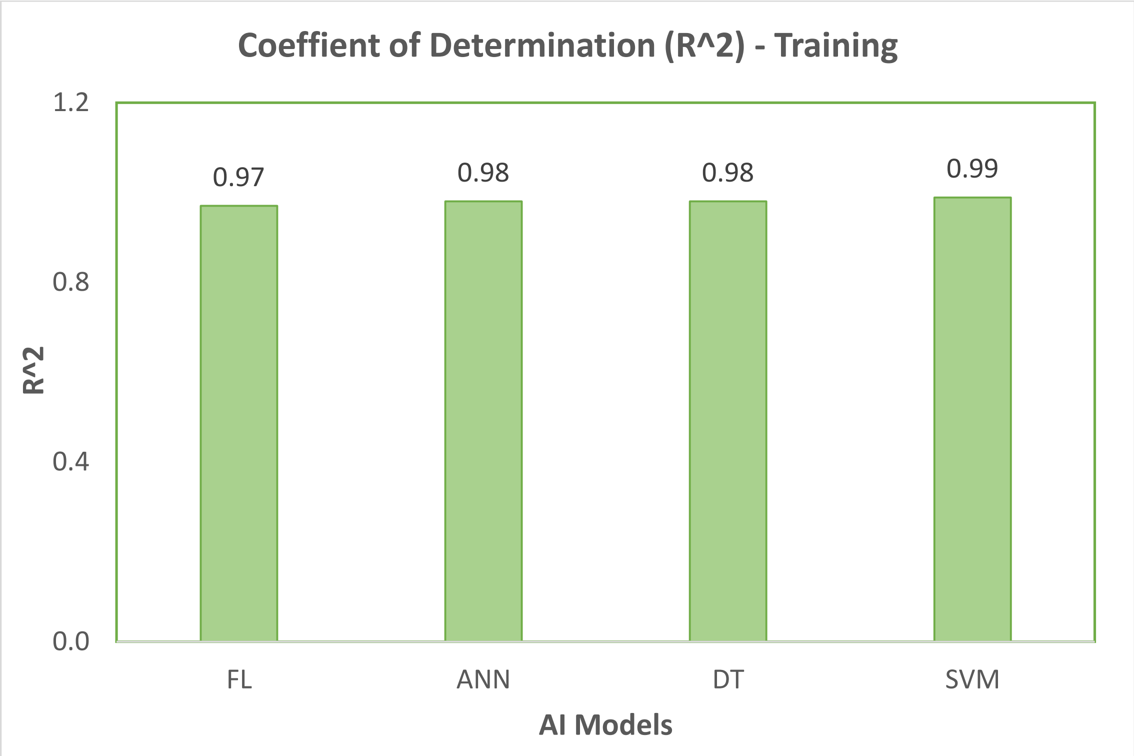

Figure 0.11: R-Square for Predicted Oil Rates from AI Models in H Wells – Training

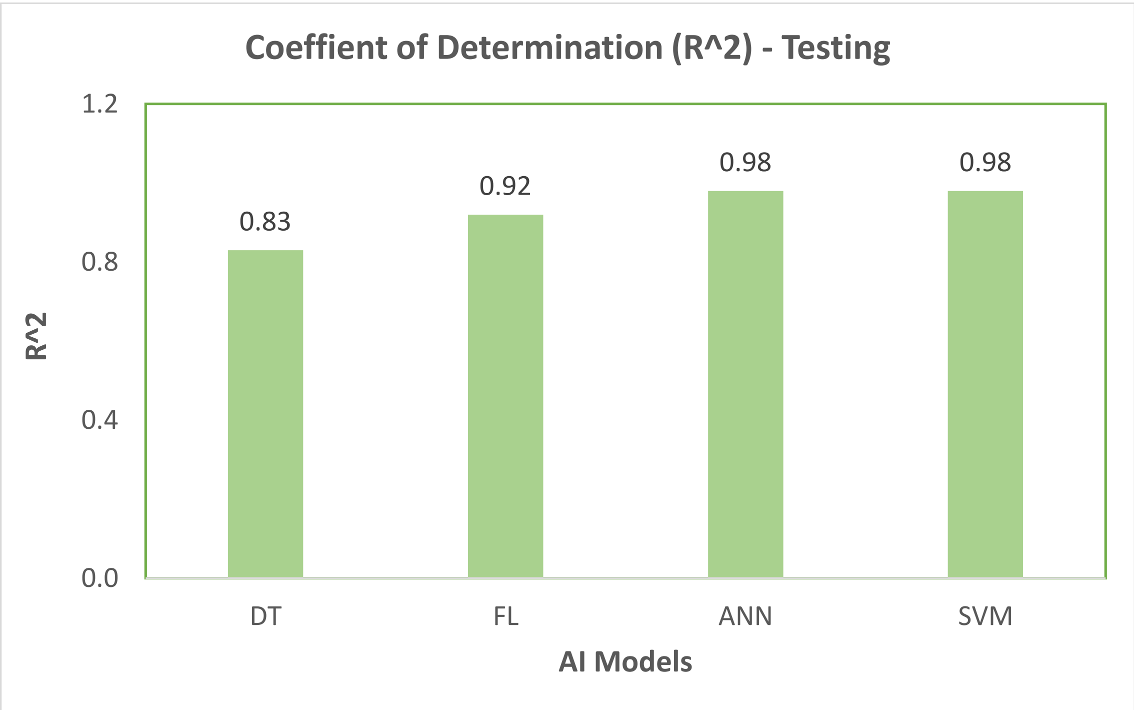

Figure 0.12: R-Square for Predicted Oil Rates from AI Models in H Wells – Testing

The AAPE results for predicted oil flow rates from H data set for training and testing of all AI models are illustrated in **Figures 5.13 & 5.14**. While DT is showing the best training results with an AAPE of 4%, FL had the least prediction accuracy among all the training models with AAPE of 7.5%. On the testing models in **Figure 5.14**, DT provided the highest AAPE of 19.2% comparing to the other AI models. The lowest AAPE value on the testing models, however, was 6.9% achieved by the ANN model.

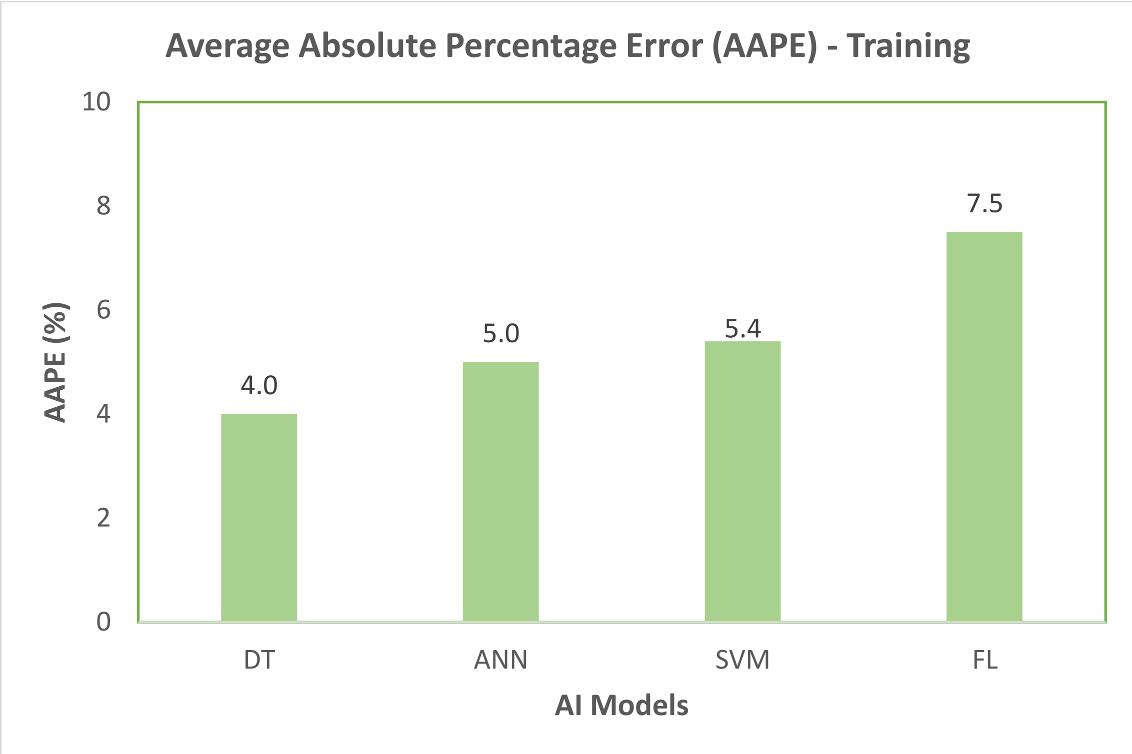

Figure 0.13: AAPE of Predicted Oil Rates from AI Models in H Wells – Training

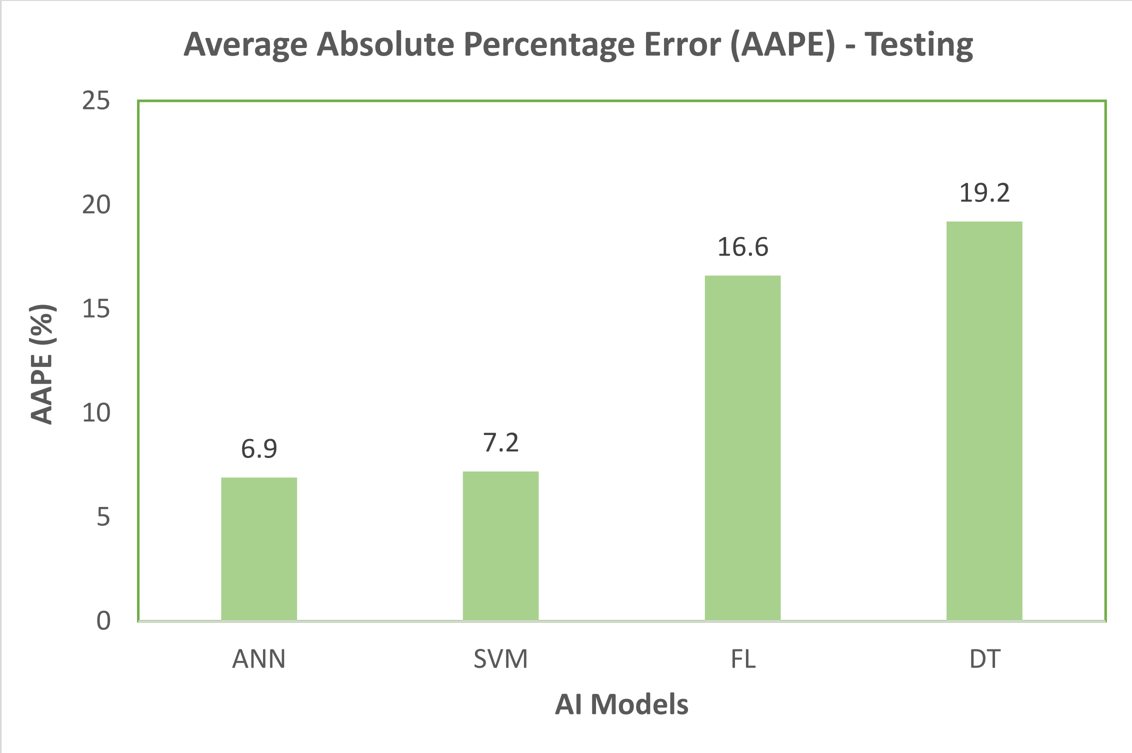

Figure 0.14: AAPE for Predicted Oil Rates from AI Models in H Wells – Testing

Figure 5.15 & 5.16 are depicting the predicted results of the R^2 for the oil rates from ML wells for all AI techniques for training and testing models. In training models, the minimum R^2 value is 0.58 for ANN while 0.89 is the highest value that obtained from FL. On the testing models in **Figure 5.20**, the lowest value of R^2 was 0.2 by FL and the highest value was 0.83 by the SVM model.

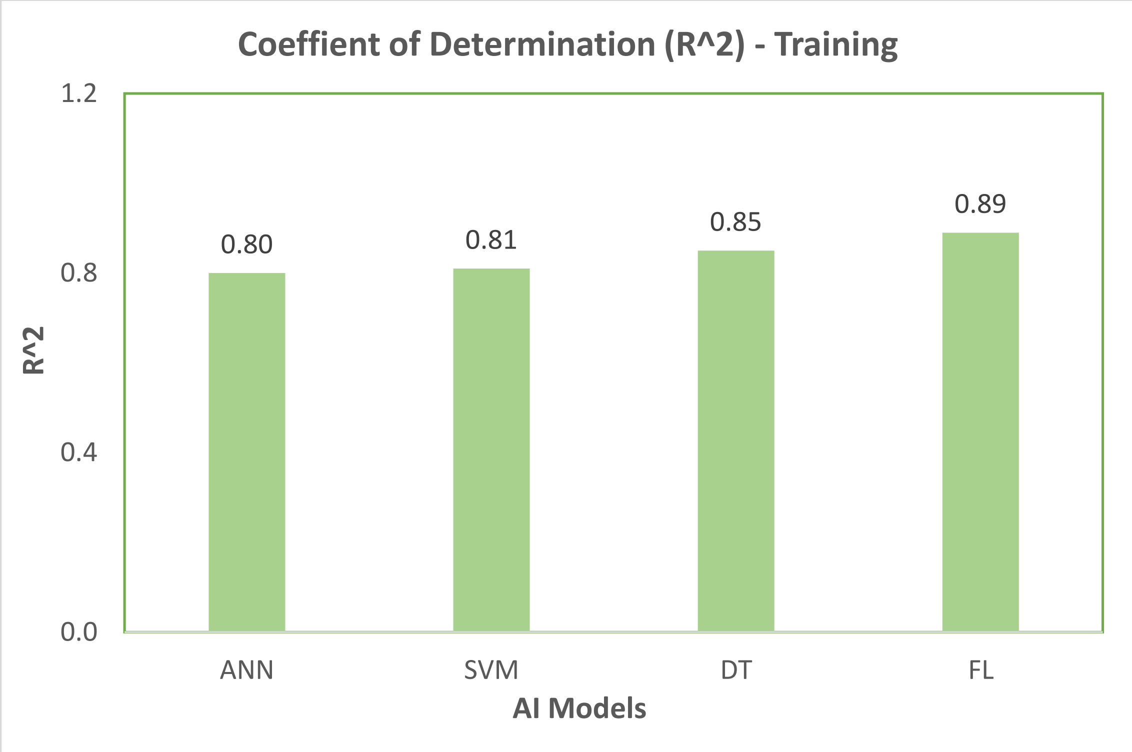

Figure 0.15: R-Square for Predicted Oil Rates from AI Models in ML Wells – Training

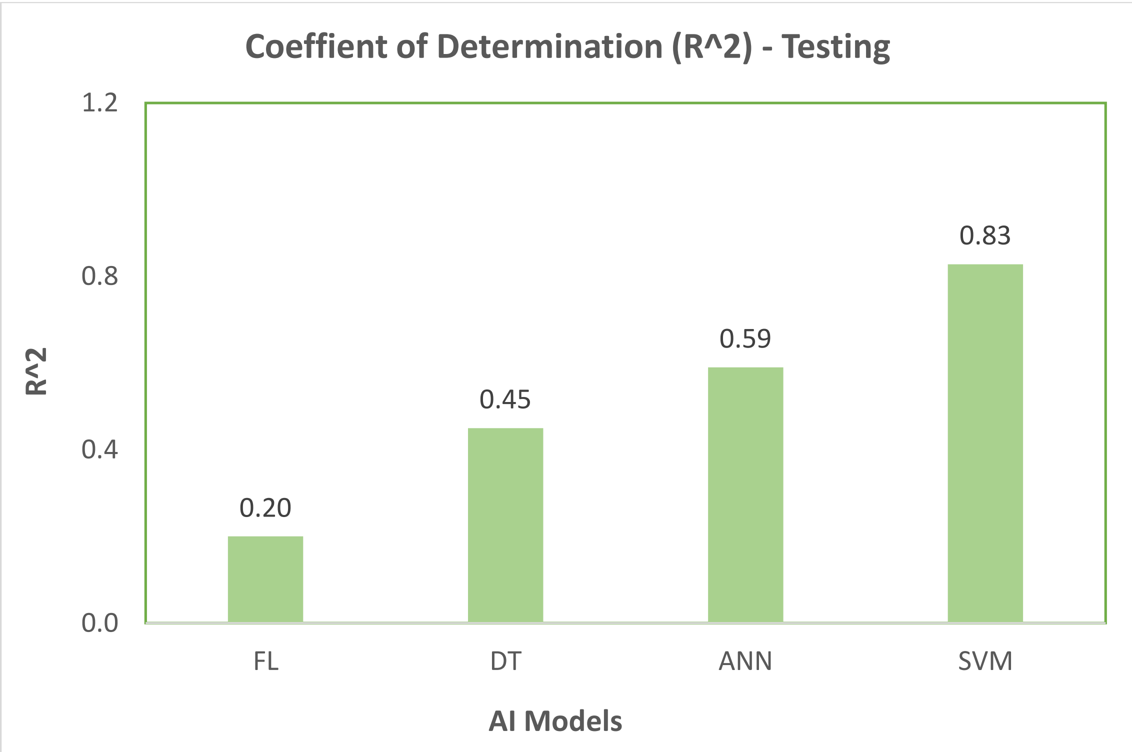

Figure 0.16: R-Square for Predicted Oil Rates from AI Models in ML Wells – Testing

Figures 5.17 & 5.18 are presenting AAPE of predicted oil flow rates from training and testing AI models for ML wells data sets. The results showed the highest AAPE was 18.9% from SVM and 10.3% was the lowest value that achieved from FL in the training models based on **Figure 2.17**. For the testing models, the maximum value of AAPE was given by FL with 36.8% whereas SVM gave the lowest AAPE value of 11.7% as plotted in **Figure 5.18**.

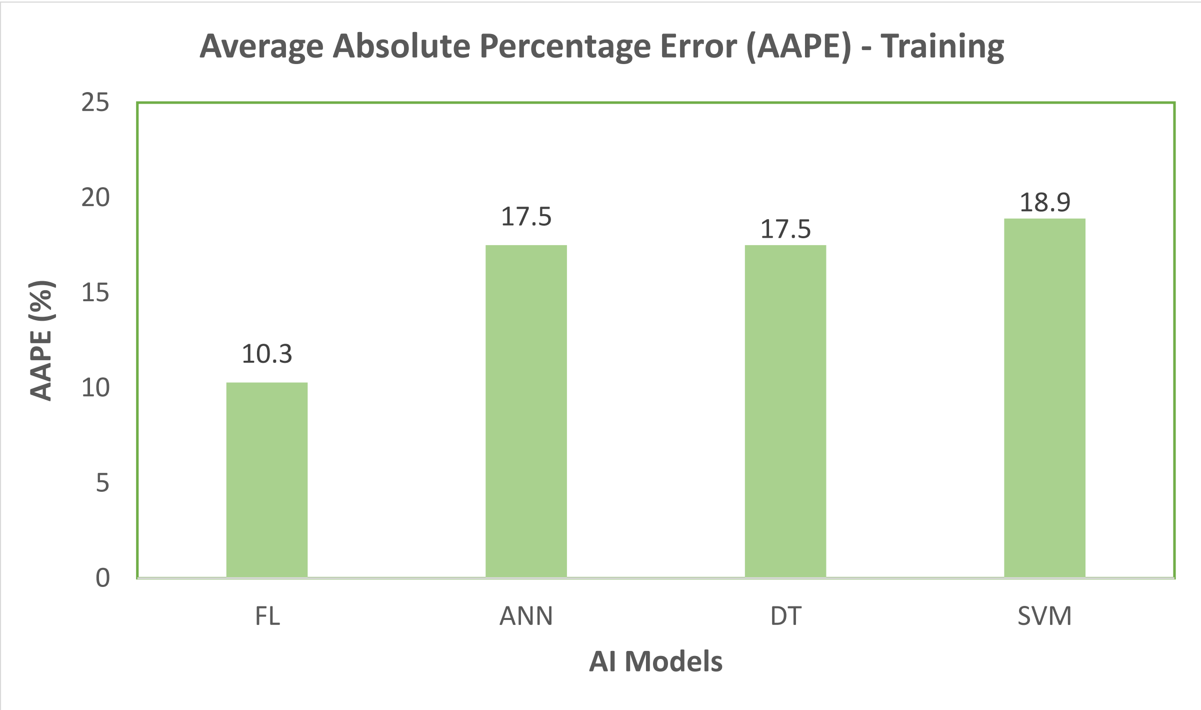

Figure 0.17: AAPE for Predicted Oil Rates from AI Models in ML Wells – Training

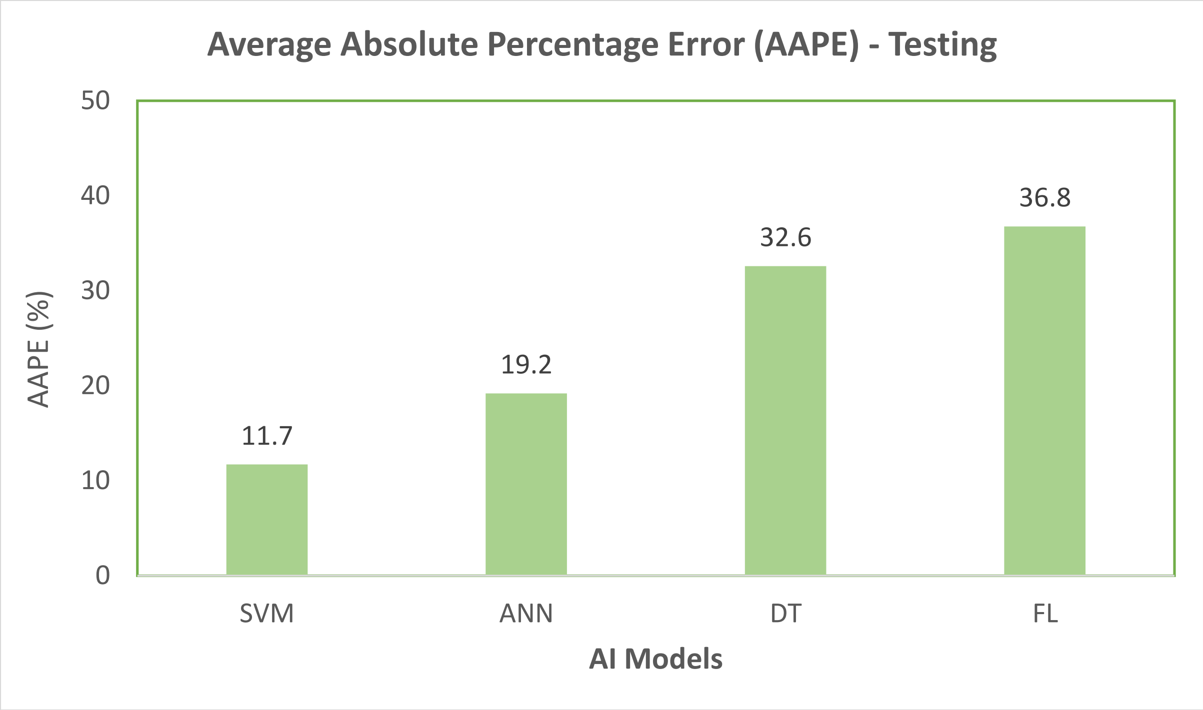

Figure 0.18: AAPE for Predicted Oil Rates from AI Models in ML Wells – Testing

Figures 5.19 & 5.20 are showing R^2 of predicted oil rates from training and testing AI models for combination data set of H & ML wells. The results showed the maximum R^2 was obtained by the ANN, DT and SVM models with a value of 0.98 whereas FL was giving the lowest R^2 value of 0.94 for the training models as shown in **Figure 5.19**. On the testing models in **Figure 5.20**, the minimum value of R^2 was obtained from DT with a value of 0.87 and the highest value was 0.94 from SVM model.

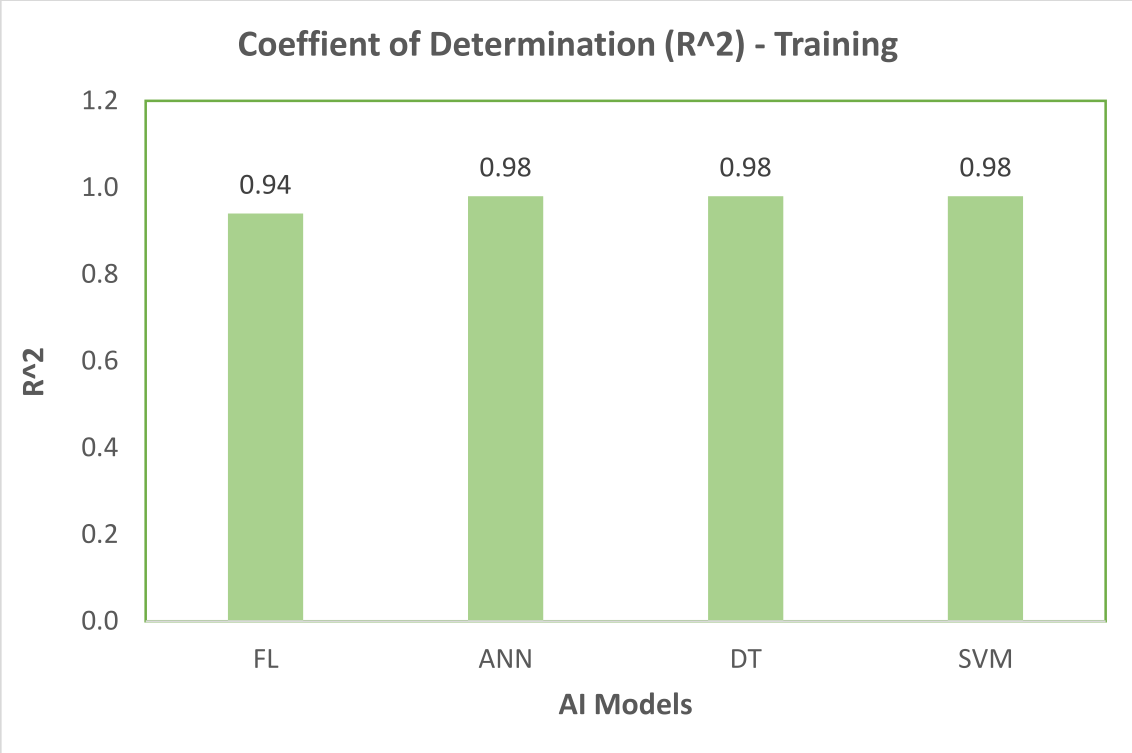

Figure 0.19: R-Square for Predicted Oil Rates from AI Models in H & ML Wells – Training

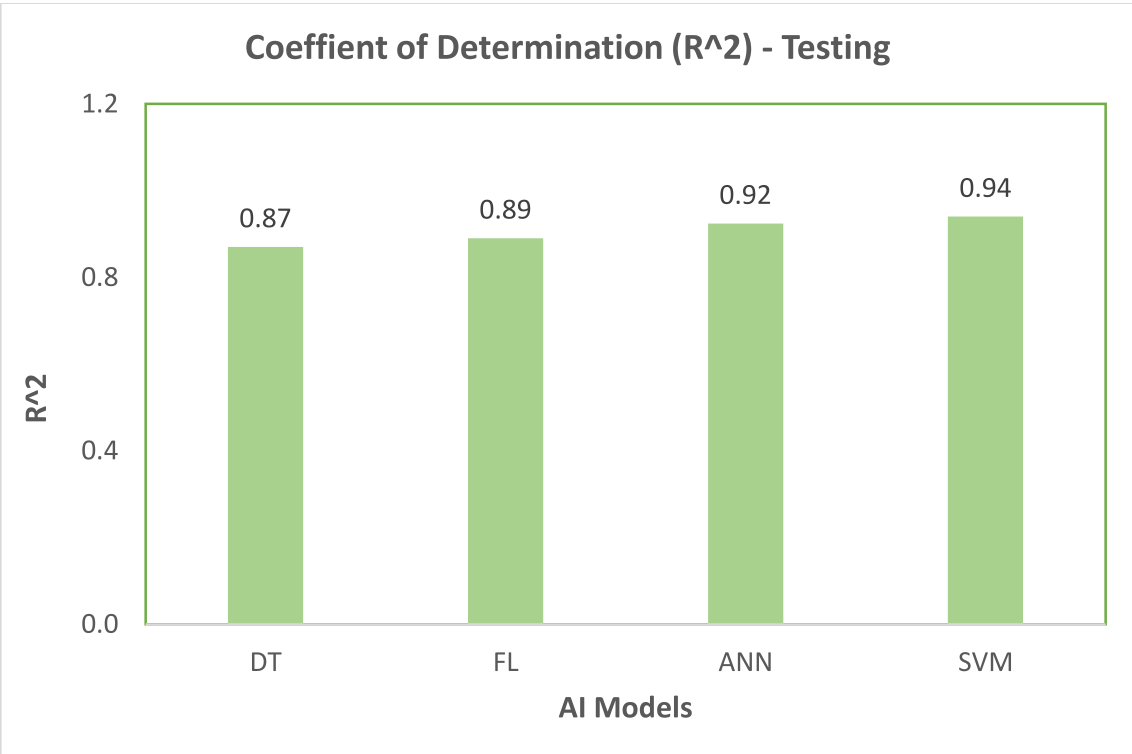

Figure 0.20: R-Square for Predicted Oil Rates from AI Models in H & ML Wells – Testing

The results of AAPE of predicted oil rates from training and testing AI models for the combination data sets of H & ML wells are plotted in **Figures 5.21 & 5.22.** The results showed that DT was the best training model for prediction oil rates with an AAPE of 4.3%. The least accuracy training model was FL with AAPE of 8.7%. For the testing models, the maximum value of AAPE was achieved by ANN with 9.5% whereas FL gave the lowest AAPE value of 18% as plotted in **Figure 5.22**.

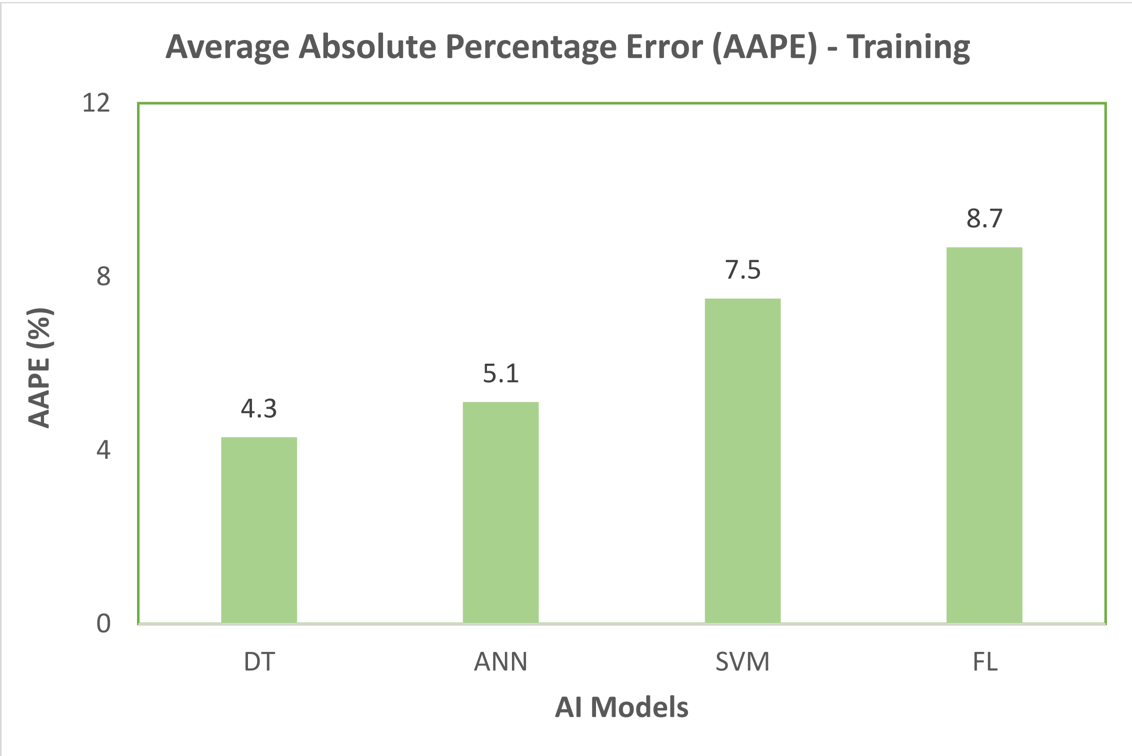

Figure 0.21: AAPE for Predicted Oil Rates from AI Models in H & ML Wells – Training

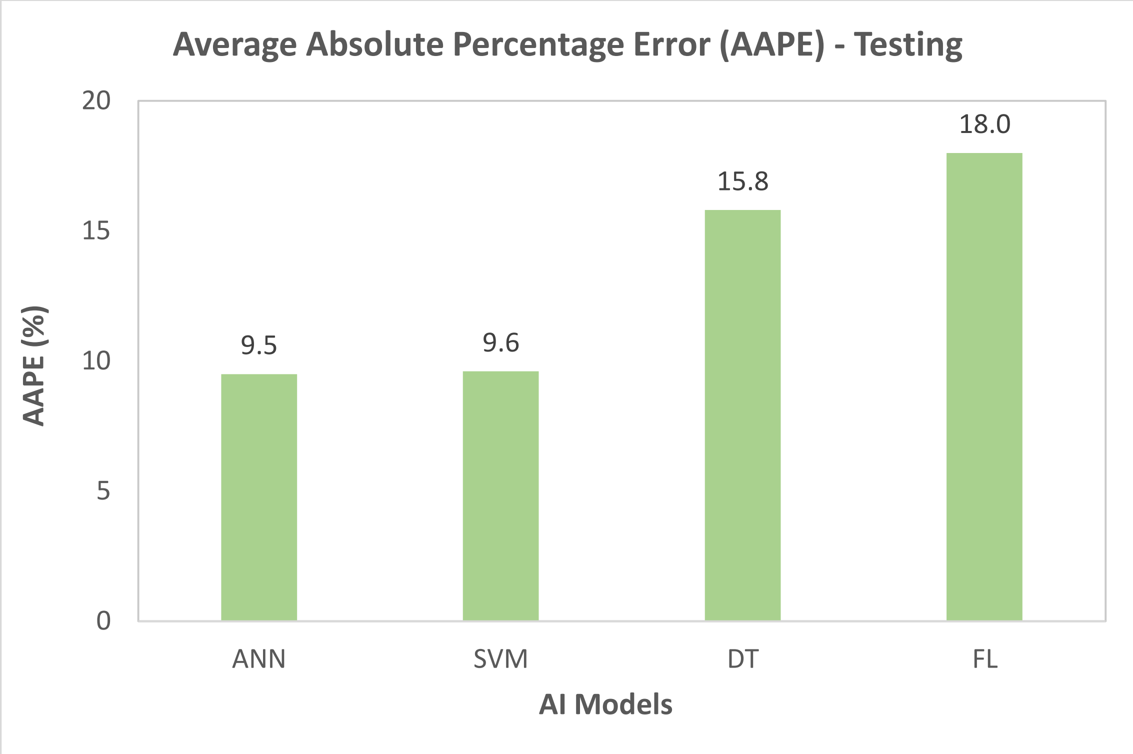

Figure 0.22: AAPE for Predicted Oil Rates from AI Models in H & ML Wells – Testing

The crossplots for of the predicted oil rates from all AI models versus the actual oil rates from H wells, ML wells and combination of H & ML Wells are shown in the following figures.

Figure 5.23 & 5.24 are showing the plotted results of training and testing models of the predicted oil rates from ANN versus the actual oil rates for H wells. The results of training & testing ANN models are: 5% & 6.9% for AAPE and 0.98 & 0.98 for R^2.

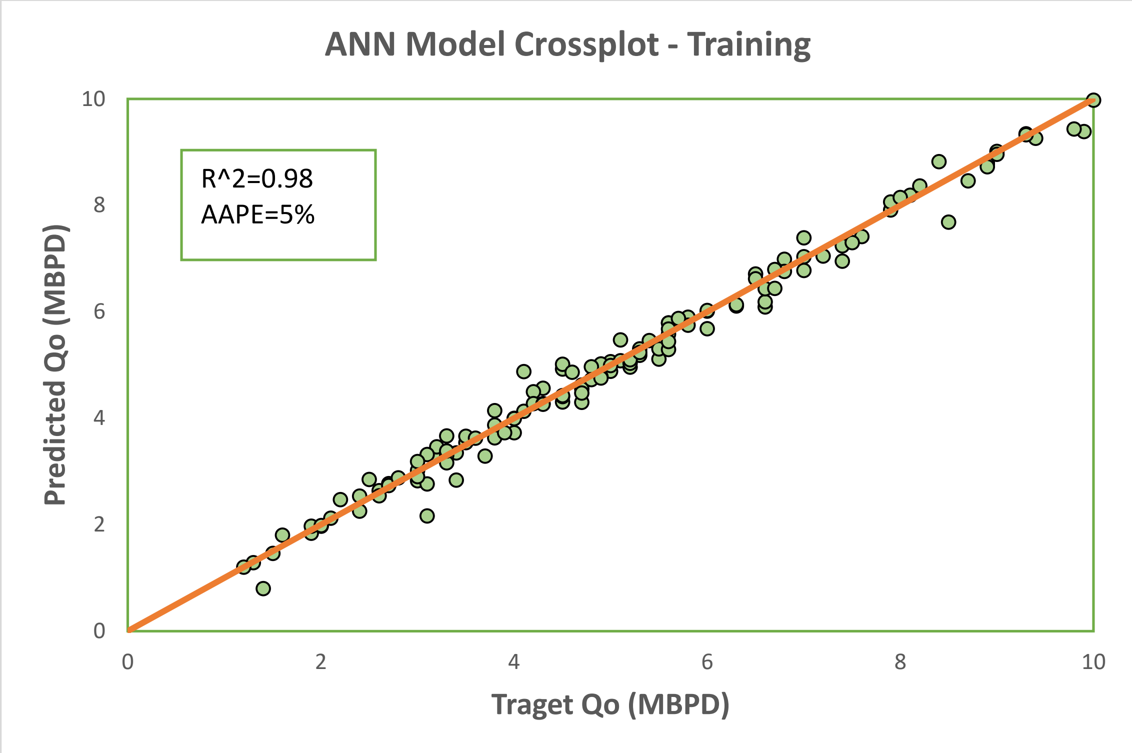

Figure 0.23: Crossplot of Predicted Oil Rates with ANN Model in H Wells – Training

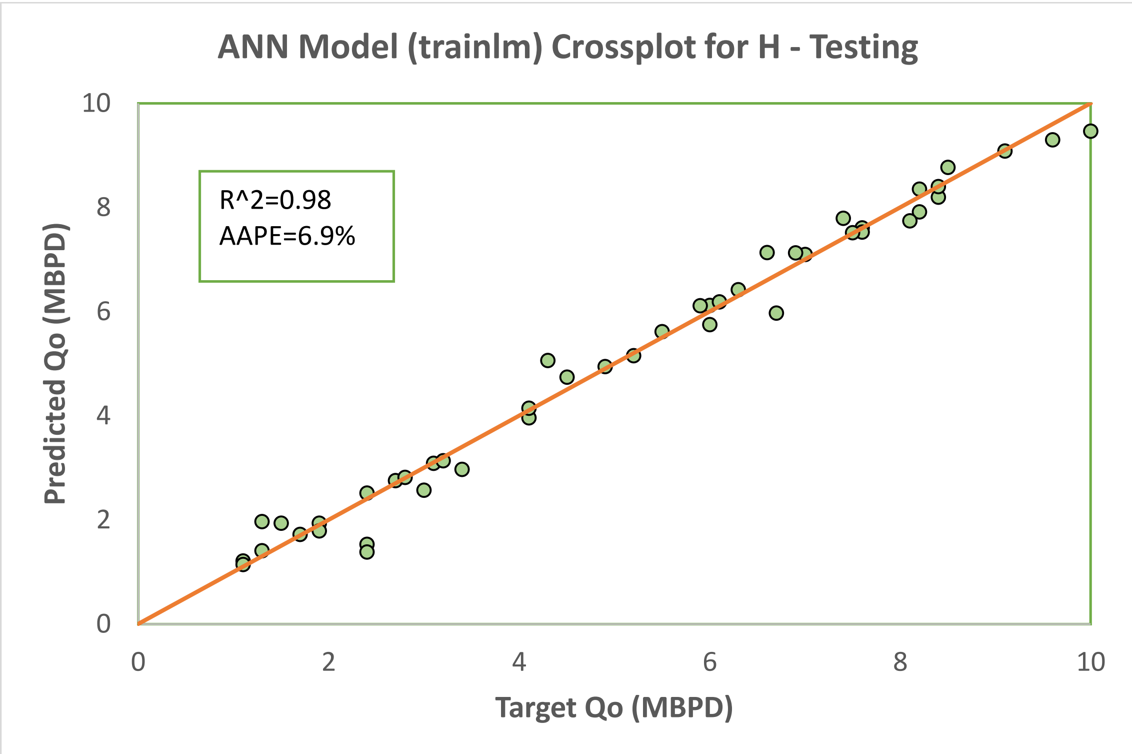

Figure 0.24: Crossplot of Predicted Oil Rates with ANN Model in H Wells - Testing

Figure 5.25 & 5.26 are showing the results of the predicted oil rates from FL models versus the actual oil rates of H wells. On training model, the results of FL technique were: 7.5% of AAPE, 0.97 of R^2. On the testing model, FL provided the results of and AAPE of 16.6%, 0.92 of R^2.

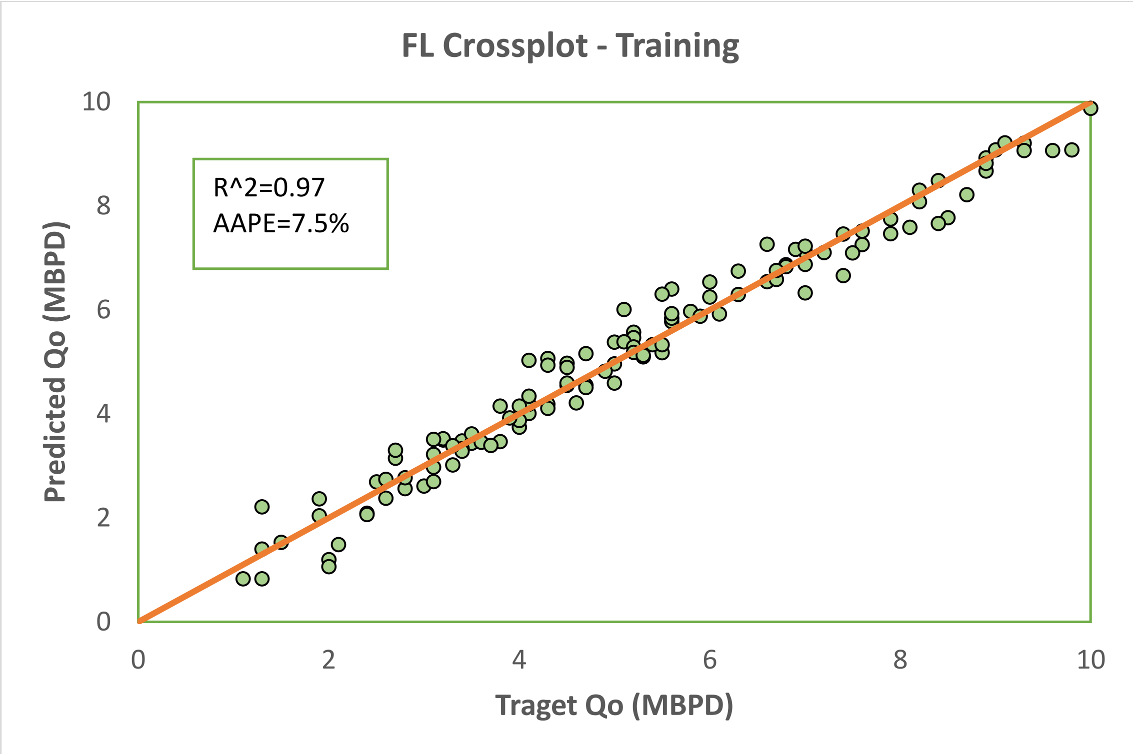

Figure 0.25: Crossplot of Predicted Oil Rates from FL Model for H Wells – Training

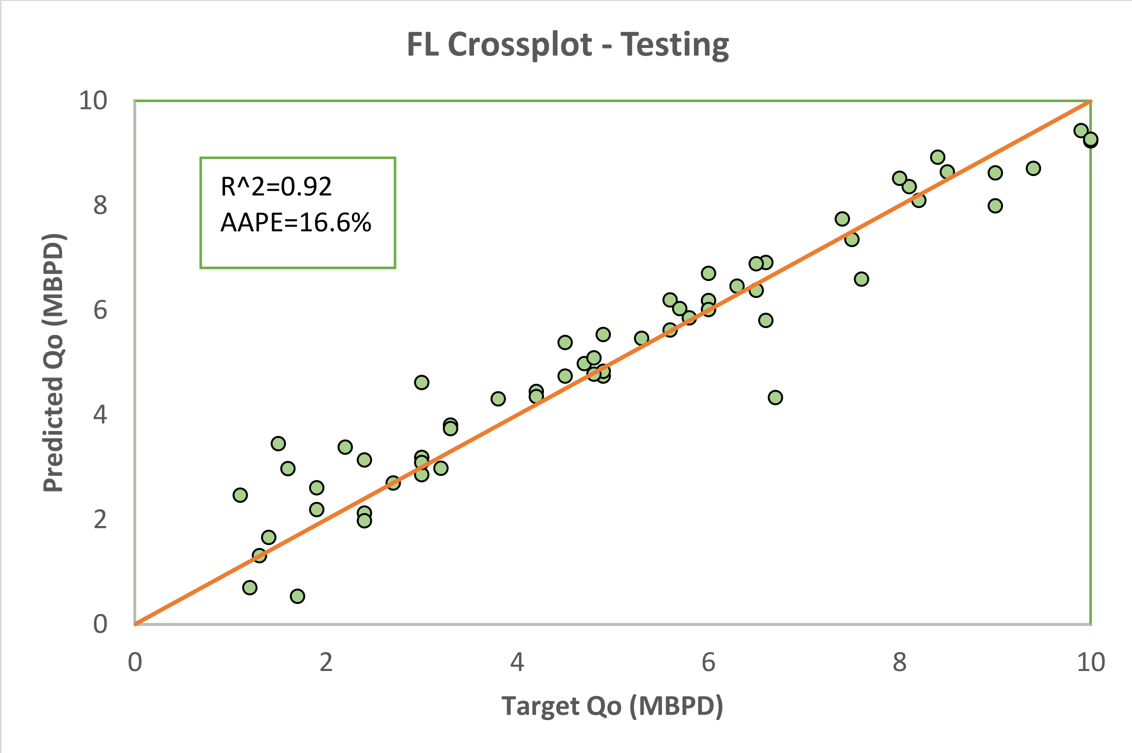

Figure 0.26: Crossplot of Predicted Oil Rates from FL Model for H Wells – Testing

Figure 5.27 & 5.28 are showing the results of the predicted oil flow rates from DT for training and testing models versus the actual oil rates of H wells. The results showed the DT models provided AAPE of 4% and R^2 of 0.94 for the training model. On testing model, however, the results were: AAPE is 19.2% and R^2 is 0.83.

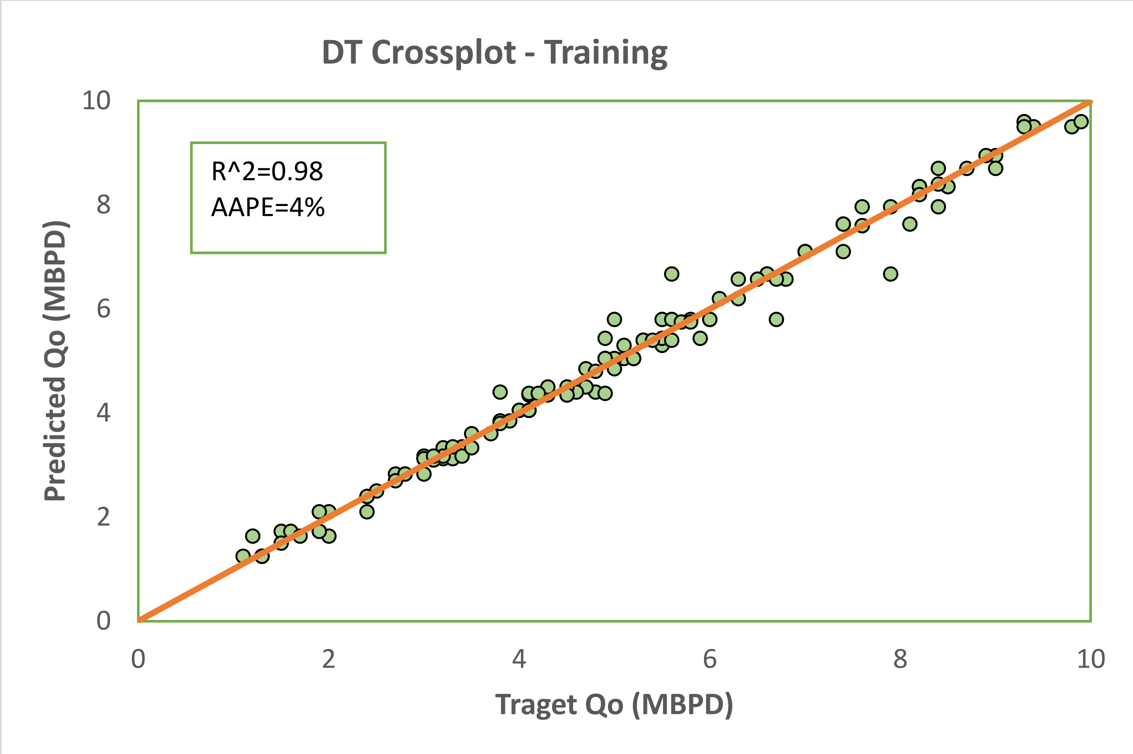

Figure 0.27: Crossplot of Predicted Oil Rates from DT Model for H Wells – Training

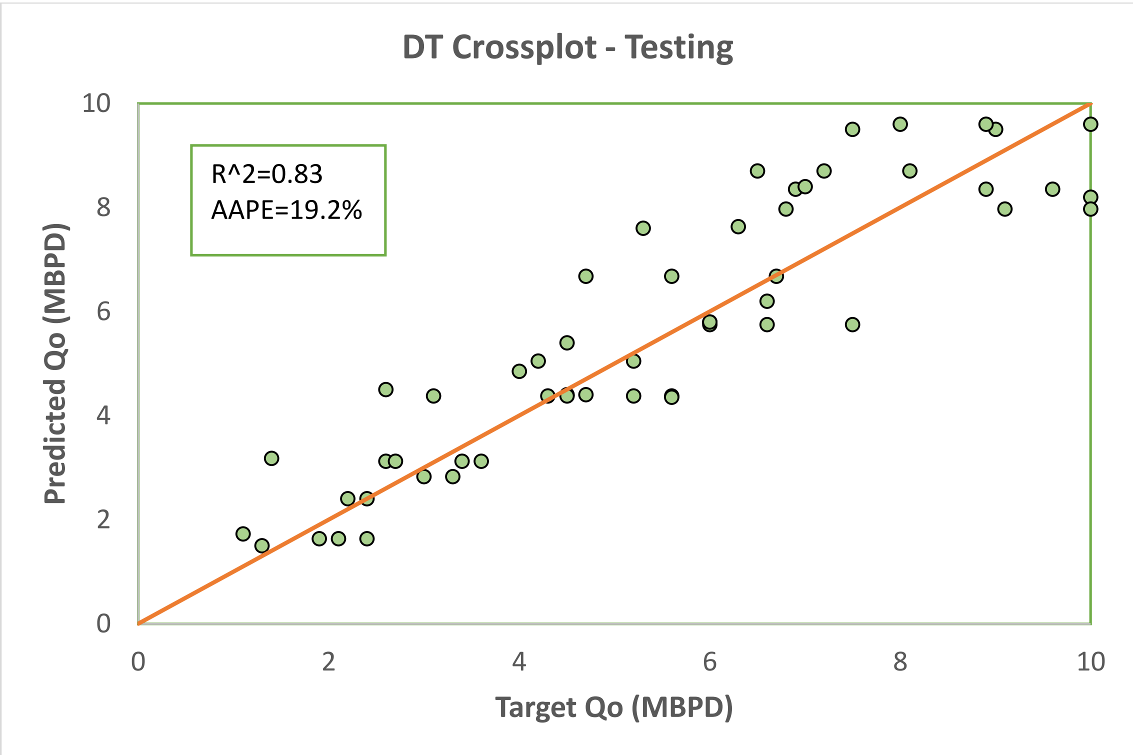

Figure 0.28: Crossplot of Predicted Oil Rates from DT Model for H Wells – Testing

Figure 5.29 & 5.30 are plotting results of the predicted oil rates from SVM for training and testing models versus the actual oil rates of H wells. The results of the SVM model were giving R^2 value of 0.99 and AAPE of 5.4% on the training AI models of H wells. On the testing model, AAPE of 7.2% and R^2 of 0.98 were obtained from SVM.

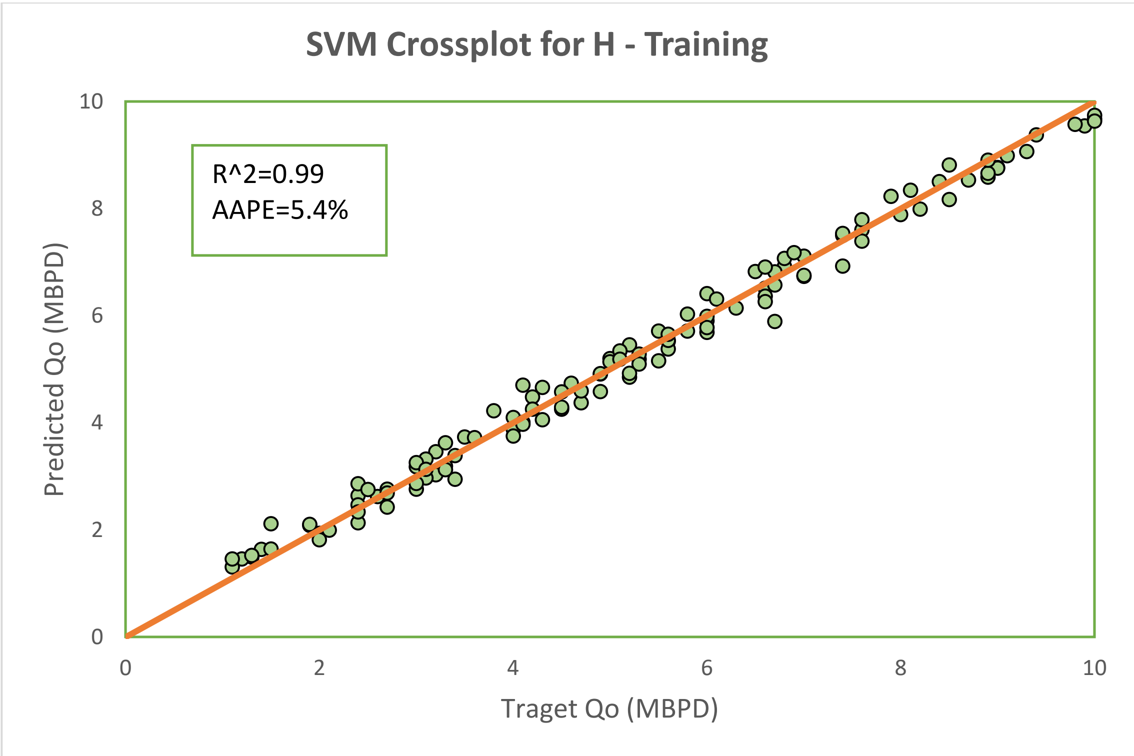

Figure 0.29: Crossplot of Predicted Oil Rates from SVM Model for H Wells - Training

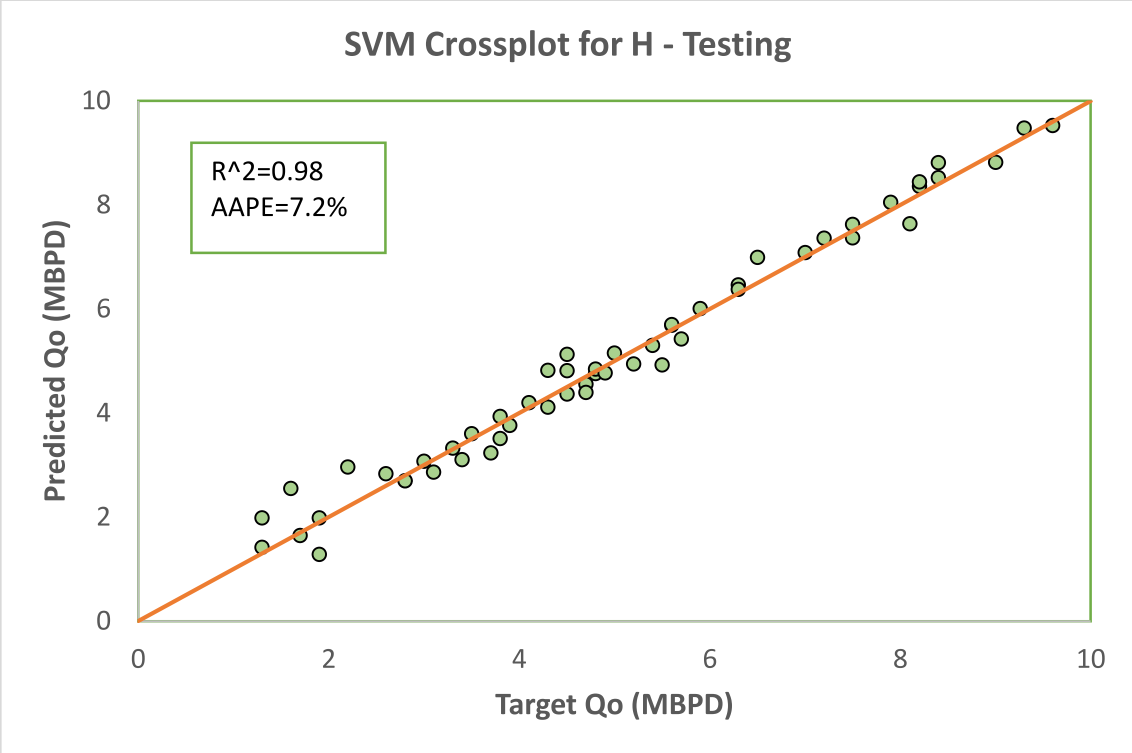

Figure 0.30: Crossplot of Predicted Oil Rate from SVM Model for H Wells – Testing

Figure 5.31 & 5.32 are illustrating the cross-plot results of the predicted oil flow rates from ANN for training and testing models versus the actual oil rates of ML wells. The results showed the ANN models were giving AAPE of 17.5% and R^2 of 0.8 from training models and AAPE of 19.2% and R^2 of 0.59 from testing model.

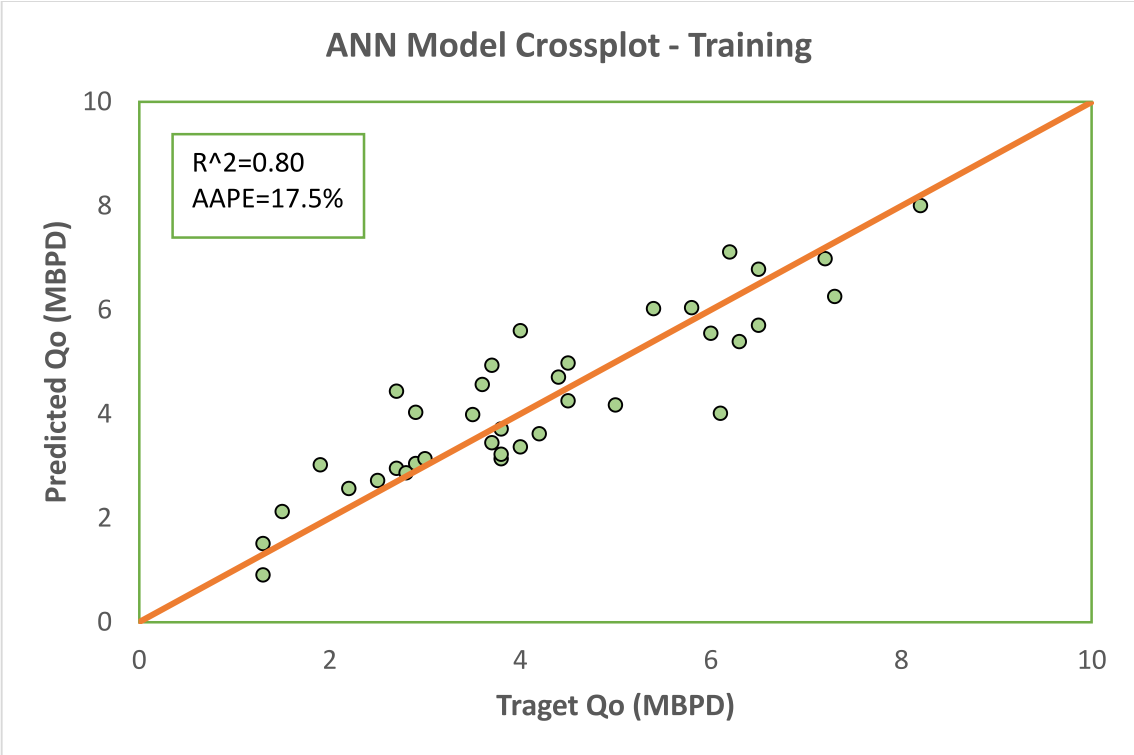

Figure 0.31: Crossplot of Predicted Oil Rates from ANN Model for ML Wells -Training

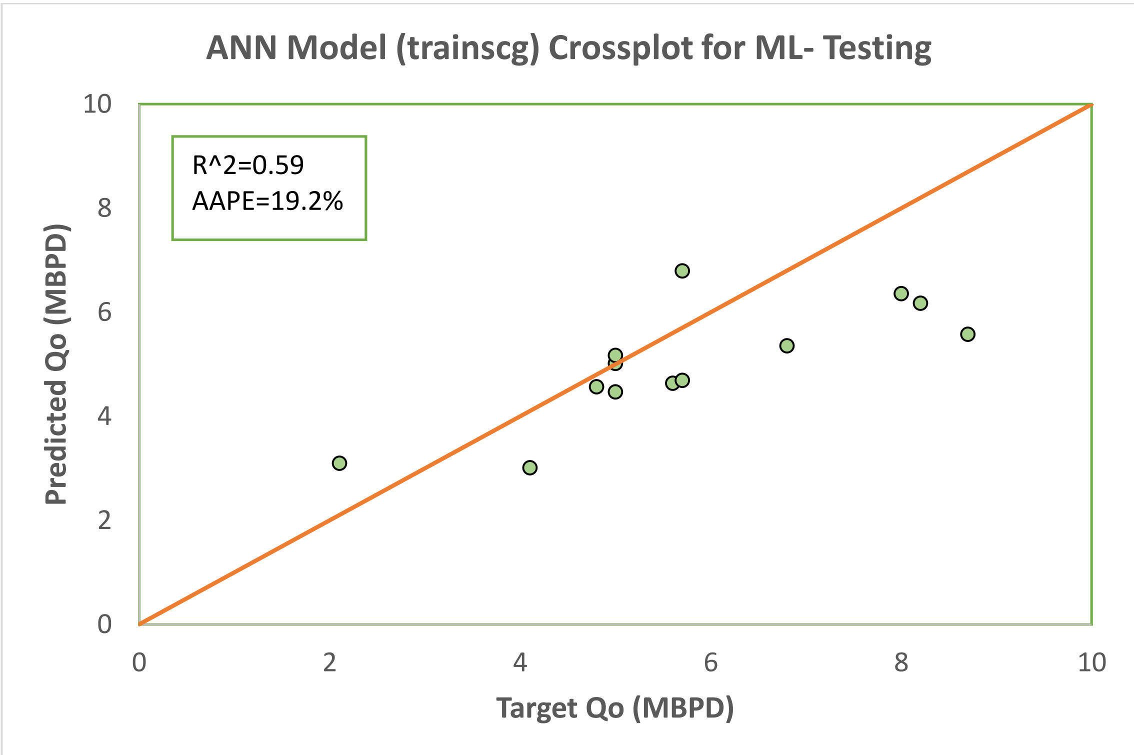

Figure 0.32: Crossplot of Predicted Oil Rates from ANN Model for ML Wells - Testing

Figure 5.33 & 5.34 are showing the results of the predicted oil rates from FL for training and testing models versus the actual oil rates of ML wells. The results showed the training FL models was providing the best prediction method for ML wells with AAPE of 10.3% and R^2 of 0.89. On testing model, the results were: AAPE is 36.8% and R^2 is 0.2.

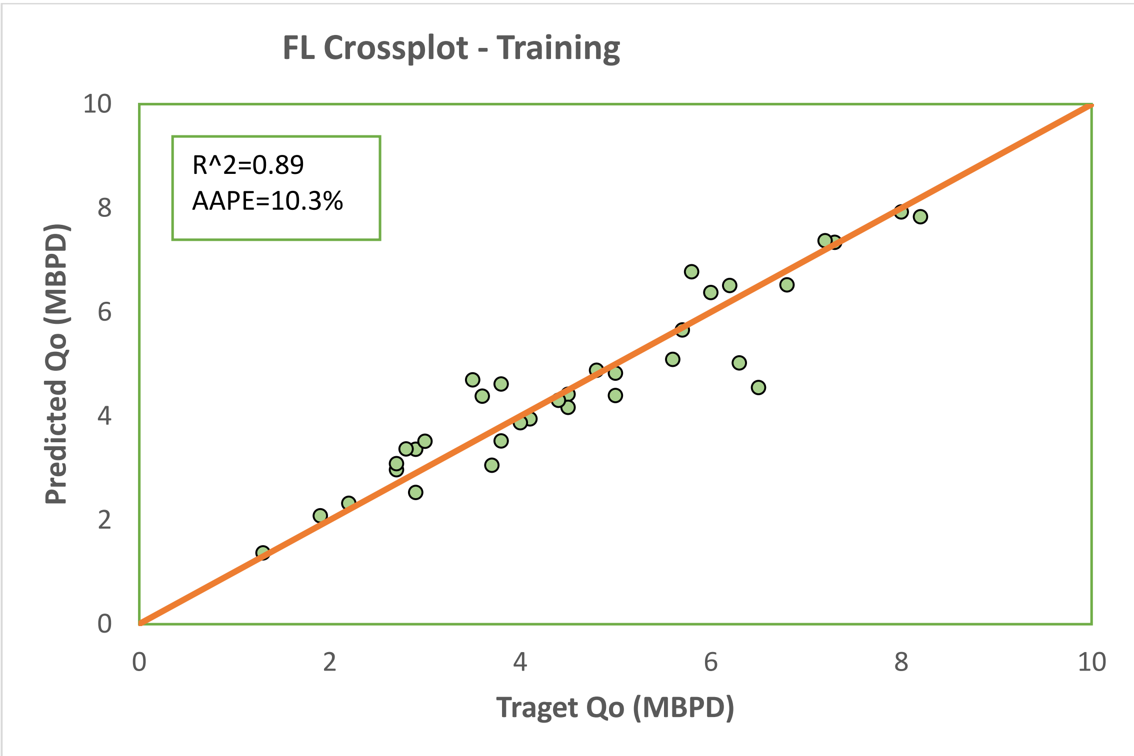

Figure 0.33: Crossplot of Predicted Oil Rates from FL Model for ML Wells – Training

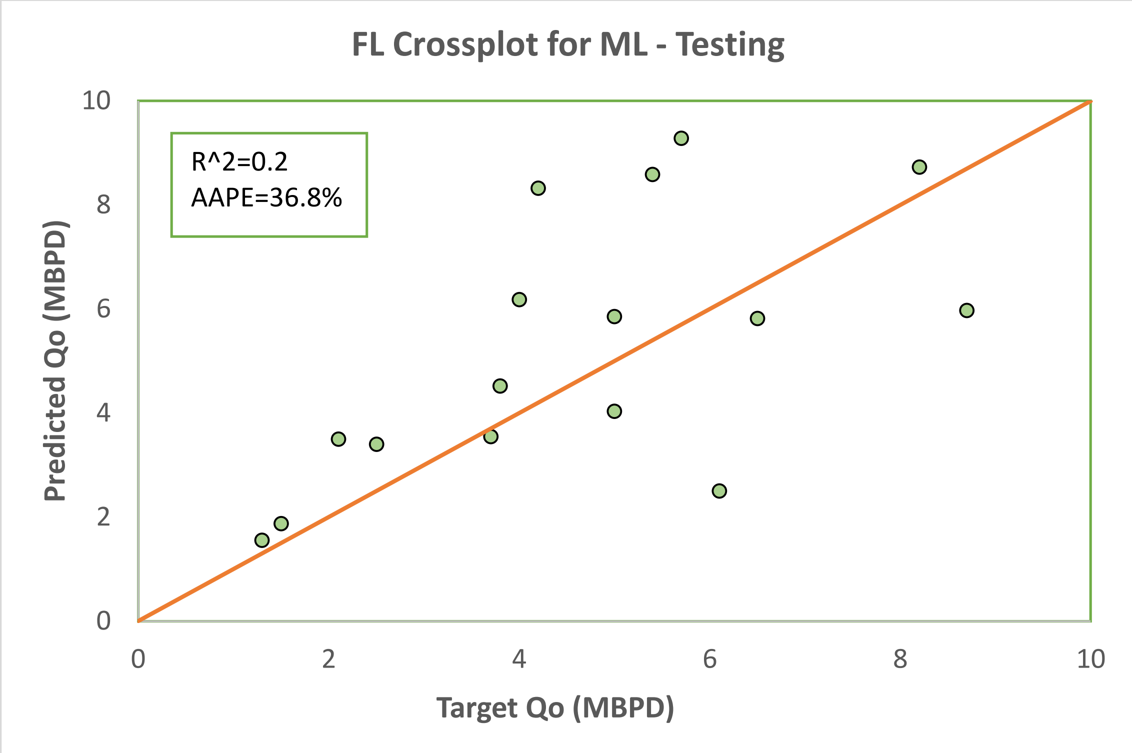

Figure 0.34: Crossplot of Predicted Oil Rates from FL Model for ML Wells – Testing

Figure 5.35 & 5.36 are plotting the results of training and testing models of the predicted oil rates from DT versus the actual oil rates for ML wells. The results of training & testing from DT models are: 17.5% & 32.6% for AAPE, and 0.85 & 0.45 for R^2 respectively.

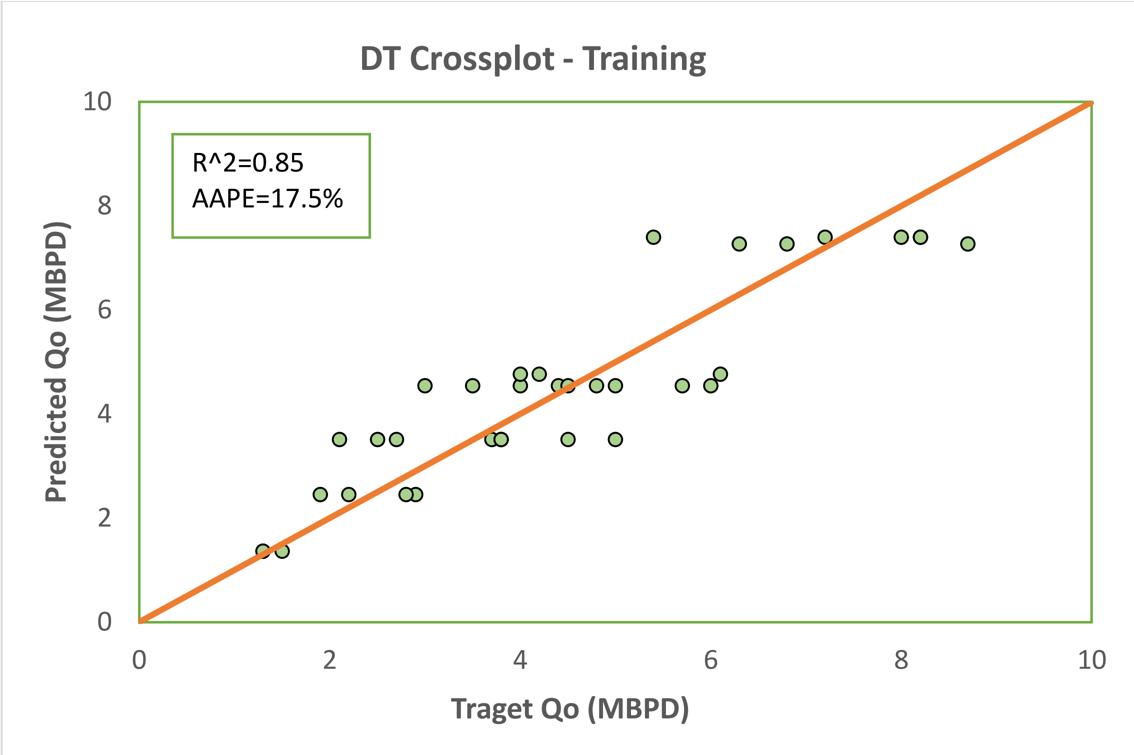

Figure 0.35: Crossplot of Predicted Oil Rates from DT Model for ML Wells – Training

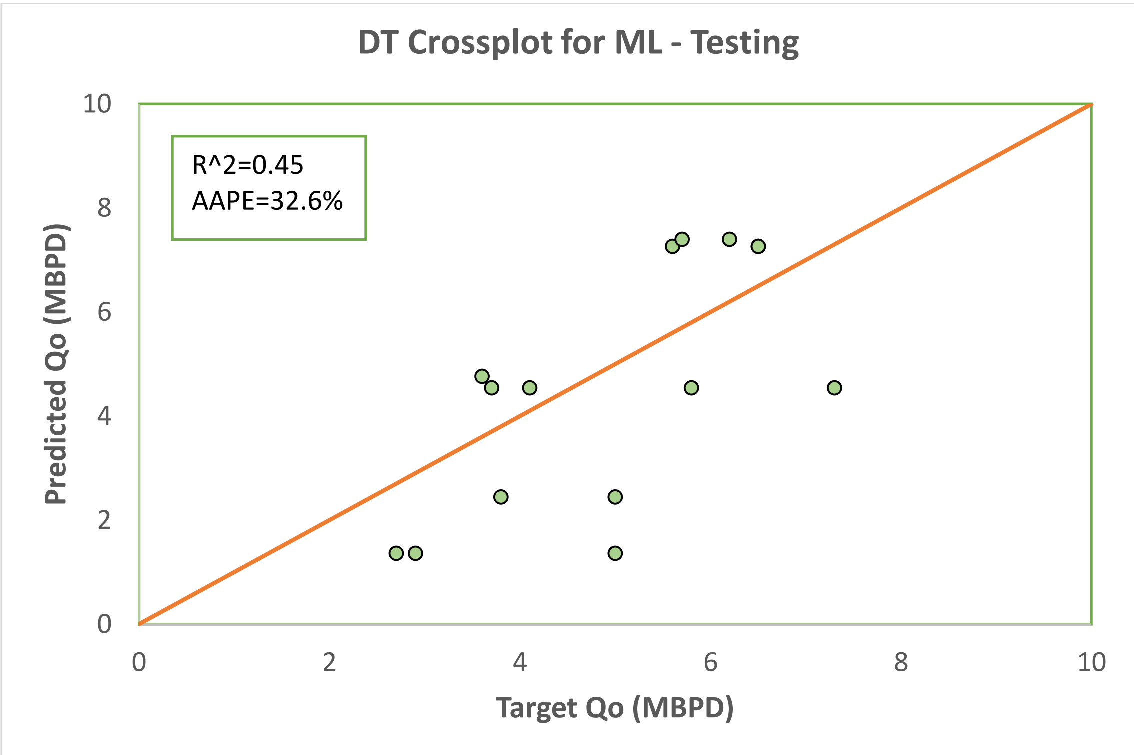

Figure 0.36: Crossplot of Predicted Oil Rates from DT Model for ML Wells – Testing

Figure 5.37 & 5.38 are illustrating the plotted results of the predicted oil rates from SVM for training and testing models versus the actual oil rates of ML wells. The results of the testing SVM models were giving the best estimation technique on oil rates forecasting of ML wells. The testing results of SVM were: AAPE of 11.7% and 0.83 of R^2. On the training model at **Figure 5.37**, the results are: AAPE of 18.90% and 0.81 for R^2.

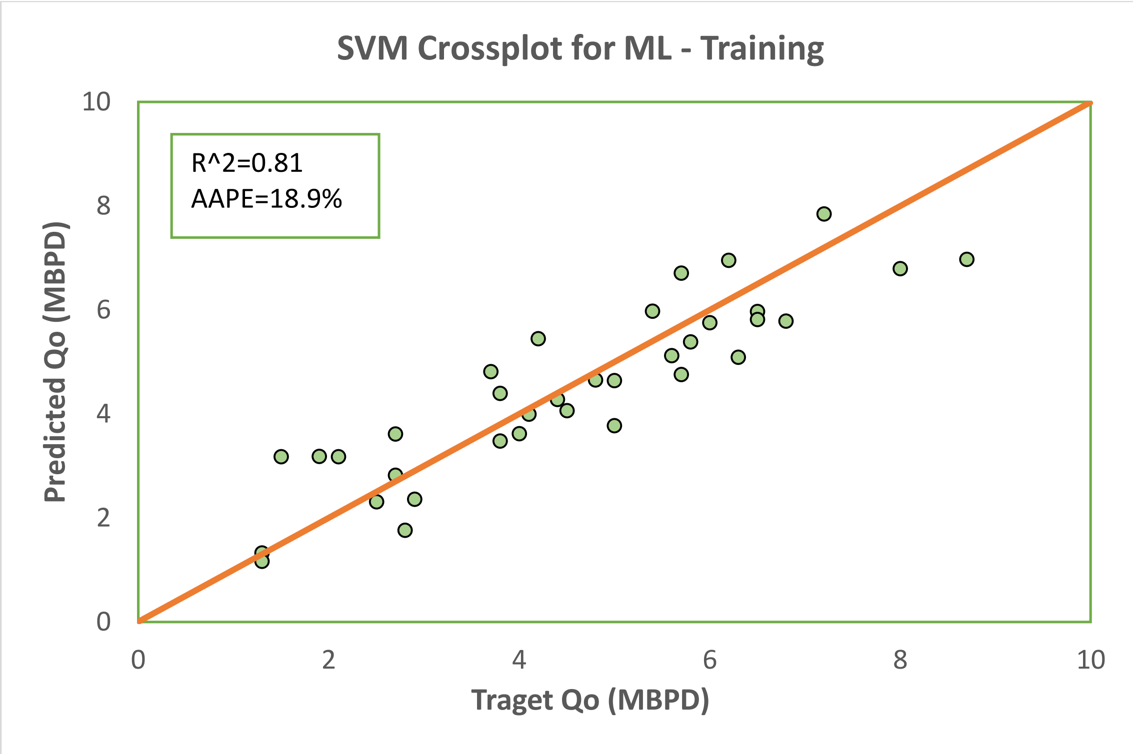

Figure 0.37: Crossplot of Predicted Oil Rates from SVM Model for ML Wells – Training

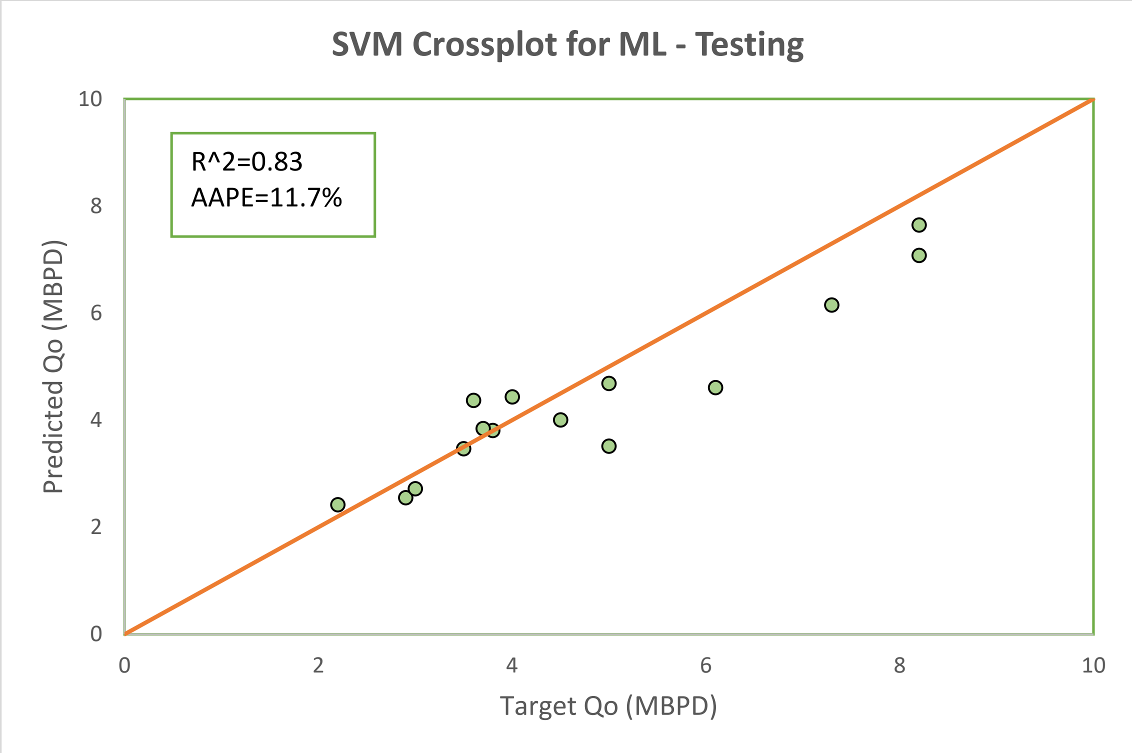

Figure 0.38: Crossplot of Predicted Oil Rates from SVM Model for ML Wells – Testing

Figure 5.39 & 5.40 are illustrating the results of the predicted oil flow rate from ANN for training and testing models versus the actual oil rates of combination data sets from H & ML wells. The results showed the ANN models were giving AAPE of 5.1% and R^2 of 0.98 from training models. The best predicting accuracy on the testing model was achieved by ANN with an AAPE of 9.5% for H & ML wells data sets. The testing model was giving R^2 value of 0.92.

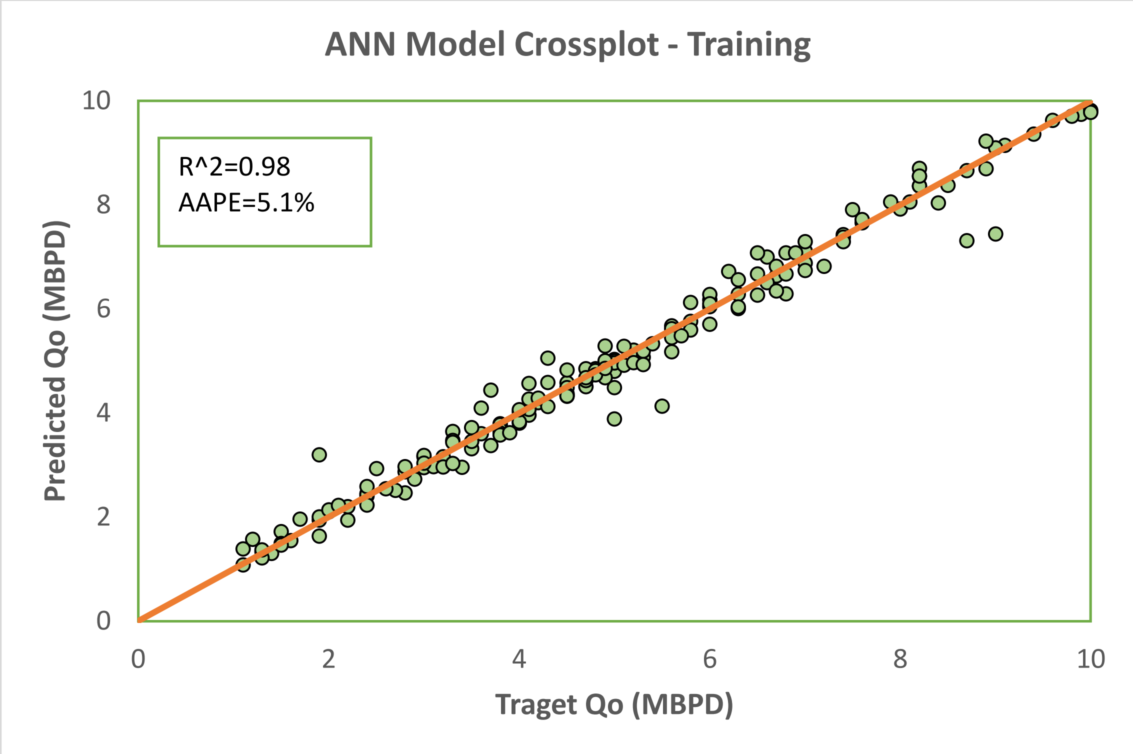

Figure 0.39: Crossplot of Predicted Oil Rate from ANN Models for H & ML Wells – Training

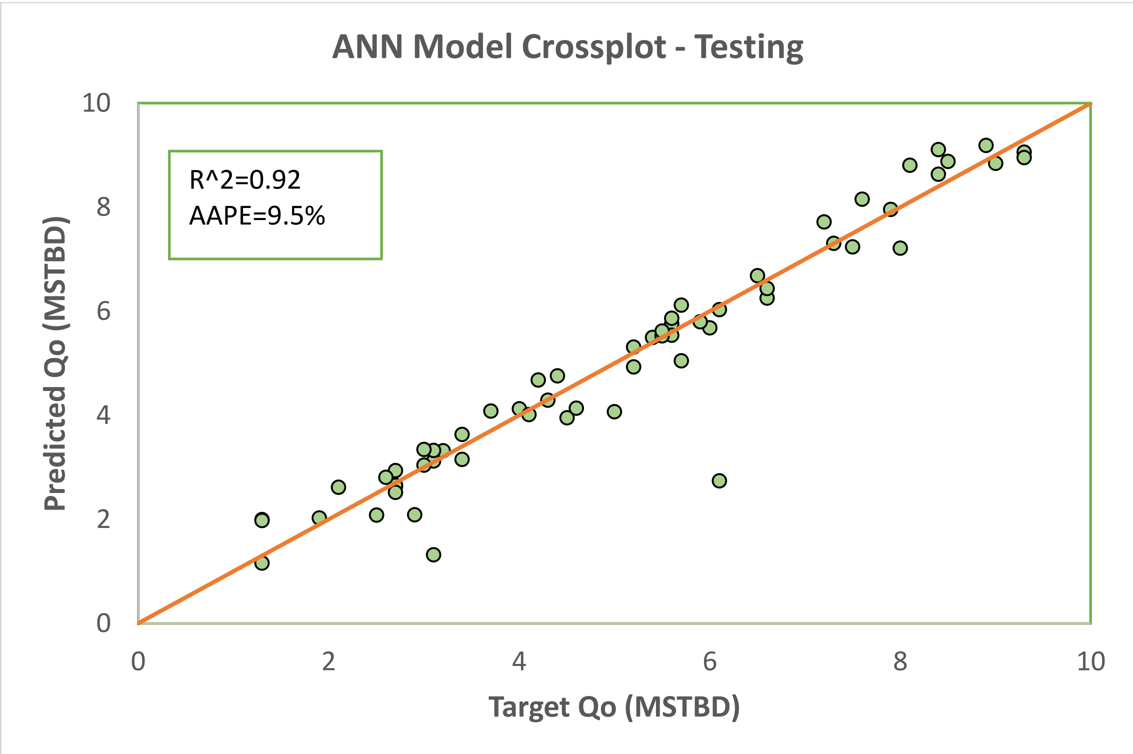

Figure 0.40: Crossplot of Predicted Oil Rate from ANN Models for H & ML Wells – Testing

Figure 5.41 & 5.42 are depicting the results of training and testing models of the predicted oil rates from FL versus the actual oil rates of H & ML wells data sets. The results of training & testing from FL models are: 8.7% & 18% for AAPE and 0.94 & 0.89 for R^2 respectively.

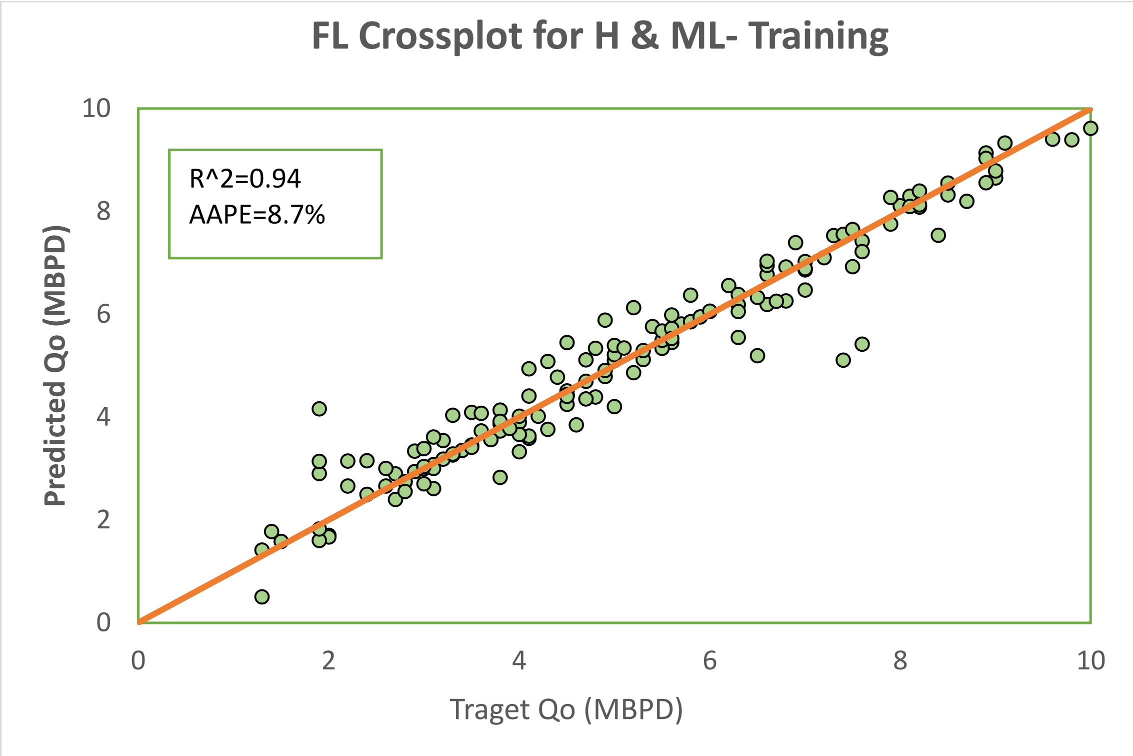

Figure 0.41: Crossplot of Predicted Oil Rates from FL Model for H & ML Wells – Training

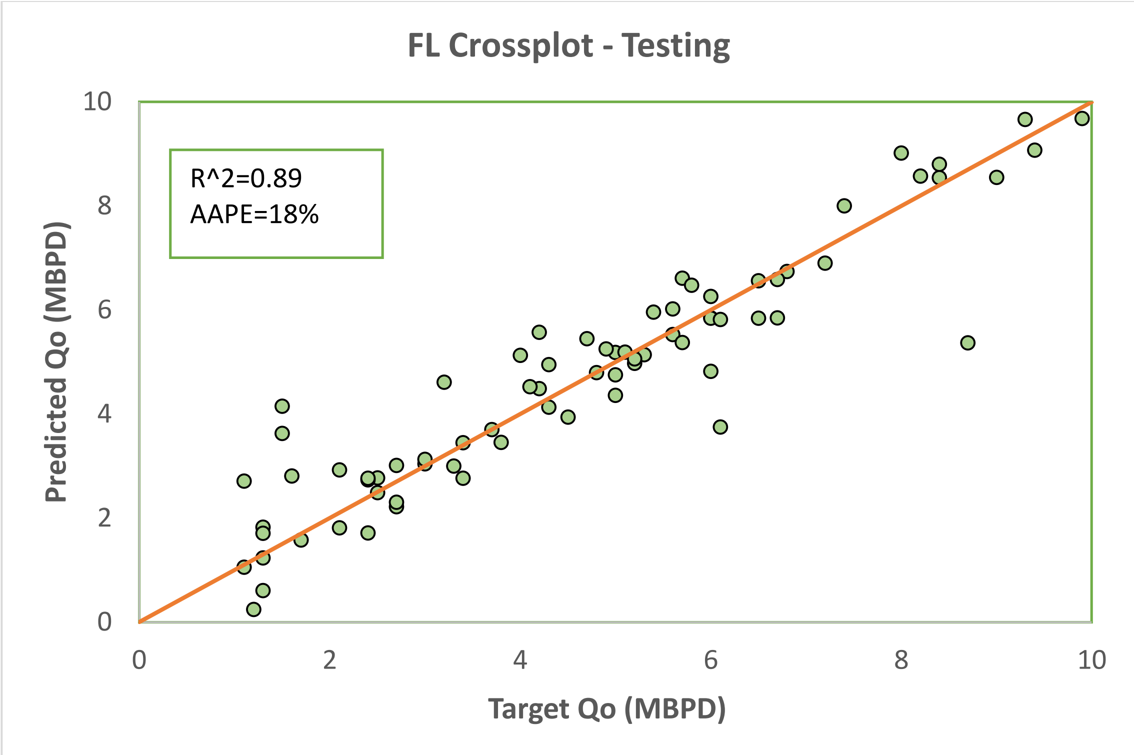

Figure 0.42: Crossplot of Predicted Oil Rates from FL Model for H & ML Wells – Testing

Figure 5.43 & 5.44 are illustrating the cross-plot results of the predicted oil rates from DT for training and testing models versus the actual oil rates of H & ML wells. The results showed DT model was providing the best prediction training AI method for combination data sets of H & ML wells with AAPE of 4.3%. The training model gave result of 0.98 for R^2. On testing model, the results were: AAPE is 15.8% and R^2 is 0.87.

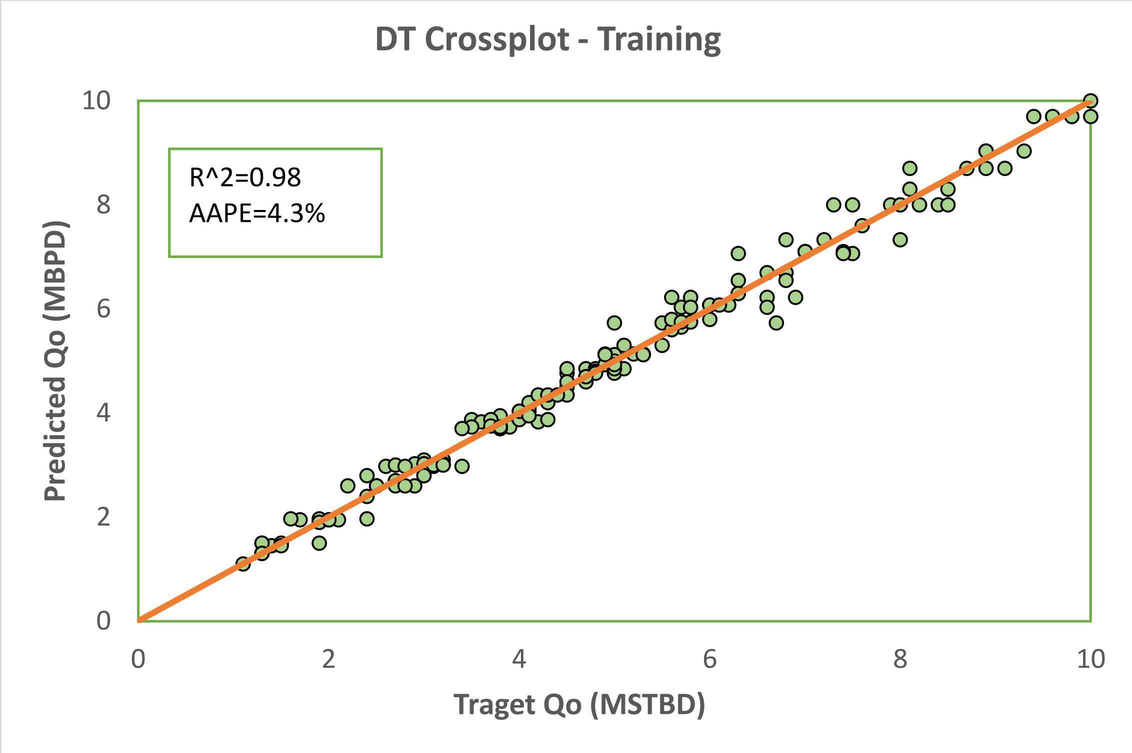

Figure 0.43: Crossplot of Predicted Oil Rates from DT Model for H & ML Wells – Training

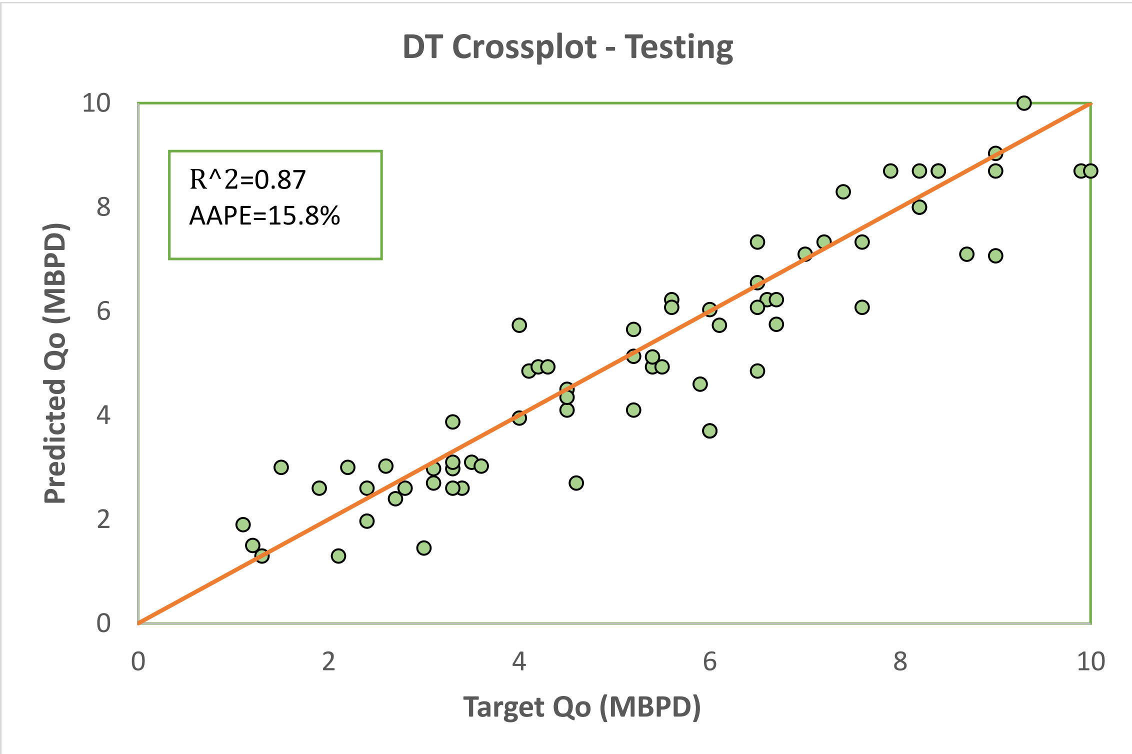

Figure 0.44: Crossplot of Predicted Oil Rates from DT Model for H & ML Wells – Testing

Figure 5.45 & 5.46 are showing the results of the predicted oil rates from SVM models versus the actual oil rates of H & ML wells. On training model, the results of SVM technique were: 7.5% of AAPE and 0.98 of R^2. For testing model, the results were: AAPE is 9.6% and 0.94 for R^2.

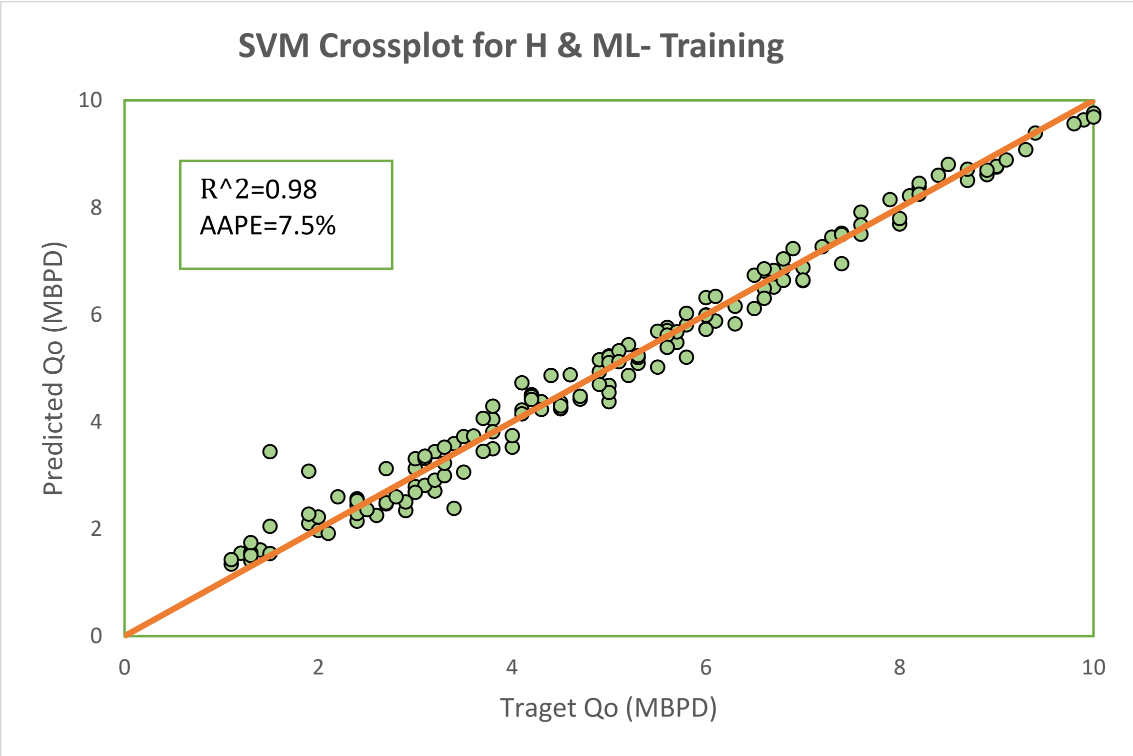

Figure 0.45: Crossplot of Predicted Oil Rates from SVM Model for H & ML Wells – Training

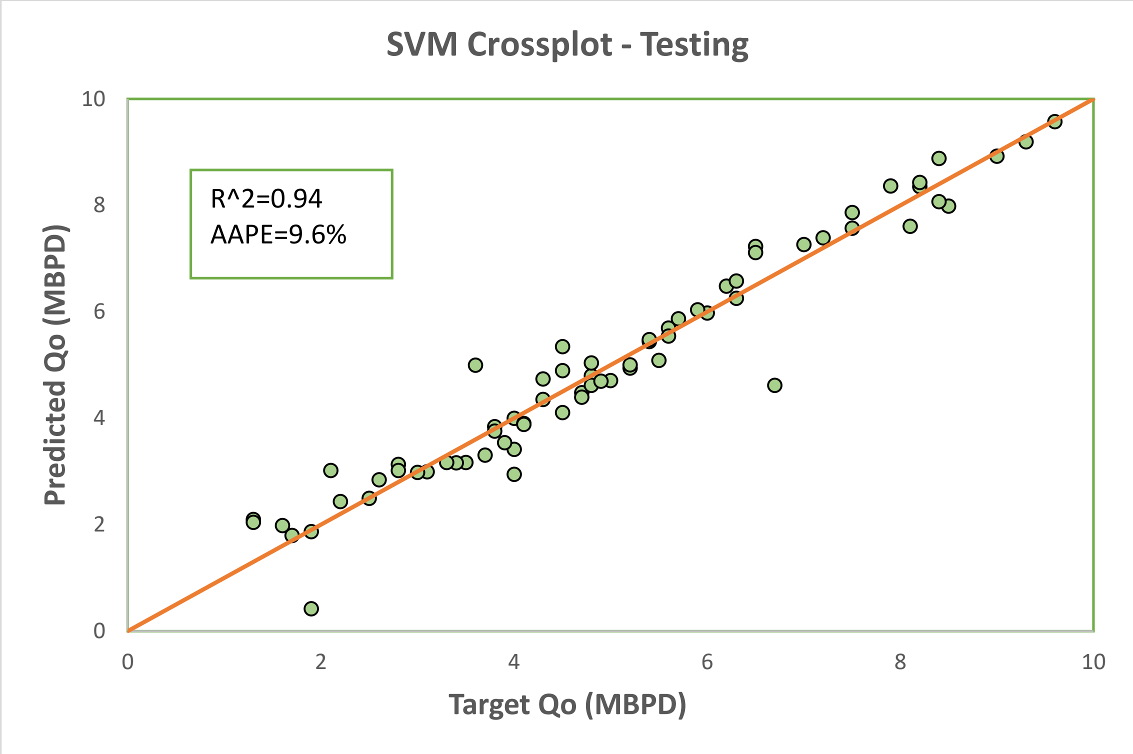

Figure 0.46: Crossplot of Predicted Oil Rates from SVM Model for H & ML Wells – Testing

The graphical plot for all AAPE results obtained from all oil rates predicting methods are illustrated in Figure 5.47. The final results shows that ANN was giving the best estimation of oil rates with AAPE of 6.9% while Butler correlations was providing the highest AAPE of 61.4%. Additionally, all AI techniques offered better estimation results than the existing correlations.

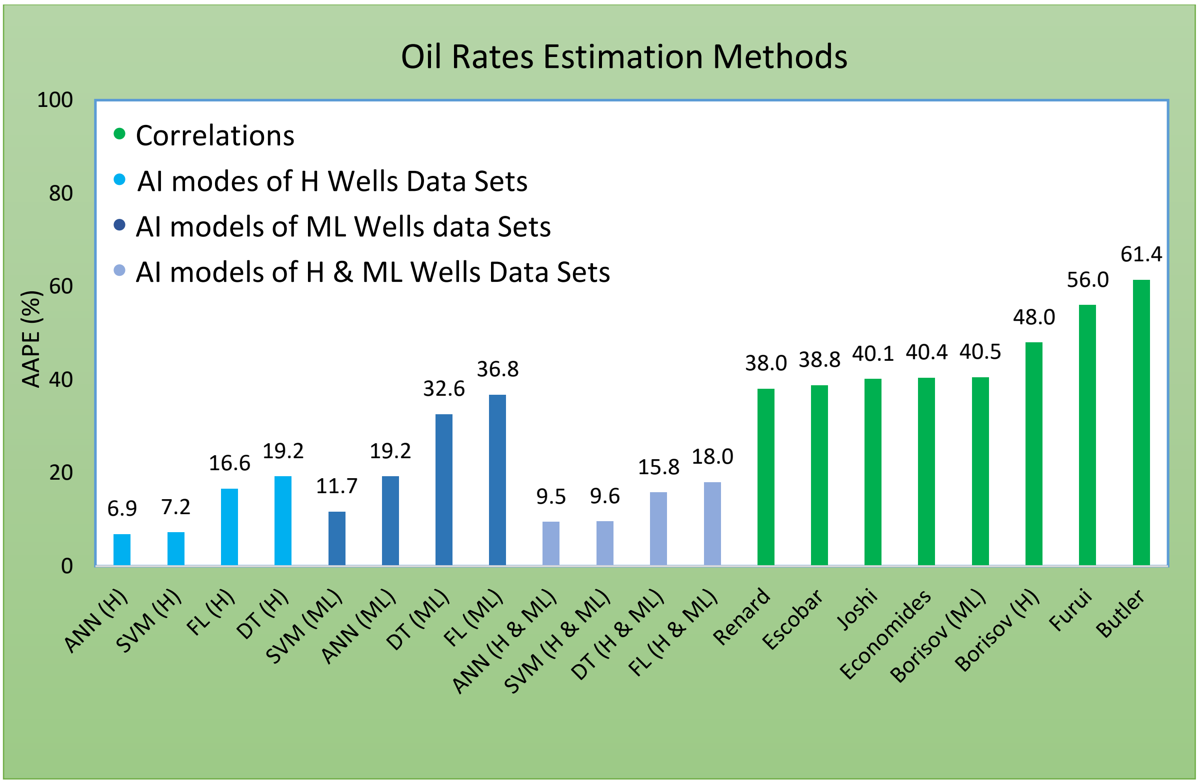

Figure 0.47: Summary Results of AAPE for All Estimation Methods of Oil Rates

5.3 Empirical Correlation using Artificial Neural Network Models

With application of AAN modelling, new empirical correlations have been derived for estimating oil flow rates in H wells and combination of H & ML wells data sets. The new correlations were obtained based on the results of weights and biases from the optimum results for H and the combination data sets of H & ML wells with application of the training function 'trainlm' of tan sigmoidal transfer function. The final form of the proposed correlation for all both well confirmation is giving by (**Equation 5.1**):

$$Qo_{\mathrm{n}} = \left[\sum_{\mathrm{i}=1}^{\mathrm{N}} \mathrm{w}_{2_i} \left(\frac{2}{1+\mathrm{e}^{-2\left(W_{1_{i,1}} P_{1_n} + W_{1_{i,2}} P_{2_n} + W_{1_{i,3}} P_{3_n} + W_{1_{i,4}} P_{4_n} + W_{1_{i,5}} P_{5_n} + W_{1_{i,6}} P_{6_n} + W_{1_{i,7}} P_{7_n} + \mathrm{b}_{1_i}\right)}} \right) - 1 \right] + \mathrm{b}_2 \tag{5.1}$$

Where:

Q_{o_n} : Normalized predicted oil rate

W_{1_j} *and* W_{1_j}: Weights in between hidden and outer layers and the values are given in **Table 5.6** for H wells and **Table 5.7** for H & ML wells data sets.

b_{1_i} & b_2: Bias and the values for H wells and H & ML wells are given in **Table 5.6 & 5.7** respectively.

P_{1_n}: Normalized value of choke size

P_{2_n}: Normalized value of logarithmic wellhead pressure (log (P_w))

P_{3_n}: Normalized value of water cut

P_{4_n}: Normalized value of pressure difference between reservoir and flowing bottom hole pressure ($\Delta P = P_r - P_{wf}$)

P_{5_n}: Normalized value of horizontal effective length (log (L_e))

P_{6_n}: Normalized value of reservoir thickness

P_{7_n}: Normalized value of the ratio of average horizontal permeability to oil formation volume factor and oil viscosity ($\frac{K_h}{B_o \mu_o}$)

Following are the main steps for utilization of the new correlations to predict oil flow rates in complex wells:

1. Make the input parameters in normalized values with ranges of -1 to 1. It is done by two slope points in the following equation:

$$\frac{y-y_{min}}{y_{max}-y_{min}} = \frac{x-x_{min}}{x_{max}-x_{min}} \tag{5.2}$$

Where;

y_{min}: is equal to -1

y_{max}: is equal to 1

x: Current input parameter

x_{min}: Minimum input parameter

x_{min}: Maximum input parameter.

The normalization equation-5.1 becomes:

$$y = 2 * \left[\frac{x-x_{min}}{x_{min}-x_{max}}\right] - 1 \tag{5.3}$$

2. Calculate the oil flow rates in normalized form with using equation (5.3) by applying the values of bias, weights and normalized parameters.
3. Convert the results of oil flow rates from normalized to real values with using the following equation:

$$Q_o = \frac{(10-1.1)}{2} * (Qo_{\mathrm{n}} + 1) + 1.1 = 4.45\ Qo_{\mathrm{n}} + 5.5 \tag{5.4}$$

Table 0.6: Weights and Biases of ANN Empirical Model for H Wells

Hidden Layer Neurons (N)	**Weights between Input & Hidden Layer (W1)**							**Weights between Hidden & output Layer (W2)**	**Hidden Layer Bias (b1)**	**Output Layer Bias (b2)**
1	0.1	0.1	0.1	0.8	0.1	-1.6	0.0	-2.2	-1.9	-0.5
2	-0.7	-0.4	-0.9	-1.5	-1.0	-1.0	-0.8	-1.0	1.1	
3	0.1	0.2	0.1	-1.3	0.0	0.9	0.0	-1.3	-1.7	
4	0.0	0.0	0.0	-0.7	0.0	-0.8	0.0	-2.5	-0.3	
5	0.0	1.1	-0.7	-0.1	0.0	-0.2	1.0	0.0	1.9	
6	-0.8	-0.1	0.1	-0.4	-0.9	0.8	1.2	0.6	-2.1	

Table 0.7: Weights and Biases of ANN Empirical Model for H & ML Wells

Hidden Layer Neurons (N)	**Weights between Input & Hidden Layer (W1)**							**Weights between Hidden & output Layer (W2)**	**Hidden Layer Bias (b1)**	**Output Layer Bias (b2)**
1	-1.51	-1.15	0.14	-0.23	-0.07	2.69	-0.69	0.19	1.02	-2.45
2	-2.08	0.85	1.03	1.53	-0.55	2.05	0.94	0.21	0.84	
3	-1.31	-1.43	1.50	-0.96	-0.58	3.02	1.62	0.73	6.31	
4	-0.49	-0.36	-0.13	0.67	-0.11	-1.01	-0.15	-0.79	-1.02	
5	-1.04	0.85	-2.09	-0.88	1.95	3.49	-2.80	0.17	1.38	
6	-1.70	2.01	-1.47	-1.40	-2.11	0.45	0.48	0.92	-2.04	
7	-1.82	2.45	-1.42	-1.88	-2.61	0.70	0.27	-0.82	-2.59	
8	0.16	-0.06	-0.12	1.50	0.05	1.64	-0.28	1.19	0.65	
9	0.02	-0.08	0.10	1.36	0.03	-0.68	0.12	1.30	1.70	
10	1.65	-0.03	-0.60	-2.16	-0.70	0.42	-1.35	0.86	1.56	

To validate the accuracy of the new correlation, a new data sets from 10 wells were used to estimate the oil rates. The results of AAPE from the proposed correlation and other productivity correlations in reference with actual measurement are shown in Figure 5.47. The new correlations have the least AAPE of 8.3% for H wells and 8.9% for H & ML wells while other published correlations provided higher AAPE that range from 38 to 58%. Hence, the proposed new correlations are offering high accuracy estimation of oil rates in easier and faster ways over all the available methods.

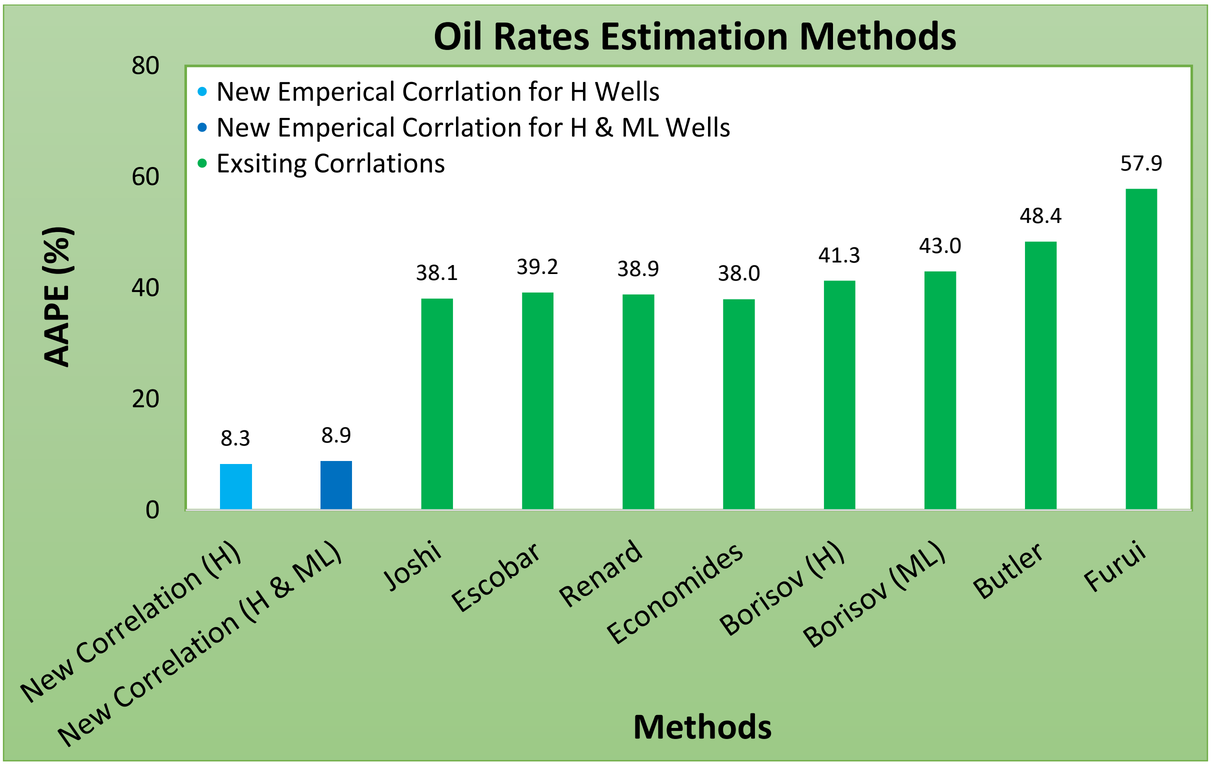

Figure 0.48: Comparison Results of AAPE from New and Existing Correlations

CHAPTER 6

CONCLUSIONS & RECOMMENDATIONS

6.1 Conclusions

Based on the results and discussion in chapter 5 and previous sections, followings are the conclusions:

- Available well performance correlations for horizontal & multilateral wells failed in a big margin in estimating oil rate for the used dataset.
- AI models proved superiority over other available well performance correlations by achieving acceptable error.
- ANN outperformed among all other AI techniques in estimating oil rate in Horizontal & Multilateral wells with AAPE of 9.5%. Moreover, the highest accuracy of production performance on horizontal wells was achieved by ANN model with an AAPE of 6.9%.
- New data sets was used to validate the proposed model which gave the best oil rate estimation with AAPE of 8.3%.

6.2 Recommendations:

- Test the new models in other fields with different well types
- Validate the developed model on saturated reservoirs with two phase condition
- Predict flow rate and contribution from each lateral in multilateral wells with using surface and downhole data

REFERENCES

- AlMosa, T. S. and Ertekin, T.: “Development and Utilization of Integrated Artificial Expert Systems for Designing Multi-Lateral Well Configurations, Estimating Reservoir Properties and Forecasting Reservoir Performance”, SPE Paper 167462, Presented at the SPE Middle East Intelligent Energy Conference and Exhibition, Dubai, UAE, 28-30 October 2013.

- Alarifi, S., AlNuaim, S. and Abdulraheem, A. :”Productivity Index Prediction for Oil Horizontal Wells Using Different Artificial Intelligence Techniques”, SPE Paper 172729, Presented at the Middle East Oil & Gas Show and Conference, Manama, Bahrain, 8 -11 March 2015.

- Choi, S. K., Ouyang, L. B. and Huang, W. S.: “A Comprehensive Comparative Study on Analytical PI/IPR Correlations”, SPE Paper 116580, Presented at the SPE Annual Energy Conference and Exhibition, Colorado, USA, 21-24 September 2008.

- Boomer, R. J.:” Predicting Production Using a Neural Network (Artificial Intelligence Beats Human Intelligenc0e)”, SPE Paper 30202, Presented at Petroleum Computer Conference, Huston, TX, USA., 11-14 June 1995.

- Weiss, W. W., Blach, R. S. and Stubbs, B. A. :”How Artificial Intelligence Methods Can Forecast Oil Production”, SPE Paper 75143, Presented at SPE/DOE Improved Oil Recovery Symposium, Tulsa, Oklahoma, USA., 13-17 April 2002.

- Alarfaj, M. K., Abdulrahim, A., Al-Majed, A., and Hussain, E.:” Estimating Layers Deliverability in Multi-Layered Gas Reservoirs Using Artificial Intelligence”, SPE Paper 60893, SPE Saudi Section Technical Symposium and Exhibition, Al-Khobar, KSA, 8-11 April 2012.

- Alarfaj, M. K., Abdulrahim, A., Al-Majed, A., and Busaleh, Y.:” Estimating Dewpoint Pressure Using Artificial Intelligence”, SPE-160919, Presented at the SPE Saudi Arabia section Young Professionals Technical Symposium, Dhahran, Saudi Arabia, 19-21 March 2012.

- Chukwuka E. and Turgay E. :"Performance Prediction for Advanced Well Structures in Unconventional Oil and Gas Reservoirs Using Artificial Intelligent Expert Systems", SPE Paper 187037, Presented at SPE annual Technical Conference and Exhibitions, San Antonio, Texas, USA, 9-11 October 2017.

- Olivares, G., Escalona, C. and Gimenez, E. :" Production Monitoring Using Artificial Intelligence, APLT Asset", SPE Paper 149594, Presented at the SPE Intelligent Energy International, Utrecht, Netherlands, 27-29 March 2012.

- Borisov, J. P.:"Oil Production Using Horizontal and Multiple Deviation Wells", R&D Library, Nedra, Moscu, 1954, Translated by J. Strauss and S. D. Joshi, Phillips Petroleum Co., Bartleville, Oklahoma, USA.

- Guo, B., Zhou, J., Liu, Y. and Ghalambor, A. :" A Rigorous Analytical Model for Fluid Flow in Drain holes of Finite Conductivity Applied to Horizontal and Multilateral Wells", SPE Paper 106947, Presented at the 2007 Production Operations Symposium, Oklahoma, USA, March 31 – April 3, 2007.

- Joshi, S. D. :"Production Forecasting Methods for Horizontal Wells", SPE Paper 17580, Presented at SPE International Meeting on Petroleum Engineering, Tianjin, China, November 1-4, 1988.

- AlAjmi, M. D., Alarifi, S. A. and Mahsoon, A. H.: "Improving Multiphase Choke Performance and Well Production Test Validation Using Artificial Intelligence: A New Milestone", SPE Paper 173394, Presented at the SPE Digital Energy Conference and Exhibition, Texas, USA, 3 – 5 March 2015.
- El-Sayed, A. H. and Amro, M. M. :" Production Performance of Multilateral Wells", SPE/IADC 57542, Presented at Middle East Drilling Technology Conference, Abu Dhabi, UAE, 8-10 November 1999.

- Ecobar, F. H., Saaverda, N. F., Aranda, R. F. and Herrera, J. F. :" An Improved Correlation to Estimate Productivity Index in Horizontal Wells", SPE Paper 88540, Presented at the SPE Asia Pacific Oil and Gas Conference and Exhibition, Perth, Australia, 18-20 October 2004.

- Chidambaram, P. :'Development and Testing of an Artificial Neural Network Based History Matching Protocol to Characterize Reservoir Properties", Dissertation, University Park: The Pennsylvania State University, USA, 2009.

- Zeeshan, T., Elkatatny, S., Mahmoud, M., Abdulwahab, A., and Abdulraheem, A. :" A New Technique to Develop Rock Strength Correlation Using Artificial Intelligence Tools", SPE-186062-MS, Presented at the SPE Reservoir Characterisation and simulation Conference and Exhibition held in Abu Dhabi, UAE, 08-10 May 2017.

- Busaleh, Y. R., and Abdulraheem, A. :"Prediction of Capillary for Oil Carbonate Reservoirs by Artificial Intelligence Technique", SPE-182173-MS, Presented at the SPE Asia Pacific Oil & Gas Conference and Exhibition held on Perth, Australia, 25-27 October 2016.

- Technical Advancements of Multilaterals (TAML) – URL: taml-intl.blogspot.com/.

- Pacontrol.com, (2014). PAControl.com – Artificial Neural Networks. Online website:
- http://www.pacontrol.com/Neural .html.

- U.S Energy information Administration System, Office of Oil and Gas as from "Horizontal Drilling", Lynn Helms
- Nelson, A. L (2012): http://www.nelsonrobotics.org/puplications.html.
- "Fuzzy Logic Toolbox User's Guide", MathWorks, Inc, September 2010.

- Hagan, M. T., Demuth, H. B., & Beale, M.: "Neural Network Design", University of Colorado, USA, 2002

- Chidambaram, P., Development and Testing of an Artificial Neural Network Based History Matching Protocol to Characterize Reservoir Properties University Park: The Pennsylvania State University, USA, 2009

- Robert, M., Dandy, G. and Maier, H.: "Artificial Neural Network - Methodological Advances and Biomedical Applications", 2011

- Demuth, B., Beal, M. and Hagan, M.: "Neural Network Design", University of Colorado, USA, 1995

- Badde, S., Gupta, A and Patki, V.:"Cascade and Feed Forward Back propagation Artificial Neural", IOSR Journal of Mechanical and Civil Engineering (IOSR-JMCE). 2278-1684, PP: 01-06 , 2011
- Demuth, B., Hagan, B., and Martin, T.:"Neural Network Toolbox for use with MATLAB", Natick, MA, MathWorks Inc., 2009.

APPENDIX A

A) ANN for H wells data sets

1) ANN modelling results and optimum conditions with ‘trainlm’ Function

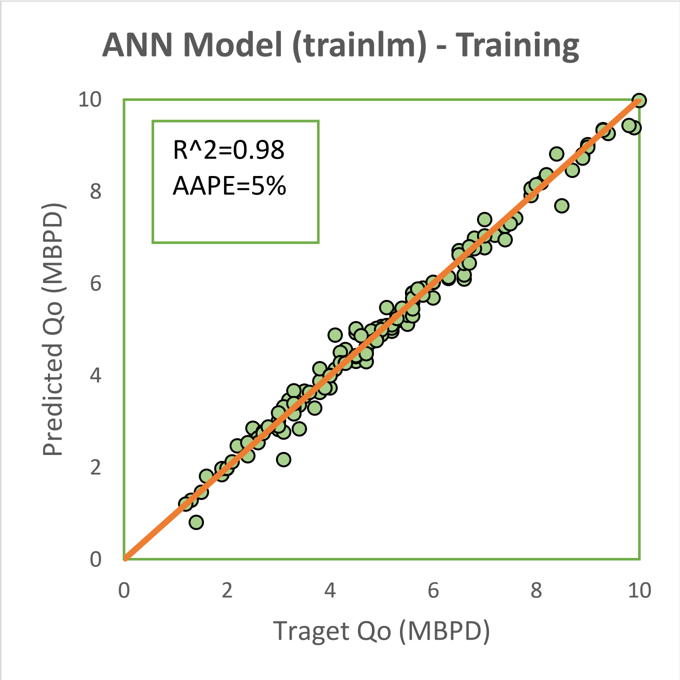

Figure A.1: Crossplot of Oil Rates with ANN ‘trainlm’ Model in H Wells – Training

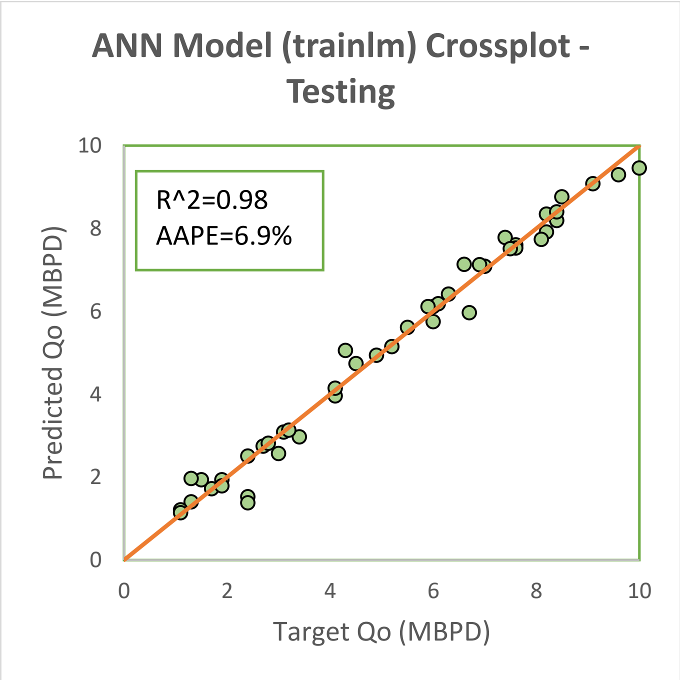

Figure A.2: Crossplot of Oil Rates with ANN ‘trainlm’ Model in H Wells – Testing

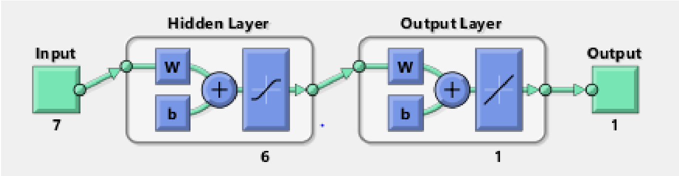

Figure A.3: Neural Network Structure for ‘trainlm’ Function for H Wells

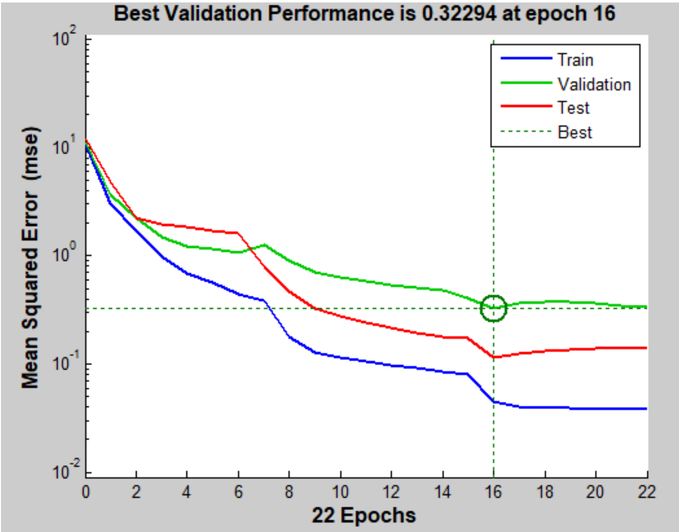

Figure A.4: Best Validation Performance of ‘trainlm’ Function for H Wells

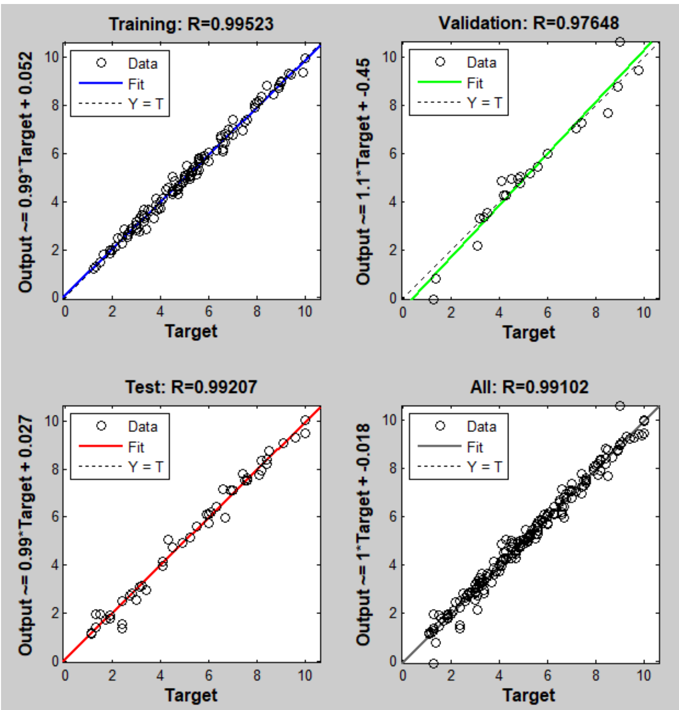

Figure A.5: Performance Plots for ‘trainlm’ Function for H Wells

2) ANN modelling results and optimum conditions with ‘trainlm -2L’ Function

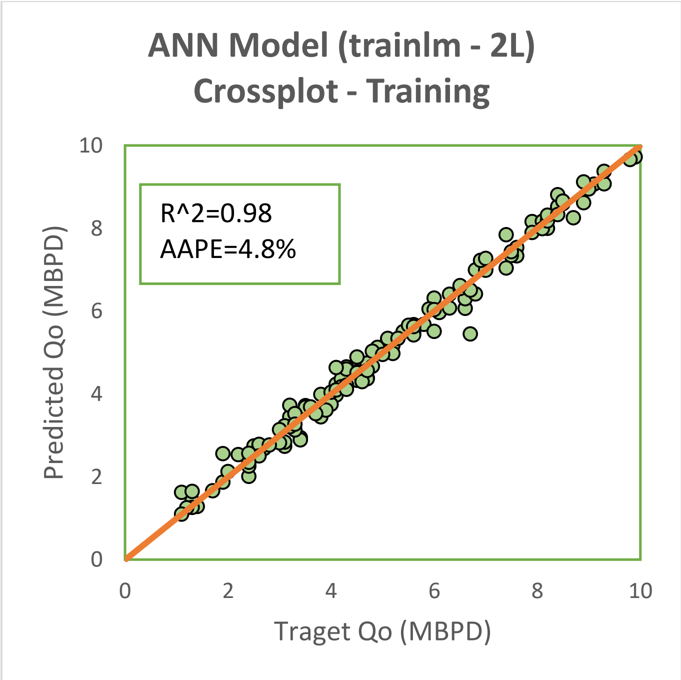

Figure A.6: Crossplot of Oil Rates with ANN ‘trainlm-2L’ Model in H Wells – Training

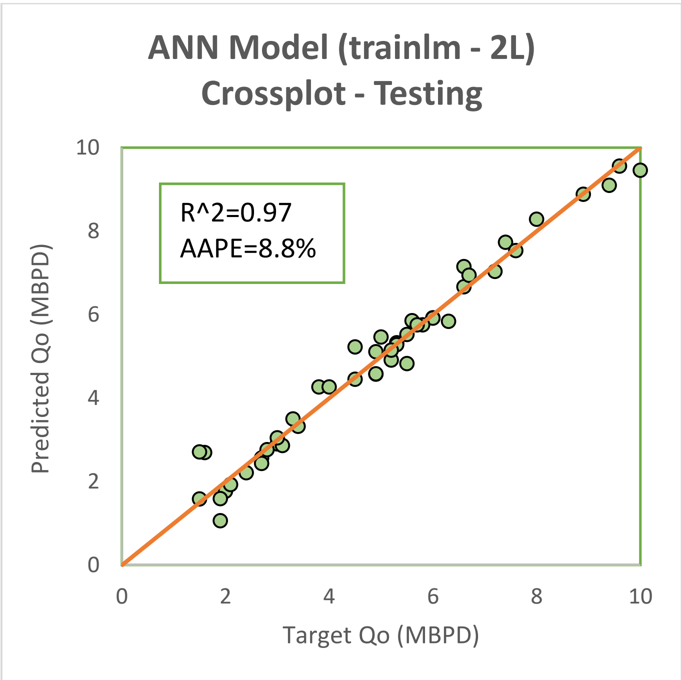

Figure A.7: Crossplot of Oil Rates with ANN ‘trainlm-2L’ Model in H Wells – Testing

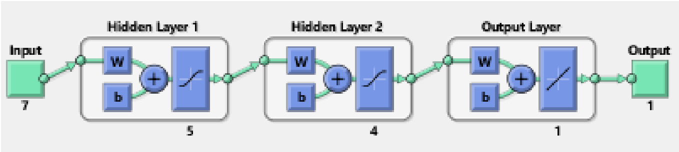

Figure A.8: Neural Network Structure for ‘trainlm-2L’ Function for H Wells

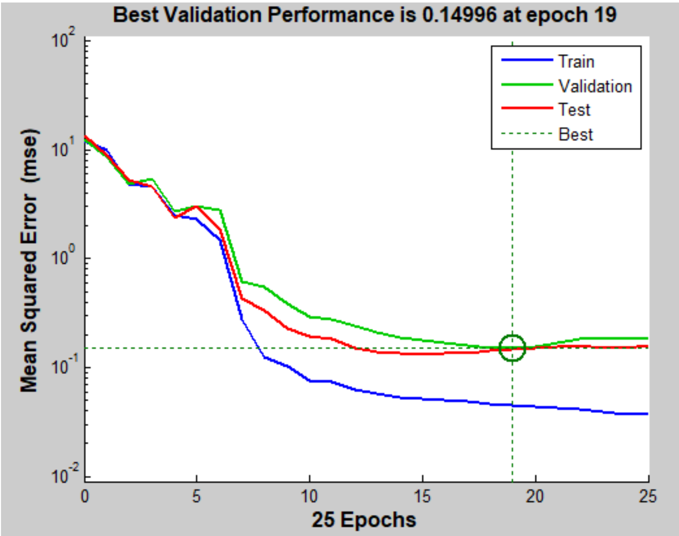

Figure A.9: Best Validation Performance of ‘trainlm-2L’ Function for H Wells

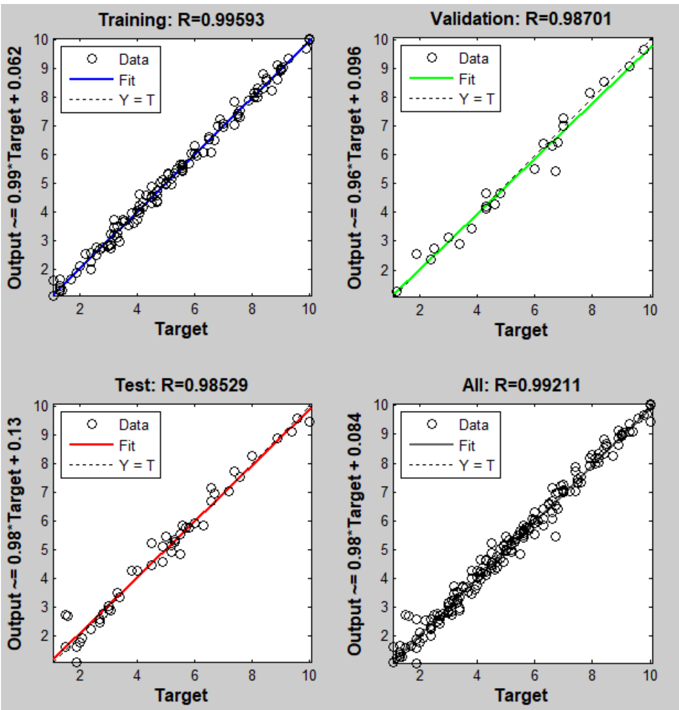

Figure A.10: Performance Plots for ‘trainlm-2L’ Function for H Wells

3) ANN modelling results and optimum conditions with ‘traingd’ Function

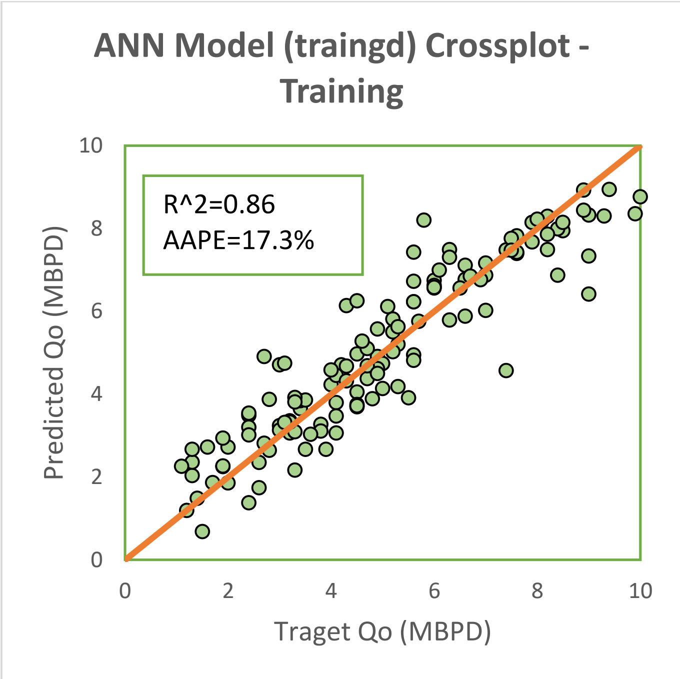

Figure A.11: Crossplot of Oil Rates with ANN ‘traingd’ Model in H Wells – Training

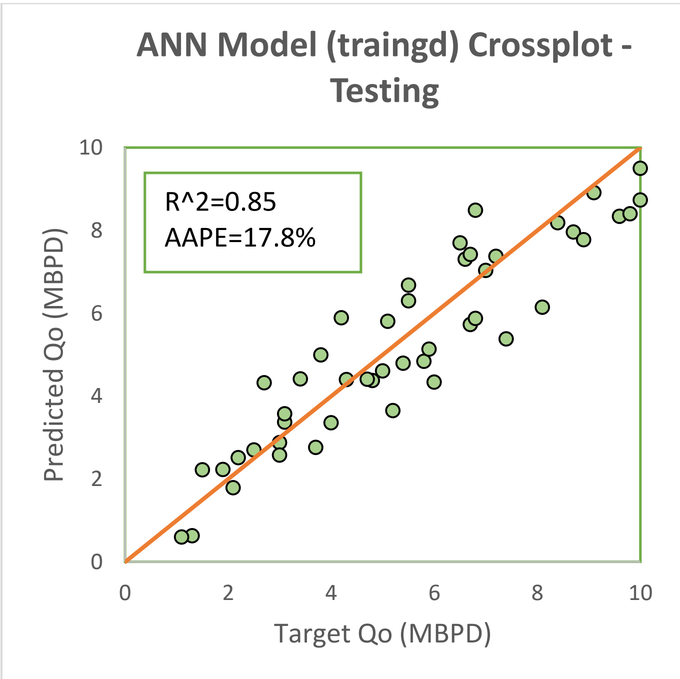

Figure A.12: Crossplot of Oil Rates with ANN ‘traingd’ Model in H Wells – Testing

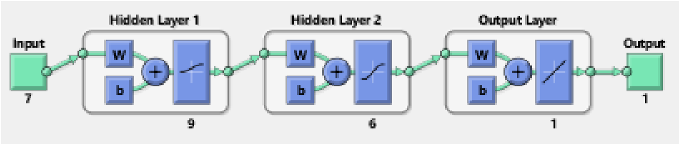

Figure A.13: Neural Network Structure for ‘traingd’ Function for H Wells

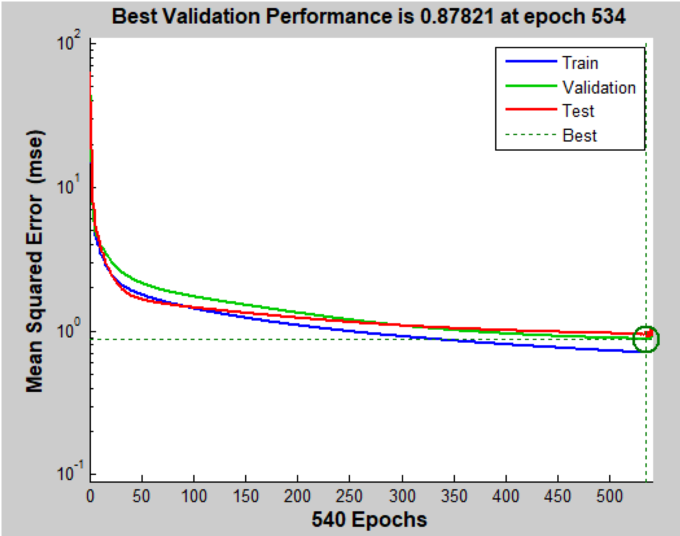

Figure A.14: Best Validation Performance of ‘traingd’ Function for H Wells

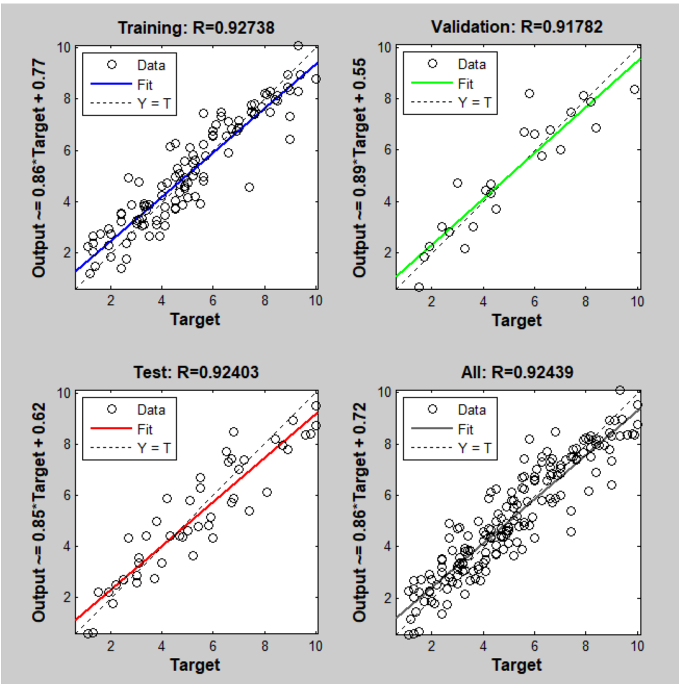

Figure A.15: Performance Plots for ‘traingd’ Function for H Wells

4) ANN modelling results and optimum conditions with ‘traingdx’ Function

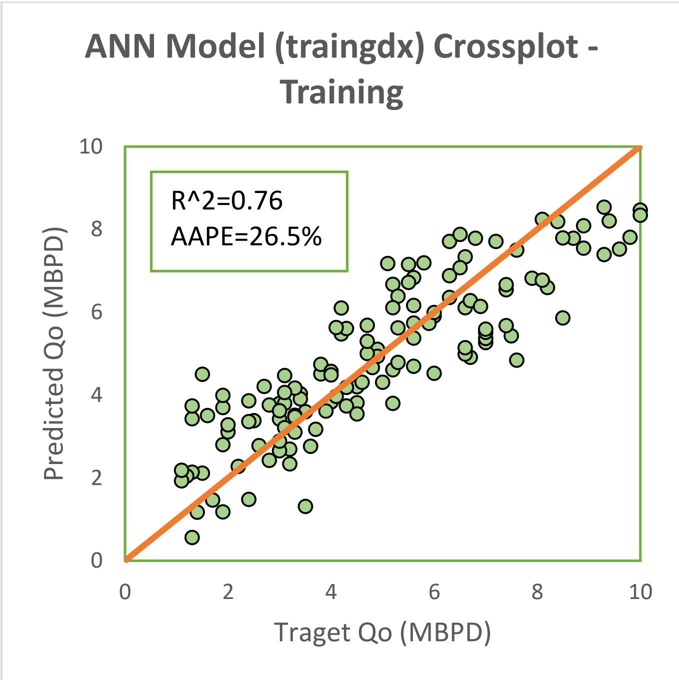

Figure A.16: Crossplot of Oil Rates with ANN ‘traingdx’ Model in H Wells – Training

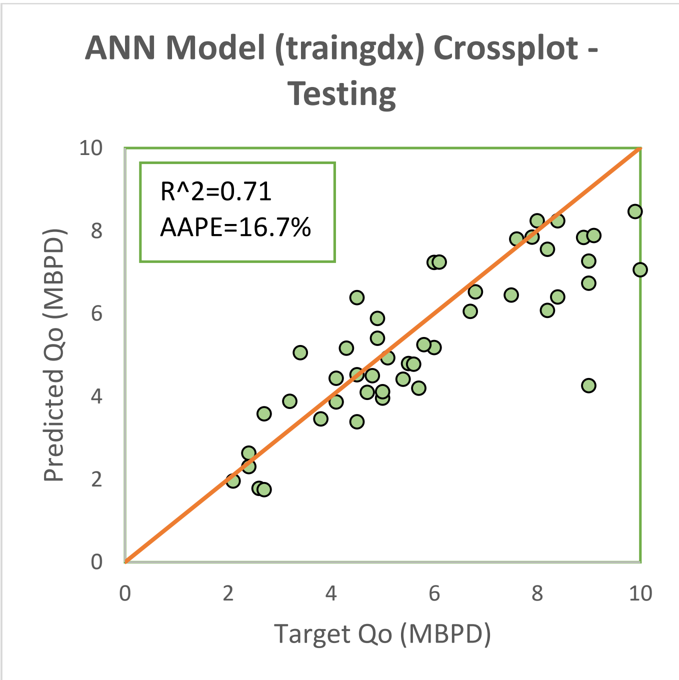

Figure A.17: Crossplot of Oil Rates with ANN ‘traingdx’ Model in H Wells – Testing

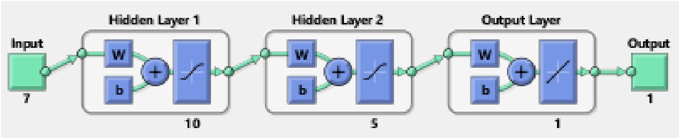

Figure A.18: Neural Network Structure for ‘traingdx’ Function for H Wells

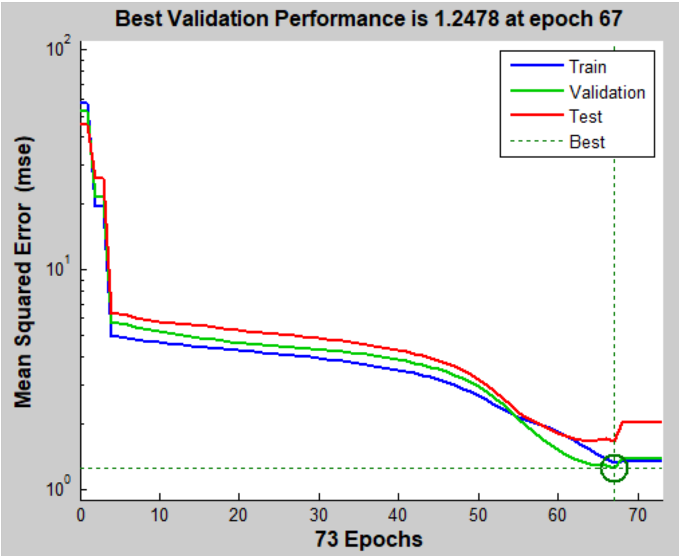

Figure A.19: Best Validation Performance of ‘traingdx’ Function for H Wells

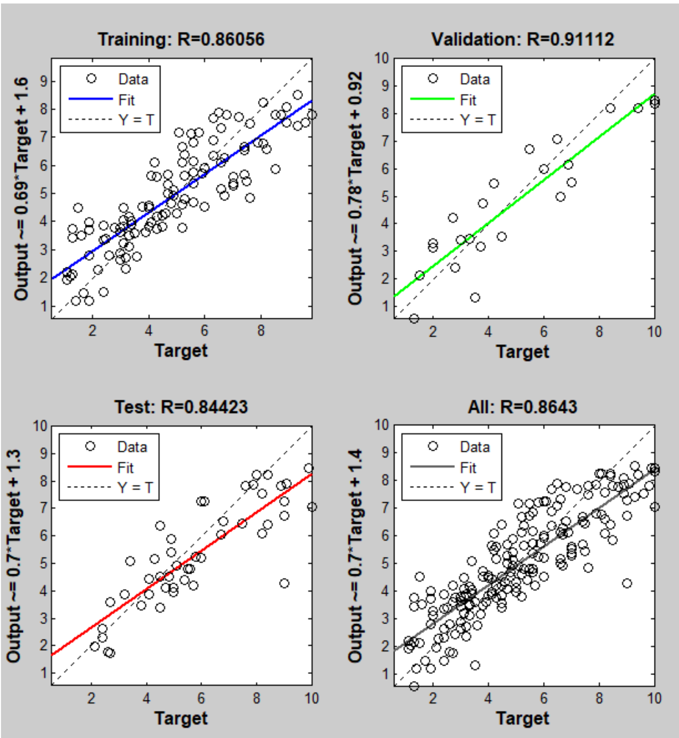

Figure A.20: Performance Plots for ‘traingdx’ Function for H Wells

5) ANN modelling results and optimum conditions with ‘trainbfg’ Function

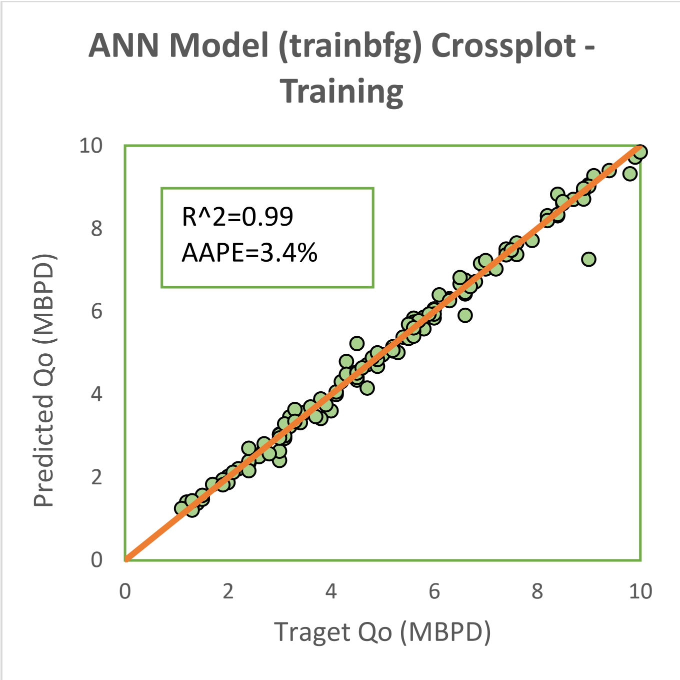

Figure A.21: Crossplot of Oil Rates with ANN ‘trainbfg’ Model in H Wells – Training

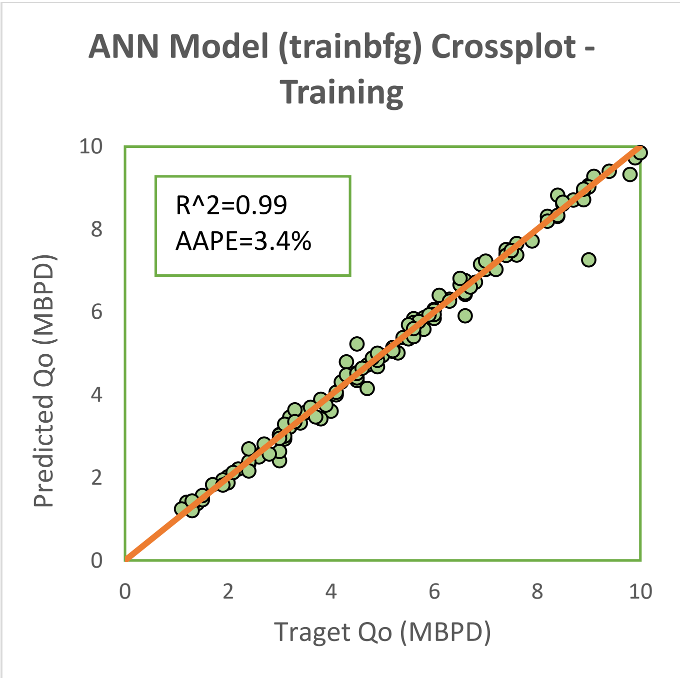

Figure A.22: Crossplot of Oil Rates with ANN ‘trainbfg’ Model in H Wells – Testing

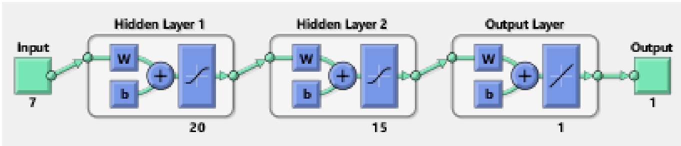

Figure A.23: Neural Network Structure for ‘trainbfg’ Function for H Wells

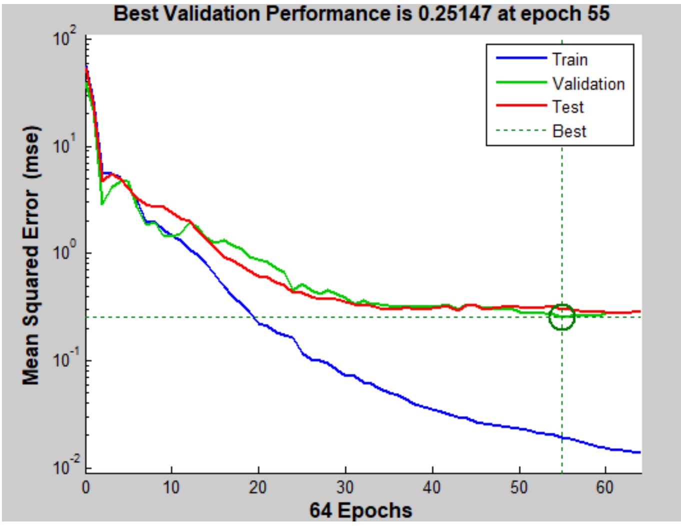

Figure A.24: Best Validation Performance of ‘trainbfg’ Function for H Wells

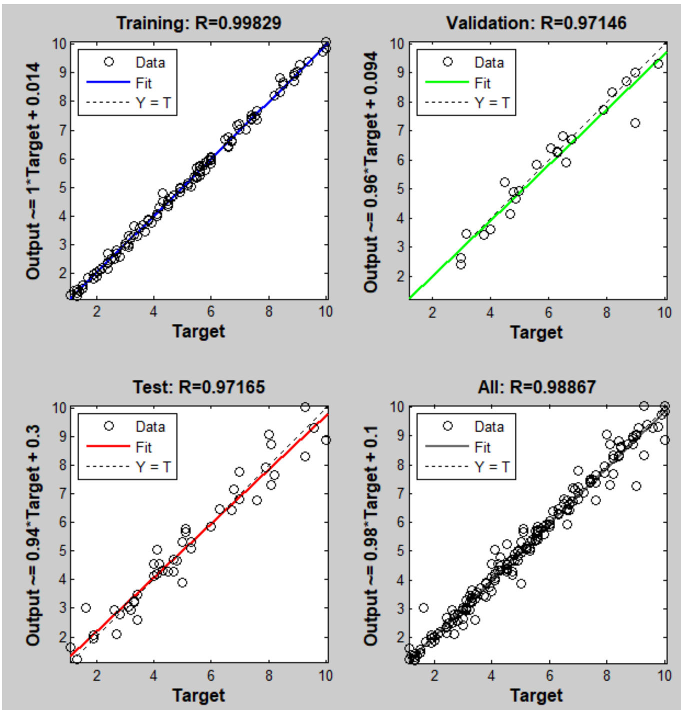

Figure A.25: Performance Plots for ‘trainbfg’ Function for H Wells

6) ANN modelling results and optimum conditions with ‘trainscg’ Function

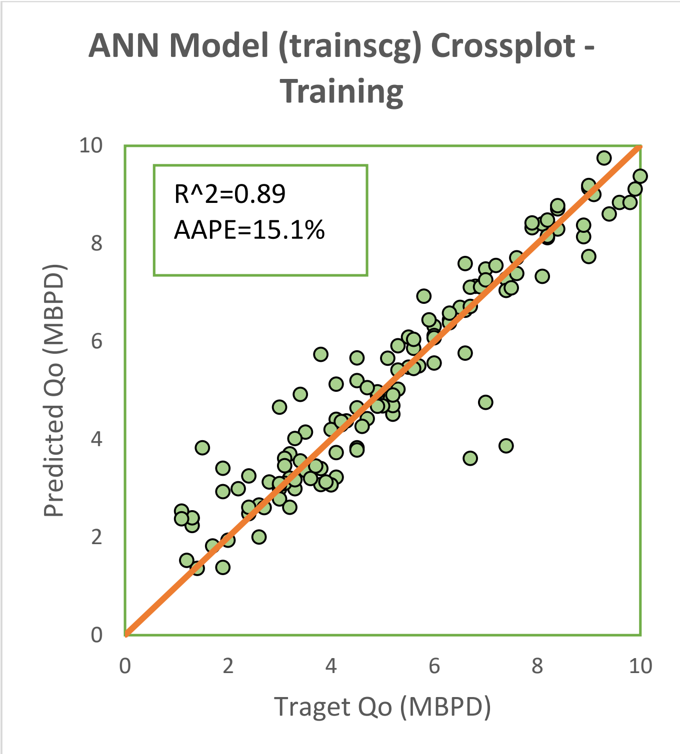

Figure A.26: Crossplot of Oil Rates with ANN ‘trainscg’ Model in H Wells – Training

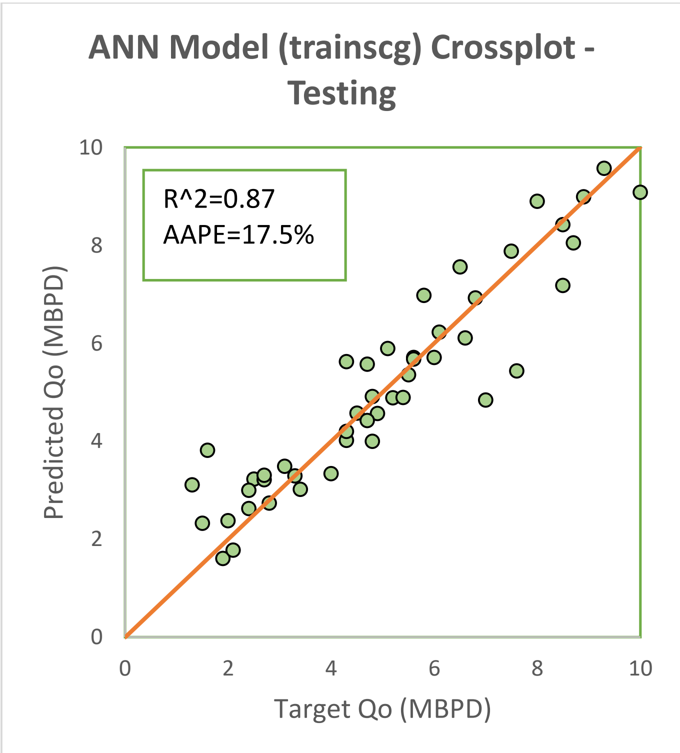

Figure A.27: Crossplot of Oil Rates with ANN ‘trainscg’ Model in H Wells – Testing

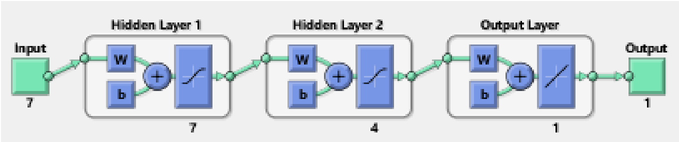

Figure A.28: Neural Network Structure for 'trainscg' Function for H Wells

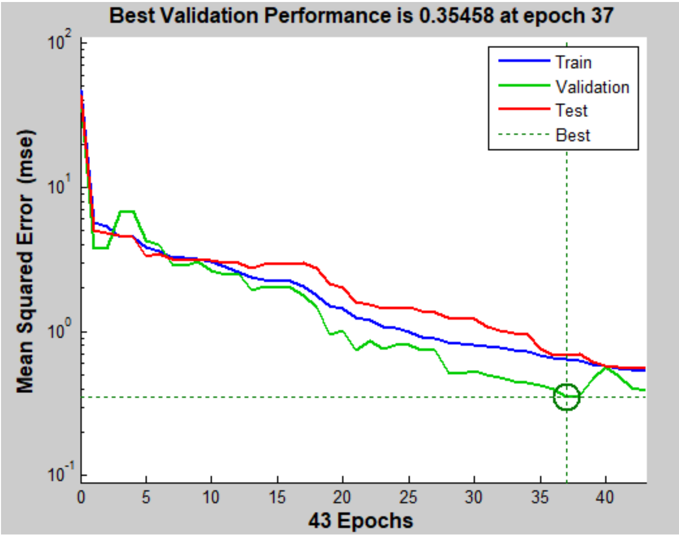

Figure A.29: Best Validation Performance of 'trainscg' Function for H Wells

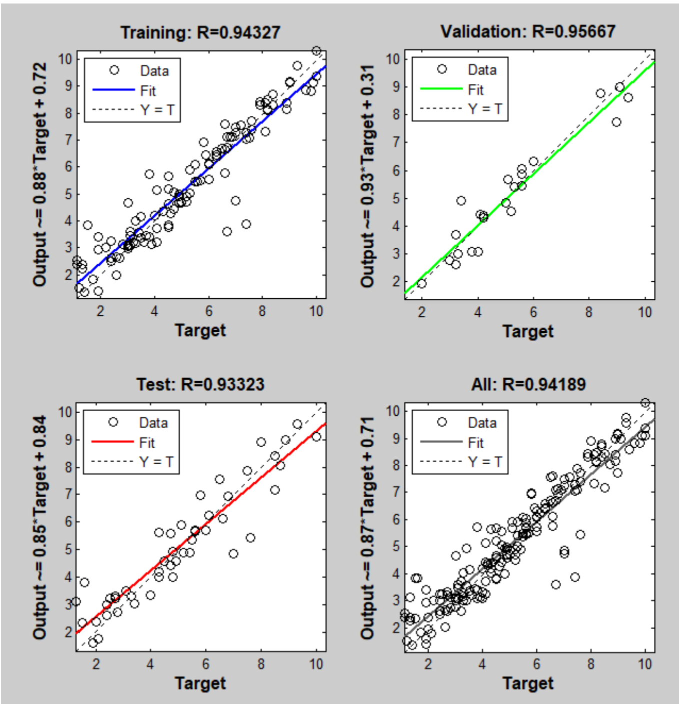

Figure A.30: Performance Plots for 'trainscg' Function for H Wells

7) ANN modelling results and optimum conditions with ‘trainoss’ Function

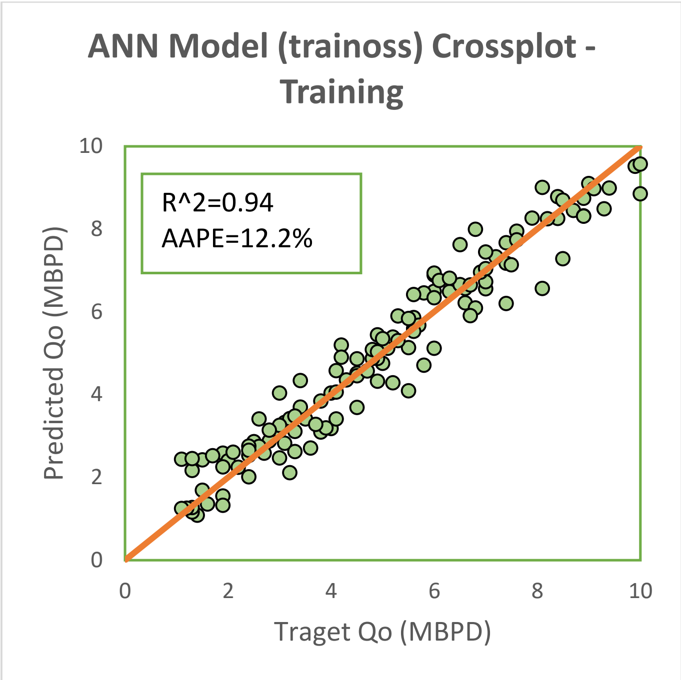

Figure A.31: Crossplot of Oil Rates with ANN ‘trainoss’ Model in H Wells – Training

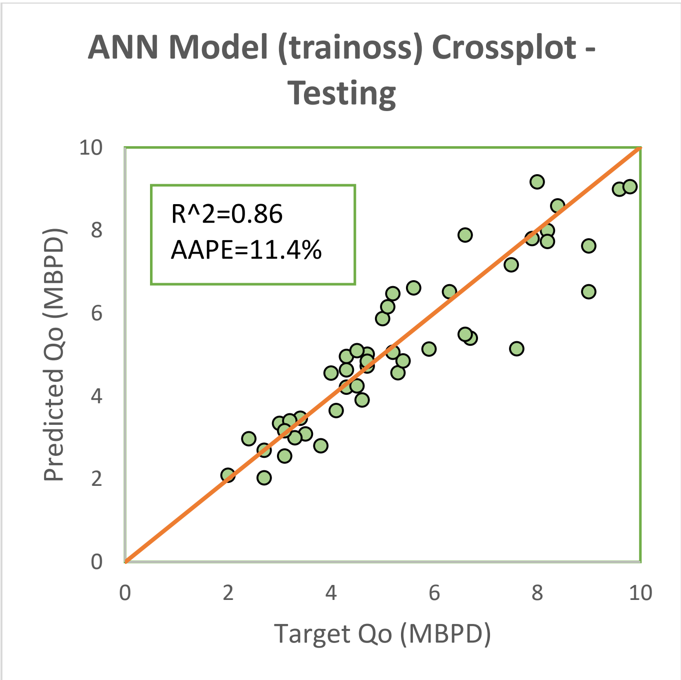

Figure A.32: Crossplot of Oil Rates with ANN ‘trainoss’ Model in H Wells – Testing

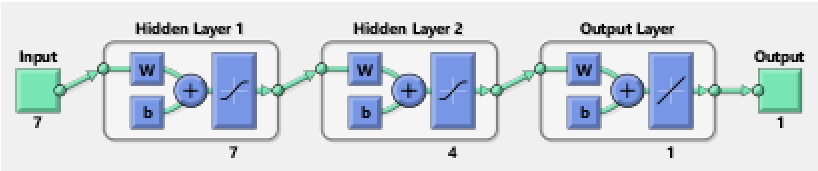

Figure A.33: Neural Network Structure for ‘trainoss’ Function for H Wells

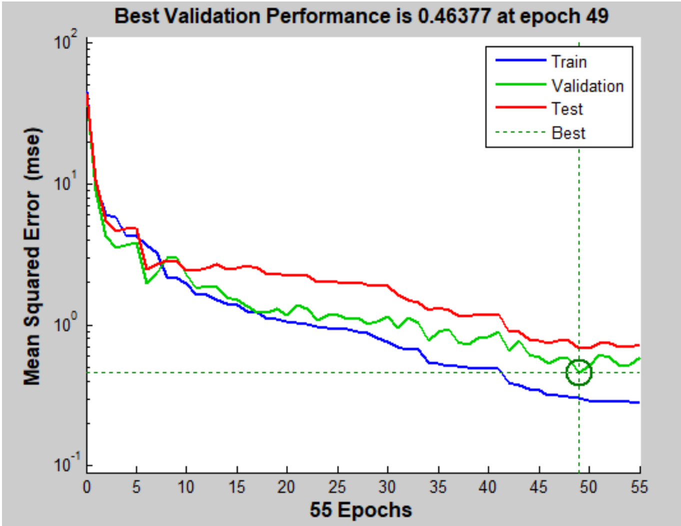

Figure A.34: Best Validation Performance of ‘trainoss’ Function for H Wells

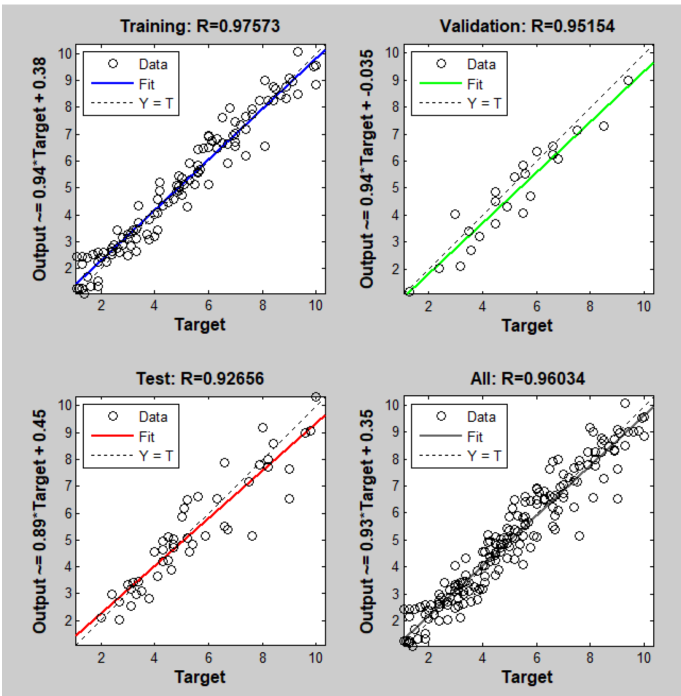

Figure A.35: Performance Plots for ‘trainoss’ Function for H Wells

8) ANN modelling results and optimum conditions with ‘trainrp’ Function

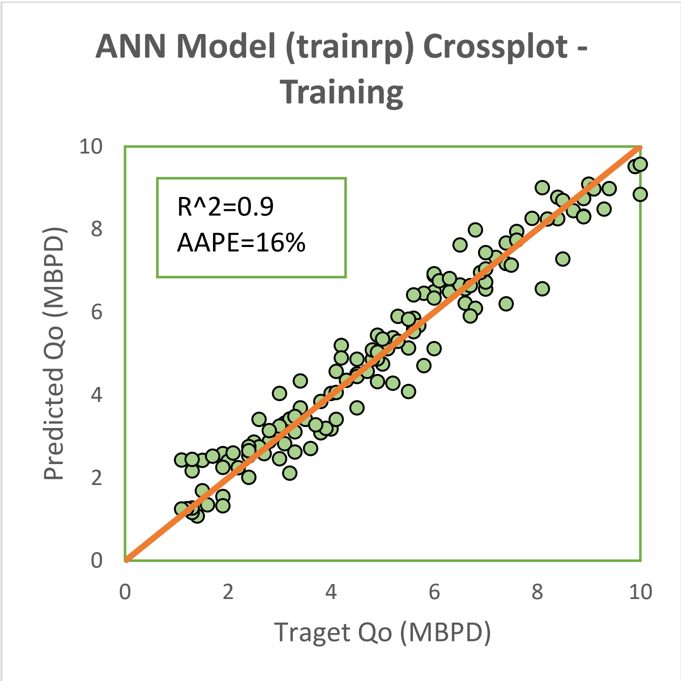

Figure A.36: Crossplot of Oil Rates with ANN ‘trainrp’ Model in H Wells – Training

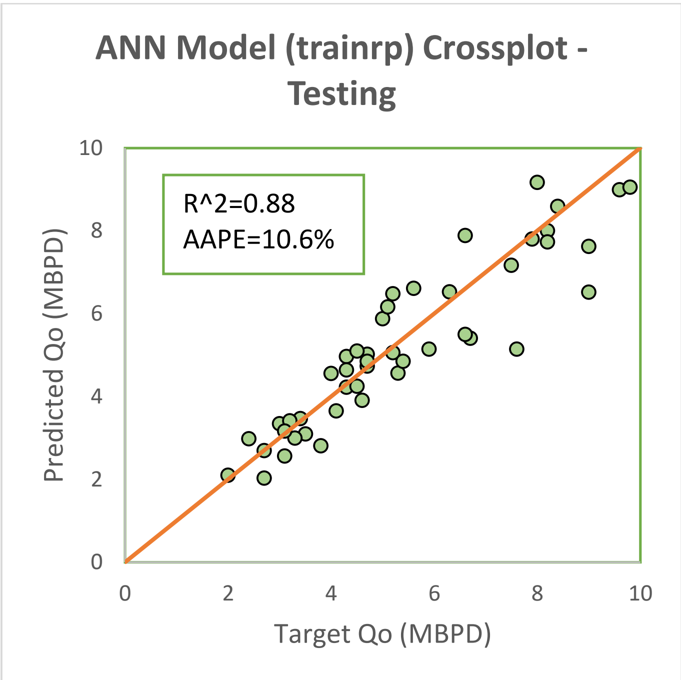

Figure A.37: Crossplot of Oil Rates with ANN ‘trainrp’ Model in H Wells – Testing

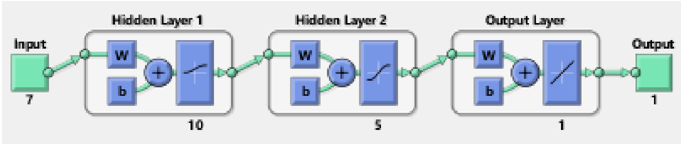

Figure A.38: Neural Network Structure for ‘trainrp’ Function for H Wells

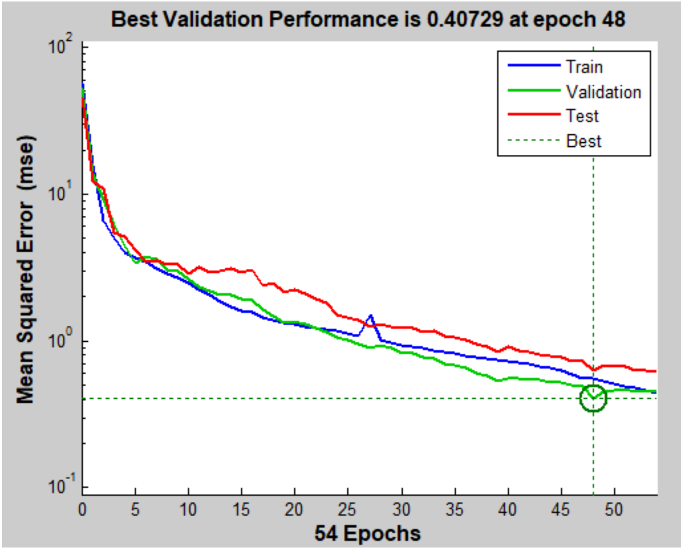

Figure A.39: Best Validation Performance of ‘trainrp’ Function for H Wells

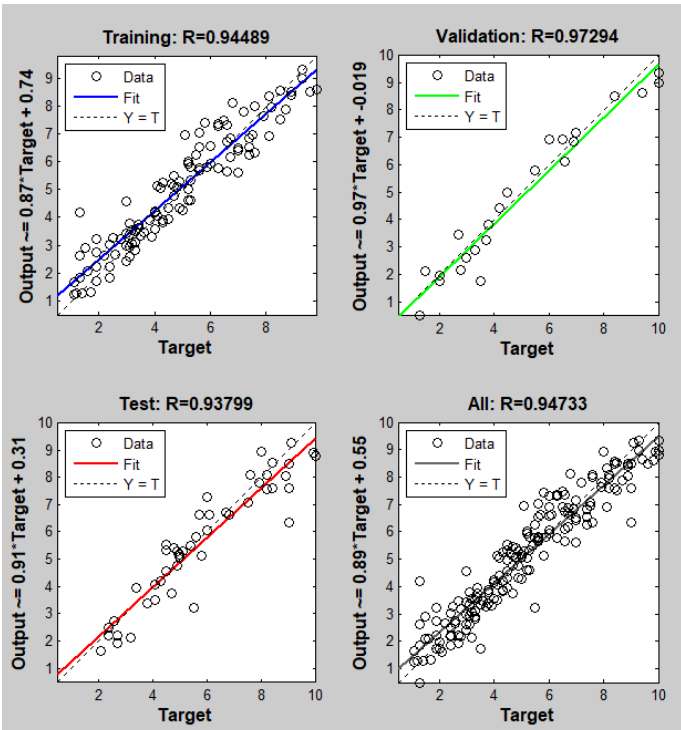

Figure A.40: Performance Plots for ‘trainrp’ Function for H Wells

9) ANN modelling results and optimum conditions with ‘trainrb’ Function

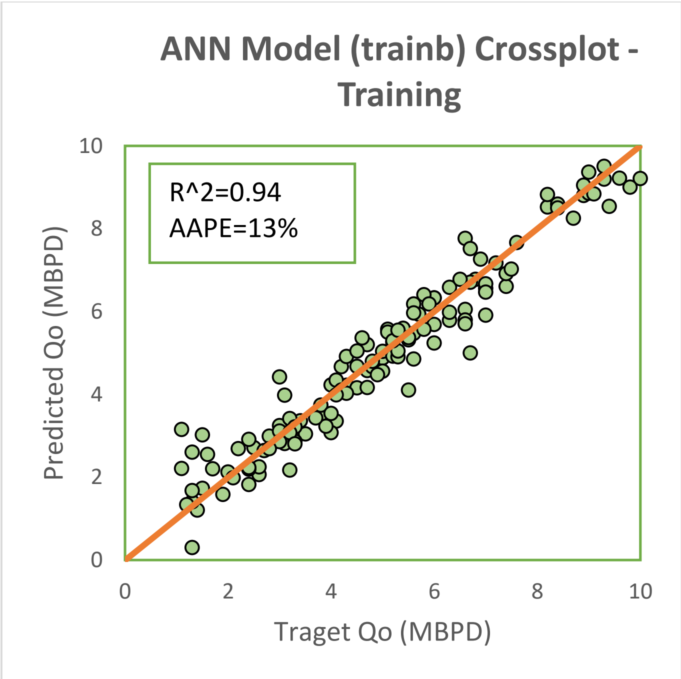

Figure A.41: Crossplot of Oil Rates with ANN ‘trainb’ Model in H Wells – Training

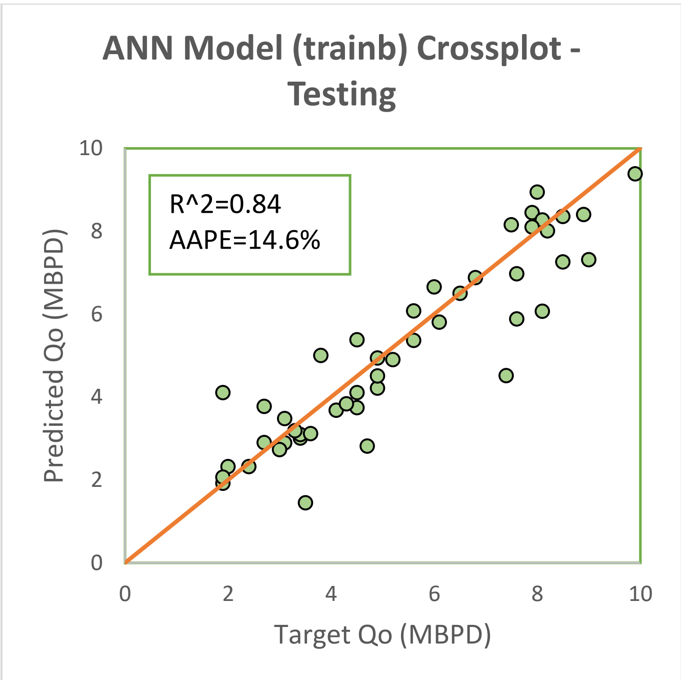

Figure A.42: Crossplot of Oil Rates with ANN ‘trainb’ Model in H Wells – Testing

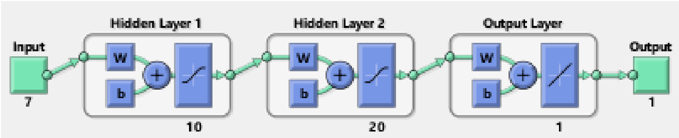

Figure A.43: Neural Network Structure for ‘trainrb’ Function for H Wells

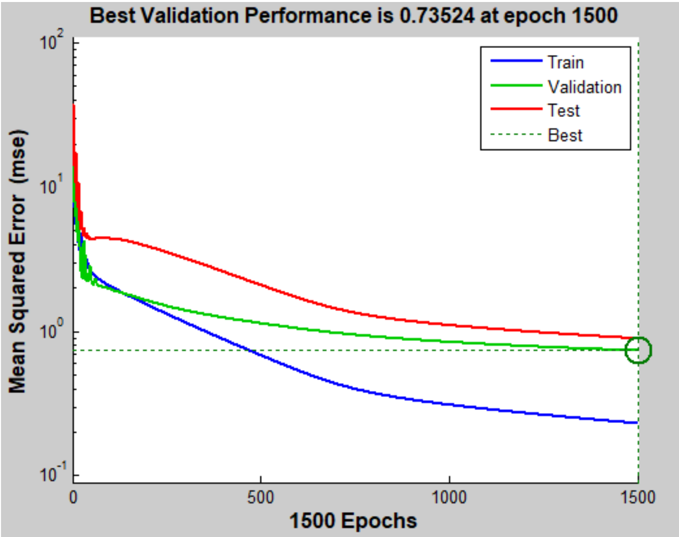

Figure A.44: Best Validation Performance of ‘trainrb’ Function for H Wells

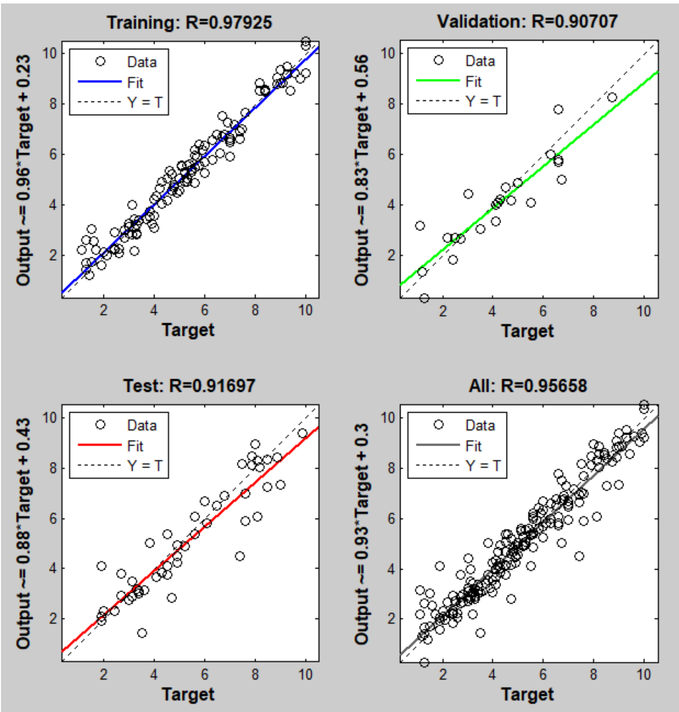

Figure A.45: Performance Plots for ‘trainrb’ Function for H Wells

B) ANN for ML wells data sets

1) ANN modelling results and optimum conditions with ‘trainlm’ Function

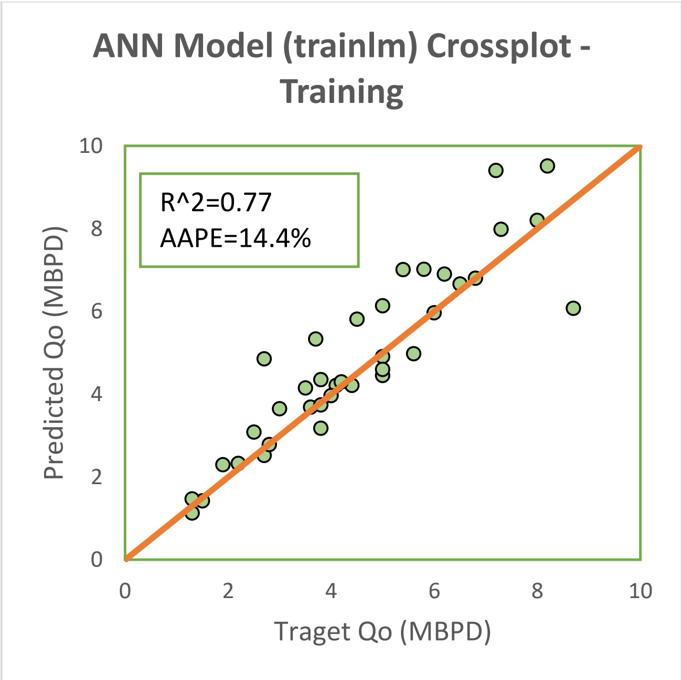

Figure A.46: Crossplot of Oil Rates with ANN ‘trainlm’ Model in ML Wells – Training

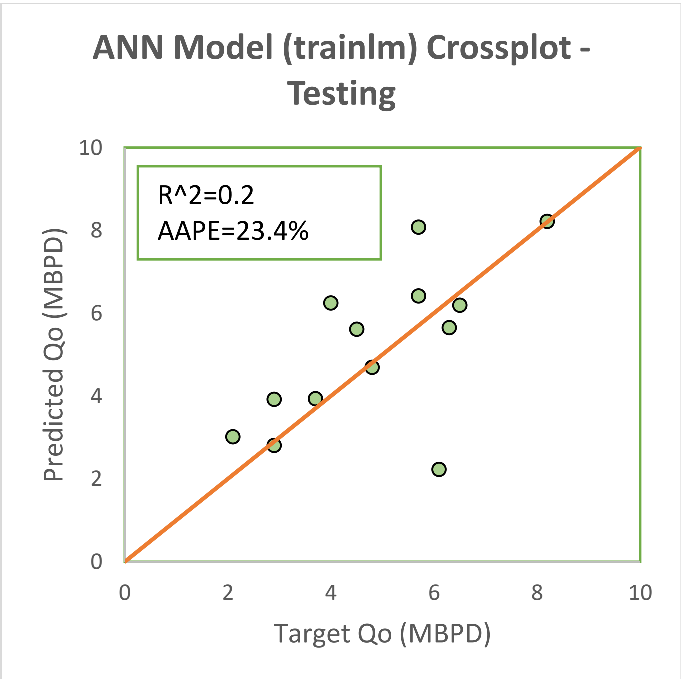

Figure A.47: Crossplot of Oil Rates with ANN ‘trainlm’ Model in ML Wells – Testing

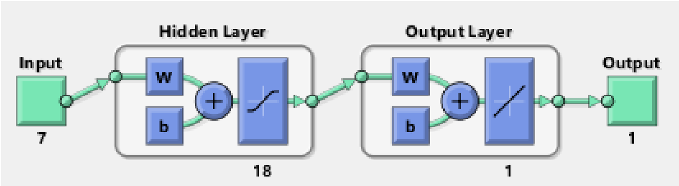

Figure A.48: Neural Network Structure for ‘trainlm’ Function for ML Wells

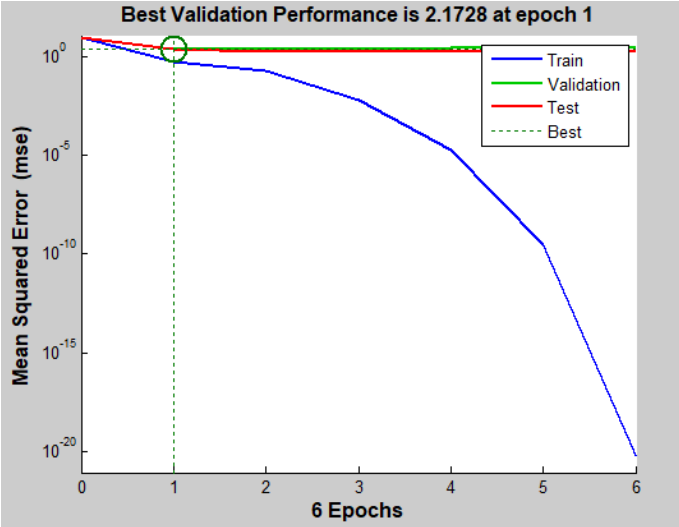

Figure A.49: Best Validation Performance of ‘trainlm’ Function for ML Wells

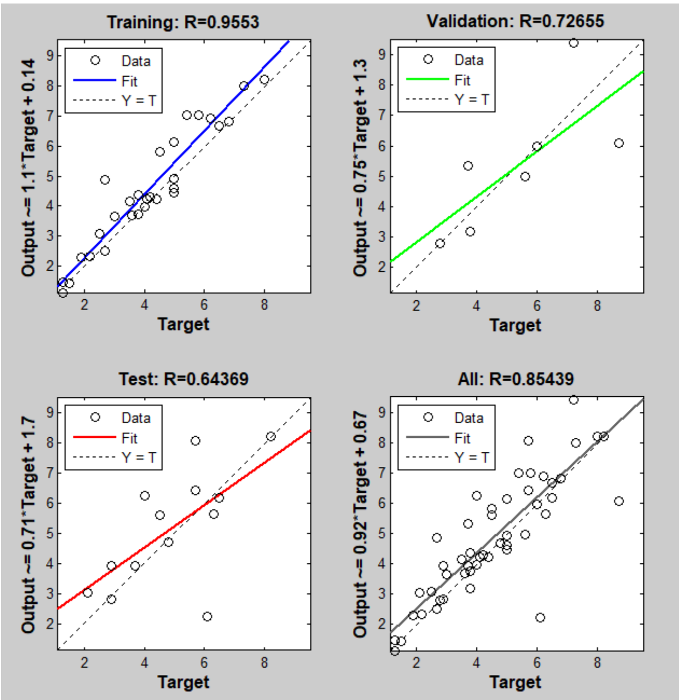

Figure A.50: Performance Plots for ‘trainlm’ Function for ML Wells

2) ANN modelling results and optimum conditions with 'trainlm -2L' Function

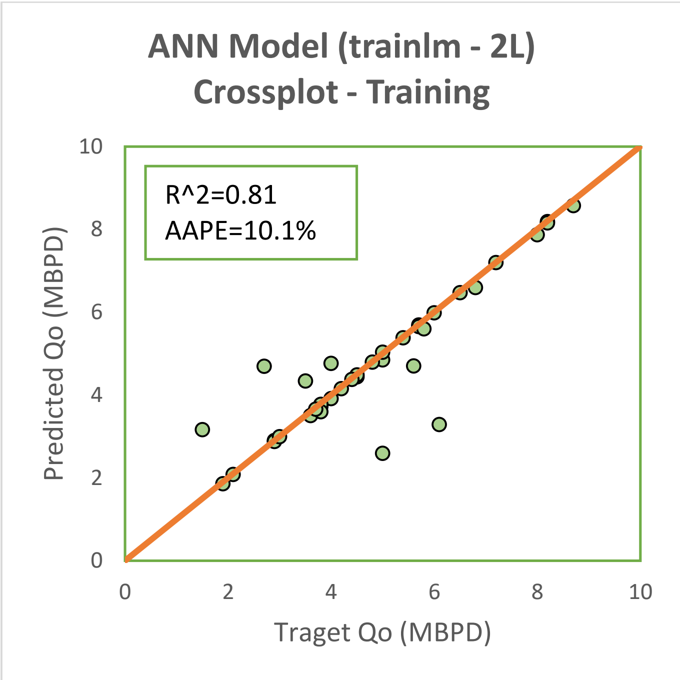

Figure A.51: Crossplot of Oil Rates with ANN 'trainlm-2L' Model in ML Wells – Training

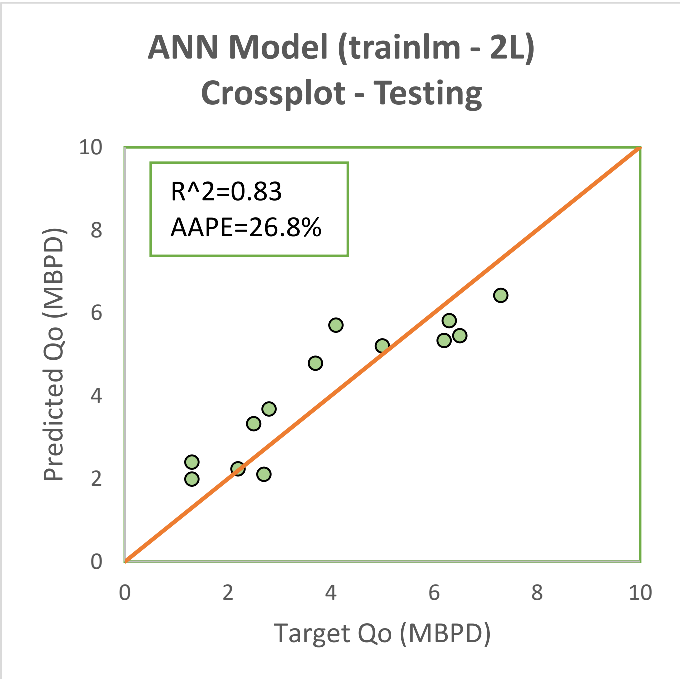

Figure A.52: Crossplot of Oil Rates with ANN 'trainlm-2L' Model in ML Wells – Testing

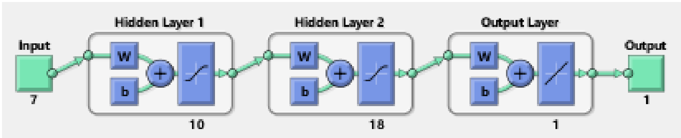

Figure A.53: Neural Network Structure for ‘trainlm-2L’ Function for ML Wells

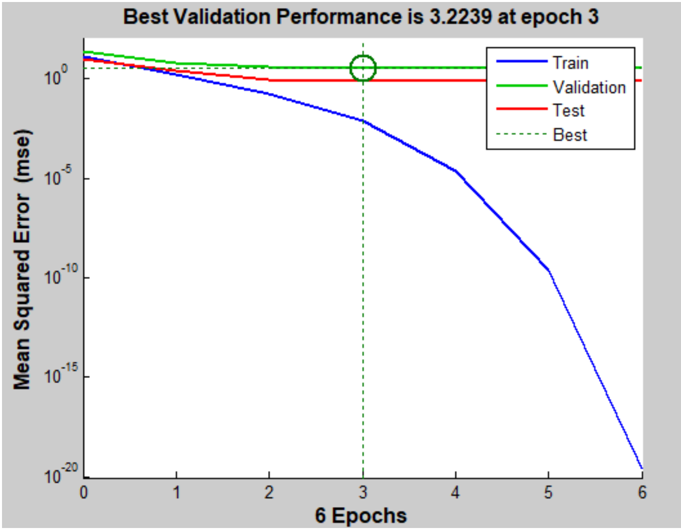

Figure A.54: Best Validation Performance of ‘trainlm-2L’ Function for ML Wells

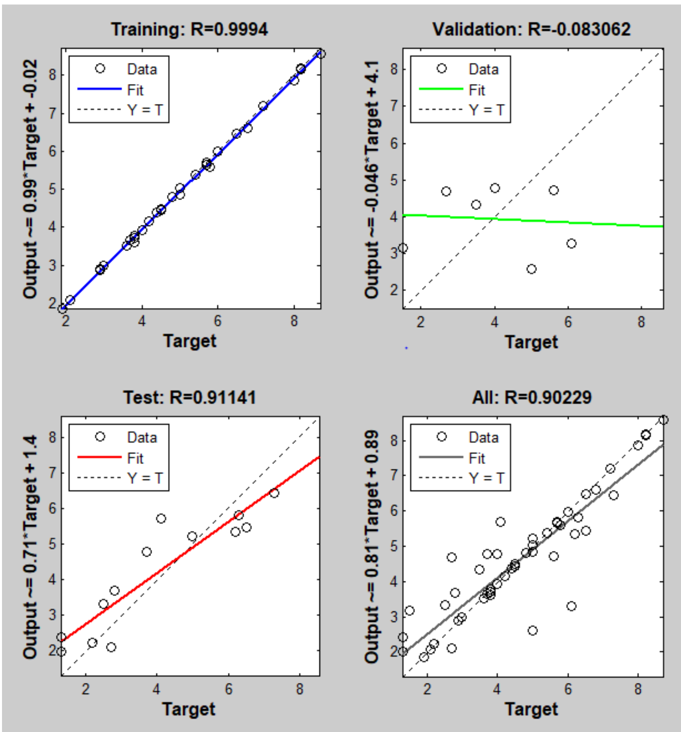

Figure A.55: Performance Plots for ‘trainlm-2L’ Function for ML Wells

3) ANN modelling results and optimum conditions with ‘traingd’ Function

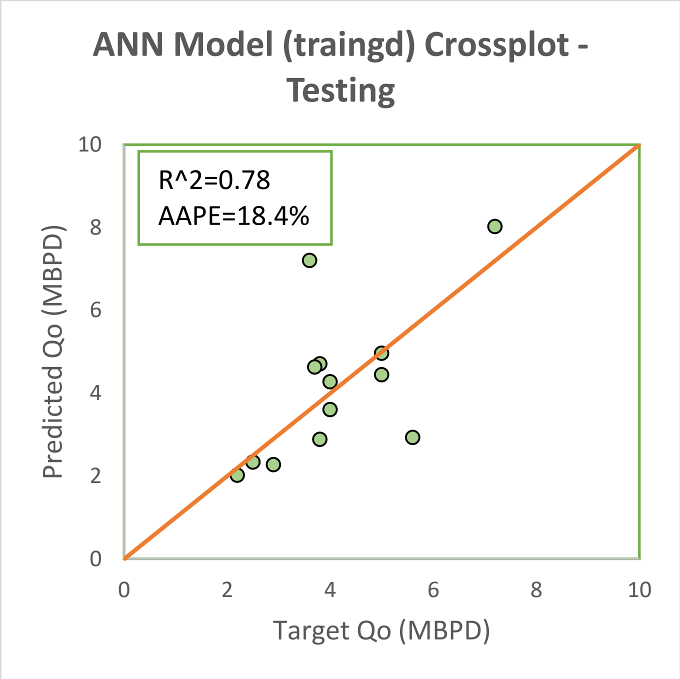

Figure A.56: Crossplot of Oil Rates with ANN ‘traingd’ Model in ML Wells – Training

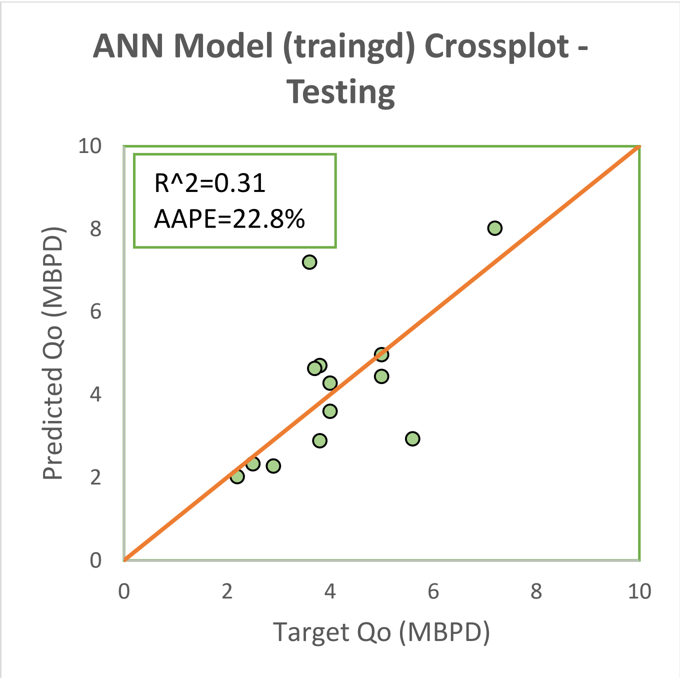

Figure A.57: Crossplot of Oil Rates with ANN ‘traingd’ Model in ML Wells – Testing

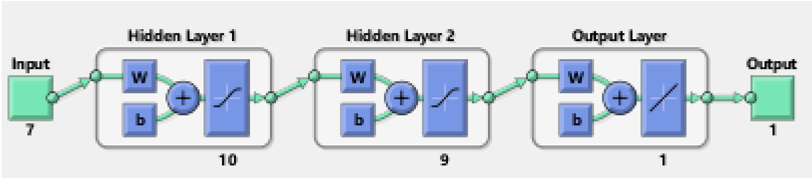

Figure A.58: Neural Network Structure for 'traingd' Function for ML Wells

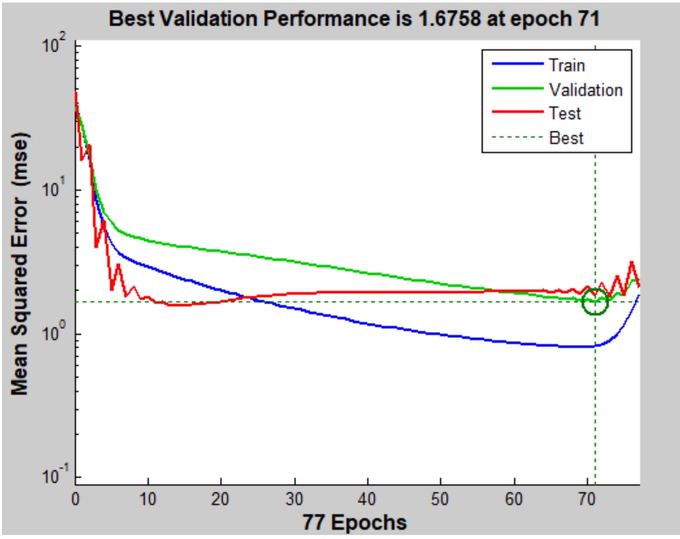

Figure A.59: Best Validation Performance of 'traingd' Function for ML Wells

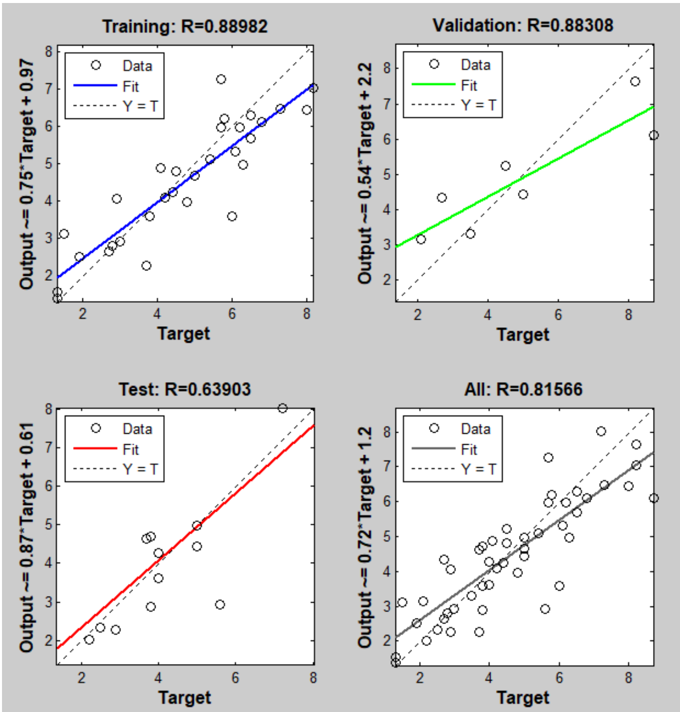

Figure A.60: Performance Plots for 'traingd' Function for ML Wells

4) ANN modelling results and optimum conditions with ‘traingdx’ Function

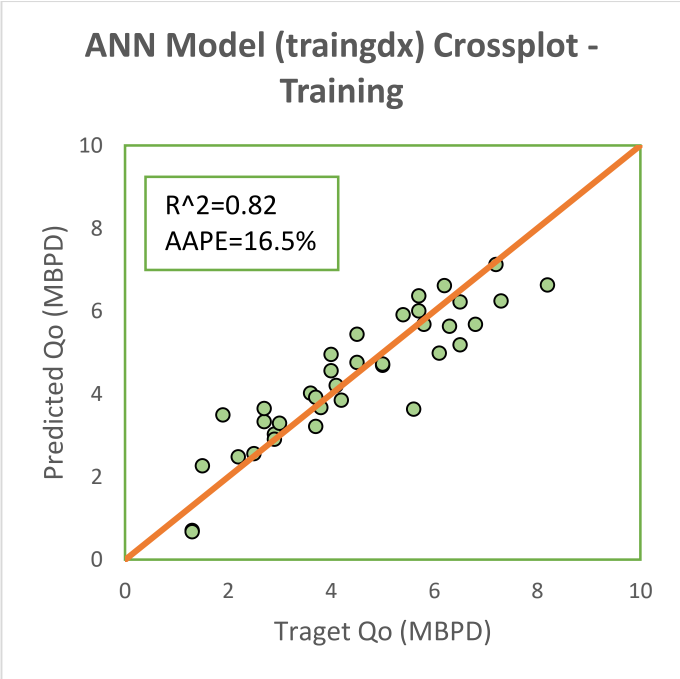

Figure A.61: Crossplot of Oil Rates with ANN ‘traingdx’ Model in ML Wells – Training

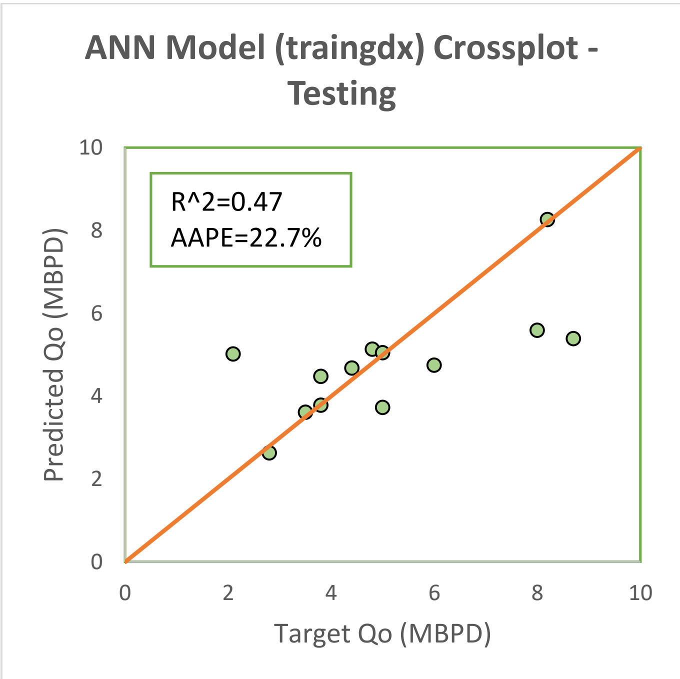

Figure A.62: Crossplot of Oil Rates with ANN ‘traingdx’ Model in ML Wells – Testing

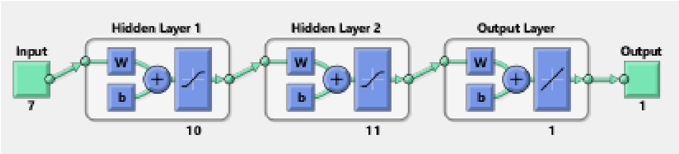

Figure A.63: Neural Network Structure for ‘traingdx’ Function for ML Wells

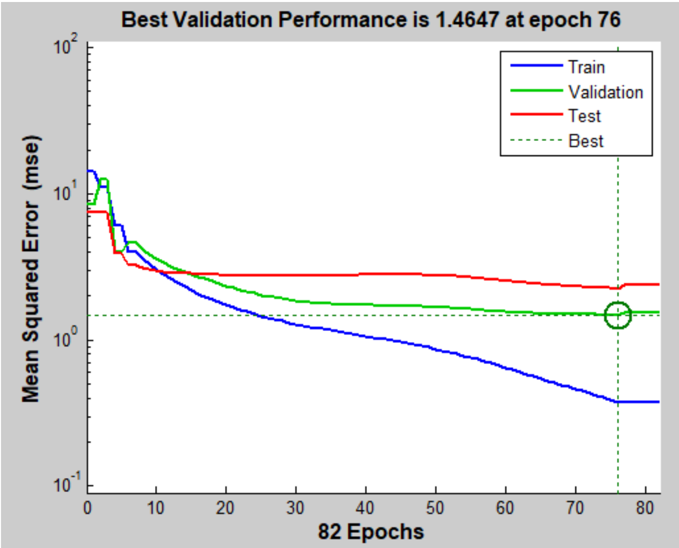

Figure A.64: Best Validation Performance of ‘traingdx’ Function for ML Wells

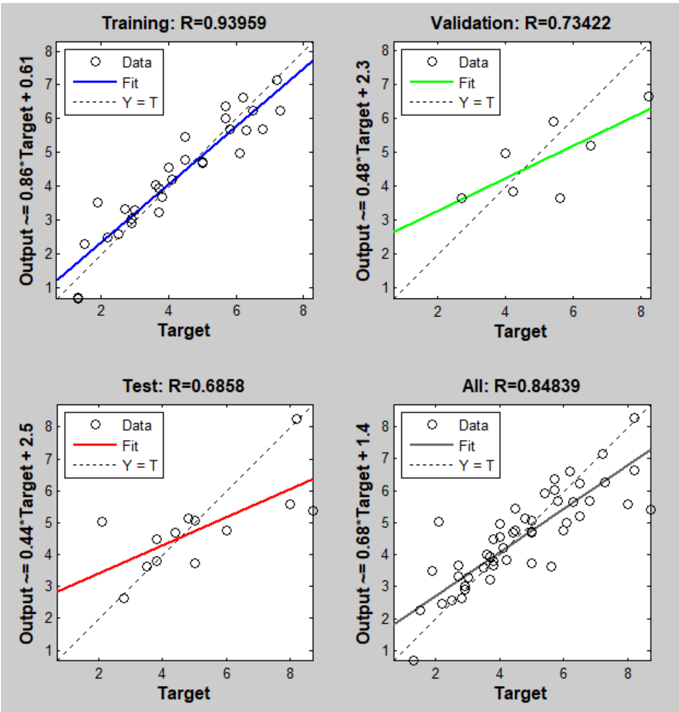

Figure A.65: Performance Plots for ‘traingdx’ Function for ML Wells

5) ANN modelling results and optimum conditions with ‘trainbfg’ Function

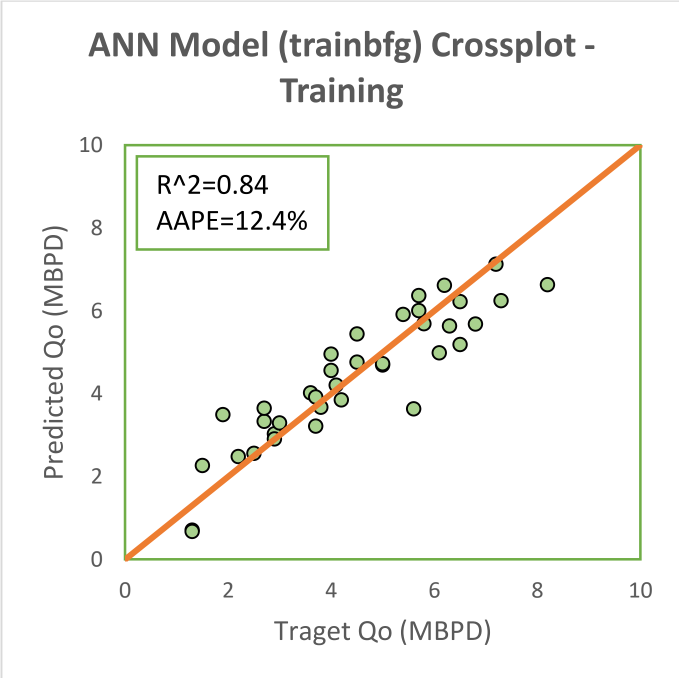

Figure A.66: Crossplot of Oil Rates with ANN ‘trainbfg’ Model in ML Wells – Training

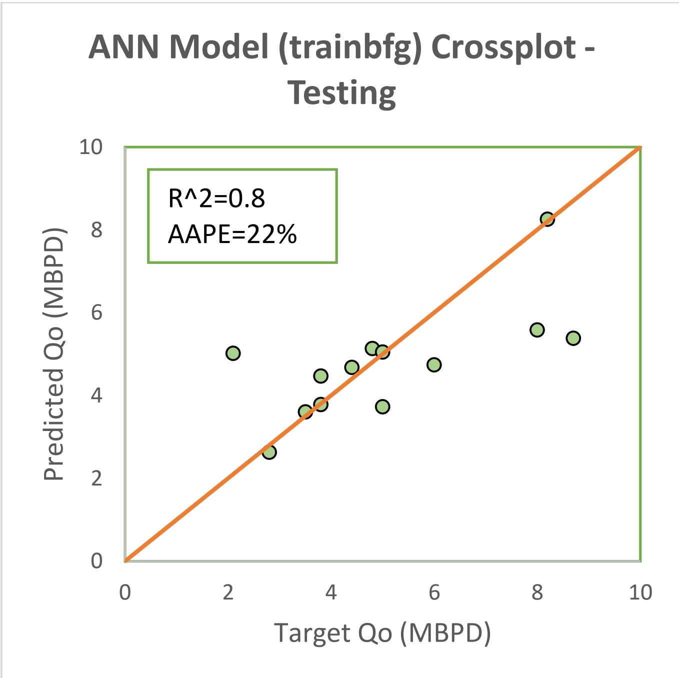

Figure A.67: Crossplot of Oil Rates with ANN ‘trainbfg’ Model in ML Wells – Testing

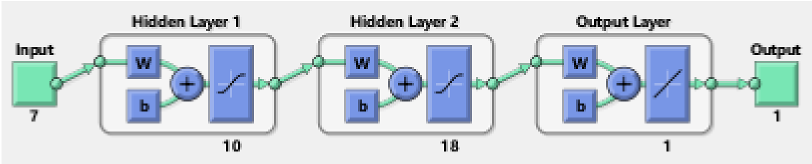

Figure A.68: Neural Network Structure for ‘trainbfg’ Function for ML Wells

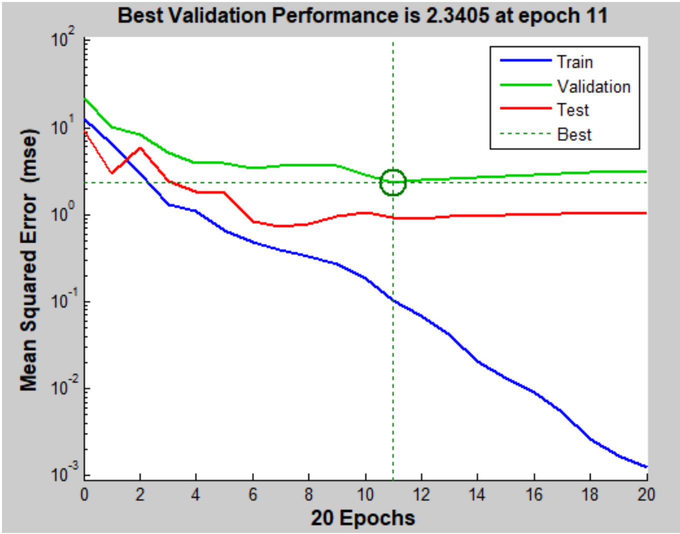

Figure A.69: Best Validation Performance of ‘trainbfg’ Function for ML Wells

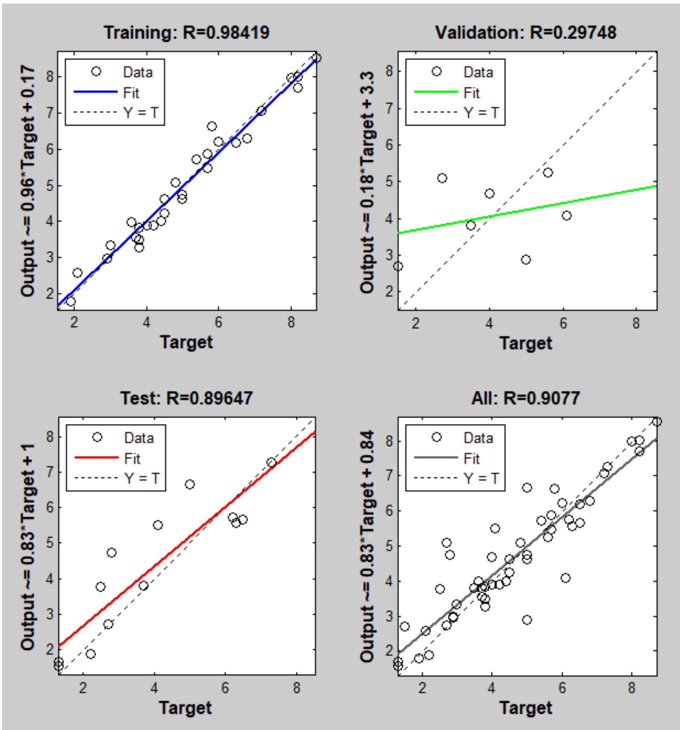

Figure A.70: Performance Plots for ‘trainbfg’ Function for ML Wells

6) ANN modelling results and optimum conditions with ‘trainscg’ Function

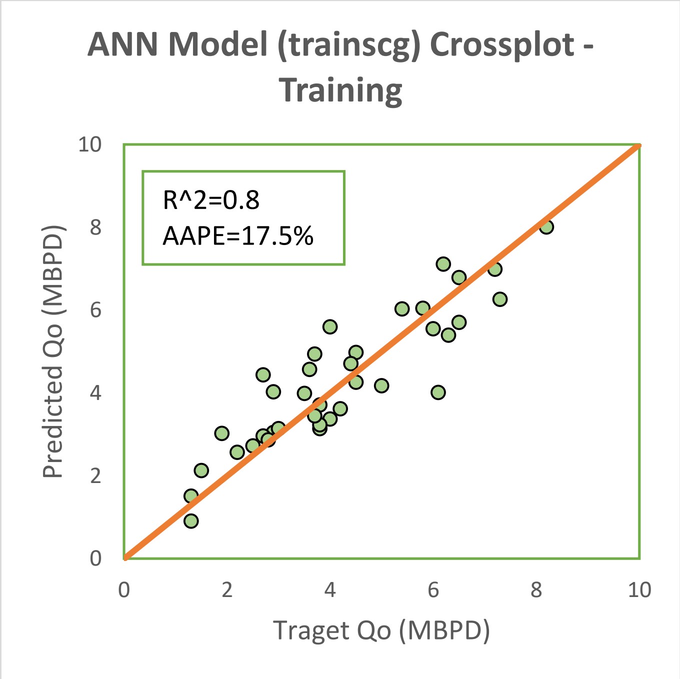

Figure A.71: Crossplot of Oil Rates with ANN ‘trainscg’ Model in ML Wells – Training

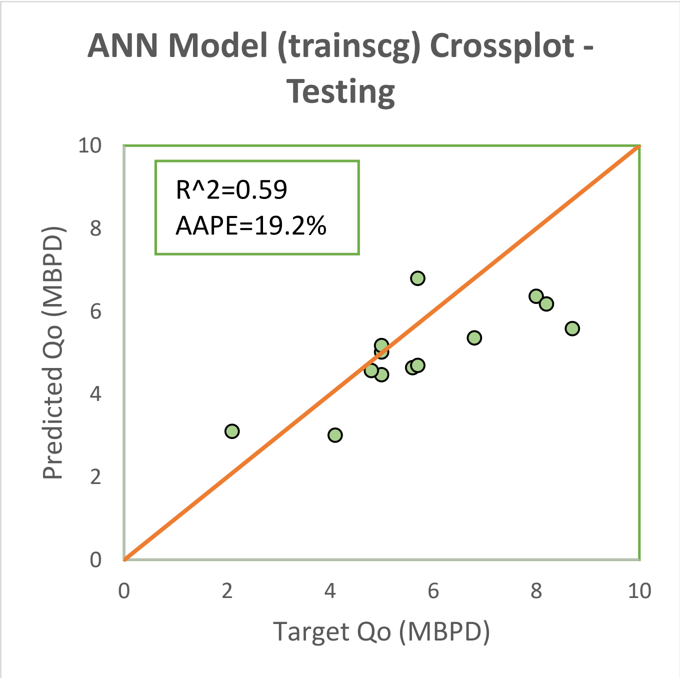

Figure A.72: Crossplot of Oil Rates with ANN ‘trainscg’ Model in ML Wells – Testing

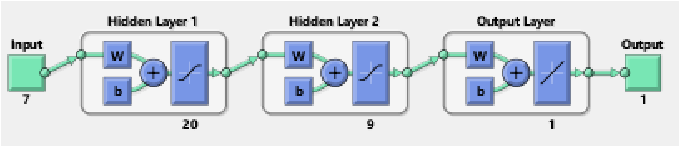

Figure A.73: Neural Network Structure for ‘trainscg’ Function for ML Wells

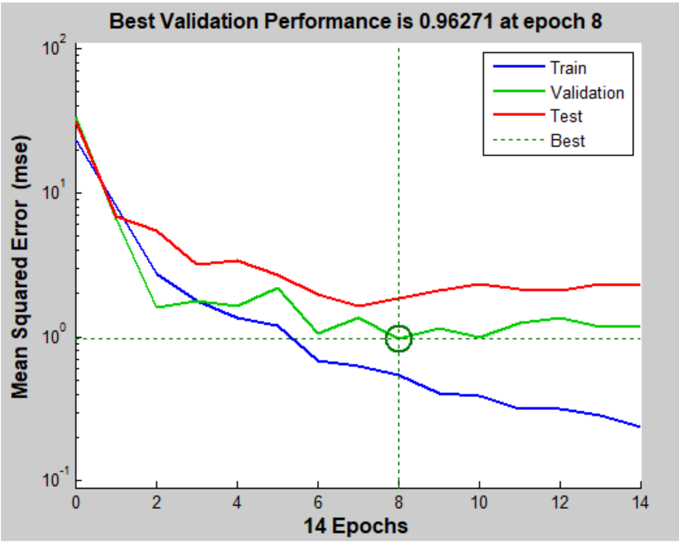

Figure A.74: Best Validation Performance of ‘trainscg’ Function for ML Wells

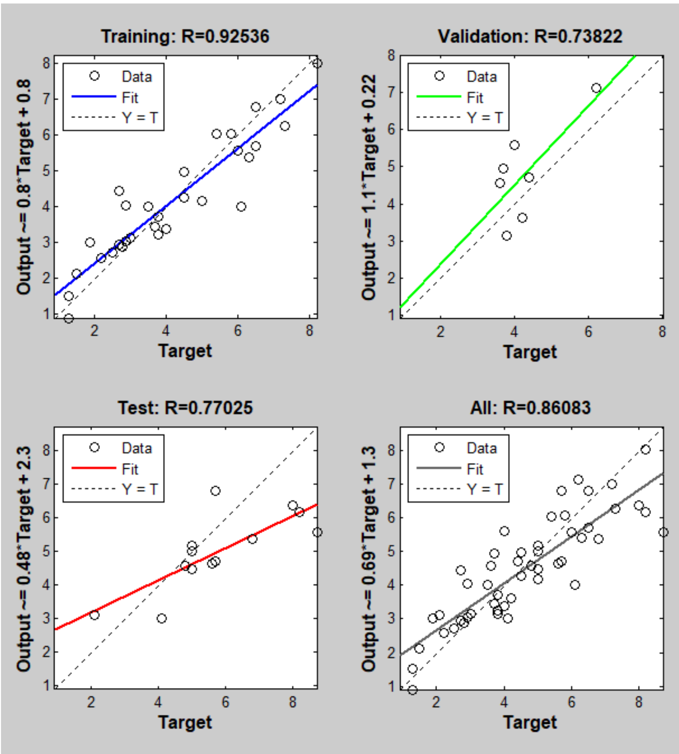

Figure A.75: Performance Plots for ‘trainscg’ Function for ML Wells

7) ANN modelling results and optimum conditions with ‘trainoss’ Function

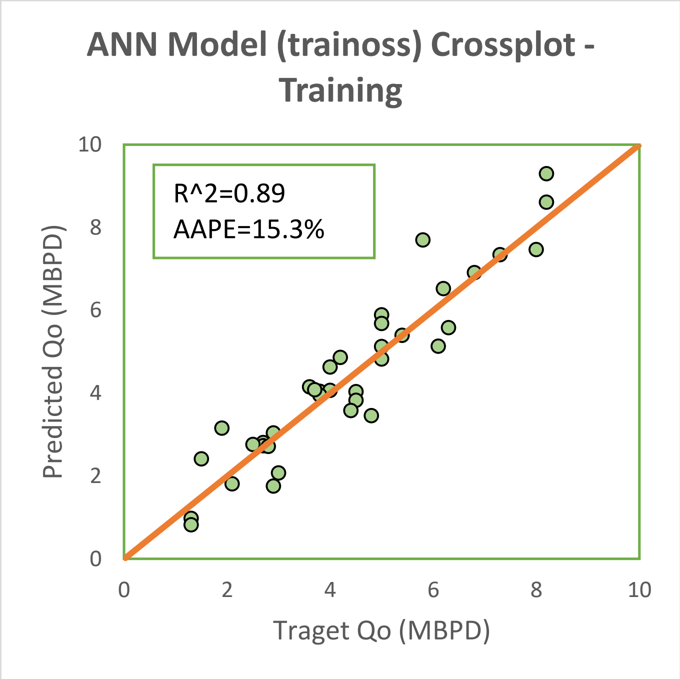

Figure A.76: Crossplot of Oil Rates with ANN ‘trainoss’ Model in ML Wells – Training

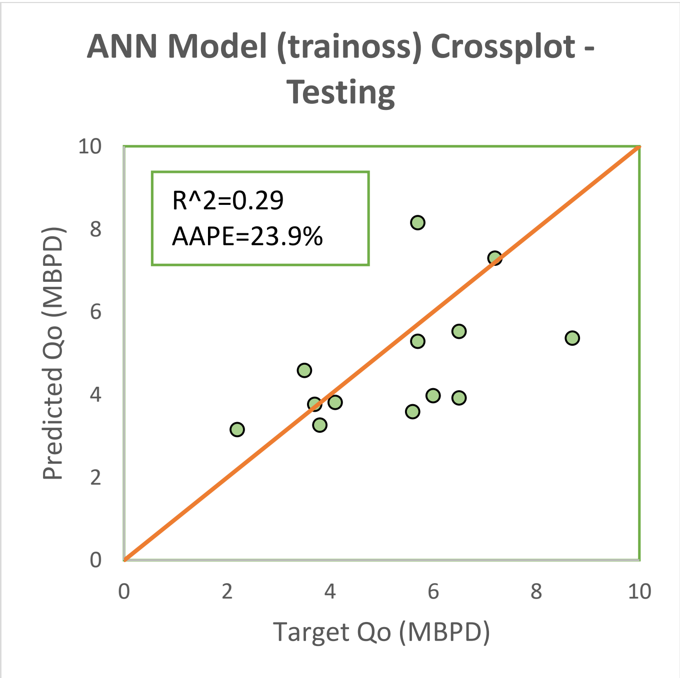

Figure A.77: Crossplot of Oil Rates with ANN ‘trainoss’ Model in ML Wells – Testing

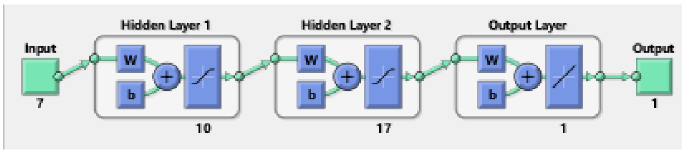

Figure A.78: Neural Network Structure for ‘trainoss’ Function for ML Wells

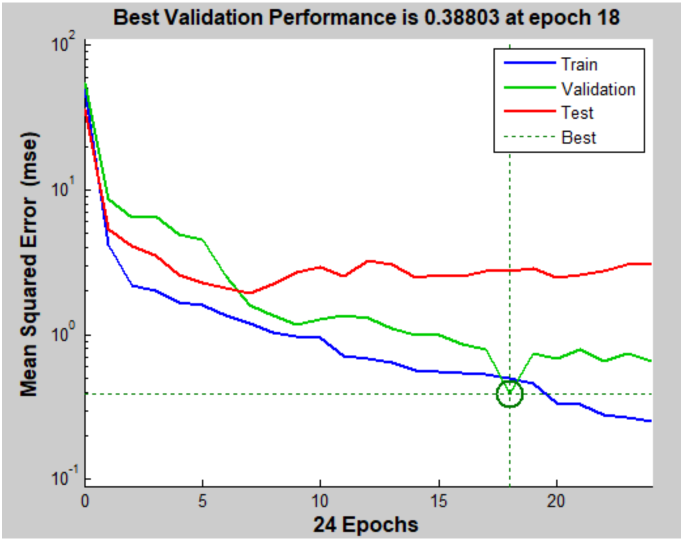

Figure A.79: Best Validation Performance of ‘trainoss’ Function for ML Wells

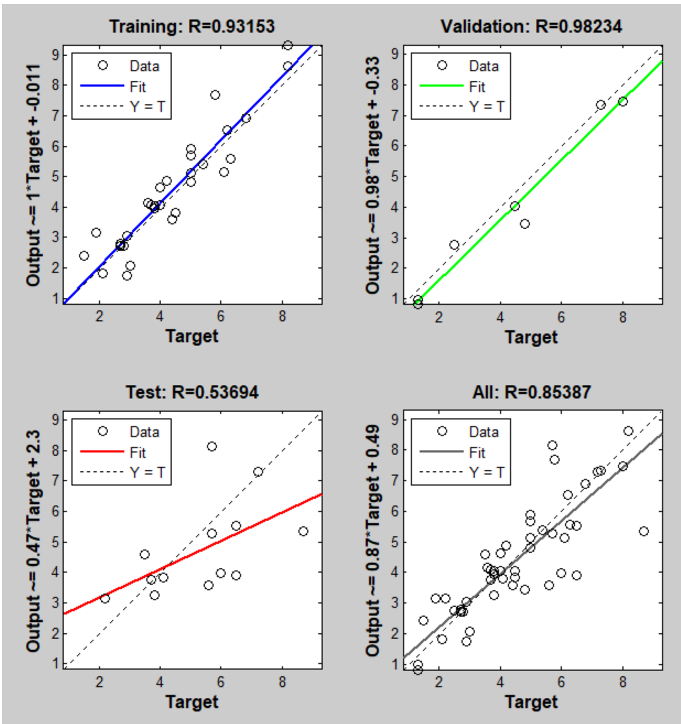

Figure A.80: Performance Plots for ‘trainoss’ Function for ML Wells

8) ANN modelling results and optimum conditions with ‘trainrp’ Function

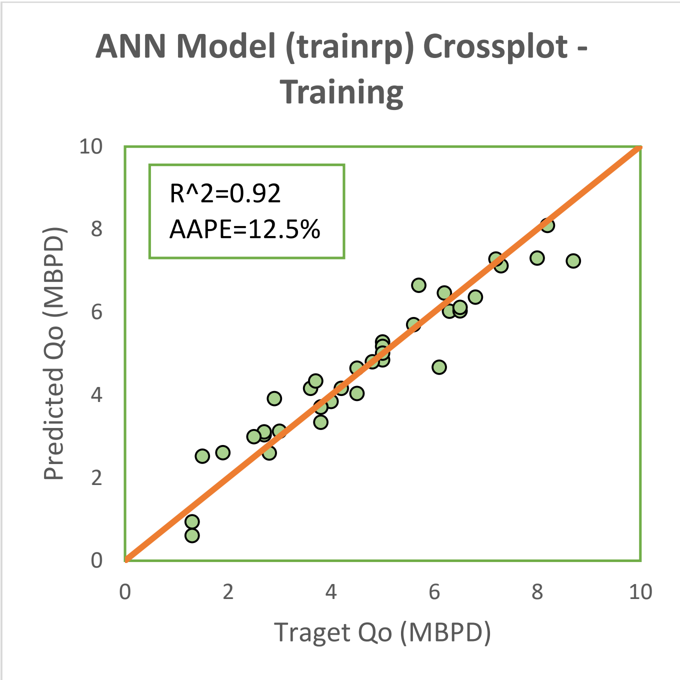

Figure A.81: Crossplot of Oil Rates with ANN ‘trainrp’ Model in ML Wells – Training

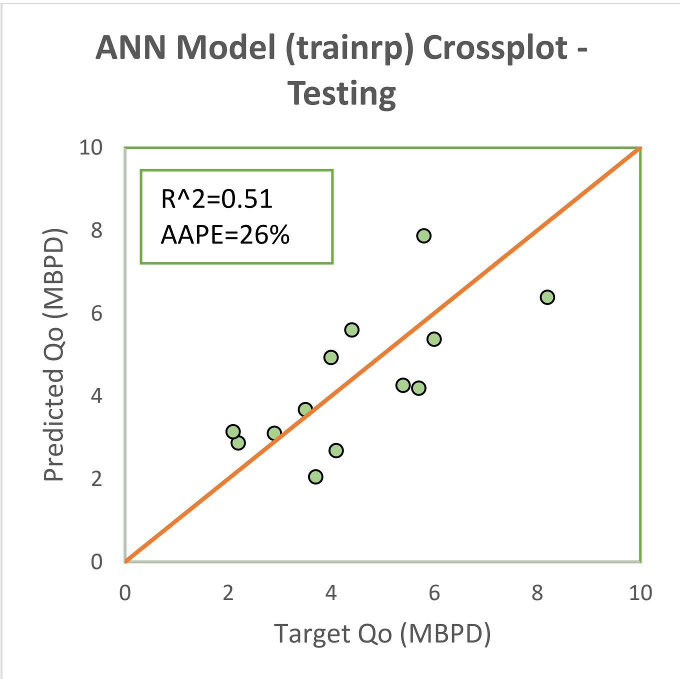

Figure A.82: Crossplot of Oil Rates with ANN ‘trainrp’ Model in ML Wells – Testing

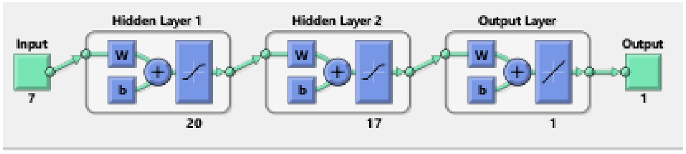

Figure A.83: Neural Network Structure for ‘trainrp’ Function for ML Wells

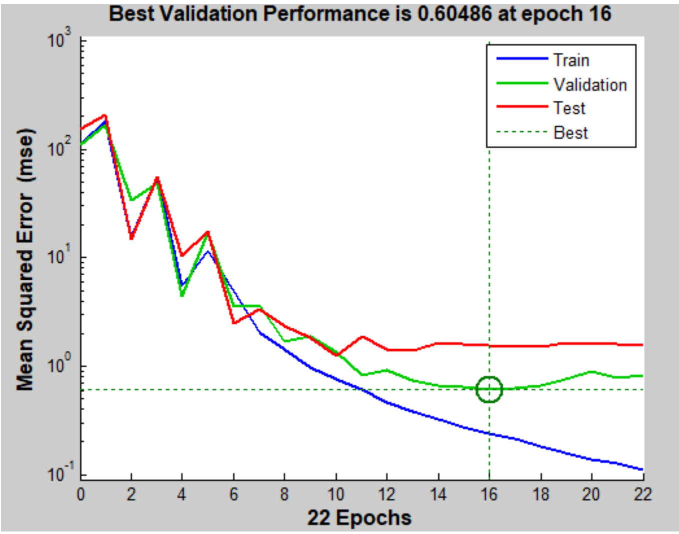

Figure A.84: Best Validation Performance of ‘trainrp’ Function for ML Wells

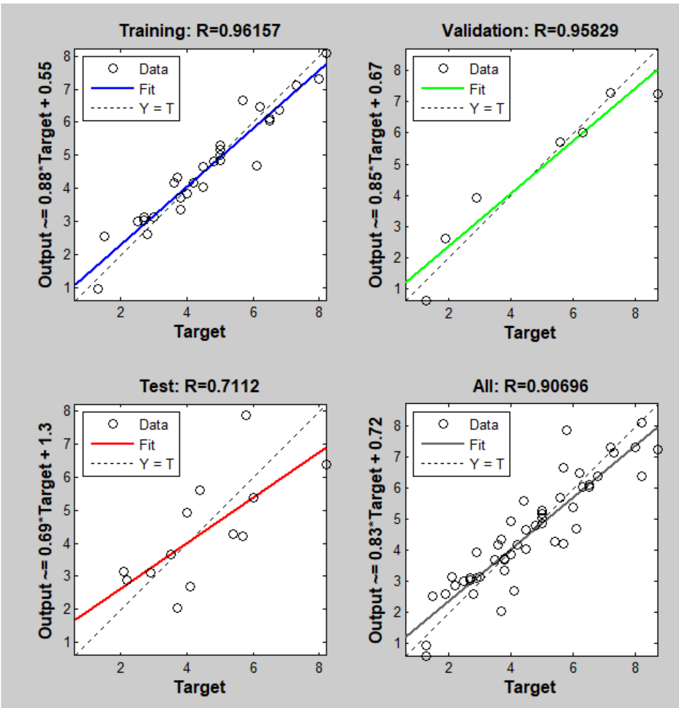

Figure A.85: Performance Plots for ‘trainrp’ Function for ML Wells

9) ANN modelling results and optimum conditions with ‘trainb’ Function

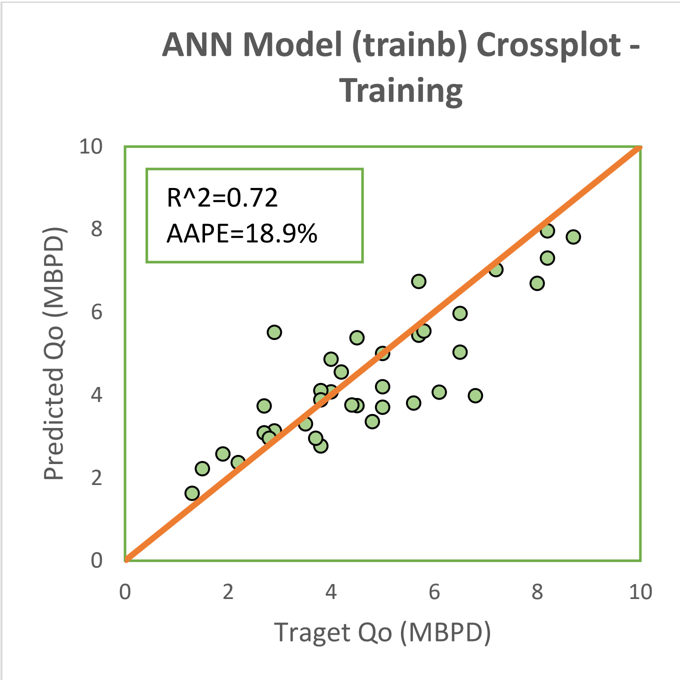

Figure A.86: Crossplot of Oil Rates with ANN ‘trainb’ Model in ML Wells – Training

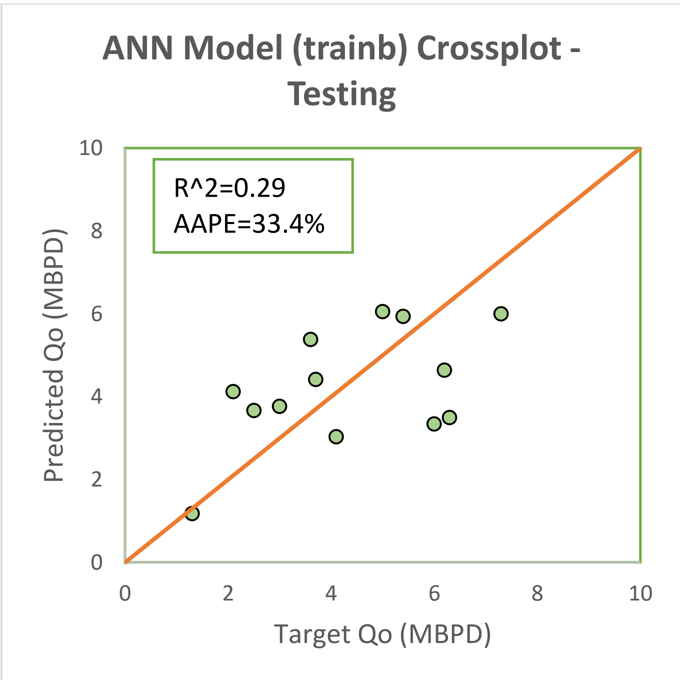

Figure A.87: Crossplot of Oil Rates with ANN ‘trainb’ Model in ML Wells – Testing

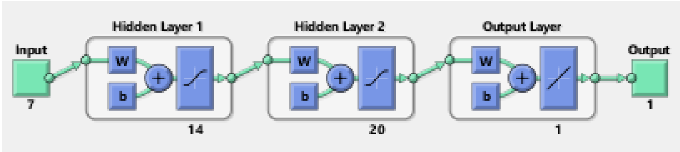

Figure A.88: Neural Network Structure for ‘trainb’ Function for ML Wells

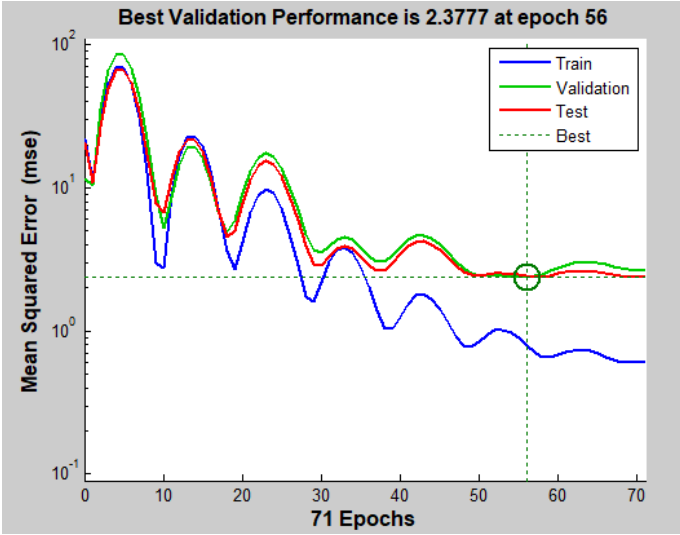

Figure A.89: Best Validation Performance of ‘trainb’ Function for ML Wells

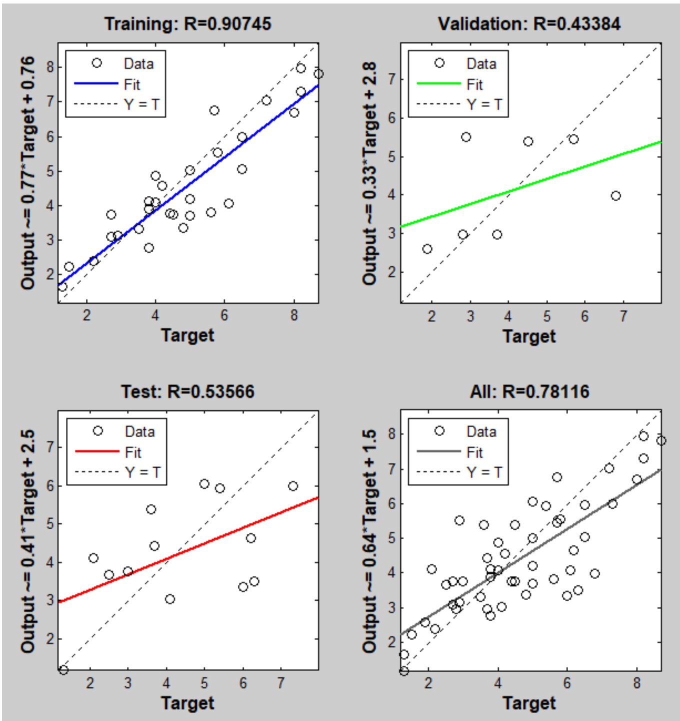

Figure A.90: Performance Plots for ‘trainb’ Function for ML Wells

C) ANN model for the combination data sets from H & ML wells

1) ANN modelling results and optimum conditions with ‘trainlm’ Function

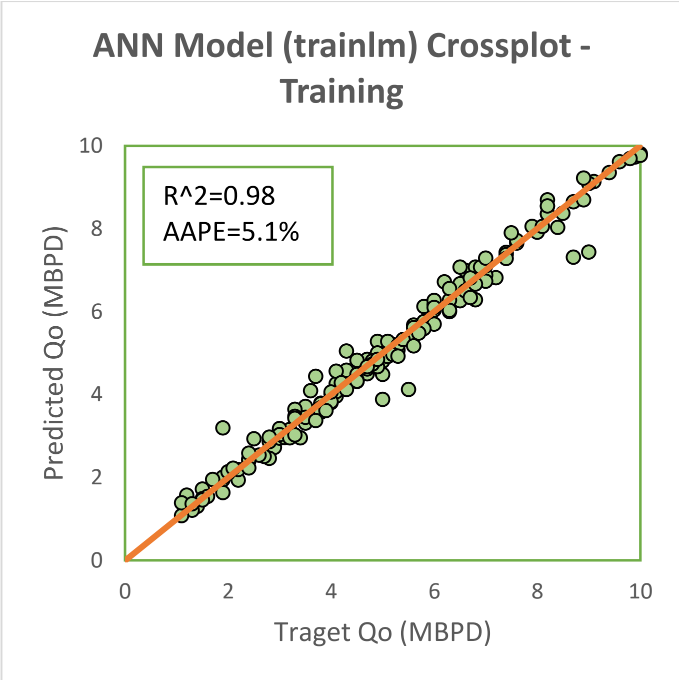

Figure A.91: Crossplot of Oil Rates with ANN ‘trainlm’ Model in H & ML Wells – Training

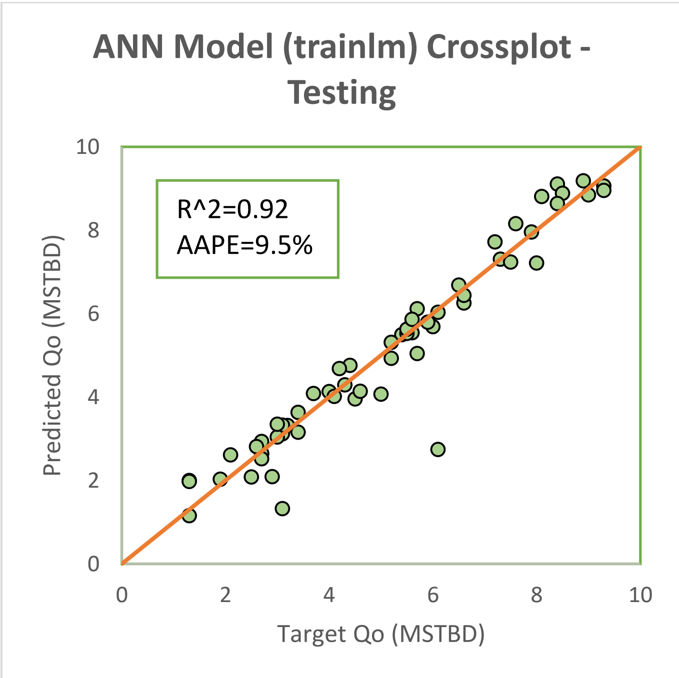

Figure A.92: Crossplot of Oil Rates with ANN ‘trainlm’ Model in H & ML Wells – Testing

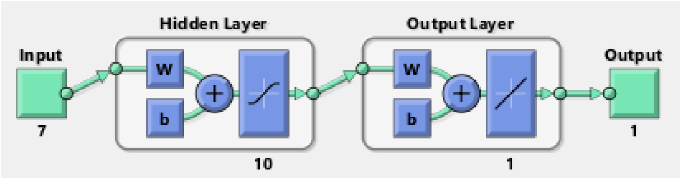

Figure A.93: Neural Network Structure for ‘trainlm’ Function for H & ML Wells

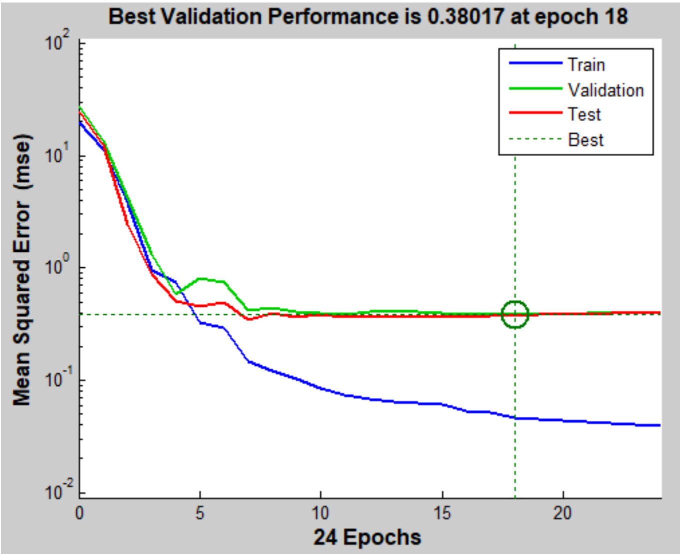

Figure A.94: Best Validation Performance of ‘trainlm’ Function for H & ML Wells

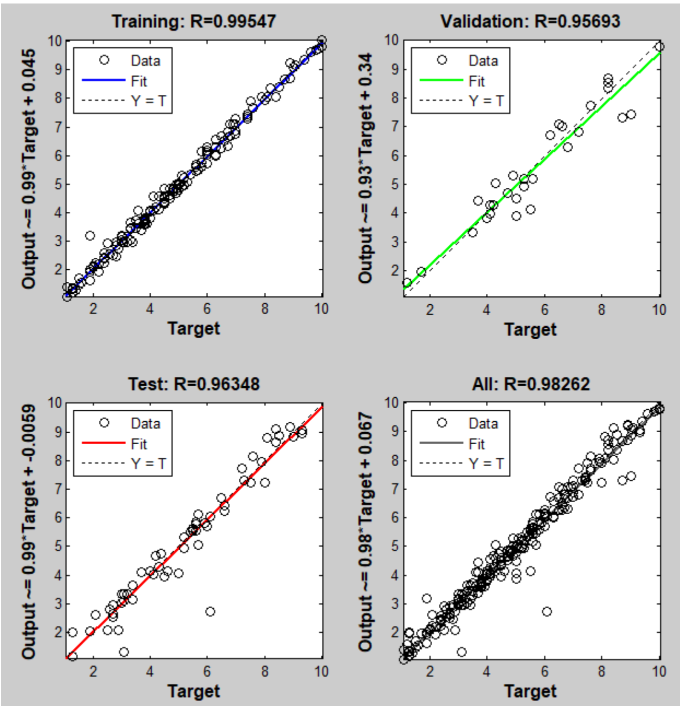

Figure A.95: Performance Plots for ‘trainlm’ Function for H & ML Wells

2) ANN modelling results and optimum conditions with 'trainlm -2L' Function

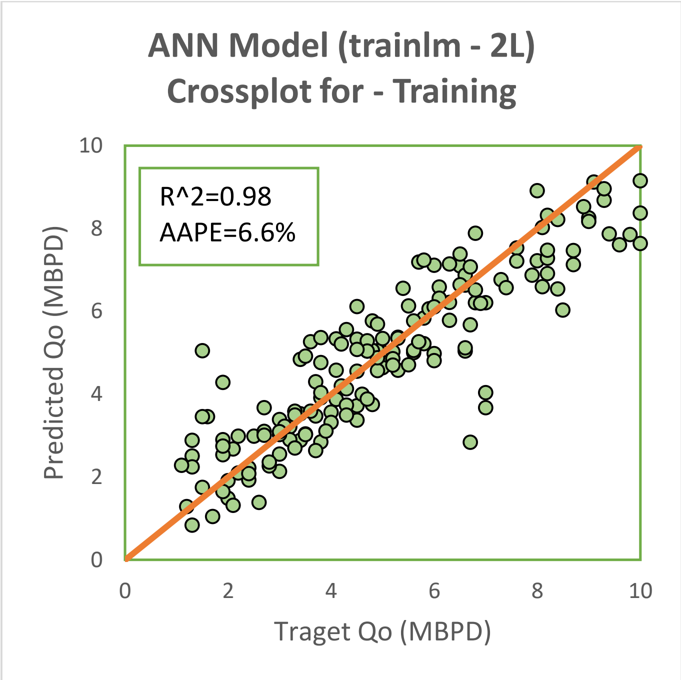

Figure A.96: Crossplot of Rates with ANN 'trainlm-2L' Model in H & ML Wells – Training

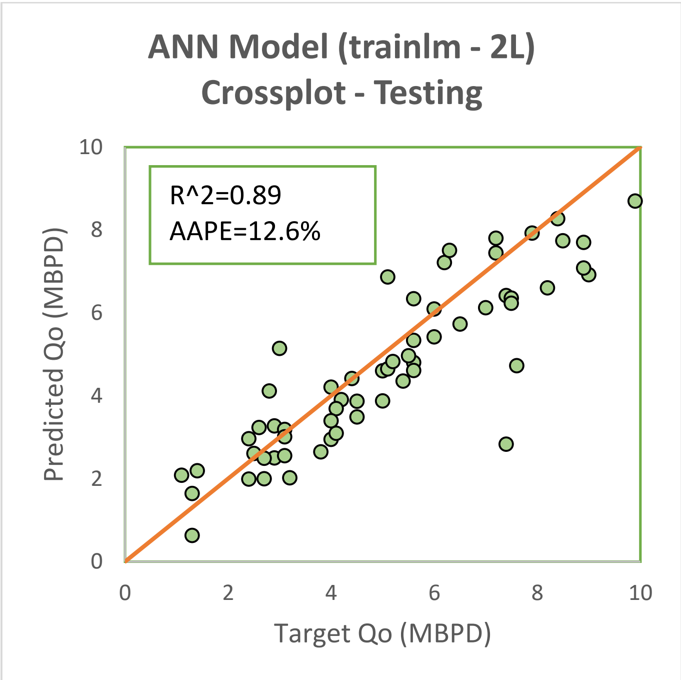

Figure A.97: Crossplot of Rates with ANN 'trainlm-2L' Model in H & ML Wells – Testing

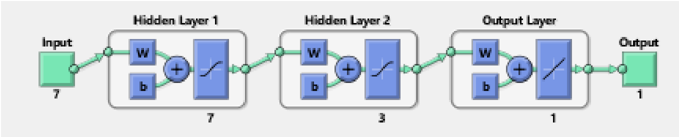

Figure A.98: Neural Network Structure for ‘trainlm-2L’ Function for H & ML Wells

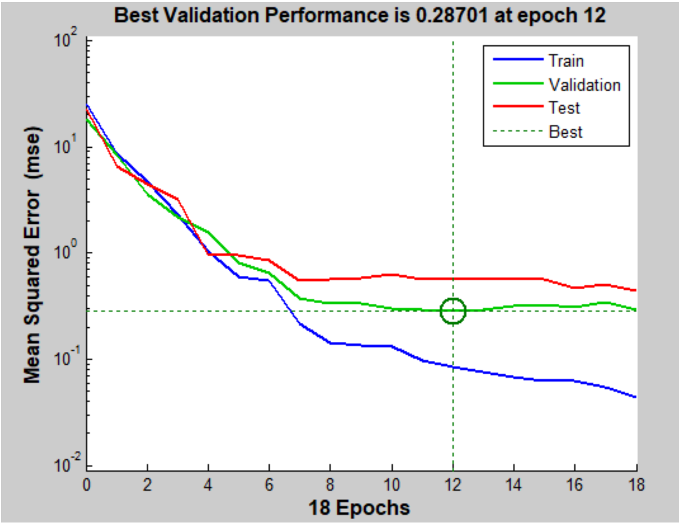

Figure A.99: Best Validation Performance of ‘trainlm-2L’ Function for H & ML Wells

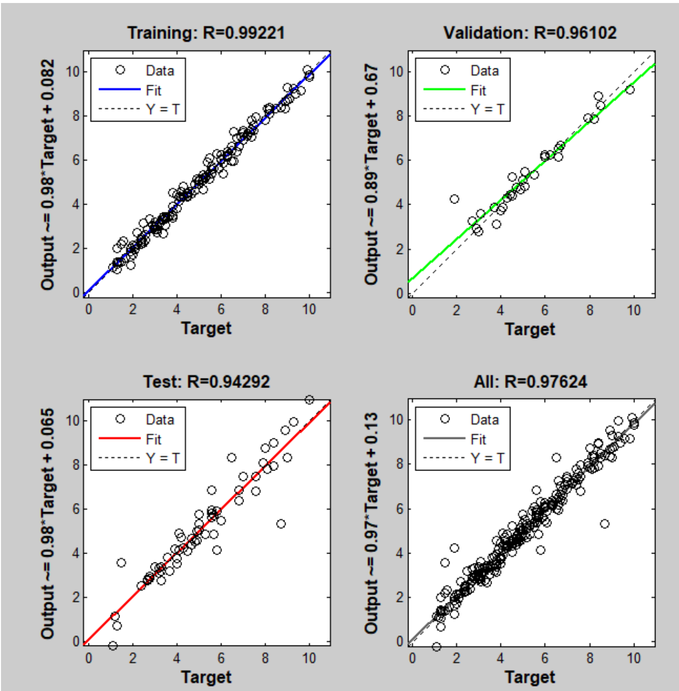

Figure A.100: Performance Plots for ‘trainlm-2L’ Function for H & ML Wells

3) ANN modelling results and optimum conditions with 'traingd' Function

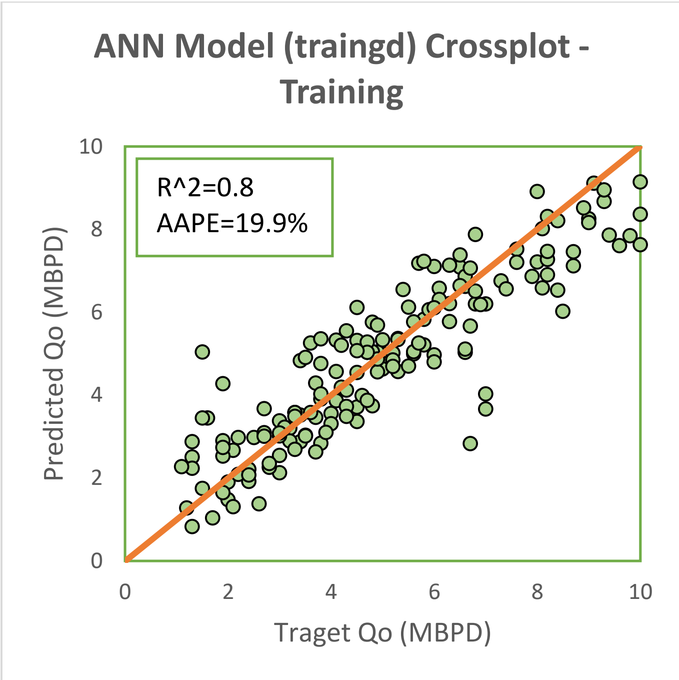

Figure A.101: Crossplot of Oil Rates with ANN 'traingd' Model in H & ML Wells – Training

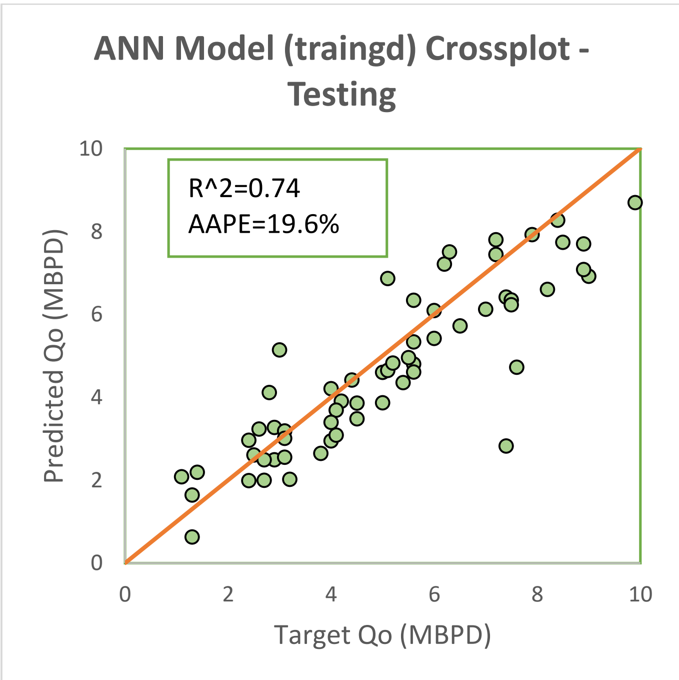

Figure A.102: Crossplot of Oil Rates with ANN 'traingd' Model in H & ML Wells – Testing

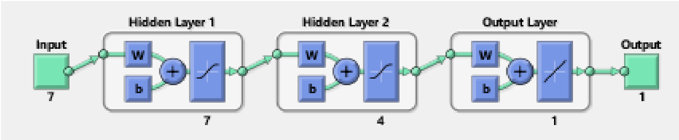

Figure A.103: Neural Network Structure for ‘traingd’ Function for H & ML Wells

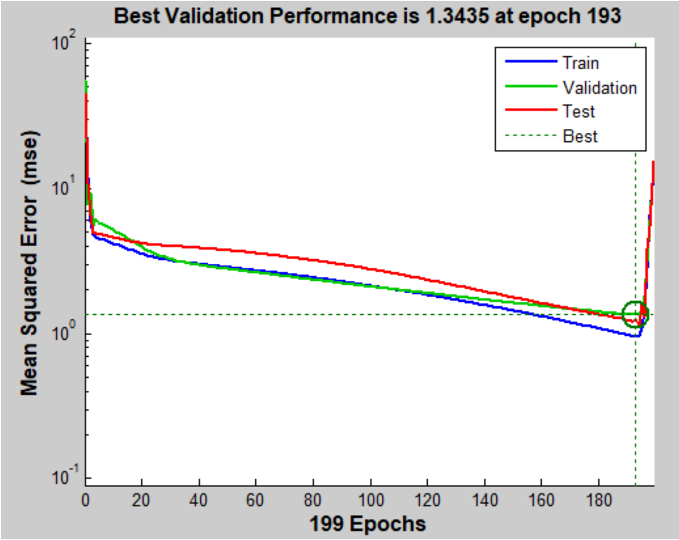

Figure A.104: Best Validation Performance of ‘traingd’ Function for H & ML Wells

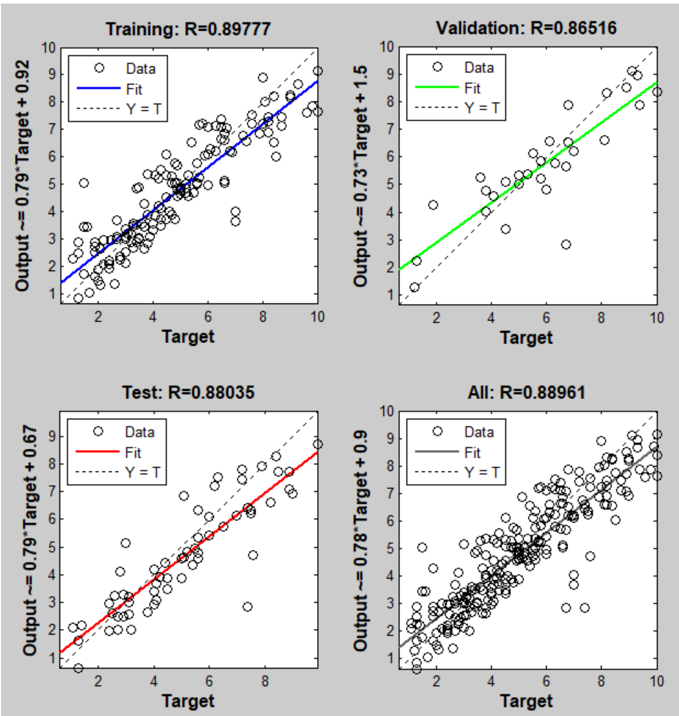

Figure A.105: Performance Plots for ‘traingd’ Function for H & ML Wells

4) ANN modelling results and optimum conditions with ‘traingdx’ Function

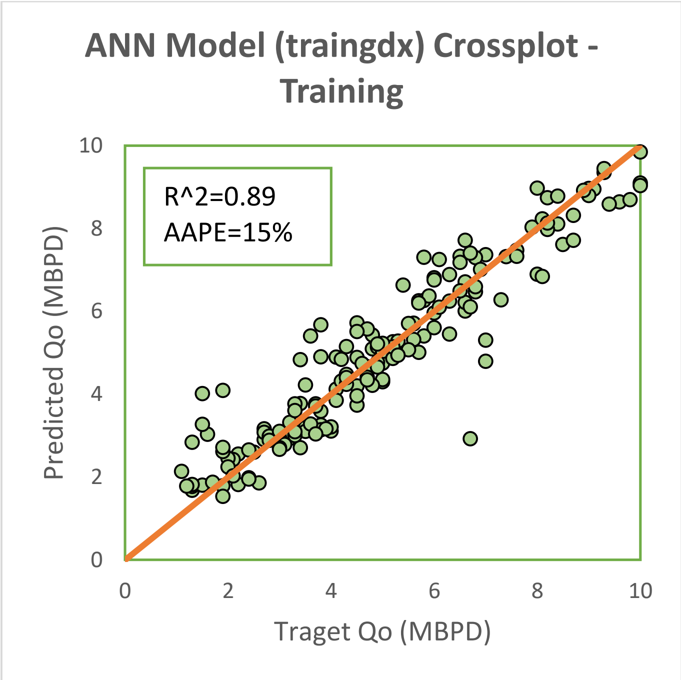

Figure A.106: Crossplot of Oil Rates with ANN ‘traingdx’ Model in H & ML Wells – Training

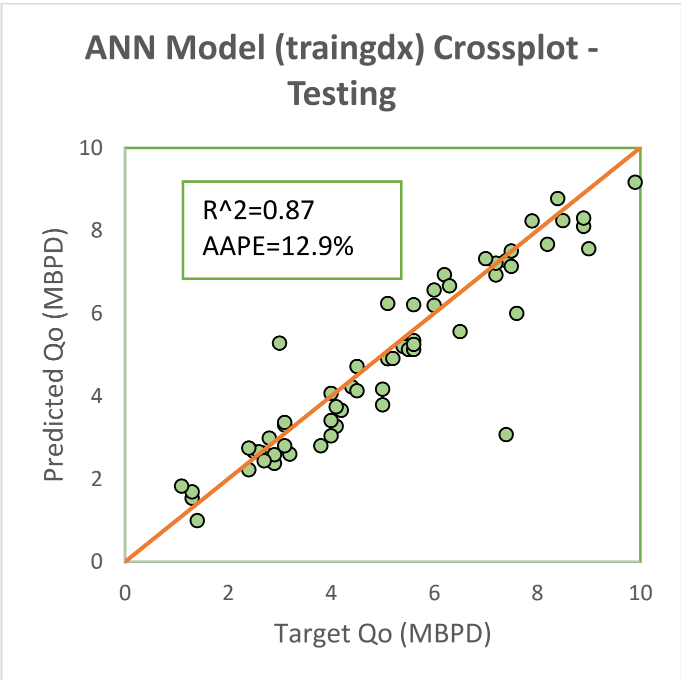

Figure A.107: Crossplot of Oil Rates with ANN ‘traingdx’ Model in H & ML Wells – Testing

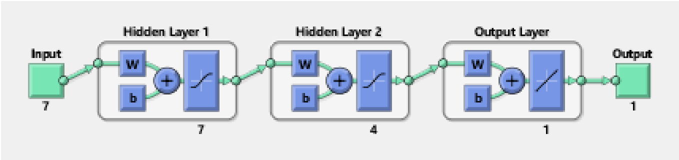

Figure A.108: Neural Network Structure for ‘traingdx’ Function for H & ML Wells

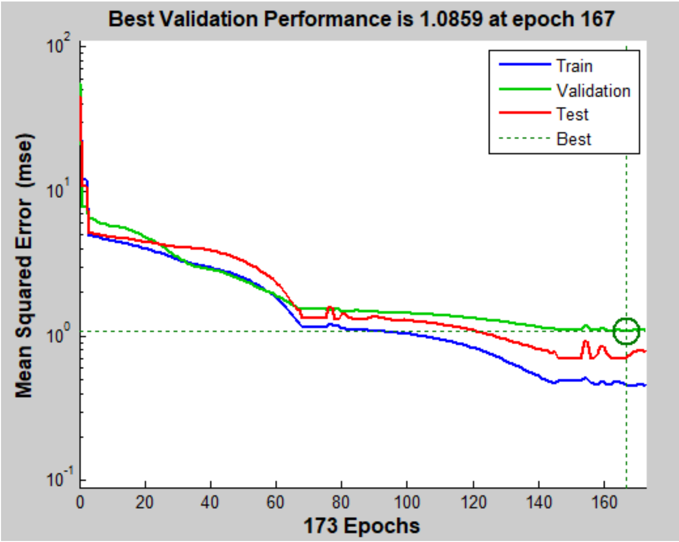

Figure A.109: Best Validation Performance of ‘traingdx’ Function for H & ML Wells

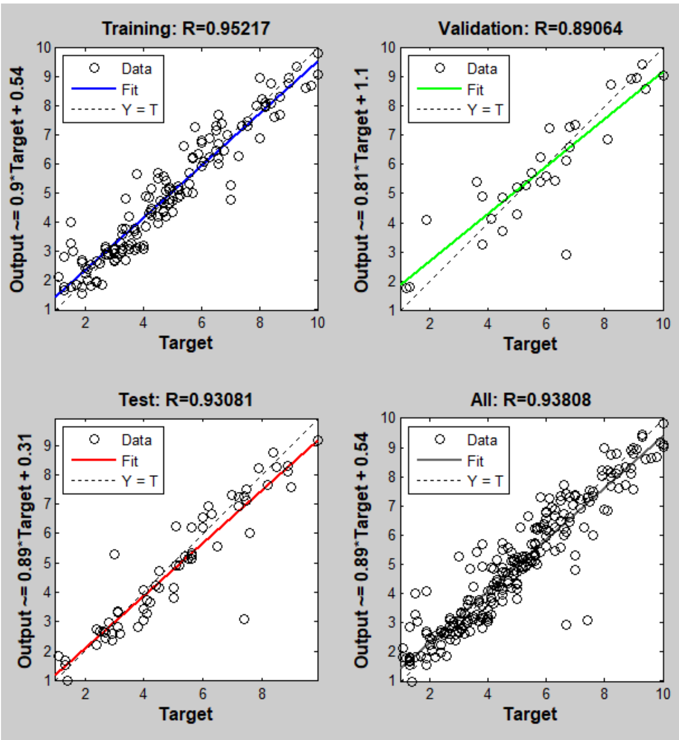

Figure A.110: Performance Plots for ‘traingdx’ Function for H & ML Wells

5) ANN modelling results and optimum conditions with ‘trainbfg’ Function

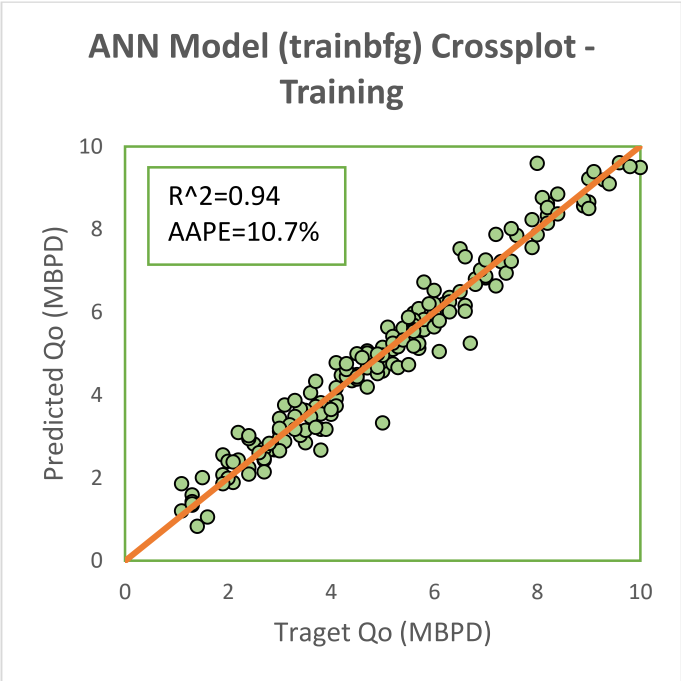

Figure A.111: Crossplot of Oil Rates with ANN ‘trainbfg’ Model in H & ML Wells – Training

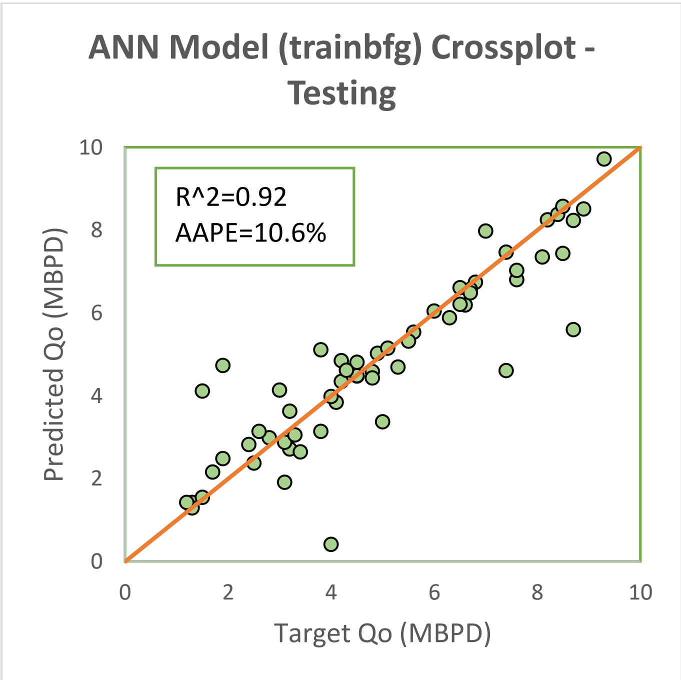

Figure A.112: Crossplot of Oil Rates with ANN ‘trainbfg’ Model in H & ML Wells – Testing

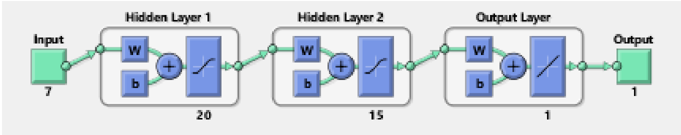

Figure A.113: Neural Network Structure for ‘trainbfg’ Function for H & ML Wells

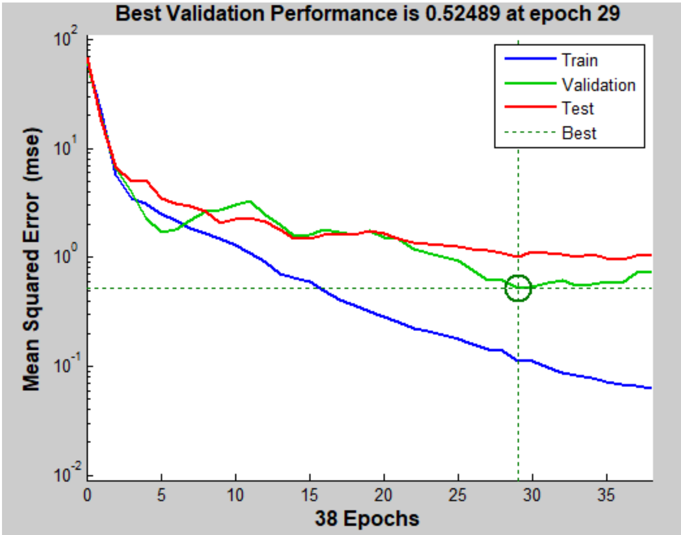

Figure A.114: Best Validation Performance of ‘trainbfg’ Function for H & ML Wells

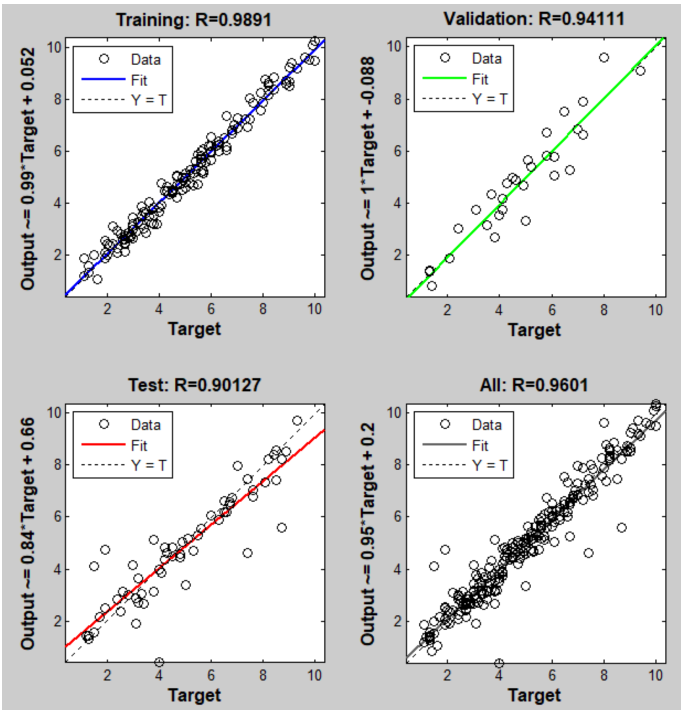

Figure A.115: Performance Plots for ‘trainbfg’ Function for H & ML Wells

6) ANN modelling results and optimum conditions with 'trainscg' Function

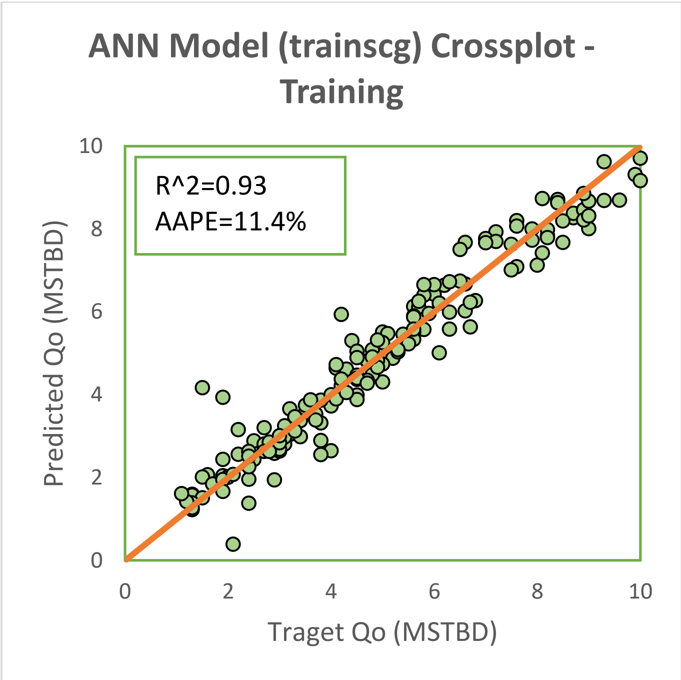

Figure A.116: Crossplot of Oil Rates with ANN 'trainscg' Model in H & ML Wells – Training

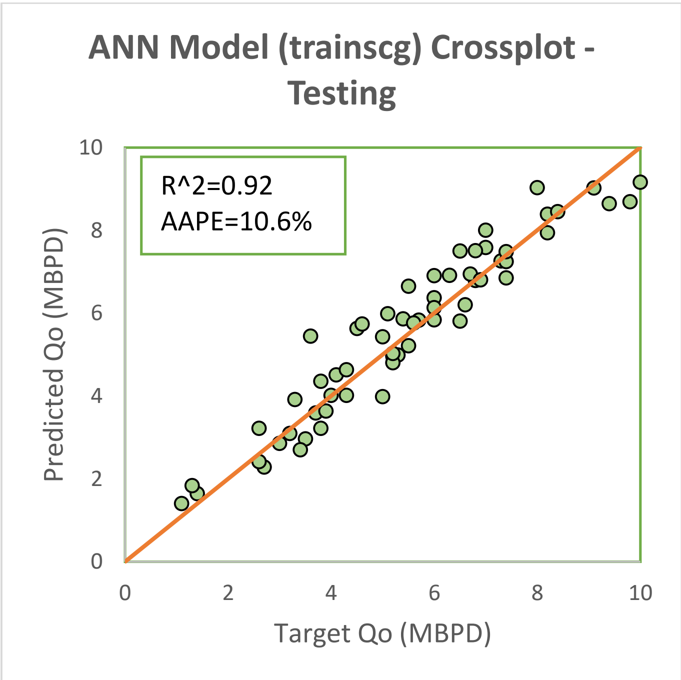

Figure A.117: Crossplot of Oil Rates with ANN 'trainscg' Model in H & ML Wells – Testing

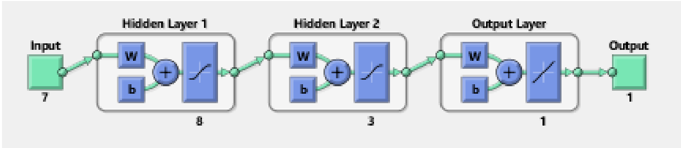

Figure A.118: Neural Network Structure for ‘trainscg’ Function for H & ML Wells

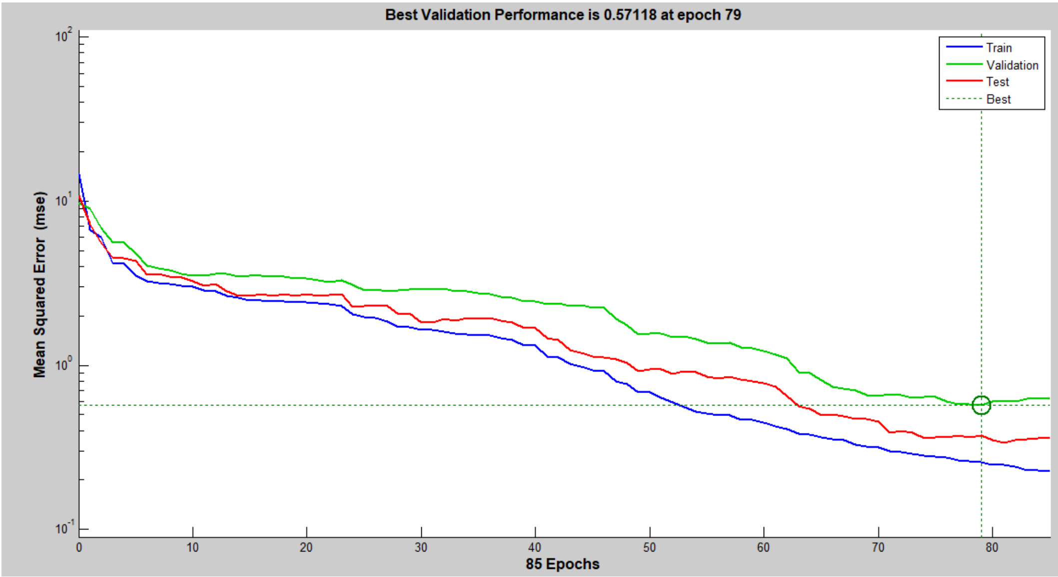

Figure A.119: Best Validation Performance of ‘trainscg’ Function for H & ML Wells

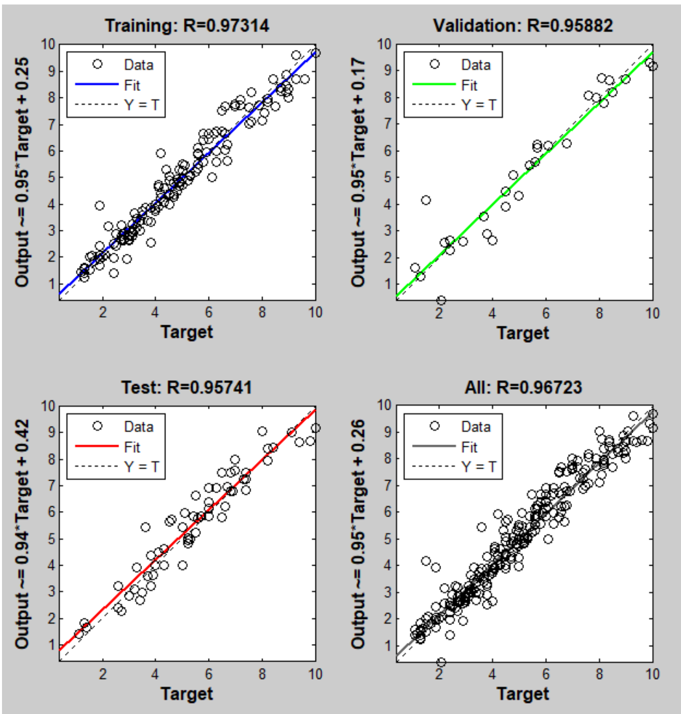

Figure A.120: Performance Plots for ‘trainscg’ Function for H & ML Wells

7) ANN modelling results and optimum conditions with ‘trainoss’ Function

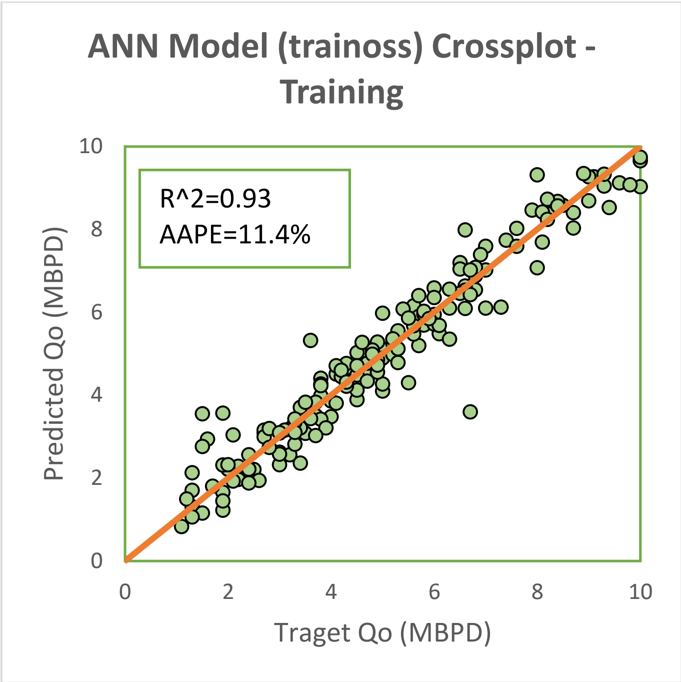

Figure A.121: Crossplot of Oil Rates with ANN ‘trainoss’ Model in H & ML Wells – Training

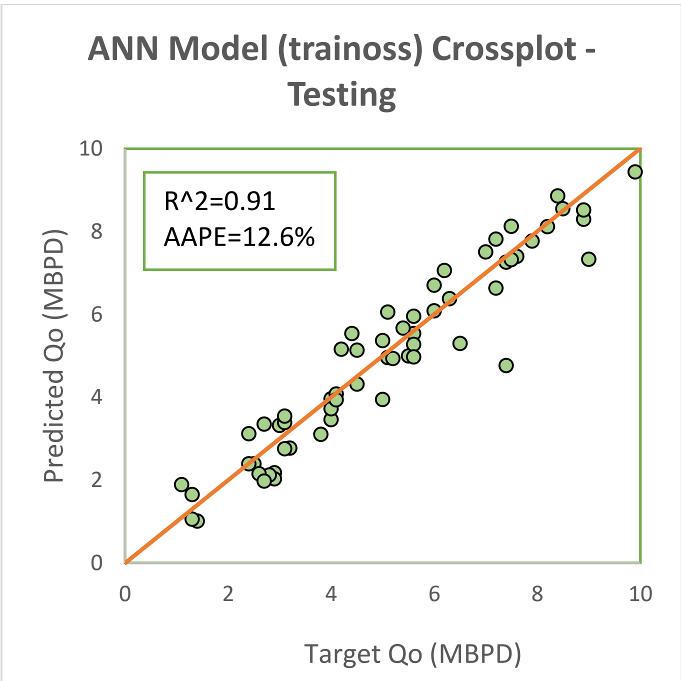

Figure A.122: Crossplot of Oil Rates with ANN ‘trainoss’ Model in H & ML Wells – Testing

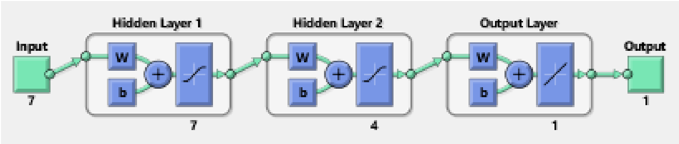

Figure A.123: Neural Network Structure for ‘trainoss’ Function for H & ML Wells

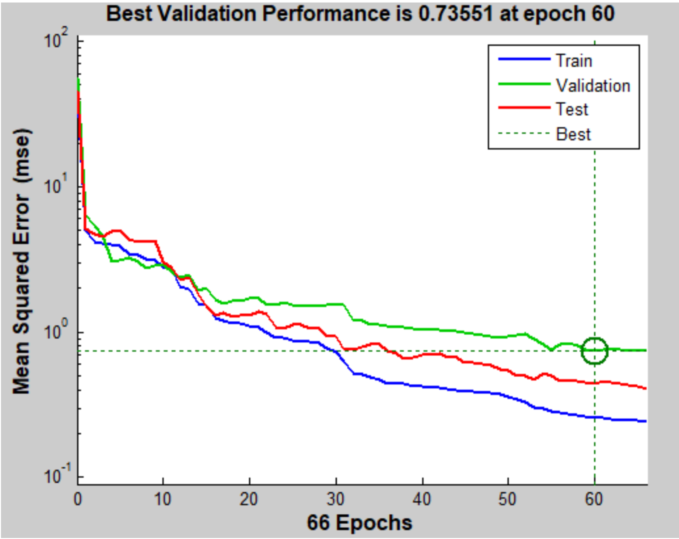

Figure A.124: Best Validation Performance of ‘trainoss’ Function for H & ML Wells

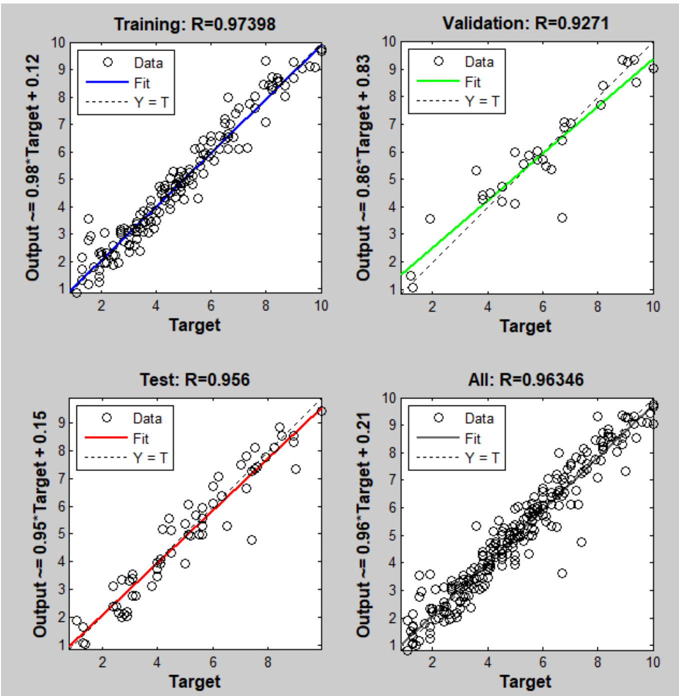

Figure A.125: Performance Plots for ‘trainoss’ Function for H & ML Wells

8) ANN modelling results and optimum conditions with ‘trainrp’ Function

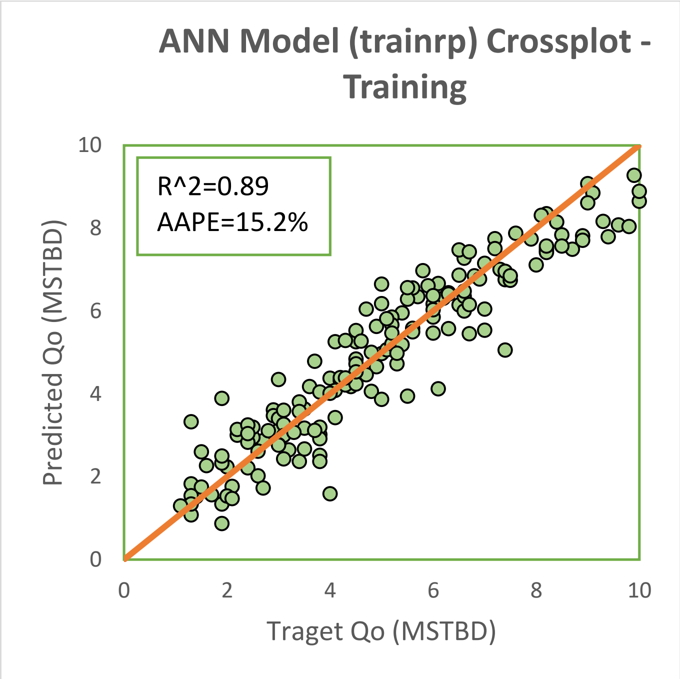

Figure A.126: Crossplot of Oil Rates with ANN ‘trainrp’ Model in H & ML Wells – Training

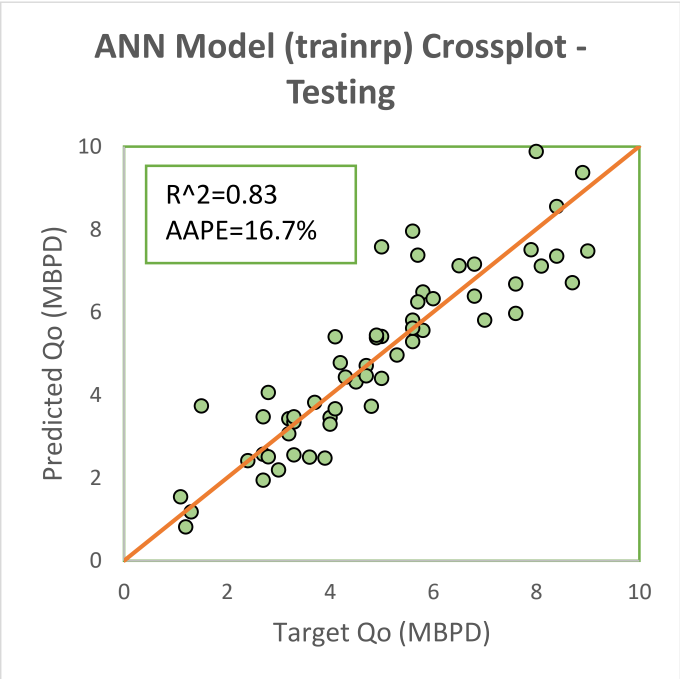

Figure A.127: Crossplot of Oil Rates with ANN ‘trainrp’ Model in H & ML Wells – Testing

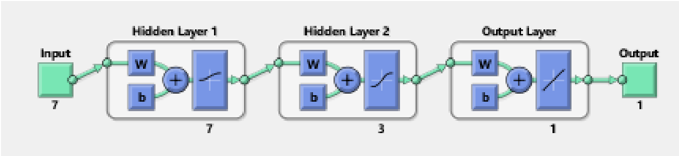

Figure A.128: Neural Network Structure for ‘trainrp’ Function for H & ML Wells

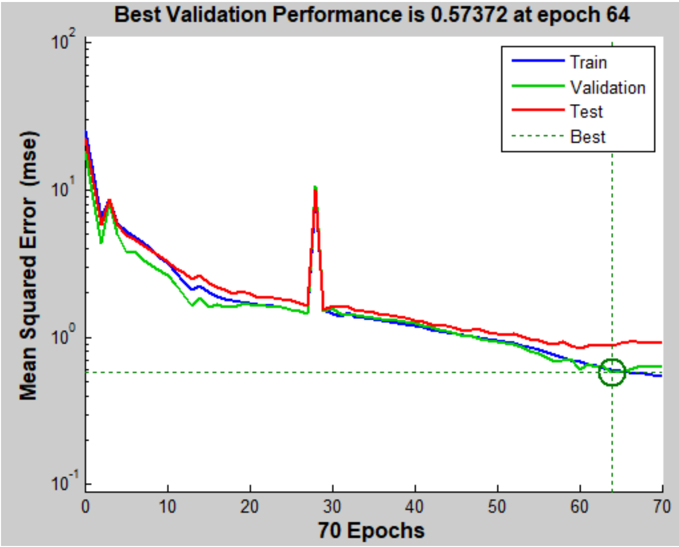

Figure A.129: Best Validation Performance of ‘trainrp’ Function for H & ML Wells

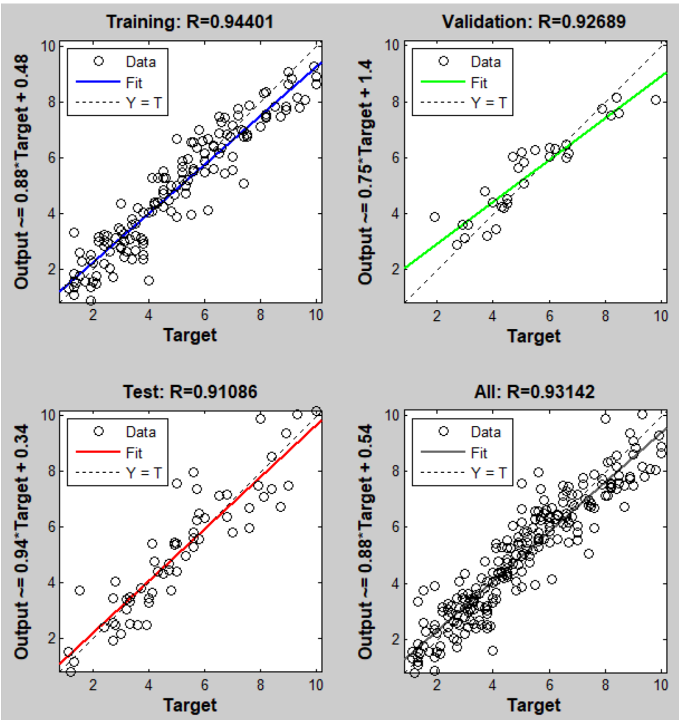

Figure A.130: Performance Plots for ‘trainrp’ Function for H & ML Wells

9) ANN modelling results and optimum conditions with ‘trainb’ Function

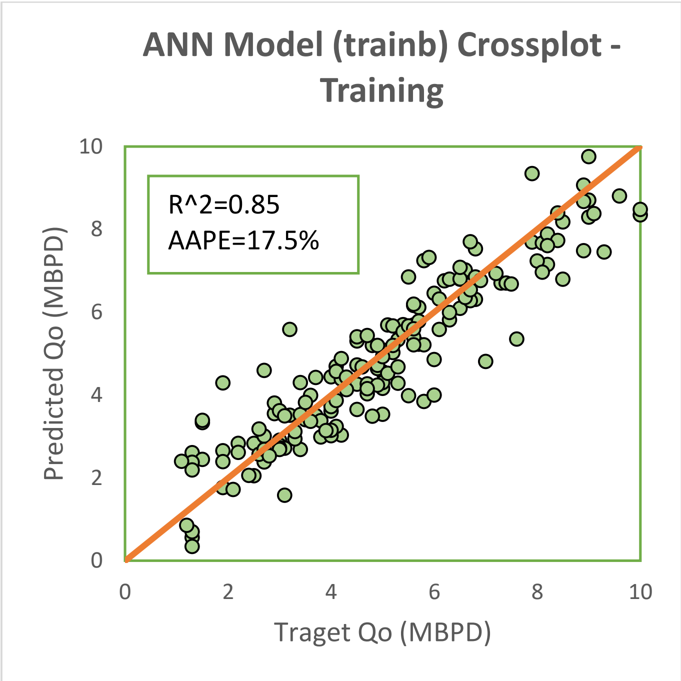

Figure A.131: Crossplot of Oil Rates with ANN ‘trainb’ Model in H & ML Well– Training

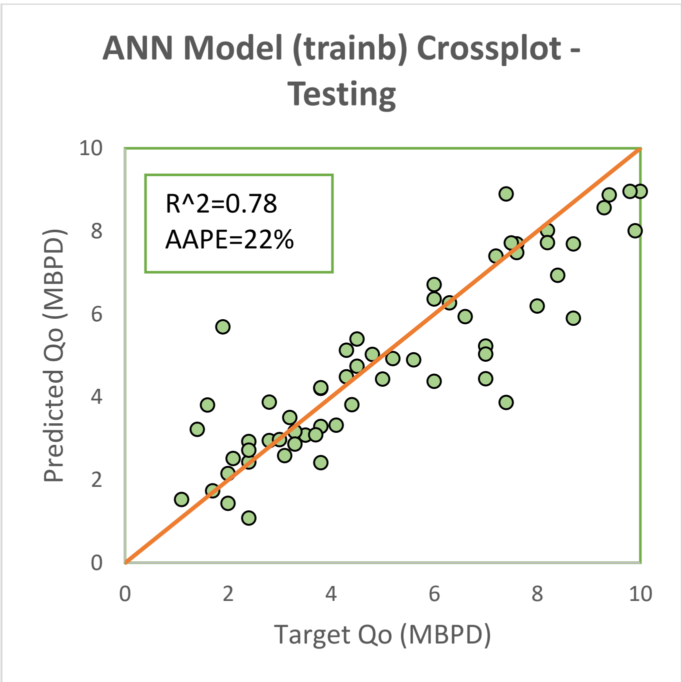

Figure A.132: Crossplot of Oil Rates with ANN ‘trainb’ Model in H & ML Well – Testing

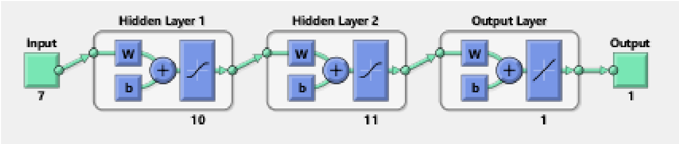

Figure A.133: Neural Network Structure for ‘trainb’ Function for H & ML Wells

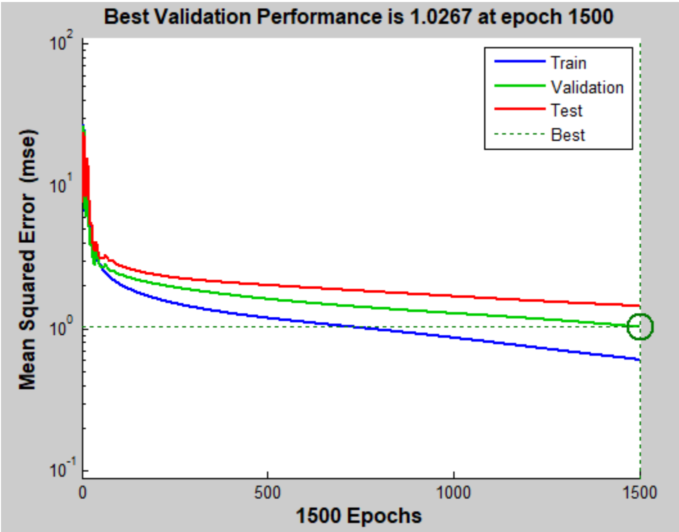

Figure A.134: Best Validation Performance of ‘trainb’ Function for H & ML Wells

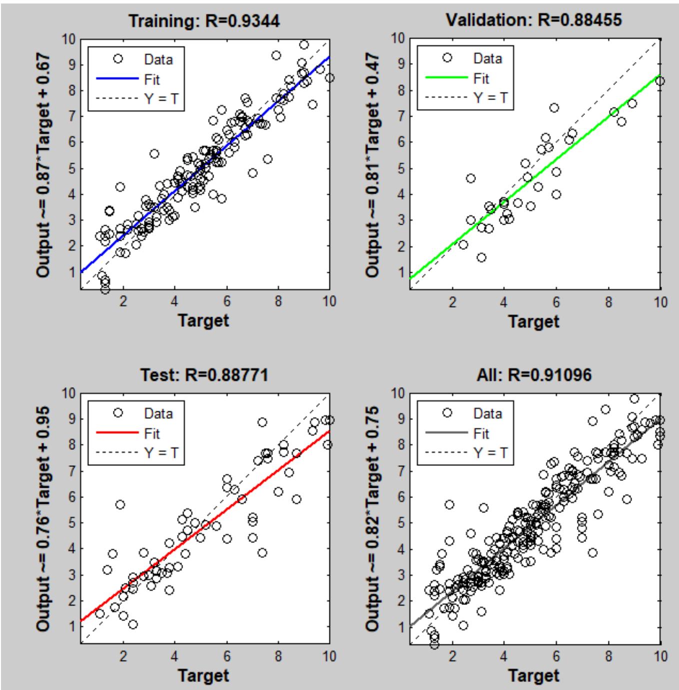

Figure A.135: Performance Plots for ‘trainb’ Function for H & ML Wells

APPENDIX B

The section is presenting in the details the statistical and graphical errors analysis for all AI models.

Table B.1: Statistical Errors from AI Models for H Wells

Statistical parameter	Set	ANN									FL	DT	SVM
		trainlm	trainlm-2L	traingd	traingdx	trainbfg	trainscg	trainoss	trainrp	trainb			
Standard Deviation	Training	0.30	0.25	0.86	1.10	0.24	0.77	0.57	0.73	0.56	0.38	0.26	0.25
	Testing	0.34	0.39	0.96	1.20	0.55	0.83	0.82	0.78	0.90	0.70	1.10	0.32
Mean Absolute Error	Training	0.20	0.19	0.66	0.94	0.15	0.52	0.44	0.57	0.43	0.30	0.17	0.21
	Testing	0.23	0.27	0.81	0.96	0.41	0.60	0.62	0.57	0.67	0.51	0.87	0.24
Mean Squared Error	Training	0.09	0.06	0.74	1.30	0.06	0.59	0.33	0.53	0.32	0.14	0.07	0.06
	Testing	0.12	0.15	0.93	1.65	0.30	0.69	0.68	0.63	0.89	0.49	1.10	0.10
Root Mean Squared Error	Training	0.31	0.25	0.86	1.10	0.24	0.77	0.57	0.73	0.56	0.37	0.26	0.24
	Testing	0.34	0.38	0.96	1.28	0.54	0.83	0.83	0.79	0.94	0.70	1.10	0.32
Mean Absolute Relative Error	Training	0.05	0.05	0.17	0.26	0.03	0.15	0.12	0.16	0.13	0.08	0.04	0.05
	Testing	0.07	0.09	0.18	0.17	0.10	0.18	0.11	0.11	0.15	0.17	0.19	0.07
Mean Squared Relative Error	Training	0.01	0.01	0.07	0.17	0.00	0.08	0.04	0.08	0.07	0.02	0.00	0.01
	Testing	0.02	0.03	0.05	0.04	0.03	0.11	0.02	0.02	0.06	0.10	0.08	0.02
Root Mean Squared Relative Error	Training	0.11	0.08	0.26	0.42	0.05	0.29	0.20	0.30	0.26	0.12	0.06	0.08
	Testing	0.13	0.18	0.22	0.21	0.17	0.33	0.14	0.14	0.24	0.31	0.28	0.14
Mean Absolute Percentage Error	Training	5.0	4.8	17.3	26.5	3.4	15.1	12.2	16.0	13.0	7.5	4.0	5.4
	Testing	6.9	8.8	17.8	16.7	10.0	17.5	11.4	10.6	14.6	16.6	19.2	7.2
Mean Squared Percentage Error	Training	128	62	688	1743	27	833	405	835	693	152	41	64
	Testing	169	320	498	425	304	1077	198	203	580	989	785	185
Root Mean Squared Percentage Error	Training	11.3	7.8	26.2	41.7	5.2	28.8	20.1	28.9	26.3	12.3	6.4	8.0
	Testing	13.0	17.9	22.3	20.6	17.4	32.8	14.1	14.2	24.1	31.4	28.0	13.6
Determination of Coeffecient	Training	0.98	0.98	0.86	0.76	0.99	0.89	0.94	0.90	0.94	0.97	0.98	0.99
	Testing	0.98	0.97	0.85	0.71	0.94	0.87	0.86	0.88	0.84	0.92	0.83	0.98

Table B.2: Statistical Errors from AI Models for ML Wells

Statistical parameter	Set	ANN									FL	DT	SVM
		trainlm	trainlm-2L	traingd	traingdx	trainbfg	trainscg	trainoss	trainrp	trainb			
Standard Deviation	Training	0.88	0.79	0.98	0.77	0.74	0.79	0.70	0.56	1.00	0.61	0.90	0.85
	Testing	1.60	0.89	1.40	1.53	0.92	1.20	1.60	1.30	1.60	2.10	1.70	0.68
Mean Absolute Error	Training	0.63	0.35	0.75	0.59	0.46	0.63	0.54	0.42	0.79	0.43	0.70	0.70
	Testing	1.05	0.79	0.93	0.99	0.73	1.10	1.30	1.10	1.35	1.64	1.50	0.59
Mean Squared Error	Training	0.86	0.62	0.98	0.58	0.53	0.62	0.48	0.31	1.10	0.36	0.80	0.70
	Testing	2.30	0.78	1.90	2.24	0.91	1.80	2.70	1.55	2.40	4.40	3.00	0.58
Root Mean Squared Error	Training	0.93	0.79	0.99	0.76	0.73	0.79	0.69	0.55	1.00	0.59	0.78	0.84
	Testing	1.50	0.88	1.40	1.50	0.96	1.40	1.60	1.24	1.55	2.10	1.70	0.76
Mean Absolute Relative Error	Training	0.15	0.10	0.18	0.17	0.12	0.18	0.15	0.13	0.19	0.10	0.18	0.19
	Testing	0.23	0.27	0.23	0.23	0.22	0.19	0.24	0.26	0.34	0.37	0.33	0.12
Mean Squared Relative Error	Training	0.05	0.06	0.07	0.06	0.05	0.05	0.05	0.04	0.07	0.02	0.05	0.08
	Testing	0.10	0.12	0.12	0.18	0.09	0.05	0.08	0.08	0.16	0.20	0.14	0.02
Root Mean Squared Relative Error	Training	0.21	0.25	0.28	0.24	0.23	0.32	0.22	0.19	0.26	0.13	0.23	0.30
	Testing	0.32	0.35	0.34	0.42	0.30	0.23	0.30	0.29	0.40	0.45	0.36	0.14
Mean Absolute Percentage Error	Training	14.4	10.1	18.4	16.5	12.4	17.5	15.3	12.5	18.9	10.3	17.5	18.9
	Testing	23.4	26.8	22.8	22.7	22.0	19.2	23.9	26.0	33.4	36.8	32.6	11.7
Mean Squared Percentage Error	Training	445	635	765	572	523	537	473	377	695	180	518	807
	Testing	1006	1209	1157	1788	885	527	823	841	1622	2027	1359	203
Root Mean Squared Percentage Error	Training	21.1	25.2	27.0	23.9	22.9	23.2	21.7	19.4	25.5	13.4	22.7	28.4
	Testing	31.7	34.0	34.0	42.3	30.0	23.0	28.7	29.0	40.3	45.0	36.9	14.4
Determination of Coeffecient	Training	0.77	0.81	0.78	0.82	0.84	0.80	0.89	0.92	0.72	0.89	0.85	0.81
	Testing	0.20	0.83	0.31	0.47	0.80	0.59	0.29	0.51	0.29	0.20	0.45	0.83

Table B.3: Statistical Errors from AI Models for H & ML Wells

Statistical parameter	Set	ANN									FL	DT	SVM
		trainlm	trainlm-2L	traingd	traingdx	trainbfg	trainscg	trainoss	trainrp	trainb			
Standard Deviation	Training	0.32	0.35	1.00	0.76	0.43	0.56	0.59	0.78	0.82	0.50	0.26	0.33
	Testing	0.62	0.77	1.10	0.82	1.00	0.60	0.66	0.94	1.20	0.83	0.85	0.50
Mean Absolute Error	Training	0.21	0.24	0.75	0.54	0.32	0.41	0.42	0.60	0.64	0.34	0.19	0.25
	Testing	0.38	0.49	0.86	0.56	0.61	0.48	0.51	0.70	0.86	0.56	0.66	0.34
Mean Squared Error	Training	0.11	0.12	1.00	0.57	0.19	0.31	0.34	0.60	0.68	0.26	0.07	0.11
	Testing	0.38	0.58	1.30	0.72	1.01	0.37	0.44	0.89	1.44	0.68	0.76	0.25
Root Mean Squared Error	Training	0.32	0.35	1.00	0.75	0.43	0.56	0.58	0.78	0.83	0.51	0.26	0.33
	Testing	0.62	0.76	1.10	0.85	1.00	0.61	0.67	0.94	1.20	0.83	0.87	0.50
Mean Absolute Relative Error	Training	0.05	0.07	0.20	0.15	0.08	0.11	0.11	0.15	0.18	0.08	0.04	0.08
	Testing	0.10	0.13	0.20	0.13	0.17	0.11	0.13	0.17	0.22	0.19	0.16	0.10
Mean Squared Relative Error	Training	0.01	0.02	0.12	0.07	0.02	0.04	0.04	0.06	0.08	0.03	0.00	0.02
	Testing	0.03	0.07	0.10	0.04	0.12	0.02	0.03	0.07	0.16	0.14	0.05	0.03
Root Mean Squared Relative Error	Training	0.09	0.14	0.34	0.27	0.12	0.21	0.20	0.23	0.29	0.16	0.06	0.14
	Testing	0.16	0.26	0.30	0.19	0.35	0.14	0.17	0.27	0.40	0.37	0.23	0.17
Mean Absolute Percentage Error	Training	5.1	6.6	19.9	15.0	8.1	10.7	11.4	15.2	17.5	8.7	4.3	7.5
	Testing	9.5	12.6	19.6	12.9	17.0	10.6	12.6	16.7	22.0	18.0	15.8	9.6
Mean Squared Percentage Error	Training	77	186	1183	743	152	441	414	546	837	263	38	209
	Testing	265	696	688	376	1235	207	303	726	1616	1372	544	303
Root Mean Squared Percentage Error	Training	8.8	13.7	34.4	27.3	12.3	21.0	20.3	23.3	28.9	16.0	6.2	14.5
	Testing	16.3	26.4	26.2	19.4	35.1	14.4	17.4	26.9	40.2	37.0	23.3	17.4
Determination of Coeffecient	Training	0.98	0.98	0.80	0.89	0.96	0.94	0.93	0.89	0.85	0.94	0.98	0.98
	Testing	0.92	0.89	0.74	0.87	0.81	0.92	0.91	0.83	0.78	0.89	0.87	0.94

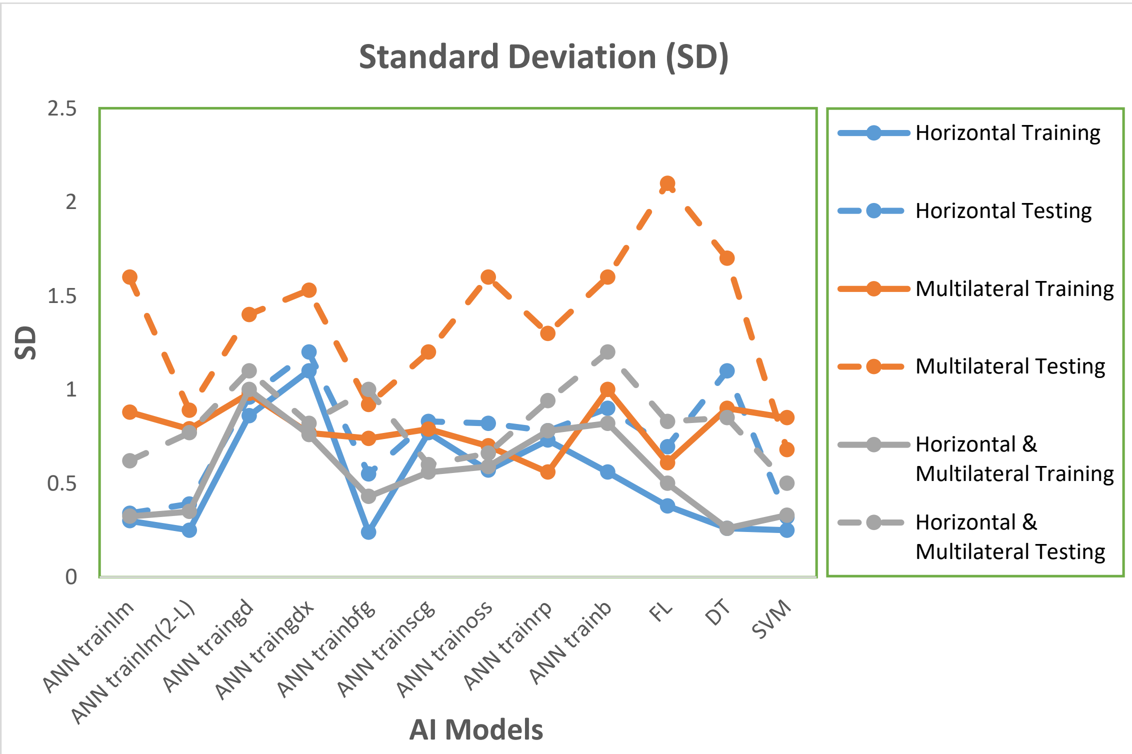

Figure B.1: Standard Deviation Plots for All AI Models

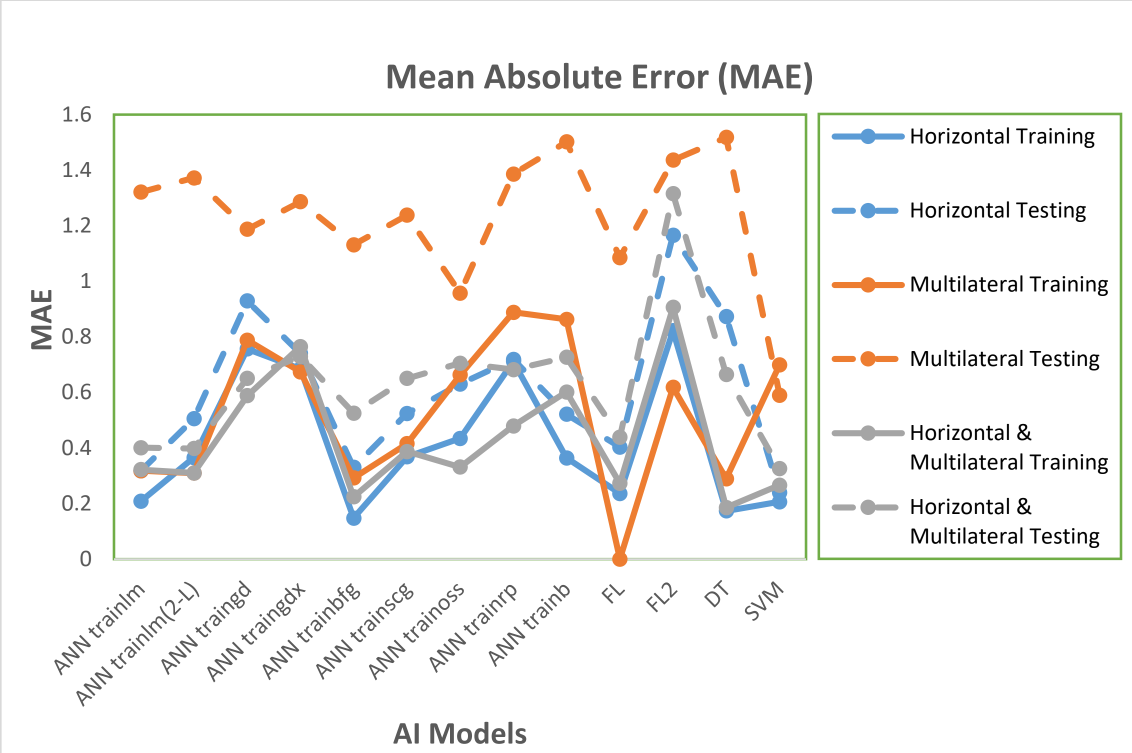

Figure B.2: Mean Absolute Error Plots for All AI Models

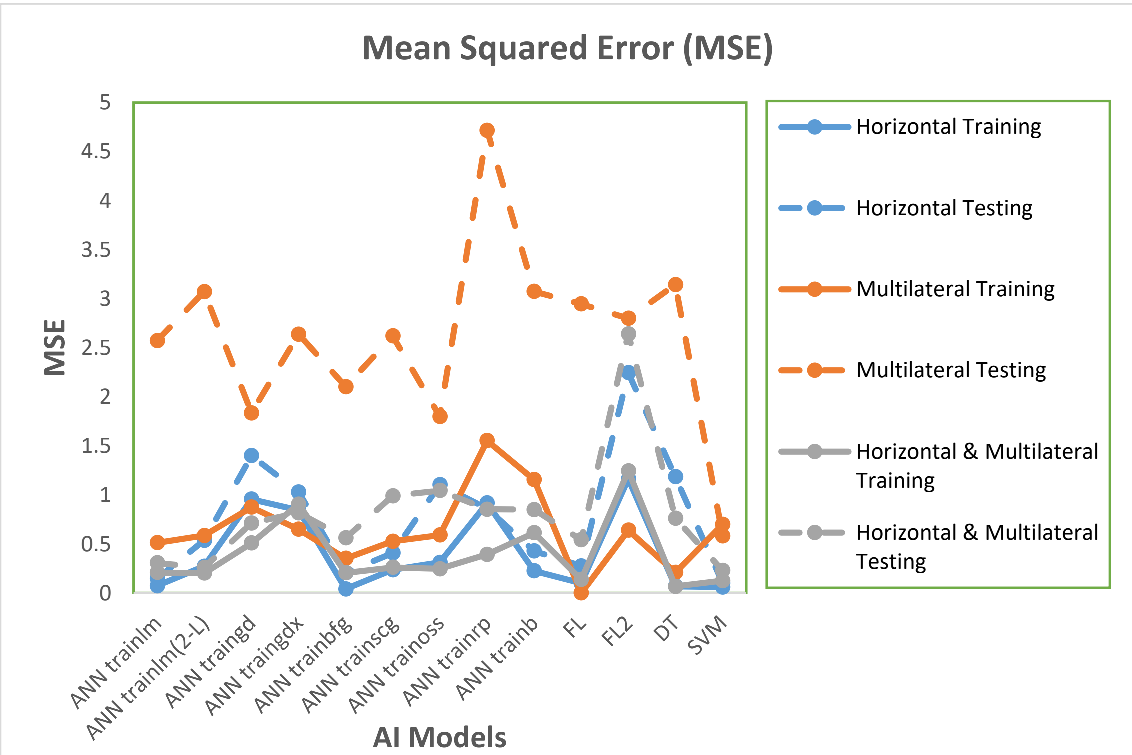

Figure B.3: Mean Square Error Plots for All AI Models

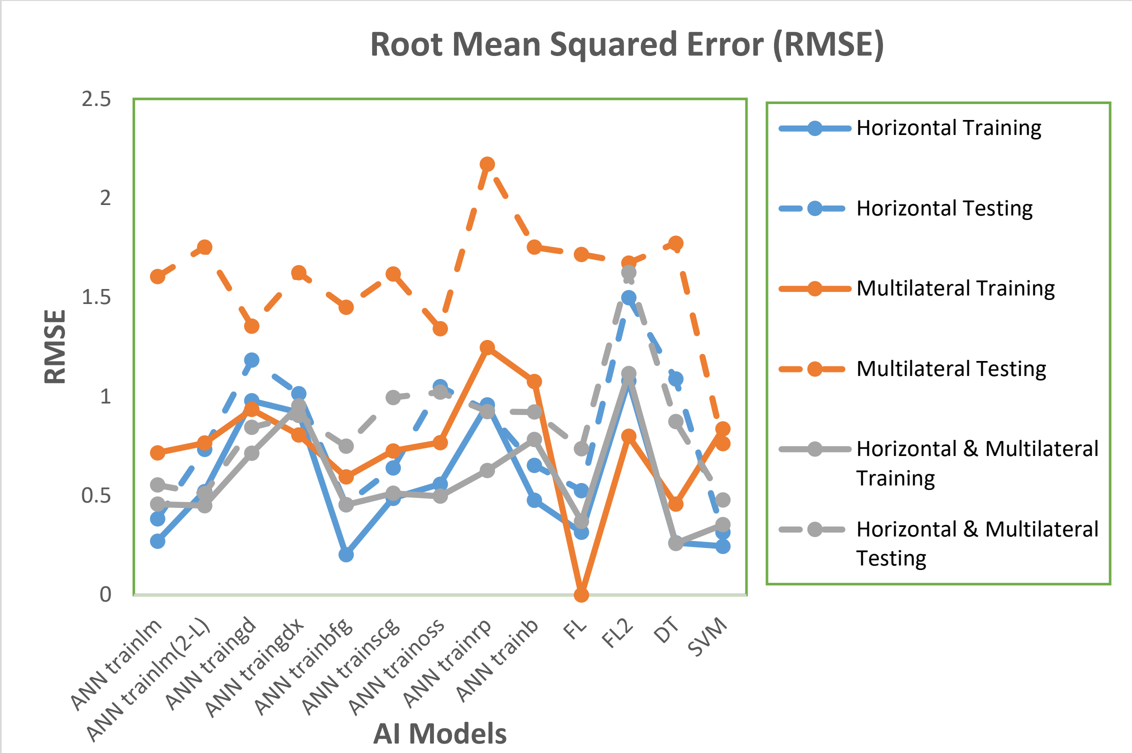

Figure B.4: Root Mean Square Error Plots for All AI Models

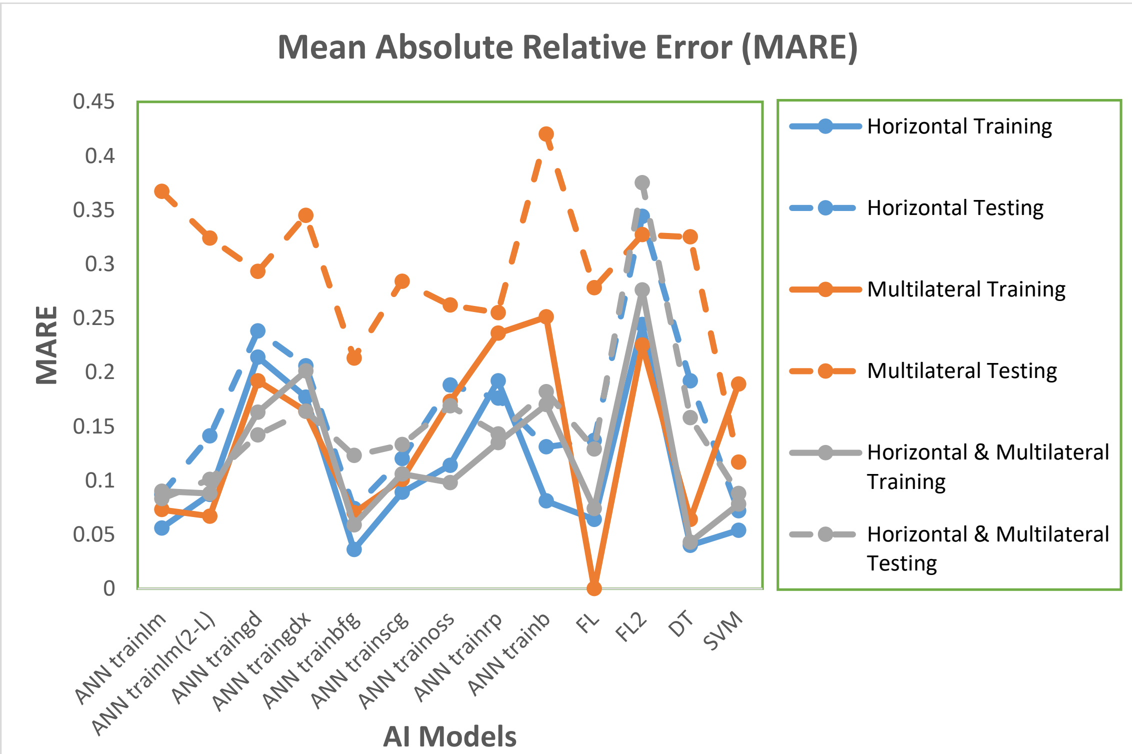

Figure B.5: Mean Absolute Relative Error Plots for All AI Models

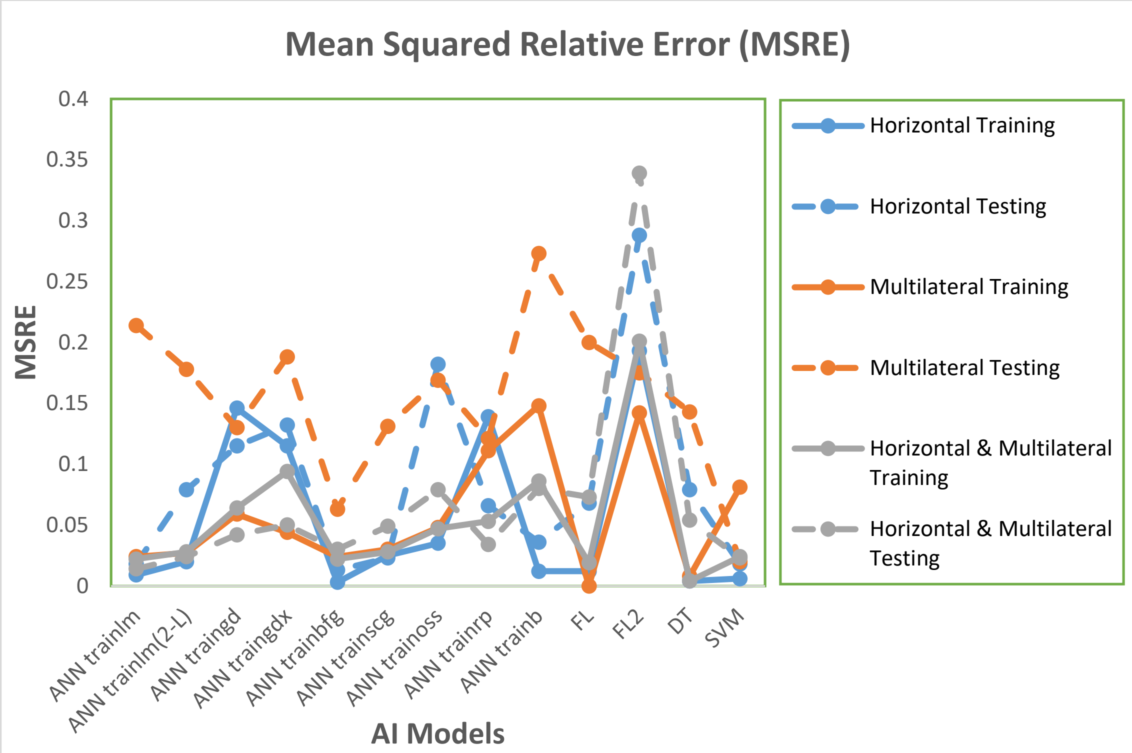

Figure B.6: Mean Squared Relative Error Plots for All AI Models

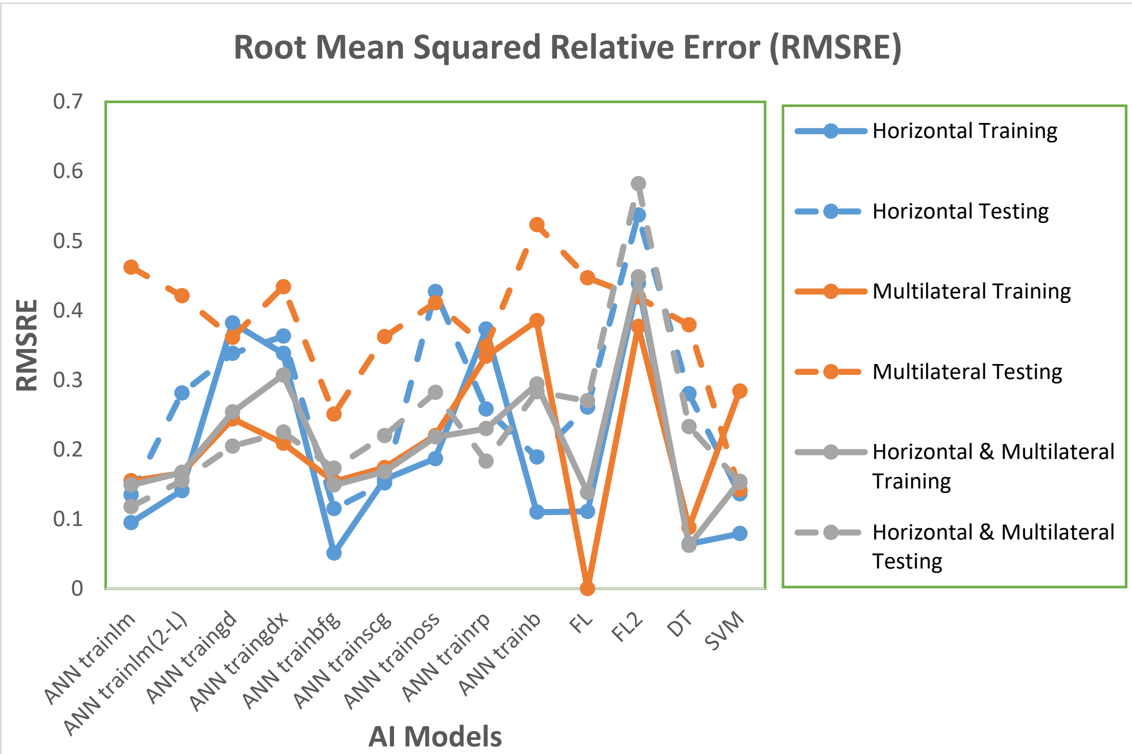

Figure B.7: Root Mean Squared Relative Error Plots for All AI Models

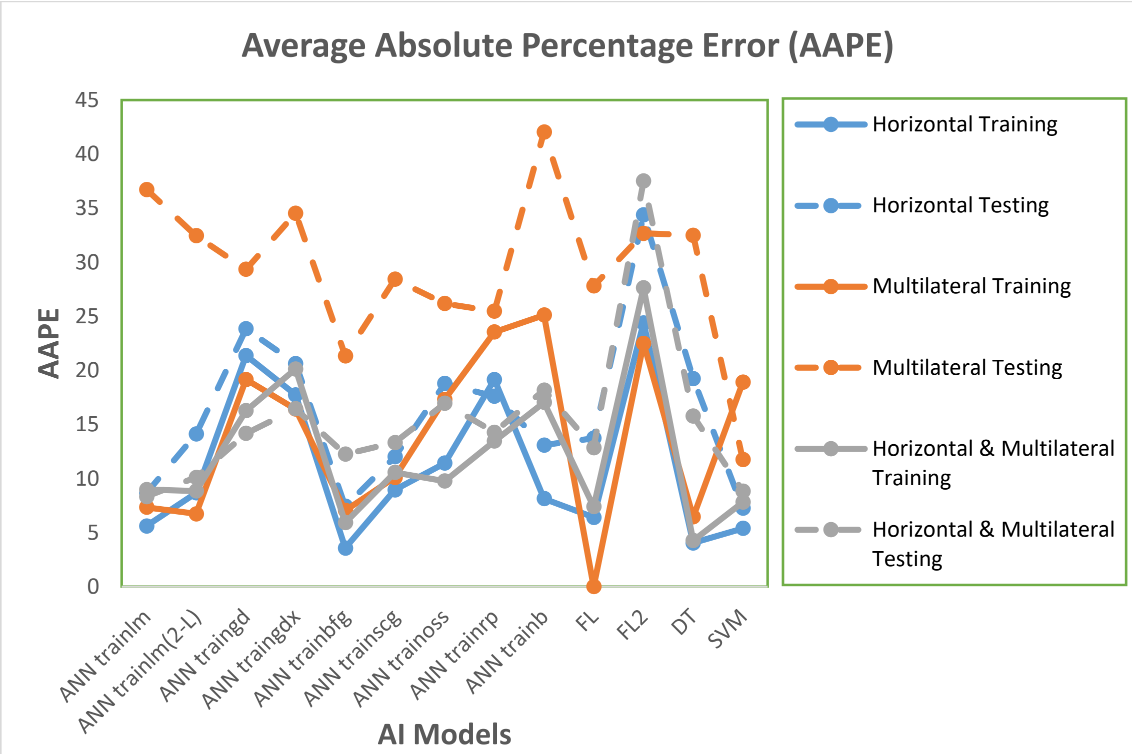

Figure B.8: AAPE Absolute Percentage Error Plots for All AI Models

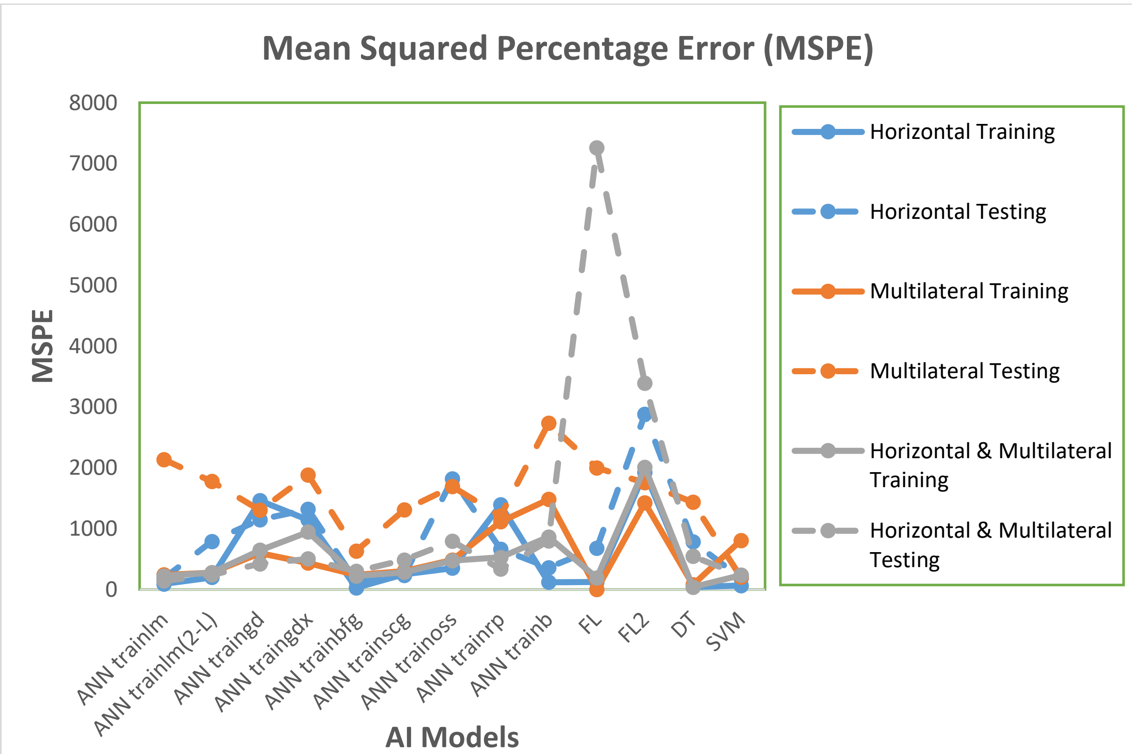

Figure B.9: Mean Squared Percentage Error Plots for All AI Models

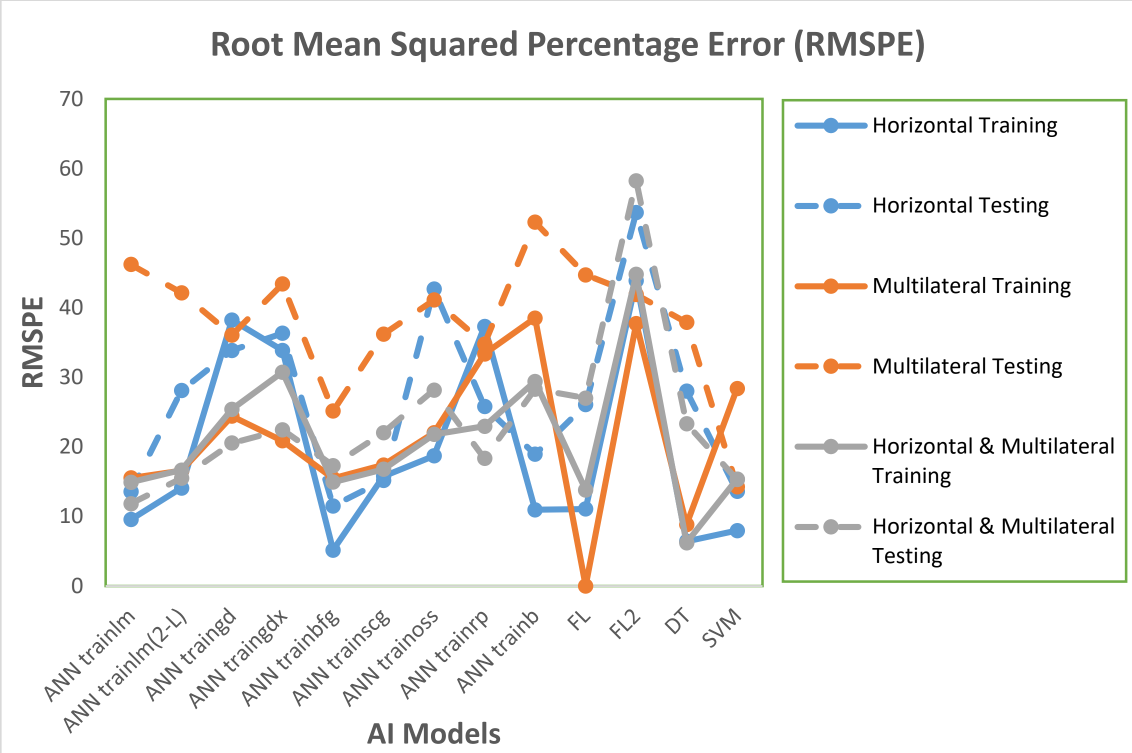

Figure B.10: Root Mean Squared Percentage Error Plots for All AI Models

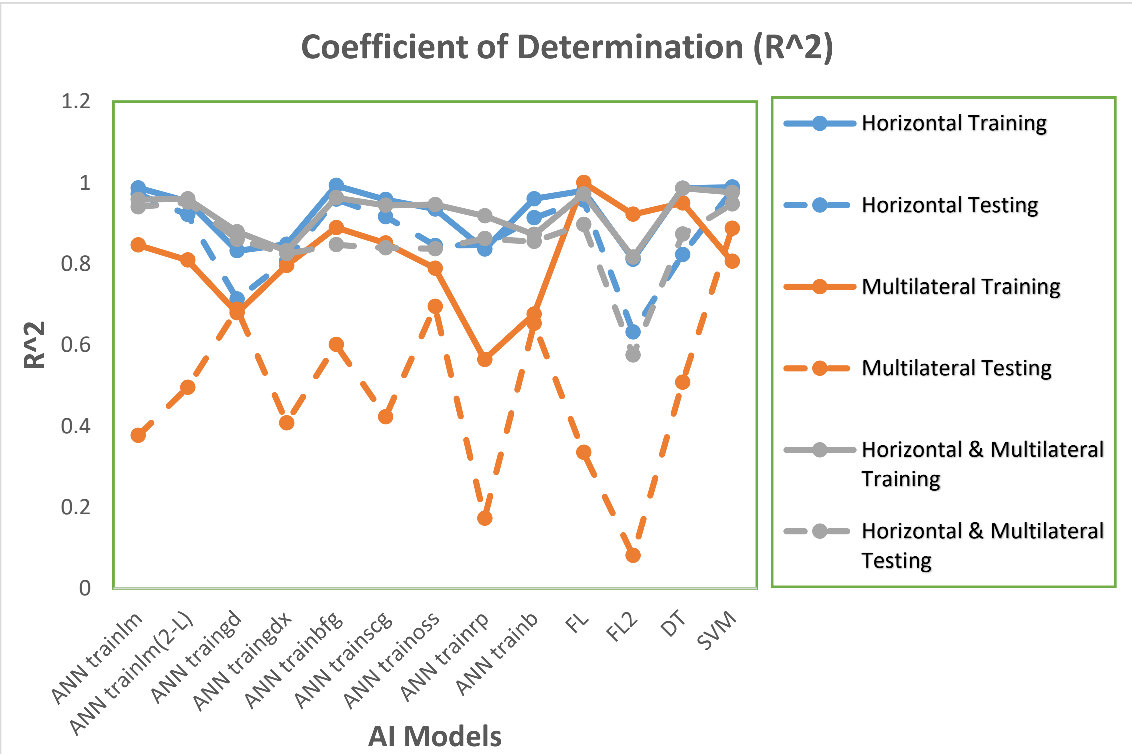

Figure B.11: Coefficient of Determination Plots for All AI Models

VITAE

Name: Ali Salman Al-Mashhad

Nationality: Saudi

Date of Birth 01/29/1985

E-mail: as_mashhad@hotmail.com

Address: Post Office Box # 5432
Ras Tanura 31311
Eastern Province, Saudi Arabia

Education: Bachelor of Science in Petroleum Engineering, 2008
King Fahd University of Petroleum & Minerals,
Dhahran 31261, Saudi Arabia.

Master of Science in Petroleum Engineering, 2018
King Fahd University of Petroleum & Minerals
Dhahran 31261, Saudi Arabia.

Areas of Interest: Well Performance, Production Engineering and I-Field Technologies

Professional Affiliations: Saudi Aramco

Experience: Ten years' experience in oil and gas industry through working on production engineering, reservoir management, production facility and I-Field engineering technologies.